

WADC TECHNICAL REPORT 53-10

**THE INFLUENCE OF TEMPERATURE AND RATE OF STRAIN
ON THE PROPERTIES OF METALS IN TORSION**

*C. E. Work
T. J. Dolan*

University of Illinois

February 1953

*Materials Laboratory
Contract No. AF 33(038)21587
RDO No. 614-13*

Wright Air Development Center
Air Research and Development Command
United States Air Force
Wright-Patterson Air Force Base, Ohio

Contrails

FOREWORD

This investigation was conducted in the research laboratories of the Department of Theoretical and Applied Mechanics, University of Illinois, on Air Force Contract No. AF 33(038)-21587, and Research and Development Order No. 614-13, "Strain Rate Effects on Torsional Properties at Elevated Temperatures." The work was administered under the direction of the Materials Laboratory, Directorate of Research, Wright Air Development Center, with R. F. Klinger acting as project engineer. Acknowledgement is due to F. C. Rally, T. Dimoff and other research personnel who have helped with the experimental phase of this investigation.

WADC TR 53-10

Contrails

ABSTRACT

An experimental study was made to determine the effect of temperature and rate of strain on the strength, ductility and energy absorbing capacity of seven different structural metals in torsion. Cylindrical specimens 0.25 in. in diameter were tested at four different constant strain-rates from 0.0001 in./in./sec. to 12.5 in./in./sec. and at four different temperatures from room temperature up to 1200F. Two series of tests were conducted: (A) specimens were held at the test temperature for one-half hour before loading, and (B) specimens were given a two-hundred hour aging treatment at the test temperature before testing.

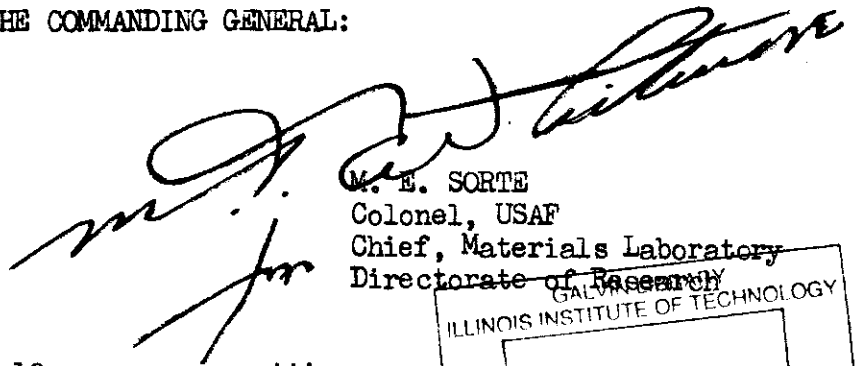
Torque, angle of twist, and time were continuously recorded and the torsional properties determined. The detailed results are presented in three-dimensional charts and analyzed in terms of the mechanisms altering the material behavior. In general, it was found that an increase in strain-rate caused an increase in strength, whereas an increase in temperature reduced the strength of all metals except in the blue-brittle temperature range for steel. Extremely great ductility was exhibited by some of the metals at the highest elevated temperatures employed, particularly at the slower rates of straining. The two-hundred hour aging treatment had no appreciable effect on the properties of most of the metals tested; significant changes were produced only in the aluminum alloys at 400F and 600F and in alloy steel at 1200F.

The experimental observations were compared with several theories that have been proposed to express mathematically the effects of strain-rate and temperature on mechanical properties. By proper selection of empirical constants, several equations involving a general relation for flow stress or new parameters of a "temperature-modified" strain-rate or a "velocity-modified" temperature were found to express approximately the variations obtained in mechanical properties.

PUBLICATION REVIEW

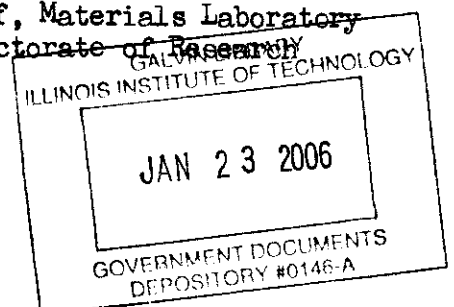
This report has been reviewed and is approved.

FOR THE COMMANDING GENERAL:


M. E. SORTE
Colonel, USAF
Chief, Materials Laboratory
Directorate of Research

WADC TR 53-10

iii



Contrails

TABLE OF CONTENTS

<u>Chapter</u>		<u>Page</u>
I	INTRODUCTION.	1
	1. Evaluation of the Mechanical Properties of Materials	1
	2. Immediate Importance of Temperature and Strain-Rate Studies.	2
	3. Object and Scope of this Investigation	3
	4. Review of the Literature	4
	a. General.	4
	b. Ferrous Metals	6
	c. Aluminum Alloys.	7
	d. Magnesium Alloys	7
	e. Titanium	8
II	EXPERIMENTAL PROGRAM.	10
	5. Description of Testing Equipment	10
	a. Mechanical Features of the Torsion Testing Machine . .	10
	b. Recording System	12
	c. Torque Measuring Device.	13
	d. Twist Measuring Devices.	14
	Rapid Tests.	14
	Lower Speed Tests.	15
	Elevated Temperatures.	17
	e. Sequence Control System.	17
	f. Furnace and Control System	19
	6. Interpretation of the Oscillograph Records	21
III	RESULTS OF EXPERIMENTS.	22
	7. Presentation of the Data	22
	a. Explanation of the Torsional Properties Reported . . .	23
	b. Evaluation of the Proportional Limit	24
	c. Determination of the Modulus of Elasticity	25
	d. Explanation of the Graphs.	26
	8. Discussion of Results.	29
	a. SAE 1018 Steel	29
	b. SAE 4340 Steel	32
	c. 24S-T Aluminum Alloy	33

Contrails
TABLE OF CONTENTS (CONT'D)

<u>Chapter</u>	<u>Page</u>
d. 75S-T Aluminum Alloy	35
e. FS-1 Magnesium Alloy	37
f. RC-70 Titanium	39
g. RC-130-B Titanium Alloy.	42
h. Effect of Aging Treatment.	43
75S-T Aluminum Alloy	43
24S-T Aluminum Alloy	44
Steel.	46
FS-1 Magnesium Alloy	47
Titanium	47
i. Energy Absorption.	47
j. Deformation and Fracture Characteristics	48
k. Shape of the Torque-Twist Curves	49
l. Comparative Strengths of the Seven Metals.	51
m. Influence of Structural Changes on Experimental Observations.	51
9. Comparison of Strain-Rate and Temperature Effects with Mathematical Theories.	56
a. Simplifications Used	56
b. Equivalent Strain-Rate Parameter	57
c. General Equation for Flow.	58
Constant Strain-Rate and Temperature	59
Constant Strain and Temperature.	60
Constant Strain and Strain-Rate.	61
d. Velocity-Modified Temperature Parameter.	62
10. Correlation with Other States of Stress.	64
IV SUMMARY AND CONCLUSIONS	66
BIBLIOGRAPHY	71
APPENDIX	
I Derivation of the Equation for Shearing Stress in Torsion .	80
II Discussion of a General Equation for Flow	84
III Discussion of the Velocity-Modified Temperature Parameter .	86
IV Tables of Individual Test Results	88
V Tables and Figures	153

Contrails

LIST OF TABLES

APPENDIX IV

TABLE NO.		PAGE
1.	Torsion Properties of SAE 1018 Steel at Room Temperature	88
2.	Torsion Properties of SAE 1018 Steel at 400°F (Not Aged)	89
3.	Torsion Properties of SAE 1018 Steel at 400°F (Aged)	90
4.	Torsion Properties of SAE 1018 Steel at 700°F (Not Aged)	91
5.	Torsion Properties of SAE 1018 Steel at 700°F (Aged)	92
6.	Torsion Properties of SAE 1018 Steel at 1000°F (Not Aged)	93
7.	Torsion Properties of SAE 1018 Steel at 1000°F (Aged)	94
8.	Torsion Properties of SAE 4340 Steel at Room Temperature.	95
9.	Torsion Properties of SAE 4340 Steel at 400°F (Not Aged)	96
10.	Torsion Properties of SAE 4340 Steel at 400°F (Aged)	97
11.	Torsion Properties of SAE 4340 Steel at 700°F (Not Aged)	98
12.	Torsion Properties of SAE 4340 at 700°F (Aged)	99
13.	Torsion Properties of SAE 4340 Steel at 1000°F (Not Aged)	100
14.	Torsion Properties of SAE 4340 Steel at 1000°F (Aged)	101

LIST OF TABLES (CONT'D)

APPENDIX IV

TABLE NO.		PAGE
15.	Torsion Properties of SAE 4340 Steel at 1200°F (Not Aged)	102
16.	Torsion Properties of SAE 4340 Steel at 1200°F (Aged)	103
17.	Torsion Properties of 24S-T Aluminum Alloy at Room Temperature	104
18.	Torsion Properties of 24S-T Aluminum Alloy at 200°F (Not Aged)	105
19.	Torsion Properties of 24S-T Aluminum Alloy at 200°F (Aged)	106
20.	Torsion Properties of 24S-T Aluminum Alloy at 400°F (Not Aged)	107
21.	Torsion Properties of 24S-T Aluminum Alloy at 400°F (Aged)	108
22.	Torsion Properties of 24S-T Aluminum Alloy at 600°F (Not Aged)	109
23.	Torsion Properties of 24S-T Aluminum Alloy at 600°F (Aged)	110
24.	Torsion Properties of 75S-T Aluminum Alloy at Room Temperature	111
25.	Torsion Properties of 75S-T Aluminum Alloy at 200°F (Not Aged)	112
26.	Torsion Properties of 75S-T Aluminum Alloy at 200°F (Aged)	113
27.	Torsion Properties of 75S-T Aluminum Alloy at 400°F (Not Aged)	114
28.	Torsion Properties of 75S-T Aluminum Alloy at 400°F (Aged)	115

Contrails

LIST OF TABLES (CONT'D)

APPENDIX IV

TABLE NO.		PAGE
29.	Torsion Properties of 75S-T Aluminum Alloy at 600°F (Not Aged)	116
30.	Torsion Properties of 75S-T Aluminum Alloy at 600°F (Aged)	117
31.	Torsion Properties of FS-1 Magnesium at Room Temperature	118
32.	Torsion Properties of FS-1 Magnesium at 200°F (Not Aged)	119
33.	Torsion Properties of FS-1 Magnesium at 200°F (Aged)	120
34.	Torsion Properties of FS-1 Magnesium at 400°F (Not Aged)	121
35.	Torsion Properties of FS-1 Magnesium at 400°F (Aged)	122
36.	Torsion Properties of FS-1 Magnesium at 600°F (Not Aged)	123
37.	Torsion Properties of FS-1 Magnesium at 600°F (Aged)	124
38.	Torsion Properties of RC-70 Titanium at Room Temperature	125
39.	Torsion Properties of RC-70 Titanium at 400°F (Not Aged)	126
40.	Torsion Properties of RC-70 Titanium at 400°F (Aged)	127
41.	Torsion Properties of RC-70 Titanium at 700°F (Not Aged)	128
42.	Torsion Properties of RC-70 Titanium at 700°F (Aged)	129
43.	Torsion Properties of RC-70 Titanium at 1000°F (Not Aged)	130
44.	Torsion Properties of RC-70 Titanium at 1000°F (Aged)	131

LIST OF TABLES (CONT'D)

APPENDIX IV

TABLE NO.		PAGE
45.	Torsion Properties of RC-130B Titanium Alloy at Room Temperature	132
46.	Torsion Properties of RC-130B Titanium Alloy at 400°F (Not Aged)	133
47.	Torsion Properties of RC-130B Titanium Alloy at 400°F (Aged)	134
48.	Torsion Properties of RC-130B Titanium Alloy at 700°F (Not Aged)	135
49.	Torsion Properties of RC-130B Titanium Alloy at 700°F (Aged)	136
50.	Torsion Properties of RC-130B Titanium Alloy at 1000°F (Not Aged)	137
51.	Torsion Properties of RC-130B Titanium Alloy at 1000°F (Aged)	138
52.	Torsion Properties of SAE 1018 Steel at 400°F (Not Aged)	140
53.	Torsion Properties of SAE 1018 Steel at 400°F (Aged)	141
54.	Torsion Properties of SAE 1018 Steel at 700°F (Not Aged)	142
55.	Torsion Properties of SAE 1018 Steel at 1000°F (Not Aged)	143
56.	Torsion Properties of 24S-T Aluminum Alloy at 200°F (Not Aged)	144
57.	Torsion Properties of 24S-T Aluminum Alloy at 200°F (Aged)	145

LIST OF TABLES (CONT'D)

APPENDIX IV

TABLE NO.		PAGE
58.	Torsion Properties of 24S-T Aluminum Alloy at 400°F (Not Aged)	146
59.	Torsion Properties of 24S-T Aluminum Alloy at 400°F (Aged)	147
60.	Torsion Properties of 24S-T Aluminum Alloy at 600°F (Not Aged)	148
61.	Torsion Properties of 24S-T Aluminum Alloy at 600°F (Aged)	149
62.	Torsion Properties of FS-1 Magnesium Alloy at 200°F (Not Aged)	150
63.	Torsion Properties of FS-1 Magnesium Alloy at 400°F (Not Aged)	151
64.	Torsion Properties of FS-1 Magnesium Alloy at 600°F (Not Aged)	152

APPENDIX V

TABLE NO.		PAGE
I.	CHEMICAL ANALYSIS OF METALS TO BE TESTED	153
II.	STATIC TENSILE PROPERTIES OF METALS TESTED	154
III.	INSTRUMENTATION AND CONDITIONS FOR CONDUCTING VARIOUS TESTS	155
IV.	SAMPLE CALCULATIONS	156

Contrails

LIST OF ILLUSTRATIONS

FIGURE NO.		PAGE
1	Torsion Testing Machine Set Up for the Slowest Rate of Loading.	157
2	Details of the Torsion Test Specimen	158
3	Details of the Water-Cooled Torsion Weigh-Bar	158
4	Apparatus for Measurement of the Angle of Twist by Means of a Photoelectric Cell	159
5	Twist Measuring Apparatus for Slower Speed Tests	160
6	Circuit Diagram for the Slide Wire Component of the Twist Indicator, Fig. 5	160
7	Timing and Switching Mechanisms for Controlling the Sequence of Events When Testing at the High Rates of Strain	161
8	Sectional View of the Electric Furnace for Elevated Temperature Torsion Tests	162
9	Wiring of the Furnace and Control Circuit	162
10	Electric Furnace and Control Panel for Elevated Temperature Tests	163
11	Typical Oscillograph Record from Torsion Test at Room Temperature and Strain Rate of 0.005 in./in./sec.	164
12	Typical Oscillograph Record from Torsion Test at Room Temperature and Strain-Rate of 12.5 in./in./sec.	165
13	Torque-Twist Diagram for 75S-T Aluminum Alloy in Torsion (Test No. 133, 2nd Speed, Room Temperature).	166
14	True Tensile Stress-Strain Curves for the Seven Metals Studied	166
15	Ordinary Tensile Stress-Strain Curves for the Seven Metals Studied	167

LIST OF ILLUSTRATIONS (CONT'D)

FIGURE NO.		PAGE
16	Effect of Temperature on the Shearing Yield Strength of SAE 1018 Steel in Torsion	168
17	Combined Effects of Rate of Strain and Temperature on the Shearing Yield Strength of SAE 1018 Steel in Torsion	168
18	Combined Effects of Rate of Strain and Temperature on the Modulus of Rupture of SAE 1018 Steel in Torsion . .	169
19	Effect of Temperature on the Total Shearing Strain of SAE 1018 Steel in Torsion	169
20	Combined Effects of Rate of Strain and Temperature on the Total Shearing Strain of SAE 1018 Steel in Torsion	170
21	Effect of Rate of Strain on the Total Shearing Strain of SAE 1018 Steel at 1000 ^{OF} in Torsion	170
22	Combined Effects of Rate of Strain and Temperature on the Energy Absorbed in Specimens of SAE 1018 Steel in Torsion	171
23	Combined Effects of Rate of Strain and Temperature on the Yield Point Ratio for SAE 1018 Steel in Torsion . .	171
24	Effect of (a) Rate of Strain and (b) Temperature on the Shearing Yield Strength of SAE 4340 Steel in Torsion. .	172
25	Combined Effects of Rate of Strain and Temperature on the Shearing Yield Strength of SAE 4340 Steel in Torsion	173
26	Combined Effects of Rate of Strain and Temperature on the Modulus of Rupture of SAE 4340 Steel in Torsion . .	173
27	Effect of Temperature on the Total Shearing Strain of SAE 4340 Steel in Torsion	174
28	Combined Effects of Rate of Strain and Temperature on the Total Shearing Strain of SAE 4340 Steel in Torsion	174
29	Combined Effects of Rate of Strain and Temperature on the Energy Absorbed in Specimens of SAE 4340 Steel in Torsion	175

LIST OF ILLUSTRATIONS (CONT'D)

FIGURE NO.		PAGE
30	Effect of (a) Rate of Strain and (b) Temperature on the Shearing Yield Strength of 24S-T Aluminum Alloy in Torsion	175
31	Combined Effects of Rate of Strain and Temperature on the Shearing Yield Strength of 24S-T Aluminum Alloy in Torsion	176
32	Combined Effects of Rate of Strain and Temperature on the Modulus of Rupture of 24S-T Aluminum Alloy in Torsion . .	176
33	Combined Effects of Rate of Strain and Temperature on the Total Shearing Strain of 24S-T Aluminum Alloy in Torsion.	177
34	Combined Effects of Rate of Strain and Temperature on the Energy Absorbed in Specimens of 24S-T Aluminum Alloy in Torsion	177
35	Effect of (a) Rate of Strain and (b) Temperature on the Shearing Yield Strength of 75S-T Aluminum Alloy in Torsion	178
36	Combined Effects of Rate of Strain and Temperature on the Shearing Yield Strength of 75S-T Aluminum Alloy in Torsion	178
37	Combined Effects of Rate of Strain and Temperature on the Modulus of Rupture of 75S-T Aluminum Alloy in Torsion . .	179
38	Effect of (a) Rate of Strain and (b) Temperature on the Total Shearing Strain of 75S-T Aluminum Alloy in Torsion.	179
39	Combined Effects of Rate of Strain and Temperature on the Total Shearing Strain of 75S-T Aluminum Alloy in Torsion.	180
40	Effect of Rate of Strain on the Total Shearing Strain of 75S-T Aluminum Alloy at 600°F in Torsion	180
41	Combined Effects of Rate of Strain and Temperature on the Energy Absorbed in Specimens of 75S-T Aluminum Alloy in Torsion.	181
42	Effect of (a) Rate of Strain and (b) Temperature on the Shearing Yield Strength of FS-1 Magnesium Alloy in Torsion	181
43	Combined Effects of Rate of Strain and Temperature on the Shearing Yield Strength of FS-1 Magnesium Alloy in Torsion	182
44	Combined Effects of Rate of Strain and Temperature on the Modulus of Rupture of FS-1 Magnesium Alloy in Torsion . .	182

Contrails

LIST OF ILLUSTRATIONS (CONT'D)

FIGURE NO.		PAGE
45	Combined Effects of Rate of Strain and Temperature on the Total Shearing Strain of FS-1 Magnesium Alloy in Torsion	183
46	Combined Effects of Rate of Strain and Temperature on the Energy Absorbed in Specimens of FS-1 Magnesium Alloy in Torsion	183
47	Effect of (a) Rate of Strain and (b) Temperature on the Shearing Yield Strength of RC-70 Titanium in Torsion . .	184
48	Combined Effects of Rate of Strain and Temperature on the Shearing Yield Strength of ⁴ C-70 Titanium in Torsion . .	185
49	Combined Effects of Rate of Strain and Temperature on the Modulus of Rupture of RC-70 Titanium in Torsion	185
50	Effect of Temperature on the Total Shearing Strain of RC-70 Titanium in Torsion	186
51	Combined Effects of Rate of Strain and Temperature on the Total Shearing Strain of RC-70 Titanium in Torsion . . .	186
52	Combined Effects of Rate of Strain and Temperature on the Energy Absorbed in Specimens of RC-70 Titanium in Torsion	187
53	Combined Effects of Rate of Strain and Temperature on the Yield Point Ratio for RC-70 Titanium in Torsion	187
54	Effect of (a) Rate of Strain and (b) Temperature on the Shearing Yield Strength of RC-130-B Titanium Alloy in Torsion	188
55	Combined Effects of Rate of Strain and Temperature on the Yield Strength of RC-130-B Titanium Alloy in Torsion . .	189
56	Combined Effects of Rate of Strain and Temperature on the Modulus of Rupture of RC-130-B Titanium Alloy in Torsion	189
57	Effect of Temperature on the Total Shearing Strain of RC-130-B Titanium Alloy in Torsion	190
58	Combined Effects of Rate of Strain and Temperature on the Total Shearing Strain of RC-130-B Titanium Alloy in Torsion	190

Contrails

LIST OF ILLUSTRATIONS (CONT'D)

FIGURE NO.		PAGE
59	Combined Effects of Rate of Strain and Temperature on the Energy Absorbed in Specimens of RC-130-B Titanium Alloy in Torsion	191
60	Shift of Blue Brittleness Temperature for Steel with Change of Strain-Rate	191
61	RC-70 Titanium Specimens Broken in Second Speed Tests .	192
62	Oscillograph Records for Tests of SAE 1018 Steel at 400°F.	193
63	Oscillograph Records for Tests of SAE 1018 Steel at 700°F.	194
64	Initial Portions of Oscillograph Records for First Speed Tests of RC-70 Titanium	195
65	Initial Portions of Oscillograph Records for Second, Third and Fourth Speed Tests of RC-70 Titanium	196
66	Torque-Twist Curves for Fourth Speed Torsion Tests of SAE 1018 Steel at Four Temperatures	197
67	Torque-Twist Curves for Fourth Speed Torsion Tests of SAE 4340 Steel at Five Temperatures	197
68	Torque-Twist Curves for Fourth Speed Torsion Tests of 24S-T Aluminum Alloy at Four Temperatures	198
69	Torque-Twist Curves for Fourth Speed Torsion Tests of 75S-T Aluminum Alloy at Four Temperatures	198
70	Torque-Twist Curves for Fourth Speed Torsion Tests of FS-1 Magnesium Alloy at Four Temperatures	199
71	Torque-Twist Curves for Fourth Speed Torsion Tests of RC-70 Titanium at Four Temperatures	200
72	Torque-Twist Curves for Fourth Speed Torsion Tests of RC-130-B Titanium Alloy at Four Temperatures	200
73	Comparison of the Shearing Yield Strengths at Elevated Temperatures of Seven Metals Tested in Torsion	201
74	Comparison of the Moduli of Rupture at Elevated Temperatures of Seven Metals Tested in Torsion	202

Contrails

LIST OF ILLUSTRATIONS (CONT'D)

FIGURE NO.		PAGE
75	Comparison of the Torsional Strength-Weight Ratios of Seven Metals at Elevated Temperatures	203
76	Plastic True Stress-Strain Curves for Torsion	204
77	Variation of Torque at Shearing Strain $\gamma=0.50$ in./in. with the Parameter P for SAE 1018 Steel in Torsion	205
78	Effect of Rate of Strain on the Torque at Constant Shearing Strain in Torsion Tests of SAE 1018 Steel	205
79	Effect of Rate of Strain on the Torque at Constant Shearing Strain in Torsion Tests of SAE 4340 Steel	206
80	Effect of Rate of Strain on the Torque at Constant Shearing Strain in Torsion Tests of 24 S-T Aluminum Alloy	206
81	Effect of Rate of Strain on the Torque at Constant Shearing Strain in Torsion Tests of 75S-T Aluminum Alloy	207
82	Effect of Rate of Strain on the Torque at Constant Shearing Strain in Torsion Tests of FS-1 Magnesium Alloy	207
83	Effect of Rate of Strain on the Torque at Constant Shearing Strain in Torsion Tests of RC-70 Titanium	208
84	Effect of Rate of Strain on the Torque at Constant Shearing Strain in Torsion Tests of RC-130-B Titanium Alloy	208
85	Effect of Temperature on the Torque at Constant Shearing Strain in Torsion Tests of SAE 1018 Steel	209
86	Effect of Temperature on the Torque at Constant Shearing Strain in Torsion Tests of SAE 4340 Steel	209
87	Effect of Temperature on the Torque at Constant Shearing Strain in Torsion Tests of 24 S-T Aluminum Alloy	210
88	Effect of Temperature on the Torque at Constant Shearing Strain in Torsion Tests of 75S-T Aluminum Alloy	210
89	Effect of Temperature on the Torque at Constant Shearing Strain in Torsion Tests of FS-1 Magnesium Alloy	211

Contrails

LIST OF ILLUSTRATIONS (CONT'D)

FIGURE NO.		PAGE
90	Effect of Temperature on the Torque at Constant Shearing Strain in Torsion Tests of RC-70 Titanium	211
91	Effect of Temperature on the Torque at Constant Shearing Strain in Torsion Tests of RC-130-B Titanium Alloy	212
92	Variation of Torque at Shearing Strain, $\gamma=0.50$ in./in. with the Parameter T_m for SAE 1018 Steel in Torsion	212
93	Variation of Torque at Shearing Strain, $\gamma=0.30$ in./in. with the Parameter T_m for SAE 4340 Steel in Torsion	213
94	Variation of Torque at Shearing Strain, $\gamma=0.30$ in./in. with the Parameter T_m for 24S-T Aluminum Alloy in Torsion	213
95	Variation of Torque at Shearing Strain, $\gamma=0.10$ in./in. with the Parameter T_m for 75S-T Aluminum Alloy in Torsion	214
96	Variation of Torque at Shearing Strain, $\gamma=0.30$ in./in. with the Parameter T_m for FS-1 Magnesium Alloy in Torsion	214
97	Variation of Torque at Shearing Strain, $\gamma=0.05$ in./in. with the Parameter T_m for RC-70 Titanium in Torsion	215
98	Variation of Torque at Shearing Strain, $\gamma=0.20$ in./in. with the Parameter T_m for RC-130-B Titanium Alloy in Torsion	215
99	Shearing Stresses in Torsion of a Round Bar	216
100	Torque-Twist Curve for Defining T_e	216
101	Contributions to the Relative Strength Caused by Time-Dependent and Temperature-Dependent Changes During Testing	216

Contrails

I. INTRODUCTION

1. Evaluation of the Mechanical Properties of Materials.

The ability of a structure or structural part in service to carry out the function for which it is intended depends to a large extent on the behavior of the material of which it is constructed. In order that the designer may have adequate information on the significant properties of the material, these properties must be determined by appropriate tests of samples of the material.

What constitutes an appropriate test is not yet defined. Each of the tests commonly used has some advantages but also certain disadvantages and it is not always certain exactly how to extend results obtained under one limited set of conditions to include others. In the past it has been customary to accept the properties obtained in the ordinary static tension test as the most satisfactory criteria for evaluating the mechanical qualities of a material. Because of its simplicity and common usage, the tension test is used to predict the applicability of materials for a wide variety of uses, many of which involve more complex systems of stresses. Considerable doubt exists, however, as to whether any universal structural characteristics can be adequately appraised on the basis of observations of the properties when subjected only to a uniaxial state of stress.

Many of the mechanical properties for which an evaluation is usually attempted fall in one of the following classes: elastic strength and stiffness, ductility energy absorption and maximum load carrying capacity. The elastic characteristics are most easily treated theoretically and until recently have received the most attention in tension test studies. However for studying the plastic and work-hardening characteristics of a metal, the tension test is inherently at a disadvantage because of the local necking which takes place. The only portion of the metal in the tension specimen which is completely exhausted plastically is the material adjacent to the break. The final elongation, therefore, is a combination

of large deformations in the necked portion and a limited amount of stretching throughout the remaining portion of the metal which retains considerable capacity for deformation. This latter portion constitutes the largest part of the length. Furthermore, within the localized region where the fracture finally occurs, necking introduces a notch effect accompanied by a complex three-dimensional stress system which changes continuously as the necking progresses. This makes it difficult, (7, 80)⁺ if not impossible, to analyze the final fracture characteristics and relative work-hardenability of different metals.

In the torsion test many of these disadvantages are not present. The dimensions of the specimen do not change appreciably during the test even to the point of fracture, so that the original dimensions of the specimen are valid for analytical studies of strength and ductility. Deformation is fairly uniform throughout the length of the test section. The absence of localized necking eliminates the continuously increasing notch effect with its consequent localized three-dimensional stress system. Ductility as determined by the angle of twist of the specimen involves general exhaustion of the plasticity along the entire gage length. The slope of the stress-strain diagram in the torsion test is a better measure of the work-hardenability of the material since this slope is not influenced by major dimension changes as in the tension test.

2. Immediate Importance of Temperature and Strain-Rate Studies.

The behavior of a given material has been found to depend on the mechanical operations carried out during fabrication, heat treatment, stress history and upon other factors such as the type of loading, state of stress and environmental conditions.

Two important parameters, rate of strain and temperature, are known to be interrelated and frequently vary simultaneously in service. Both have been

⁺ Numbers in parentheses refer to the references listed in the Bibliography.

investigated singly but few studies have been of a wide enough scope to give attention to their combined effects.

The current trend toward jet engines and rockets for propulsion of guided missiles and military aircraft, and the extreme speeds developed, have introduced problems of elevated temperatures and severe sudden loading. Heat arising from skin friction and from the power plants is sufficient to produce elevated temperatures in wing and fuselage elements which heretofore have operated well within the ordinary room temperature range. Because of the extreme urgency for rapid advance in this field, investigation of these parameters is particularly timely and since many of the stress systems in surface and supporting elements are biaxial, torsion tests are especially appropriate.

3. Object and Scope of Investigation.

In this project, prepared specimens of several metals were subjected to a biaxial state of stress in torsion tests to investigate the effects of the two parameters, temperature and strain-rate, on their mechanical properties.

The studies covered here included two steels, two aluminum alloys, one magnesium alloy and two titanium alloys. These metals represent three different classes according to crystal lattice structure, namely, body-centered cubic for steels, face-centered cubic for the aluminum, and close-packed hexagonal for the titanium and magnesium.

Four rates of torsional strain, differing by factors of 50 to 1, were selected to produce the following nominal rates of shearing strain for the specimens tested: 12.5, 0.25, 0.005 and 0.0001 in. per in. per second.

Torsion tests were conducted at room temperature and at three or four elevated temperatures for each metal. The elevated temperature levels were: 200F, 400F and 600F for the aluminum and magnesium alloys and 400F, 700F and 1000F for the steels and titanium. For the 4340 steel a set of tests was included also at 1200F. For one series of tests, specimens were heated to the

desired temperature then held at temperature for one-half hour before each test began. A second series of tests is also reported for which specimens were given a 200-hour aging treatment in advance, at the same elevated temperature at which they were subsequently tested.

The geometric details chosen for the torsion test specimen are shown in Fig. 2. Large radius fillets at the ends of the reduced section and a slight undercutting of the central portion were necessary to prevent the fracture from occurring outside the gage length.

4. Review of the Literature.

a. General. - The technical literature contains reports on a multitude of investigations and theories which contribute to an understanding of the influence exerted by rate of loading and by temperature on the behavior of structural materials. Some of the papers, which have appeared in the literature during recent years, treating this subject are listed in the bibliography which is included at the end of this manuscript. For a more complete bibliography see the lists of references included in Refs. 115 and 116.

A large proportion of the studies involving a high rate of strain have been made in impact testing machines and, in some cases, the energy absorbed was the only property which could be measured. In impact tests the effect of reduced temperature is particularly important and for many metals it is possible to determine critical temperatures above which the fracture is ductile and energy absorption great and below which fracture is brittle and energy absorption low. Charpy notched-bar bending impact tests are easy to perform and have therefore been used frequently but the complexities involved in interpreting the meaning of this type test subtract from its worth.

In tension impact tests it is readily possible to obtain elongation and reduction of area to fracture in addition to energy, although it is not easy by mechanical methods of measurement to obtain data for complete stress-strain

Contrails

curves from impact tests. Recently, some investigators (74) have been able, by means of oscillographic recordings, to study the load-time and load-strain relationships in high speed tests.

Frequently the results from tension impact tests are compared with the ordinary static tensile properties to determine the influence of rate of strain at room temperature. For elevated temperatures most experiments have been of the long-time creep type test with constant load. A limited number of tests have been made in ordinary tensile testing machines at elevated temperatures and at rates of strain attained within the standard machine speeds (30).

Since there is a certain correspondence between the effects of time and temperature (84), theories have been developed (3, 48, 67, 112) to express the flow stress (usually defined as the "true" tensile stress) as a function of time or strain-rate, and the temperature, strain and certain other factors. In order to combine the time and temperature effects, such relations have been manipulated to provide expressions of strain-rate in terms of an equivalent temperature (70, 71) and temperature in terms of an equivalent strain-rate (46, 112). Most of the data in the literature which is applicable to test these relationships are from creep type tests but they are generally expected to be valid also when applied to data obtained by more rapid loading.

Because in the majority of applications materials are subjected to biaxial or triaxial states of stress (28, 69), considerable attention has been devoted to developing means of translating data obtained under one state of stress into terms which correspond with data for the same material under a different state of stress.

In addition to comparing ordinary tension and torsion tests to study the biaxial case (28, 63, 90, 100, 114), some investigators have subjected tubular specimens to combinations of tension and torsion or internal pressure to set up other desired ratios of two principle stresses (25, 47, 53, 78, 86, 104). Graphs have been plotted of true stresses and strains in terms of their so-called

Contrails

effective, generalized or significant values; in many cases, where anisotropy of the material was not significant (44, 114), general agreement between the flow curves for different states of stress has been reported. These generalized expressions are based on stress and strain invariants or the distortion energy principles.

A very limited number of studies of these parameters has been reported (92, 93) in which samples were tested in compression and a few in torsion (6, 38, 52, 63, 90). Of these, Itahara's (52) work covers the widest range of variables including torsion tests of many materials, temperatures up to nearly 1200F, and strain-rates covering five orders of magnitude.

b. Ferrous Metals: In iron and steel, temperature and strain rate probably have their most pronounced effect on the heterogeneous yielding and associated phenomena. Heterogeneous yielding, the upper and lower yield points, (32, 65, 90, 111) time delay before plastic yielding (12), yield point strain (111), blue brittleness (9, 27, 52, 71, 72, 85) and Lüders lines (42, 110) have been observed to be sensitive to time and temperature effects.

For the range of variables usually studied, investigators (4, 16, 22, 35, 39, 49, 52, 55, 73, 74, 81, 83, 98, 105) have generally found that the tensile strength, yield point and the strain during yielding increase with an increase in rate of strain or a decrease in temperature. For elevated temperatures, strength usually decreases after the blue brittleness range is exceeded.

Although lowering the temperature is usually considered to have an embrittling effect, the opposite is frequently the case when evaluated in terms of elongation and reduction of area (4, 30) however these measurements are often erratic (11, 110). Increase in strain-rate has also been found to reduce elongation and reduction of area (9, 55) for some ranges of speed but may have the opposite effect or none for other ranges (13, 88, 107).

The blue brittleness temperature has been observed to be elevated for

higher rates of strain according to results of tests in torsion (52), tension (85), hardness (62), crushing (93), and bending (37).

c. Aluminum Alloys: A survey of the literature on low temperature properties of aluminum alloys (4) shows general agreement concerning an increase in strength with decrease in temperature. Elongations reported for low temperature tests were generally either as great or greater than those observed at room temperature. Values of reduction of area were reported less frequently but did not necessarily increase with increased elongation. Breaking energy in impact tests usually increased as temperature was reduced. Retention of ductility at low temperatures was attributed to the face centered cubic lattice structure.

Strength of aluminum and its alloys decreases as the temperature is raised above room temperature (85, 89, 92). The decrease is quite sharp above 400F, and at 600F the strength is very low. Ductility on the other hand has been found to increase with temperature and radical increases in elongation have been reported above 400F (89).

Roberts and Heimerl (92) report a hump in the yield strength vs. temperature curve for compression with a slight increase near 400F. The yield strength of 24S-T, although lower than for 75S-T at room temperature, was higher for temperatures of 400F and above.

In general, some increase in tensile and yield strengths have been observed with increase in rate of straining (10, 13, 26, 85). In some instances (9, 60, 107), very little increase or even a decrease in strength was observed for certain speeds of testing. Ductility and energy absorption have also shown increases with rate of strain (9, 13, 88, 89, 107) although in a few cases only a negligible change or a reverse trend has been reported (10, 26).

d. Magnesium Alloys: Only a relatively few papers have reported studies of the effects of strain-rate or temperature on properties of magnesium alloys. Clark and Wood (13) report increases of from 10 to 50 per cent in tensile

Contrails

strength, elongation and energy absorption in dynamic tests as compared to static values for four magnesium alloys. According to tests by Piper (89) the tensile strength and yield strength of FS-1 magnesium alloy decrease and elongation increases with increase in temperature.

e. Titanium: Even commercially pure titanium contains sufficient quantities of other elements such as carbon, oxygen, nitrogen and hydrogen to produce mechanical properties differing sharply from the really pure metal. Strength is higher and ductility less in the commercially pure product than in the pure metal (124). Although still only in the early stages of development, titanium has received widespread publicity and attention. Only a few selected references are included in the bibliography. For a more complete bibliography on titanium see references 1, 18, 120 and 122.

Titanium in its various commercially pure forms and early alloys has received particular attention in the moderately elevated temperature ranges. Because it is light in weight and yet maintains considerable strength up to 1000F it offers considerable promise in replacing the other light metals in aircraft elements in which operating temperatures exceed room temperature. It has been shown (33, 117 etc) that the strength and hardness of titanium decrease considerably with increase in temperature in the entire useful range, and ductility and energy absorption in notched bar tests increase with increasing temperature. There is some reduction in stiffness as measured by the modulus of elasticity for higher temperatures and an increase at low temperatures.

Graphs of tensile properties versus temperature (43, 108, 120, 123, 124) show that the static tensile strength of commercially pure titanium at 1000F is about 20-30,000 psi (120, 123, 124) and for some of the alloys, 70,000 psi (123). At 400F where the strength of aluminum is essentially lost, the tensile strength of commercially pure titanium is about two-thirds of its room temperature value and this ratio is considerably higher for the alloys of titanium.

Contrails

Exposure to elevated temperatures up to 1000F for periods up to 1000 hours has no effect on the tensile properties determined at the exposure temperature (123).

All forms of titanium respond readily to cold work and tensile strengths well above 200,000 psi are regularly obtained in this manner (124). Cold working is most effective in providing increased strength for operation in the lower elevated temperature ranges because even though the annealing temperature is usually considered to be from 1200F to 1300F (23) considerable recrystallization and softening take place at 1000F (64) and the strength at 1000F is no greater for coldworked titanium than for the same alloy in the annealed condition. To achieve corresponding strengths there is more sacrifice of ductility in work hardening than in alloying. By these two methods higher room temperature strength-weight ratios can be obtained with titanium than with any other metal.

The effect of strain rate on mechanical properties of titanium is not well known. Some creep and stress rupture data are available and some impact tests have been made.

Anisotropy in both bar (29) and sheet forms (119) currently produced will make correlation between properties determined with different states of stress less consistent than for other metals.

The ordinary stress-strain tests of titanium reported in the most of the literature appear to show no sharp yield point although the possibility of strain-aging is indicated by several associated phenomena. Fontana (29) reports a yield point by drop of the beam in two titanium alloys and also reports S-N curves with sharp knees; Everhart (23) presents a strength vs. temperature curve with a hump around 800-900F. Elements such as oxygen, nitrogen and carbon are present in commercially available titanium and the presence of these elements is thought to be related to the sharp yield point and to the sharp knee commonly found in S-N diagrams for mild steel.

II. EXPERIMENTAL PROGRAM

5. Description of Testing Equipment.

a. Mechanical Features of the Torsion Testing Machine: The torsion testing machine shown in Fig. 1 is the mechanical apparatus for applying a twisting moment or pure torsional load to one end of a test specimen while holding the other end of the specimen fixed. A weighbar is utilized to measure the torque or twisting moment at any instant during the test. The right end of the specimen is clamped firmly in the torque weighbar. The right end of the weighbar is held rigidly to a supporting fixture. A loading arm A is attached to the left end of the specimen. The left face of this loading arm clears the face of the flywheel W by about $3/8$ " in the normal position. Two pins P extend out from the face of the flywheel to engage the loading arm or can be retracted to clear the loading arm as the flywheel rotates. The specimen and weighbar are aligned so that their centerlines coincide with the axis of rotation of the flywheel.

The rate of strain in the specimen is controlled by the speed of the flywheel. A half-horsepower electric motor M_1 drives the flywheel through a series of gear reducers labeled R_1 , R_2 , and R_3 in Fig. 1. The apparatus as illustrated in Fig. 1 is set up to obtain the slowest of the four testing speeds used in this research and referred to as "first speed". With this arrangement R_1 and R_2 each provide a 50 to 1 reduction in speed, and R_3 reduces the speed by a ratio of $67\frac{1}{2}$ to 1. The three in series provide a reduction of 168,750 to 1 or roughly from 1750 rpm speed of the motor to 0.01 rpm of the flywheel.

The next faster speed (second speed, 0.52 rpm flywheel speed) is obtained by removing reducer R_1 from the system and moving the motor up to drive reducer R_2 directly. For the third speed (26 rpm), R_2 also is removed, and reducer R_3 is driven directly by the motor. Thus a flywheel speed of 26 rpm is

Contrails

produced in third speed tests.

For the highest rate (fourth speed), the reducer R_3 and the coupling C are also removed, and an auxiliary motor M_2 is employed to accelerate the flywheel. The flywheel is driven through a friction pulley on the motor; the connection is maintained manually and is disconnected when the flywheel reaches a speed slightly above the test speed. The flywheel is then allowed to rotate freely until bearing friction and air resistance gradually reduce its speed to the desired rate (1300 rpm in these tests). At this time a latch is tripped by solenoid S in Fig. 1, allowing the pins P to jump out. When extended, the flywheel pins engage the loading arm attached to the specimen and apply a sudden torsional load of high strain-rate to the specimen.

In these high strain-rate tests, the speed of the flywheel shaft is measured by matching the frequency of a signal generated by a magnetic pickup with the known frequency output of an audio-oscillator ("O" in Fig. 1). The magnetic field of the pickup is varied by special depressions machined in the face of a circular steel plate mounted in place of coupling C on the end of the flywheel shaft. This pickup generates six approximately sinusoidal impulses per revolution of the flywheel. This signal, fed into the horizontal sweep of a cathode ray oscilloscope is matched with a signal of known frequency from the audio-oscillator fed into the vertical sweep. The desired speed is indicated by formation of an elliptical Lissajous figure on the screen of the oscilloscope.

Specimens of the present design tested at 1300 rpm absorb energy at rates up to 11 horsepower, which exceeds the capacity of the driving motor (M_1) used. In the mechanism as employed at this speed the inertia of the rapidly rotating flywheel loads the specimen. As energy is absorbed by the specimen, there results a corresponding loss in energy of the flywheel and hence a loss in speed. For the 75S-T aluminum alloy at room temperature this change of strain-rate is hardly noticeable because of the relatively low capacity to absorb energy before

Contrails

fracture. For tougher materials a more pronounced drop in speed is observed. However, even for the 1018 steel tested at room temperature, this loss in speed by the very end of the test was only about 30 per cent. Though appreciable, the change in strain-rate for this extreme case is relatively small when compared with the increment of 50 to 1 in strain-rate decrease for the next slowest speed of testing.

b. Recording System: All pertinent data such as twisting moment and angle of twist were recorded by use of a 6-channel Hathaway S14-A oscillograph. This instrument is supplied with galvanometers of different frequency responses and different sensitivities which can be readily interchanged to fit the range of input signal expected. The deflection of light beams by the galvanometer mirrors represents the magnitude of the quantities to be measured by the various devices utilized. The positions of the light spots from the various galvanometers are recorded on photo-sensitive linagraph paper six inches wide moving continuously in the camera of the oscillograph. This camera handles paper in rolls of 100 ft. length.

Paper speeds from $1/8$ in. per sec. to 45 in. per sec. are available with the standard oscillograph belt and pulley combinations and, by use of special pulleys, paper speeds as low as $1/30$ in. per sec. have been obtained for the slower tests. Because of limitations of the oscillograph, it was not practical to make continuous recordings of the entire tests made at the slowest speed. Therefore, only the early (elastic) portion of each test was recorded continuously. After the yield strength had been exceeded, the oscillograph was intermittently cycled on and off at regular intervals. The two cams on the output shaft of reducer R_2 in Fig. 1 operate microswitches for remote control of the oscillograph. The circuit controlled by the right cam supplies the power to the recording lamp, and the left cam switches the paper drive motor on and off 135 times during every two revolutions of the flywheel. The cams are positioned

Contrails

so that there is a delay of about one second each time for the lamp to light up before the paper begins to move. The record for one cam cycle consists of a set of short parallel dashes recorded simultaneously for an interval of about three seconds, the position of each dash representing the measurement of one quantity. The complete record resulting from intermittent operation is composed of a series of these dashes for each quantity measured.

A summary of the instrumentation and some features of tests for each speed are listed in Table III. The interval between time marks recorded (given under Item 6) is varied to suit the conditions of the total time required at a given speed and by the speed of the recording paper. Markings at every tenth second and hundredth second (for third and fourth speeds respectively) are provided by a synchronous time marking attachment built into the oscillograph. To obtain slower frequencies, a device employing a synchronous electric clock motor was built to provide a signal every five seconds for use with first and second speed tests (the two slowest strain-rates).

It should be noted in connection with Table III that the signals from the photoelectric cell, the G-beam and weigh-bar bridge circuits described in the following paragraphs are amplified before being transmitted to the galvanometer in the oscillograph.

c. Torque Measuring Device: The twisting moment or torque at any instant is measured by four electric resistance type strain gages mounted on the outside surface of a hollow cylindrical steel weigh-bar in series with the specimen (Fig. 3). The gages are connected in the form of a four-arm bridge used with a Hathaway Strain Gage Control Unit type MRC-16 with amplifier elements of type MRC-15C. The amplified output signal passes through one of the galvanometers of the oscillograph for recording.

To protect the gages from excessive heat during elevated temperature tests, the portion of the weighbar outside the furnace is hollow and tap water flows

Contrails

under the region where the gages are mounted and out through a brass tube connected to the drain as shown by the arrows in Fig. 3.

In order to interpret quantitatively the magnitude of the torque from the deflection of the trace on the record, a calibration is necessary. After some tests, the signal from the bridge is recorded when a twisting moment of known magnitude is applied to the weigh-bar by means of dead weights. This can be used to determine a calibration factor for the particular record with which it is made. However for different amplifier settings, the factor would be different so it is advisable to have a calibration for each test. The dead weight method is not a convenient one, so a controlled unbalance of the bridge is produced by shorting a precision resistor across one arm of the bridge. The resistive unbalance thus produced corresponds to that produced by a definite amount of torque, the magnitude of which can be determined by comparison with a dead weight calibration. It is very simple to apply a resistor calibration at the end of each test either by hand or automatically.

d. Twist Measuring Devices: Because of the wide range of speeds involved in these tests it was necessary to develop two different twist measuring instruments, each adapted to measure the angle of twist for a limited range of speeds. The devices used are described separately in the following paragraphs.

Rapid Tests: For measuring the angle of twist in the tests conducted at the highest strain-rate (fourth speed), the pickup device (see Fig. 4) employs two thin disks of photographic film on which are reproduced photographically alternate opaque and transparent sectors. These disks are individually fastened to the specimen at points one inch apart by means of small tubular aluminum pieces and set screws. Light projected from a bright incandescent source is transmitted through the disks to a photoelectric cell by means of lucite rods and a mirror (Fig. 4). The disks act as a set of multiple shutters to control the light transmitted to the photocell. The angular displacement of one disk

Contrails

with respect to the other corresponds with the angle of twist within the one-inch gage length. The intensity of the light transmitted through the disks varies as one disk turns with respect to the other. For disks with 2° sectors, one sinusoidally varying cycle of light intensity is completed every 4° of twist within the gage length. The varying intensity of light striking the photoelectric cell causes a corresponding variation in output electrical signal of the photo-cell circuit which, after being amplified, is transmitted to a galvanometer in the oscillograph for recording.

Because of its light weight and low moment of inertia with respect to the axis of twist, this type of pickup device can be used effectively for tests involving twisting applied suddenly at high strain-rates. It will continue measuring the twist until the specimen breaks, even for specimens of ductile metals which twist through several complete revolutions before fracture. However this device is not as sensitive as might be desired in the elastic range and therefore is not used in slower speed tests where inertia effects are not encountered.

Lower Speed Tests: The angle of twist is measured in two ways simultaneously by the device shown in Fig. 5. The angle of twist for large strains is measured by one component making use of a slide wire and rider. The other component which is sensitive to small strains, uses two electric resistance type strain gages mounted on opposite sides of a small aluminum beam. The beam has the form of a 300° circular arc. The combined indicator is mounted on two short pieces of aluminum tubing which are clamped to the specimen by means of three pointed set screws threaded through each ring. Number 28 chromel wire with a resistance of 4.1 ohms per foot extends as one continuous wire around the periphery of a 2-in. diameter lucite disk mounted on the right ring. The circumference of the slide wire is divided into four equal lengths by soldered connections to larger copper wires (see Fig. 6). Junctions separated

Contrails

by 180° on the circumference are at the same electric potential.

From the circuit diagram shown in Fig. 6, it can be seen that as the rider (which is attached to the left mounting ring) moves around the circumference of the disk, the potential output to the galvanometer varies gradually from a maximum at points A and A' to a minimum at points B and B'. The values of resistance and voltage in the circuit have been proportioned to give a linear response in deflection of the galvanometer trace on the paper with respect to the angle of twist. For a constant rate of twist and constant paper speed in the recording oscillograph, the resulting twist record consists of straight lines forming a sawtooth-shaped contour.

The electric strain gages mounted on the "C" shaped beam form two arms of a bridge which provides sensitive measurements of twist during the initial (elastic) portion of the test. A screw with a knurled head is threaded through a small block at the end of the riding arm attached to the left mounting ring. One end of the C-beam is fastened to the lucite disk, and the beam is oriented so that the point of the screw on the rider contacts the C-beam near the free end. Before a test, the screw is turned up to deflect the beam about one-fourth inch. As the specimen is twisted, the rider and screw gradually release the initial deflection of the spring. The signal from the strain gage bridge thus produces a deflection of the trace on the recording paper which is proportional to the angle of twist. After an optional angle of twist of up to about 15° , the initial deflection is completely released and the screw moves away from contact with the C-beam. The beam is pivoted so that it drops down to clear the rider and screw on subsequent revolutions. For calibration purposes, a resistor is shorted across one arm of the strain gage bridge. The resulting signal produced corresponds to a definite angle of twist carefully determined from previous calibrations.

The combined data from these two components provide twist measurements

Contrails

with the accuracy and range required for both the elastic and plastic deformation.

Elevated temperatures: There was no simple means of making twist measurements over the one-inch gage length inside the furnace for elevated temperature tests. Therefore it was necessary to depend on measurements of the over-all twist which could be made from outside the furnace. Since all bars, shafts, connections, etc. in the system were very stiff compared to the stiffness of the specimen, the angular rotation of the flywheel shaft could, for practical purposes, be considered to be taken up entirely in twist within the 1-15/16" reduced length between the shoulders of the specimen. For room temperature tests, both "flywheel twist" and gage length twist were recorded and from these measurements a constant determined for the ratio of the total (flywheel) twist to the twist within the gage length. Since specimens were geometrically identical and the temperature was known to be uniform along the entire reduced length of the specimen, it was assumed that this constant was the same at all temperatures. Gage length twist for elevated temperatures was computed by dividing the flywheel twist by this twist ratio.

For third and fourth speeds, the flywheel position was recorded from the output signal from a small magnetic pickup and a gear on the flywheel shaft. As each gear tooth passed by the magnetic pickup, it disturbed the magnetic field setting up a current which produced a deflection of the mirror in one of the galvanometers in the oscillograph. The cyclic trace recorded had one cycle for each tooth that passed the pickup.

For the two slowest tests (at first and second speeds) the position of the flywheel or over-all twist was indicated by an impulse produced by a cam on the output shaft of reducer R_2 shown in Fig. 1. One impulse was recorded for each 5.33° rotation of the flywheel.

e. Sequence Control System: The time required to break the specimen in the tests at the highest strain-rates is quite short; for example, the total time required to fracture specimens of 75S-T aluminum at room temperature at the

WADC TR 53-10

Contrails

two highest strain-rates is approximately 0.02 and 1.0 seconds, respectively. In order to record intelligible data in these short time intervals, a high speed of the oscillograph paper is necessary. A velocity of 45 inches per second is the maximum which can be readily obtained with the oscillograph used. In order to avoid using, say thirty or forty feet of paper per test of which a length of only a few inches contains the entire useful record, a rather intricate sequence switching system was developed. The control motor and attached switches are shown in Fig. 7.

The cam shaft C is driven by the small motor A through the gear reducer B. There are three cams mounted on the shaft C, the angular position of each can be set independently. The motor A (and the whole test sequence) is started by pushing the reset button on micro-switch E. After one revolution of the cam shaft, the motor is switched off automatically when the plunger D, operated by the cam nearest the motor, depresses the pin on the face of the microswitch E.

During this one revolution, the cam at the outer end of the shaft operates the multiple pole switch F which controls or actuates three circuits whose functions are:

- 1) to actuate a solenoid to release the brake on the oscillograph paper drive;
- 2) to turn on the motor to drive the recording paper;
- 3) to turn up the brilliancy of the oscillograph lamp for recording.

This outer cam is adjustable so that the length of time the recording paper is to run can be set in advance. At the end of this time, the paper drive motor is automatically turned off, the brake applied, and the recording lamp dimmed.

The test is initiated when two pins in the rotating flywheel are released to jump out and engage the loading arm that is attached to the end of the specimen. These pins are released by a trigger actuated by a solenoid in a circuit

Controls

closed by the middle cam on the control mechanism shaft (Fig. 7). By adjusting the angular position of this cam relative to the outer cam, the proper time delay can be preset to allow the oscillograph paper to get up to speed before the pins are tripped to start twisting the specimen.

For the third speed tests (when the total test time is several seconds) the cams are oriented to stop the control motor with the outer cam in position to leave the oscillograph and paper running. A second multiple switch, operating automatically when the specimen breaks, opens the circuits to stop the oscillograph and paper drive. This switch is not shown in Fig. 7.

This automatic sequence control system was used only for third and fourth speeds. For the slower speed tests, time intervals involved were long enough that manual control was satisfactory.

f. Furnace and Controls: An electric furnace was employed to provide the ambient temperatures required for elevated temperature tests. It was designed to provide a minimum of variation in temperature along the length of the specimen. A photograph of this furnace and control panel is shown in Fig. 10. A diagrammatic sketch of the furnace showing pertinent dimensions is given in Fig. 8. The heating coils are wound with platinum wire and the power to the four elements A, B_L, B_R and C can be controlled individually.

Extra length for insulation was allowed at the right end of the furnace to compensate for extra heat losses in the weigh-bar due to water cooling. However, it was necessary to control the proportion of heat input to the different zones of the furnace to obtain optimum uniformity of heating along the length of the specimen. Experiments were made with several different circuits for connecting the heating elements. The circuit illustrated in Fig. 9 proved to be best fitted to the requirements. It is simple, utilizing only one controller, yet flexible enough for easy adjustment to compensate for different conditions encountered at the different temperatures. The controller employed

Contrails

was a Wheelco Capacitrol (Model 292) of the on-off type. The notation in Fig. 9 is as follows:

- P_G - green pilot light
- P_R - red pilot light
- R_1 - heater type resistor, allows a limited continuous current
- V_0 - Voltmeter
- A_m - Ammeter
- R_2 - variable resistance, allowing a portion of the current to by-pass coil A.
- A, B, L, R, C - heating coils. (A, at the loading arm side; C, nearest the weighbar)

The setting of the variac determines the current during the "on" period of the heating cycle and the value of R_1 determines the current during the "off" period. The value of R_2 is adjusted so that the temperature is the same at the two ends of the specimen.

In experiments to check the uniformity of the temperature in the furnace, chromel-alumel thermocouples were peened into the surface of a dummy specimen. By using five such couples, the temperatures were measured at the following five locations along the length of the specimen: at the center, at points 1/2 inch to either side of the center (i.e., at the ends of a one-inch gage length), and at points at the base of the end fillets. It was discovered that for higher temperatures, a larger proportion of the current was required by coil A to keep the left end of the specimen at the same temperature as the right end.

Using settings determined in the experiments described above, uniformity of temperature along the entire reduced length of the specimen is maintained within about two degrees Fahrenheit for lower temperatures and within ten degrees at the highest temperatures (1200F) required in this program.

6. Interpretation of Oscillograph Records.

Two typical oscillograph records obtained in room temperature torsion tests are shown in Figs. 11 and 12. The traces representing each quantity recorded are labeled and some of the measurements made from the record are illustrated. Fig. 13 shows the curves for twisting moment vs. angle of twist plotted from measurements obtained from the record in Fig. 11. A set of sample calculations have been included as Table IV to illustrate how each physical quantity is computed from the data read from the oscillograph records.

For elevated temperature tests, the quantities recorded are the same except there are no direct twist measurements for the one-inch gage length. Since ductility is generally substantially greater at some of the elevated temperatures, longer records resulted and in some cases paper speeds were reduced somewhat to prevent them from being unreasonably long.

III. RESULTS OF EXPERIMENTS

7. Presentation of the Data.

Although this study was primarily in torsion, ordinary room-temperature static tensile tests were conducted to provide a means of establishing the general material properties in terms of the more standardized type tests. The tensile tests were performed by employing an Amsler testing machine of the hydraulic type. The tensile properties as determined by tests of three specimens of each material are given in Table II. Sample stress-strain curves for each metal are given in Figs. 14 and 15. Fig. 15 shows the ordinary stress-strain curves and Fig. 14 the "true" stress-strain curves according to the following definitions:

$$\sigma = \frac{P}{A_0} = \text{ordinary stress}$$

P = load

$$\epsilon = \frac{l - l_0}{l_0} = \text{ordinary strain}$$

A_0 = area before loading

$$\sigma_t = \frac{P}{A} = \text{"true stress"}$$

A = actual (minimum) area

l_0 = original gage length

$$\epsilon_t = \ln \frac{A_0}{A} = \text{"true strain"}$$

l = actual length

A pronounced yield point was observed in tensile tests of both steels and both titanium alloys tested whereas a smooth stress-strain curve was obtained for the magnesium and aluminum alloys (Fig. 15).

The accuracies of the values of the torsional properties reported here are governed by the instruments and methods used to record and interpret the data. Torque values depend on the faithfulness of the pickup and amplifier circuits, on the accuracy of calibration and on the precision with which values are scaled from the records. Large angles of twist in the gage length can be measured at room temperature with an accuracy of about 1 or 2 degrees, but at elevated temperatures the error may be somewhat greater if the rela-

Contrails

tive distribution of strain along the length of the specimen changes with temperature. The per cent error in measurements of small angles of twist was somewhat higher depending on the rate of travel of the recording paper as compared to the rate of strain. In general the values determined represent the property exhibited in the sample with an error of no more than six per cent. In a few instances there was reason to believe the error may have been somewhat larger than six per cent, but in most cases it was substantially smaller.

The torsional properties determined in this investigation are discussed briefly in the following sections.

a. Explanation of the Torsional Properties Reported.— In determination of the properties for torsion the strain at a given section is assumed to vary in direct proportion to the radial distance from the central axis; all computations for stress and strain apply to the material at the extreme fiber or periphery of the test section. As illustrated in the Sample Calculations, Table IV, the properties reported in terms of stress units (psi) are all computed according to the elastic relation $\tau = T/(J/c)$, where: τ = strength property (proportional limit, yield point, etc.) in psi.; T = Torque (or twisting moment) in lb-in.; J/c = section modulus of minimum section of specimen in in^3 .

In cases where the contour of the torque-twist curve was smooth during the initiation of inelastic deformation the "yield strength" was determined from the torque corresponding to an offset of 0.2 per cent shearing strain (or approximately 0.92° twist in the T vs. θ diagram).

The upper and lower "yield points" were determined for tests in which the observed torque on the test specimen dropped suddenly at the beginning of yielding and then increased again as twisting progressed further. The values of yield points recorded are based on the torque at the maximum and minimum points in this region of the torque-time record.

Contrails

The modulus of rupture by definition is calculated from the same equation by using for T the maximum resisting torque developed during the test.

The shearing strain γ was computed from the angle of twist θ' in radians⁺ within the gage length l and for a radius c by the relation:

$$\gamma = \frac{c\theta'}{l} \quad (1)$$

Application of this relation for determining strains for large angles of twist may be questioned (63). However it is considered to give an accuracy consistent with other assumptions on which the present calculations are based and is useful here because of its simplicity.

The values of "energy absorbed" that are tabulated represent the total energy to fracture for the one-inch gage length and not the energy per unit volume as usually reported for tension tests. Because of the strain gradient in the torsion specimens the energy absorption would be highest in the material at the circumference and less for points nearer the axis.

b. Evaluation of the Proportional limit: - Although the values of the proportional limit were determined for each specimen, they are not shown graphically or considered in the analysis since this property is so indefinite. Although it is affected by the rate of strain, it has been pointed out (103) that the proportional limit measured depends also on the type of testing machine, sensitivity of extensometer, scale to which results are plotted, the personal element in choosing the point of departure from a straight line, and the presence of small amounts of residual stress, cold work etc. Dolan and Sidebottom (19) have pointed out some of the difficulties encountered in detecting the actual point of departure from linearity

+ θ' is used to indicate the angle of twist in radians; θ without the prime is reserved in this manuscript to represent the angle of twist expressed in degrees.

when a stress gradient exists.

The proportional limits determined were based on the departure from the straight line in the curve representing torque versus angle of twist. For certain combinations of circumstances, mainly at elevated temperatures and high strain-rates, where the initial rise in torque was very rapid with respect to the speed of the paper in the camera of the oscillograph, the end of the linear range was the only point that could be accurately plotted. In such cases the proportional limit represents the end of proportionality of the torque-time relationship which coincides exactly with the proportional limit for torque vs. strain only when the strain-rates are perfectly constant.

It was observed from the original data that the scatter in proportional limit for the individual specimens for a given set of conditions was generally greater than is observed for yield strength or modulus of rupture.

c. Determination of the Modulus of Elasticity: In calculation of the modulus of elasticity or modulus of rigidity, the slope of the linear portion of the stress-strain or torque-twist curve must be determined. This calculation involves taking the ratio of an ordinate and abscissa with magnitudes of the order of the proportional limit stress and proportional limit strain respectively. The proportional limit stress is a large proportion of full deflection in the torque record and therefore can be measured with reasonable accuracy. This was not generally the case for the strain increment. For test conditions which did not develop large amounts of ductility, the proportional limit strain was only about 5 per cent of the total strain during the test; for specimens having great ductility the proportional limit strain was as small as 0.03 per cent of the total strain. It is clear that, for continuous recording, a speed of oscillograph paper that would stretch the record out sufficiently to provide reliable measurement of the proportional limit strain would be prohibitive in length to record the entire test.

Contrails

Only in first speed tests were the time intervals long enough to permit a switch from continuous recording during the elastic deformation to intermittent recording for the remainder of the test in order to stretch the length of the record for the elastic deformation but shrink the length of the record for the plastic deformation. Therefore, the first speed tests were the only ones in which any effect of elevated temperature on the elastic stiffness of the metals could be measured.

Shearing modulus of elasticity measurements were determined for room temperature tests and conformed reasonably well with generally accepted nominal values. However it is generally felt that only a limited significance should be attached to values of modulus of elasticity determined from such a short gage length (one-inch).

Because of the considerations which have been outlined above, no values for modulus of elasticity are included in this report.

d. Explanation of the Graphs: The magnitudes of the properties measured in these experiments are plotted in the graphs given in Figs. 16-59. Except where otherwise indicated, each point plotted in these figures represents the average from three or more tests. Curves are sketched in to show the average trends in the data. Since the variation of each property with the two parameters of strain-rate and temperature was studied, most of these graphs are three dimensional plots; each graph is intended to show the combined effects of the two parameters on one property of a metal. However, some two -dimensional plots are included to aid in visualizing magnitudes and to show certain individual effects more clearly. The temperature in Fahrenheit in these graphs is plotted on a uniform linear scale whereas the rate of strain is plotted to a logarithmic scale. Since the ratio of any two consecutive testing speeds was 50:1 the scale used for rate of strain is linear with respect to the speed number.

In all graphs where both solid and open circles are used, the data

Contrails

represented by the solid black circles refer to the series of tests in which specimens were heated to the temperature specified for the test and held at this temperature for one half hour before the beginning of loading. This condition is referred to as "unaged". Open circles refer to the series of tests made on specimens which were given the 200-hour aging treatment at the test temperature prior to the test. Except in special cases, mainly for aluminum, where both curves are shown, the curves sketched are intended to represent the average trend of the data for the solid points. In graphs in which only one set of symbols appears, the symbols represent the data for unaged specimens.

Fig. 35-b shows a family of curves which illustrate the effect of temperature on the yield strength of 75S-T aluminum alloy in torsion tests. Each curve shows the variation of yield strength with temperature at one given rate of strain. Subscripts for strain-rate $\dot{\gamma}$ are in accordance with the usual speed notations designated as follows:

$$\dot{\gamma}_1 = 0.0001 \text{ in./in./sec.} = \text{first speed}$$

$$\dot{\gamma}_2 = 0.005 \text{ in./in./sec.} = \text{second speed}$$

$$\dot{\gamma}_3 = 0.25 \text{ in./in./sec.} = \text{third speed}$$

$$\dot{\gamma}_4 = 12.5 \text{ in./in./sec.} = \text{fourth speed}$$

Fig. 35-a shows the same data replotted to show the variation of yield strength with rate of strain for each temperature. The data in Figs. 35-a and 35-b are combined in the three-dimensional plot in Fig. 36 and experimental values for unaged specimens are represented by the solid black dots and solid curves. The vertical planes are shaded to illustrate how the two-dimensional curves in Fig. 35 fit into the three-dimensional plot (viewed from front and left).

The open circles and broken curves superimposed on the graph in Fig. 36 show the yield strengths for specimens which were given an aging treatment of 200 hours at the test temperature before being tested.

Contrails

In Fig. 37 the modulus of rupture for the 75S-T aluminum alloy is plotted in the same manner as the yield strength in Fig. 36. Figs. 38-a and b illustrate how the variation in total shearing strain to fracture is affected by rate of strain and temperature respectively; the combined three-dimensional curves are shown in Fig. 39. Fig. 41 shows the energy absorbed to fracture for the same material and test conditions.

Similar curves are shown in Figs. 16-34 and 42-59 for the other six metals tested. In tests of SAE 1018 steel a sharp break in the torque-twist curve was observed at the yield point for certain temperatures and rates of strain (Figs. 62, 63 and 66). In these cases upper and lower "yield points" were determined. At high temperatures and slow rates of strain, however, the torque did not drop during yielding but increased continuously. In the latter cases a yield strength based on 0.2 per cent shearing strain offset was computed. The "yield strength" plotted in graphs such as Figs. 16 and 17 represents the "lower yield point" when present, or the offset yield strength for instances in which no sharp yield point was observed.

Some of the torque-twist curves for titanium also exhibited maximum and minimum points in the region of initial yielding (Figs. 64 and 65); thus, upper and lower yield points were determined as in the case of SAE 1018 steel. This phenomenon was not observed for all temperatures and strain-rates; therefore, the curves for yield strength in Figs. 47 and 48 are plotted in the same manner as described above for SAE 1018 steel.

The influence of temperature and rate of strain on the magnitude of the drop in torque at yielding is illustrated in Fig. 23 for 1018 steel and Fig. 53 for RC-70 titanium. In these figures the "Y.P. Ratio - 1" represents the decimal fraction by which the ratio of the upper yield point to the lower yield point exceeds unity. It can be seen that the maximum ratio of upper to lower yield point for RC-70 titanium occurs at different temperatures and

speeds than for the 1018 steel.

8. Discussion of Results.

Because of the wide differences observed in the behavior of the metals studied here, the experimental results for each metal are discussed separately in the following sections.

a. SAE 1018 Steel: The SAE 1018 steel was received in hot rolled round bars 5/8 in. in diameter and fulfilled the specifications set up in Spec. AN-QQ-S-646. Its specific gravity was about 7.86. The chemical analysis as furnished by the manufacturer is included in Table I. Specimens were machined from the bars in the condition as received without further heat treatment. This metal falls under the classification of mild steel and, because of the vast amount of study already devoted to this type of metal, most of the tendencies exhibited in the present study have been observed before. Unfortunately however, despite the extent of previous research, the mechanisms governing the characteristics observed have not all been determined.

Strength: The experimental results plotted in Fig. 18 show that, for temperatures of 700F and below, the strain-rate had little effect on the modulus of rupture of 1018 steel, but for 1000F there was a marked decrease in strength with decreasing speed. This latter temperature probably was sufficient to allow a substantial amount of softening or recrystallization which progressed more completely as time went on, therefore very little benefit was derived from work hardening; whereas the rate of recrystallization was too slow at temperatures below 800F to produce measurable effect before fracture.

Strength was higher for temperatures around 400F than at room temperature, as is expected for strain aging materials, and was progressively lower for temperatures above about 400F. The lowest strengths measured were for

the highest temperature and the slowest speed.

The yield strength or yield point, Fig. 17, was more sensitive than the modulus of rupture to rate of strain, since initial yielding in this type of steel is through development and propagation of Lüders bands, a highly time-dependent phenomenon. For more rapid loading or lower temperatures higher elastic strengths resulted.

The yield point ratio, defined here as the ratio of upper and lower values of torque in cases where yielding was accompanied by a sudden drop in the torque, showed considerable sensitivity to both temperature and time (Fig. 23). It is well known that the upper yield point (and hence the ratio) is also affected by factors other than speed and temperature. In tension tests the magnitude of the upper yield point depends on the machine used, a "hard" or stiff machine giving higher values than a "soft" machine which tends to iron out the jog in the force-deformation curve. The occurrence of an upper yield point depends on the geometry of the specimen, the surface finish, etc. A more complete discussion and review of the literature on the yield point phenomenon is given in Ref. 66.

The yield point is generally considered to be related to strain aging and is associated with the presence of carbon and nitrogen in the steel. The detailed mechanism which results in the observation of a yield point is, however, not clear. One explanation based on the theory of dislocations (14) attributes the sudden yielding to the tearing free of dislocations from "atmospheres" of solute carbon and/or nitrogen atoms, leaving the dislocations mobile and able to produce rapid flow under smaller forces. The force required to release a dislocation from its atmosphere is less at higher temperatures due to the added thermal energy present.

Ductility: Ductility of 1018 steel as measured by the total shearing strain was found in general to increase with higher temperature and longer

Contrails

time (slower rates of loading) except as modified by the blue-brittleness effect at intermediate temperatures. These trends are illustrated in Figs. 19 and 20.

Blue-brittleness shows up as a lowering of ductility for moderately elevated temperatures which would otherwise be expected to increase ductility. This usually occurs over a fairly wide temperature band so that the minimum point for one set of data might be chosen anywhere within a range of a hundred or more degrees. An increase in strength frequently accompanies the loss in ductility in this temperature range but not always to the same degree. The maximum strength is usually observed at a temperature slightly different from the minimum ductility.

Blue-brittleness is considered to be the result of strain aging (27, 64, 59) and the temperature at which it occurs is a function of the rate of straining. Fig. 60 shows the temperature for minimum ductility plotted versus rate of strain for data scaled from the curves in Fig. 19. For the sake of comparison, a few data from the literature are also plotted in Fig. 60. Data from all three sources fall within the same general scatter-band represented by the dashed lines. The general trend of this scatter-band can be expressed mathematically in the form

$$A = \dot{\gamma} e^{B/T_R} \quad (2)$$

or

$$T_R = \frac{B}{C - \ln \dot{\gamma}} \quad (3)$$

where A, B and C are constants, $\dot{\gamma}$ the shearing strain-rate and T_R the absolute temperature in Rankine units. Evaluating the constants for the solid average line in Fig. 60 we find $A = 1.77 \times 10^{12}$, $B = 3.25 \times 10^4$, $C = \ln A = 28.2$. Equation 3 then becomes

Contrails

$$T_R = \frac{32,500}{28.2 - \ln \dot{\gamma}} \quad (4)$$

Other investigators (27) report qualitative agreement that the blue-brittle temperature increases with rate of strain but in most cases the actual rates of strain are not reported. The scarcity of strain-rate data is probably because it is very difficult to determine reliably the rate of strain in the bending impact test or tension tests in which necking occurs. The blue-brittleness phenomenon has not been observed in non-strain-aging metals.

b. SAE 4340 Steel: - The SAE 4340 steel was received in the form of hot-rolled round bars 5/8 in. in diameter and fulfilled the specifications set up in Spec. MIL-S-5000. The specific gravity was about 7.83. The chemical analysis as furnished by the manufacturer is given in Table I. This alloy steel can be heat-treated to very high strengths but (for the purpose of comparison with the annealed titanium alloy) was quenched in oil from 1500F and tempered at 1130F to give a hardness of approximately 33 Rockwell C which corresponds with an ultimate tensile strength of about 150,000 psi. In this condition the 4340 steel exhibited a sharp yield point in tension and considerable ductility.

Strength: The experimental results illustrated in Figs. 24-26 show a rather consistent decrease in yield strength and modulus of rupture with increasing temperature and decreasing strain-rate over the entire range of both parameters. The loss in strength was somewhat more rapid at temperatures above about 700F. Strength was sustained at higher temperatures for 4340 steel than the other metals tested here.

Ductility: Fig. 28 indicates that a general increase in total strain accompanied an increase in temperature at every rate of twisting; in Fig. 27 it can be observed that the strain also increased when the strain-rate was decreased.

Contrails

Large strains were developed at 1200F, particularly for the two slower speeds. It can be seen in Fig. 28 that at 1200F and $\dot{\gamma} = 0.0001$ in./in./sec. fracture occurred with somewhat less strain than for the next faster rate.

c. 24S-T Aluminum Alloy: In the manufacturing process the 24S-T aluminum alloy was formed into round bars 11/16 in. in diameter by hot rolling and then cold drawn to the final diameter of 5/8 in. before solution heat treatment. This metal fulfilled the specifications set up in Spec. QQ-A-354. The chemical analysis as supplied by the manufacturer is given in Table I. The specific gravity of the 24S-T alloy is 2.77. This alloy was in the condition designated T4 indicating that it was not artificially aged by the manufacturer but had been given a solution heat-treatment. The recommended treatment for increased strength of this alloy includes cold working followed by a precipitation heat-treatment at 375F. In the T4 condition natural aging is known to occur at room temperature and further aging will take place at moderately elevated temperatures.

The properties of the aluminum alloys at normal and elevated temperatures are influenced to such a large extent by precipitation aging after solution heat-treatment that a brief and simplified discussion of this phenomenon is presented here and used as a basis for explaining some of the results observed in experiments.

Precipitation: In several aluminum alloys in which the principal alloying constituent shows a marked increase in solubility at elevated temperatures, heat-treatment affords a means for additional improvement in strength. The commonly accepted explanation for the mechanism through which this strengthening or hardening is achieved seems to be in accord with the behavior observed here.

When the metal is heated to a temperature of about 900F the alloying constituents go into solution and diffuse throughout the matrix providing a

Contrails

nearly homogeneous solid solution. Upon rapid cooling or quenching the hardening elements are not allowed sufficient time to precipitate from solid solution in accordance with their reduced solubility at the lower temperature but remain in supersaturated solution. As time passes however these constituents gradually precipitate out at a rate which shows marked increase at temperatures slightly above room temperature. These tiny particles are evenly distributed throughout the matrix when they form and tend to inhibit slip, thus reducing ductility and increasing strength and hardness. By a limited increase in time or temperature in the proper combination, the number and size of these precipitated particles (and the hardness) are increased. However with further increase in time or temperature the particles begin to coalesce into larger particles which are not as effective as the smaller, more dispersed particles, in hardening the metal. This progressive precipitation and initial coalescence which results in hardening is often referred to as aging, and when allowed to proceed to excess, is called overaging.

Strength: The yield strength of 24S-T aluminum alloy was slightly increased at elevated temperatures up to about 400F as compared to room temperature values for all speeds of testing as shown in Figs. 30 and 31. This is evidence that aging occurred during heating and during the half hour at the test temperature before the torque was applied. The differences in the duration of the tests at the various speeds was not sufficient to influence appreciably the aging effect observed. At 400F more precipitation undoubtedly took place than at 200F but it was offset by the normal weakening effect of this increased temperature; approximately the same strength resulted at both 200F and 400F.

At 600F a marked decrease in yield strength was observed. This was the result of the ordinary softening effect which occurs at elevated temperatures, and possibly combined with a limited amount of over-aging. Only at

the highest temperature (600F) did the increase in strain-rate appreciably increase the yield strength of 24S-T aluminum. In room temperature tests, a larger increase in yield strength was observed at fourth speed than would be expected. Careful re-examination of the oscillograph records indicates that this increase may be partly attributed to interpretation of the record. If it had been possible to obtain higher rates of travel of the record paper a slightly earlier departure from linearity would have been revealed in this instance. At slower rates of deformation both the elastic and maximum strengths were lowered. There was more time at slower strain-rates for flow of the grain boundary material etc.

As the temperature was raised, the modulus of rupture (Fig. 32) began to decrease at about 200F. This was a lower temperature than that at which the yield strength began to diminish. Probably recrystallization and other softening tendencies progressed during the plastic portion of the tests at temperatures above 200F to an extent that prevented the full increase of strength from strain-hardening which occurred at lower temperatures.

Ductility: As shown in Fig. 33 there was no general increase in the total strain to fracture in 24S-T specimens as the temperature was increased up to about 500F. Any aging which tends to maintain the strength at elevated temperatures also tends to prevent an increase in ductility. Hence the observed variations in strength and ductility were consistent.

At 600F over-aging and recrystallization contributed to large increases in ductility at all four strain-rates. Except for a slight decrease in ductility at the highest strain-rate the rate of strain had no effects on ductility that were consistent for any two speeds of straining.

d. 75S-T Aluminum Alloy: The 75S-T aluminum alloy was received from the manufacturer in the form of round bars which had been hot rolled to 11/16 in. diameter and then cold drawn to the final diameter of 5/8 in.

Contrails

The 75S-T alloy fulfilled the specifications set up in Spec. AN-A-11. The chemical analysis as supplied by the manufacturer is given in Table I. The specific gravity of the 75S-T alloy is 2.80. This alloy was in the condition designated T6 indicating that it had been solution heat-treated and was artificially aged for 24 hours at 250F by the manufacturer.

Strength: The strength of 75S-T aluminum alloy as measured by yield strength or modulus of rupture in torsion was only slightly less at 200F than at room temperature (See Figs. 35, 36, 37). A slight strengthening effect from additional aging seems to have taken place at 200F to offset the deleterious effect of the temperature increment so that the strength was maintained almost equal to that at room temperature. This temperature is not sufficiently high to expect overaging to occur during the time intervals encountered here.

The tests at 400F were appreciably above the normal aging temperature for this alloy and therefore overaging was probably pronounced enough to add to the ordinary weakening effect of temperature, particularly for the lower rates of strain. 600F expressed in absolute units is 1060° Rankine or about two-thirds the absolute temperature of the melting point of this alloy. At this temperature the metal was quickly overaged and recrystallization or softening was rapid; it is weakened to such an extent that the strengths observed were very low. The 75S-T alloy was no longer stronger at 600F than other aluminum alloys which exhibit considerably lower strengths at room temperature.

The ratio of yield strength to modulus of rupture was highest for the highest temperature and lowest rate of strain. The maximum torque occurred at a very small per cent of the total strain for this condition. Probably a continuous recrystallization accompanied the deformation and its weakening effect progressed more rapidly than the strengthening effect due to strain

Contrails

hardening. The strain hardening capacity of the 75S-T alloy was relatively small at room temperature as shown by the small slope of the tensile true stress-strain curve illustrated in Fig. 14.

When loaded at room temperature there was no overaging. Any relaxation or creep took place slowly and there was a gradual increase in resistance to deformation as a result of work hardening so that the maximum torque was reached near the end of plastic deformation.

Ductility: For temperatures up to 400F the increase in ductility (Figs. 38 and 39 corresponded very closely with the decrease in strength. The marked increase in ductility at 600F at fourth speed over that for lower temperatures was expected to result from overaging and from recrystallization which could take place readily at this temperature as the crystals were deformed. At third speed the additional time allowed more complete recrystallization; conditions were optimum for unrestrained or maximum plastic flow. About 800 per cent shearing strain was reached in third speed tests before fracture.

However, when the rate of deformation was less than at third speed (second and first speeds) a combination of factors produced an embrittling tendency which has been observed (99) in creep and stress rupture tests where a decrease in ductility resulted from increasing the duration of the test. One possible explanation for this behavior arises from the fact that the rate effects are not the same within the grains or crystals as for the grain boundary material. It has been observed (82) that in some cases for elevated temperatures a great deal of slip and deformation of the crystal occurs at one speed and a ductile failure results, whereas at a higher speed less slip is observed and the fracture surface follows the grain boundaries. These observations are in agreement with the ductilities measured here in 600F tests of 75S-T aluminum.

e. FS-1 Magnesium Alloy: This alloy was the lightest in weight of any

Contrails

metal tested (Sp. gr. = 1.77) and lowest in tensile strength. The material was received in the form of 11/16 in. diameter round bars and was the only metal included in this study that was fabricated by the extrusion process. This alloy is sometimes designated No. AZ-31B and fulfilled the specifications set up in Spec. AN-M-27. It was not solution heat-treated or given any other heat-treatment after extrusion so that any cold work induced by the extrusion and stretching phases of the operation were not removed from the metal before the specimens were prepared. The chemical analysis as furnished by the manufacturer is given in Table I.

Strength: The torsional strength of the FS-1 magnesium alloy shown in Figs. 42-44 was very low. The linear portion of the torque-time or torque-twist curve was very short. Despite large amplification of the signal from the torque weighbar bridge, the curvature of the torque trace appeared to begin almost at zero torque, especially for elevated temperatures.

There was a general decrease in yield strength with increase in temperature for all speeds of testing (Fig. 42) although the rate of decrease was moderate. Strain-rate had a distinct influence, higher yield strengths being observed at the higher rates of deformation. The rate of loading is significant at all temperatures since pure magnesium creeps at room temperature (99).

Ductility: At room temperature the ductility was relatively low, being comparable to that of the 75S-T aluminum alloy. At higher temperatures the ductility (Fig. 45) increased, particularly at the slower rates of deformation. The deformation mechanism can be either by slip or by twinning. Because of the preferred orientations developed in the extrusion process, slip is easiest when the shearing stress is the direction of certain favorably oriented planes.

The fact that the FS-1 exhibited a continued increase in ductility and a decrease in strength as the temperature was raised may be taken as an

Contrails

indication that there was no precipitation aging or over-aging as is observed in the aluminum alloys tested here and of some other magnesium alloys. For the magnesium alloy the maximum strain of about 700 per cent occurred at 600F for the lowest strain rate (Fig. 45).

f. RC-70 Titanium: This metal was designated "commercially pure", a term which does not restrict its composition within close limits. The chemical composition as determined by the manufacturer is given in Table I. Its specific gravity is 4.5. It was received in the form of round bars 5/8 in. in diameter which were hot rolled and annealed by the manufacturer.

The relative newness of commercial availability of titanium has meant that, until recently, very little was known of its mechanical properties. Characteristics considerably different from those observed for the alloys of steel and aluminum were revealed in the current studies.

Strength: The graphs in Figs. 47-49 illustrate the sensitivity of the strength of commercially pure titanium to time and temperature effects. In general, there was a marked increase of yield strength with increase in speed of testing for all temperatures. There was a substantial decrease in yield strength with increasing temperature for all speeds of straining. However, the rate of decrease of yield strength with temperature for RC-70 was a decreasing function so that the loss of strength is less rapid with respect to increase in temperature at the higher temperatures than at the low. This is the opposite of the tendency observed for 75S-T aluminum alloy for which the loss of strength became very rapid for temperatures above 400F.

Since 570F is sufficient to provide stress relief of commercially pure titanium in an hour (123), it is logical to assume that considerable relaxation of stress and loss of strength would occur even in rapid tests at 700F or slower tests at as low as 400F.

The contour of the torque record in the region of the upper and lower

Contrails

yield points for RC-70 titanium appears to be somewhat different from that for 1018 steel. The initial portions of typical oscillograph records for tests of RC-70 for each of the test conditions are illustrated in Figs. 64 and 65. There was no sharp break to indicate that the torque decreased suddenly during yielding. For the fourth speed tests the recording paper speed was not rapid enough relative to the rate of deformation to show accurately the contour of the curve during yielding.

It has been pointed out that for 1018 steel (see Figs. 62 and 63) the drop in torque during initial yielding was sudden whenever any decrease was observed. It appears then that the yielding mechanism which has been investigated at great length for low carbon steels (but is still not clearly understood) might be somewhat different from the mechanism responsible for yielding at a reduced stress in titanium.

No drop in torque at the yield point was observed in room temperature torsion tests of RC-70 titanium at any speed. However, this phenomenon was observed in tests at elevated temperatures, particularly at the more rapid rates of strain (Figs. 64 and 65). Similarly the yield point effect in titanium alloys in tension has been observed to disappear at low temperatures (29).

Ductility: The ductility of the RC-70 titanium shown in Fig. 51 appears to be nearly the same for all temperatures and speeds except for the two slowest speed tests at 1000F. This was true for both aged and unaged specimens. Thus for the times and temperatures involved here there was no radical embrittlement due to absorption of hydrogen, oxygen or nitrogen from the air. It is generally considered that extended exposure at temperatures somewhat above 1000F is required for absorption of sufficient quantities of oxygen and nitrogen to produce drastic embrittlement (124) but some effect might have been expected at 1000F, particularly after the two-hundred hour

Contrails

exposure. Hydrogen is absorbed at temperatures above 600F but is not considered to be as serious an embrittling agent as the other two gases.

Complete removal of cold worked properties is possible by exposure to a temperature of 800F for one thousand hours (123) or more quickly at higher temperatures. Since the greatest portion of this annealing effect would take place during the first few hours or minutes it would be expected that for tests at temperatures of 1000F and involving several minutes, softening would take place continuously during the test and large values of strain might be developed before fracture. The corresponding strength would be rather low for this condition.

Ordinarily the conditions which increase strength properties of metals also tend to decrease ductility and, although there is no quantitative formulation of this relationship, qualitative correspondence is usually observed. In Figs. 48, 49, and 51 this qualitative inverse relationship between ductility and strength is not clearly obvious when comparing shearing strain in torsion with yield strength and modulus of rupture. However when the strain is plotted to a larger scale as in Fig. 50, the increases in strain can be seen to correspond with the decreases in strength. There is in general an increase in strain with increasing temperature, except for the minimum point observed for the strain at 700F for first speed.

This minimum in ductility at 700F is not considered to be the result of hydrogen embrittlement since specimens that were aged for two-hundred hours in air at 700F exhibited essentially the same ductility (compare strains in Fig. 51). Specimens tested at 1000F should have absorbed hydrogen at a more rapid rate than at 700F, but extremely large values of strain were reached before fracture at the higher temperature. Treating the six specimens (both aged and unaged) for each condition together the spread in strains measured for any one set of conditions did not appear to be large enough to suggest

that the difference in the average was purely a chance result of normal scatter.

If reduction in ductility at 700F for this slow straining speed were due primarily to absorption of hydrogen accelerated in some way by the deformation itself, then the marked increase in ductility at 1000F (when even more hydrogen would be picked up) indicates that the softening mechanism which tends to increase the ductility far outweighed the embrittling tendency of hydrogen at 1000F.

In data reported by the manufacturer (123) and others, the ductility of titanium in conventional static tension tests is not greatly effected by temperatures up to around 800F or higher. Reduction of area in tension tests has been reported to show marked increase above about 700F but elongation may be as low at 850F as at room temperature.

g. RC-130-B Titanium Alloy: This metal is a ternary alloy with nominally 4 per cent each of manganese and aluminum added. Some carbon was also present in the heat analysis (Table I) although the percentage was not as large as that in the RC-70 titanium tested. The specific gravity was 4.7. The RC-130-B was tested in the annealed condition as received; no effort was made to increase the strength by further heat-treatment or by cold rolling. Specimens were prepared from the 5/8 in. diameter hot rolled round bars that were annealed by the manufacturer.

Strength: In Figs. 54 and 55 it can be seen that the torsional yield strength of the RC-130-B titanium alloy was sensitive to both temperature and strain-rate effects. There was a continuous decrease in yield strength for every speed as the temperature was raised. The yield strength was higher at every temperature for the higher strain-rates except for some of the tests at 700F. At this temperature there was no change in yield strength apparent in the data from tests at the three lowest speeds.

Contrails

The values of modulus of rupture shown in Fig. 56 were about the same for all speeds of testing. At 1000F a sharp decline in strength was observed that was approximately inversely proportional to the logarithm of the strain-rate.

Ductility: An increase of total strain with increasing temperature is evident in Fig. 58 for all speeds. The rate of this increase in ductility was quite constant except at the highest temperature. For tests at 1000F and the slowest strain-rate an extremely high strain was observed. This strain, about 3750 per cent, was more than three times as great as that observed in RC-70 for the same conditions.

h. Effect of the Aging Heat-Treatment: Data for specimens heated to the test temperature for 200 hours in advance of the actual test appear as open circles on graphs where the data for unaged specimens are plotted by solid circles. By comparing these results the effect of the aging treatment can be determined. Since the reaction to aging was different for the different metals the discussion below has been subdivided according to metal.

75S-T Aluminum Alloy: A pronounced effect of the 200-hour aging heat-treatment on the strength of 75S-T aluminum alloy can be observed in Figs. 36 and 37 only for temperatures near 400F. Since the manufacturer's aging treatment produced precipitation for essentially optimum strength, little or no increase in strength would be expected from further aging at 200F whether for one-half hour or for 200 hours. Considerable over-aging or coalescence of the alloy particles could be expected when the material was held at 400F for 200 hours. This was evident from the reduction of yield strength and modulus of rupture after aging at 400F. One factor in the reduction of strength of unaged specimens at 400F as compared with those tested at 200F probably was the aging occurring during the half hour at temperature prior to loading. The additional time for over-aging to take place during the slower tests may contribute to the fact that at 400F the reduction in strength

WADC TR 53-10 43

Contrails

with decrease in speed of testing was more pronounced for specimens tested after a half hour at temperature than for specimens aged 200 hours.

At 600F the overaging seems to have progressed to completion within the half-hour conditioning and further aging for 200 hours did not show any significant effect on the strength at this temperature.

The ductility, like the strength, is effected by over-aging during which the coalescence of alloying elements precipitated out of solution by aging leaves these particles no longer sufficiently distributed throughout the matrix to restrict the slip. This change increases ductility as well as decreasing the strength. The effect of aging on strain (shown in Fig. 39) is therefore consistent with that observed for strength. The apparent differences between ductility for aged and unaged specimens for 600F tests are probably the result of plotting averages, each based on two or three events which are part of a widely distributed population. For example, Fig. 40 shows the strain data for each of the individual specimens of 75S-T tested at 600F. This graph illustrates the wide scatter in the points from which the averages plotted in Fig. 39 were obtained. The heavy solid curve in Fig. 40 is the curve from Fig. 39 through the average points for unaged specimens, and the broken curve is for aged specimens. The light-weight curve is sketched in to show an average trend of the data for both aged and unaged specimens. It appears likely that this is more representative of the general material behavior than the results plotted for the two small groups of specimens. The scatter in the strains measured for the individual specimens at the three lower temperatures was very much less than at 600F. Therefore it appears likely that the large apparent effect of aging on strain at 400F was real, whereas the smaller apparent effect at 600F was probably not real but due mainly to chance effects in sampling and testing.

24S-T Aluminum Alloy: The effects of the two-hundred hour aging heat-

Contrails

treatment on the strength and ductility of 24S-T aluminum alloy are illustrated in Figs. 31-33. It can be seen that there was a decrease of strength at 400F and 600F and accompanying increases in strain as compared with the specimens which were not given the 200-hour heat-treatment.

The temperature of 400F was only slightly over that for optimum strength from aging and therefore for the tests in which the specimen was at this temperature only a short time the only effect was a slight amount of beneficial aging. However, after 200 hours, over-aging had begun at 400F with a reduction of strength and ductility evident. At 600F, over-aging had no more than begun in the short time tests so that there was little if any over-aging. The increase in strain probably was due chiefly to softening and recrystallization during the test. After the 200-hour heating at 600F probably complete over-aging had occurred reducing the strength by about 50 percent and increasing the strain by a large factor. The pattern observed for the variation of strain in 24S-T aluminum alloy specimens tested at 600F in this over-aged condition was identical to that for the 75S-T aluminum alloy. For the 75S-T it was observed that over-aging was complete at 600F in both aged and unaged specimens (see Fig. 40) whereas for 24S-T the longer holding time was required for over-aging. This temperature was relatively higher above the aging temperature for 75S-T (250F) than for 24S-T (375F); therefore, over-aging was more rapid in the 75S-T. A difference could be expected because the different alloying elements employed in the two alloys would come out of the supersaturated solution at different temperatures or at different rates at a given temperature.

The peculiar loss of high-temperature ductility at the slower strain-rates did not occur in the unaged specimens of 24S-T where the coalescence of the precipitated particles was not complete. However it did occur in 24S-T when conditions were right for complete averaging (i.e. 200 hours at

600F). An explanation of this behavior on the basis of different rate effects in the crystal grains as compared with the grain boundary material was given in Section 8d. In this discussion ductility was associated with slip and a fracture through the grain itself at the one speed and loss of ductility with a decrease in speed was associated with fracture following the grain boundaries. This behavior seems consistent with the presence of accumulations of foreign (solute) atoms along the grain boundaries.

Steel: There was no reason to expect the 200-hour aging treatment to have a marked effect on the SAE 1018 steel. The only possible change might be a quench-aging resulting from air cooling after the hot-rolling operation that would be accelerated slightly by the 200-hour heating. Tempering should have eliminated the possibility of further quench-aging in the SAE 4340 steel at temperatures below the tempering temperature.

Comparisons between the aged data (open circles) and unaged data (solid circles) in Figs. 17, 18 and 20 for 1018 and Figs. 25-27 for 4340 indicate that if an aging effect were present it was too small to be distinguished from the normal scatter inherent in the experimental measurements for temperatures of 1000F and below. The differences in ordinates observed in Fig. 20 between aged and unaged specimens tested at 1000F appears to be a chance effect as in the case of 75S-T aluminum at 600F. Fig. 21 shows the points representing strain plotted for the individual specimens of 1018 steel tested at 1000F. This condition gives rise to large differences in observed strain suggesting a need for more than two or three samples to obtain a reliable mean value.

Tests of the specimens of 4340 steel aged at 1200F exhibited lower strengths and greater ductility than specimens which were at temperature only one-half hour before testing. Since the 1200F was above the temperature (1130F) at which the 4340 steel was tempered it is not surprising that the

200-hour aging treatment at this temperature did tend to soften the steel.

Apparent effects of aging on the yield point ratio observed for 1018 steel in Fig. 23 (and in Fig. 53 for titanium) also are likely to be due to chance since any deviations which occur are exaggerated by subtraction of two numbers of the same relative magnitude (Y.P. Ratio - 1). The shapes of the torque-twist diagrams in the region of initial yielding were not altered by the 200-hour heat treatments.

FS-1 Magnesium Alloy: Since this alloy was not solution heat-treated or quenched there was no possibility for precipitation or quench-aging. It was cold worked somewhat in the extrusion process but is not a strain-aging metal. The 200-hour aging treatment would not be expected to have an appreciable effect on the magnesium tested here and none was observed in Figs. 43 to 46.

Titanium: Both titanium alloys were received in the annealed condition which would eliminate the possibility of either quench-aging or strain-aging being accelerated by the 200-hour heat-treatments given here. The titanium was aged in the bar stock form before specimens were machined. Hence, any strain-aging of the outer layer that was cold worked during the machining operation could not occur during the aging treatment. It seems reasonable therefore that no significant aging effect would be expected in titanium, and none was observed in the results plotted in Figs. 48-59.

i. Energy Absorption: It will be noted by comparison of the trends which are observed for the influence of rate of strain and temperature on the modulus of rupture and the maximum strain that the energy absorbed by the specimen follows a pattern that is a combination of the trends observed in the other two properties. This follows directly because the relationship of the energy absorbed to twisting moment T and the corresponding angle of twist θ' expressed radians, is:

Contrails

$$\text{Energy in torsion} = \int_0^{\theta_1'} T d\theta' \quad (5)$$

The integral represents the area under the torque-twist curve up to the twist θ_1' . For the shapes of diagrams obtained for the ductile metals reported here the energy values were found to vary in close correspondence with the product of the maximum torque and the total angle of twist to fracture. Torque and twist are directly proportional to the modulus of rupture and the shearing strain to fracture, respectively. Discussions devoted to strength and ductility can be extended therefore to apply to the energy absorption for the same testing conditions.

The influence of temperature and strain-rate on the energy absorbed by specimens of the seven metals is illustrated in Figs. 22, 29, 34, 41, 46, 52 and 59. Comparison of the data in these figures indicates that the steels and titaniums absorbed much more energy before fracture than did the aluminum or magnesium alloys. Because any change in one or both parameters produced opposite effects on the ductility and strength of these metals any large change in one was modified by an opposite change in the other so that no conspicuously large values of energy were observed.

j. Deformation and Fracture Characteristics: One of the advantages of the torsion test over the tension test or the notched-bar impact test is that the geometry and dimensions of the specimen remain essentially unchanged during the deformation process. Specimens which are cylindrical before stressing remain cylindrical and without appreciable change in diameter or length.

In general, deformation of the specimens tested in this project did follow this pattern and fracture occurred at or near the center of the gage length as a sharp clean break in a plane perpendicular to the axis of the specimen. Just prior to fracture at the highest temperatures and slowest

Contrails

speeds there was a small contraction in area at the section where fracture was impending and there was a corresponding increase in length. Usually a small thread of material held on in these cases after the larger portion of the section had separated.

For both RC-70 and RC-130-B titanium there was evidence of non-homogeneous longitudinal layers in the material before testing or which developed during the process of deformation. Plastic deformation in torsion caused the surface of titanium specimens to warp or form ridges and valleys similar to very smooth coarse-pitch screw threads. The pitch of these "threads" was in inverse proportion to the total twist before fracture and therefore was smaller for specimens tested at the higher temperatures and lower strain-rates (see Fig. 51). Fig. 61 shows a photograph of broken specimens of RC-70 titanium as an example of this non-homogeneous deformation. The appearance of the deformed specimens of RC-130-B was the same. Specimens of all other materials remained essentially cylindrical during the deformation process.

In tension tests the cross-section of the titanium specimens became elliptical in the zone where plastic deformation was large. The major axis dimension of the ellipse at the fracture surface was about 20 per cent greater than the minor axis dimension.

k. Shape of the Torque-Twist Curves: Figs. 66 to 72 illustrate the effect of elevated temperatures on the shape of the torque-twist curves for the seven metals studied. Curves shown are for the highest strain-rate. At the slower speeds of straining less drop in torque was observed; at the yield point somewhat greater decrease in torque occurred after the maximum was reached early in the test; and there were considerable variations in strength and ductility as discussed earlier. Some further details on the shape of the curves for particular conditions are included in Section 9.

The mode of fracture progression that occurred controlled the shape of

Contrails

the final portion of the torque-twist curves. At the lower temperatures the failure was sudden and the torque dropped so rapidly the photographic paper could not record the descending trace but showed the torque immediately before fracture then zero torque immediately after fracture. At higher temperatures and slow speeds the final failure was less sudden and the records showed that the torque gradually tapered off to zero.

Continuous torque recordings (Figs. 62 and 63) for tests of SAE 1018 steel at 400F and 700F exhibited the jagged contours characteristic of the material behavior in the blue-brittle range. This recurring process of buildup and sudden drop of torque is not so clearly observed in larger specimens where an averaging tendency masks out the individual jumps. Hall (42) watched this process in thin strip specimens and could trace the advance of a Lüders band with the drop in stress followed by a buildup as soon as one band was arrested. When the stress reached a sufficiently large magnitude a new Lüders band darted through the metal, etc. This phenomenon is observed only for a limited range of combinations of temperatures and strain-rates; it is undoubtedly related to the rates of strain-aging and of slip within the crystal-structure. Portions of records from torsion tests are shown for all four strain-rates for tests at 400F and 700F in Figs. 62 and 63. The appearance of the irregularities is also influenced by the rate of travel of the paper in the camera of the oscillograph as compared with the rate of strain in the specimen. The torque scale, the time intervals and the twist increments are labeled to aid in interpreting these records.

Figs. 64 and 65 shows the initial portions of records for RC-70 titanium illustrating the yield point phenomenon observed. For several conditions the yield portion of the torque-twist curves for RC-130-B titanium was almost flat or dropped slightly. In these cases the offset yield strength differed only slightly from the lower yield point.

9. Comparative Strengths of the Seven Metals: The comparative yield strength and modulus of rupture for the seven metals in torsion at different elevated temperatures can be seen from the results plotted in Figs. 73 to 75. Data from tests at only the highest and lowest rates of strain are shown. These curves show that the strength RC-130-B titanium alloy at elevated temperatures is comparable to that on the SAE 4340 steel with some differences resulting from different strain-rate effects. These two metals stand out above the others on the basis of yield strength and modulus of rupture. RC-70 titanium ranks next for all conditions. On the basis of yield strength at slow speeds 75S-T and 24S-T aluminum alloys are comparable to the RC-70 for portions of the temperature range but the aluminum alloys are very weak at 600F or above. The yield strength of SAE 1018 steel was low at room temperature compared to the other metals but was reduced very little by elevated temperature so that it ranked more favorably with increasing temperature.

The two aluminum alloys lost strength rapidly at and above 400F but the strength of 24S-T was reduced less than the strength of 75S-T. The FS-1 magnesium alloy ranked lowest in strength at all temperatures tested.

The data in Fig. 73 are replotted in Fig. 75 in terms of the modulus of rupture divided by the specific gravity. This illustrates the relative shifts in curves when evaluated in terms of the strength-weight ratios. The RC-130-B titanium alloy apparently stands out above all others for the whole range of variables.

m. Influence of Structural Changes on Experimental Observations: In analyzing the significance of data of the type discussed in this chapter, it is common practice for engineers to plot two-dimensional curves and draw conclusions regarding the relation between two variables for conditions in which the third variable is held constant. For example, one may plot the strength (either yield strength or modulus of rupture) versus the strain-rate

Contrails

for a given fixed temperature. When this is repeated for a second (perhaps higher) temperature of testing, the general trends observed as the strain-rate is increased may be entirely contrary to those indicated by the first chart. This immediately leads the investigator to suspect errors of observation or variability of material. It is not immediately obvious why the same change in one of the variables (for example, strain-rate) may decrease the strength at one temperature yet cause an increase in strength at a higher temperature.

However, metallurgical instability and marked changes which occur in the properties of the material during a test make it impossible to draw logical conclusions from limited observations of this nature. It is believed that a study of the reasons for the hills and valleys shown on the three-dimensional surfaces of the types shown in Figs. 17, 18, 20, and the similar charts plotted for the other metals, gives a much clearer picture of the interaction of the three variables involved.

In discussing the effect of strain-rate and temperature on the strength properties of a metal, the final test data must be considered to be influenced by "time-dependent" as well as by nearly "time-independent" phenomena accompanying the structural breakdown of the material. For example, the exhibition of upper and lower yield points by metals such as low carbon steels and titanium is a process that is influenced by time (or by strain-rate) as shown by many different experimenters (11, 13, 16, 22, 30, 35, 73, 112, 128). Theories of dislocation and diffusion processes indicate that this time-dependence is markedly influenced by an alteration in temperature of testing.

We might visualize an interaction of two effects as shown diagrammatically in Fig. 101. The trend of Curve A represents for a stable material the relative strengths that may be expected as the strain-rate is increased.

Contrails

However the material may simultaneously undergo an aging phenomenon, a precipitation of hardening constituents, or some other type of diffusion process (which in the dislocation theory might be visualized as a progressive blocking of dislocations). One might represent by Curve B a second contribution to the strength caused by these time-dependent changes. That is, for the slower strain-rates, more time is available for strengthening by aging to occur; hence, curve B indicates a gradual increase in the strength as the strain-rate is decreased. If these two different phenomena contribute simultaneously to the strength of a metal, the resulting strengths observed would follow some curve such as C which represents the sum of the ordinates to Curves A and B. Curve C would then apply for only one fixed temperature, (say 80F). If the temperature of testing is increased however, the contributions to the strength by the strain-induced aging may be drastically reduced. That is, the stimulation of relaxation and recovery processes by elevated temperature will result in Curve B being depressed to a lower level such as is shown by Curve D. Thus, at an elevated temperature, the net effect of strain-rate on the strength may be represented by Curve E which exhibits somewhat different characteristics from those of Curve C for the lower temperature of testing. In Figs. 24-a, 30-a, and 35-a the data show these two types of variation for yield strength. Two-dimensional plots of the modulus of rupture vs. strain-rate also showed similar trends for several of the metals tested. It is believed that these trends are representative of the behavior of the material and are not inconsistencies in the test data.

The ductility (or total angle of twist) observed during a torsion test is also influenced by a number of these same instabilities in the structure of the metal. Deformation may occur by a number of basic processes such as follows:

Contrails

1. slip
2. twinning
3. fragmentation
4. elastic bending of crystal lamellae
5. grain boundary movements
6. transient creep and anelastic effects.

It should be pointed out that there are no fundamental data available to indicate what it is that limits the capacity of a metal for deformation or causes the onset of fracture. It has been suggested (130, 131, 132) that the primary effect of cold-working a metal is to decrease the mean size of the crystals and thereby raise the elastic strength. Wood (131) has proposed that there is a limiting crystallite size below which further deformation and fragmentation of the crystal cannot take place. However an increase in the temperature should correspondingly alter the limiting minimum stable fragmentation size because of the increased activity in place change of atoms and the greater freedom of mobility for recovery and recrystallization processes. Certainly the grain boundary movements and transient creep may be expected to increase greatly the observed deformations at elevated temperatures if sufficient time is available during the test for these effects to become pronounced. On the other hand it has been observed in long time creep tests at elevated temperatures that metallurgical changes in the material or changes in the mode of fracture sometimes result in greatly reduced ductility.

During testing, changes may occur that are dependent upon diffusion of atoms through the matrix by processes referred to by various names such as relaxation, recovery, recrystallization, aging, precipitation, etc.; these are all time-dependent and are markedly sensitive to changes in temperature. On the other hand the deformation processes of slip, twinning, elastic bending of lamellae and fragmentation are probably influenced to a much lesser

Contrails

degree by time effects and may be only mildly altered by changes in temperature. Thus in considering the ductility characteristics observed in the present tests, one must again visualize the complete interaction of temperature and strain-rate on a given metal since the relative effects observed at one temperature of testing may be entirely reversed at a different temperature of testing.

For example, in Fig. 19 the greatest ductility was developed at the highest strain-rate when strains at 400F are compared whereas when a similar comparison is made at 1000F, the greatest ductility was exhibited by the specimens tested at the lowest strain-rate. Examining the two-dimensional graphs such as Fig. 38-b, one might question the consistency of the data for 75S-T aluminum alloy at 600F. The tests conducted at the highest and lowest strain-rates exhibit roughly the same amount of ductility whereas those run at the two intermediate strain-rates show extremely high ductility. However the complete three-dimensional picture of the variation of total strain with temperature and rate of strain shown in Fig. 39 indicates that this greater ductility at the intermediate strain-rates is entirely consistent both for the material aged 200 hours at the test temperature and for that held at temperature only 1/2 hour before testing. Therefore it becomes difficult to draw general sweeping conclusions about the effect of altering either temperature or strain-rate separately without considering the interaction of both parameters.

In view of the time- and temperature-dependent instabilities and continuous change of metallurgical structure which occurs while the metal is being tested, it becomes apparent that no simple single equation of state can adequately express the effects of strain-rate and temperatures on either the strength or the ductility of a metal. If one deals only with temperatures for which the materials are entirely stable, such an equation might be developed. However, even here the very process of deformation changes

WADC TR 53-10

the crystalline structure and this break-up in crystal size and its effect on grain boundary reactions must certainly develop new instabilities such as anelastic after-effects or transient creep, which cannot be adequately expressed even for single crystals and certainly not for complex polycrystalline metals such as those commonly used for structural purposes.

9. Correlation of Strain-Rate and Temperature Effects with Mathematical Theories.

As pointed out in the previous section it appears probable that no complete and acceptable theory can be developed to express all the effects of strain-rate and temperature on the mechanical properties of structural metals. Nevertheless, it was felt desirable to investigate the usefulness of several proposed relationships in expressing mathematically the variations observed in data from these experiments. In this section the modifications necessary to adapt these equations to the torsion test are discussed, and a comparison is made between the experimental data and several mathematical functions which include parameters to express the influence of strain-rate and temperature. Some of the detailed concepts and mathematical equations are presented in Appendices II and III and only the essential final equations are discussed here.

a. Simplifications Used: Theoretical considerations for correlation of data of this type are usually intended to determine mathematical expressions relating the flow stress to the strain, rate of strain, temperature and certain material constants. The equations developed are generally stated in terms of the "true stress" in tension. For direct application to the torsion test, these expressions can be rewritten in terms of shearing stress, shearing strain, and shearing strain-rate. However, it would be more convenient in analysis of the present data to work in terms of applied torque instead of shearing stress. Arbitrary substitution of torque for stress does not seem justified since it is known that the two are not equal or even

proportional during plastic deformation.

For the plastic range, Eq. A20 of Appendix I can be used to evaluate the shearing stress at the surface of a specimen. This equation for the shearing stress τ includes a constant coefficient, $K_1 = 1/2\pi c^3$, a term involving the torque T , and a term involving another variable torque, T_0 .

$$\tau = K_1(4T - T_0) \quad (6)$$

If T_0 were negligible with respect to $4T$ or if T_0 were directly proportional to T then the substitution of a constant times T for τ would be permissible. However, in most cases T_0 is not negligible compared with T . Neither is T_0 always directly proportional to T . Nevertheless, computations have shown that for a given or constant θ (of the magnitudes examined in the three following sections), the amount by which T_0 differed from being proportional to T was small enough compared to $4T$ that valid observations for the plastic range were possible by using the following simplification⁺:

$$\tau \Big|_{\theta} = KT \quad (7)$$

In order to substantiate this reasoning the same types of plots as those shown in Figs. 76 to 98 were constructed for representative sample conditions. The curves resulting showed the same trends and scatter when values of T were plotted as when the more rigorous analysis employing values of the shearing stress τ were used.

b. Equivalent Strain-Rate Parameter: A quantitative relation between the effects of temperature and strain-rate was suggested in 1944 by Zener

+ In this notation a vertical line followed by one or two symbols will be used to indicate variables which are held constant for a given equation. In Eq. 7 the shearing stress τ is expressed as a function of the torque T for a constant angle of twist θ . Other variables such as strain-rate and temperature are not restricted in this equation.

and Hollomon (112, 113). The flow stress σ at a given strain ϵ was expressed by the function

$$\sigma \Big|_{\epsilon} = f(\dot{\epsilon} e^{Q/RT}) = f(P) \quad (8)$$

where $\dot{\epsilon}$ is the rate of strain, R is the universal gas constant, and Q is a constant depending on the material. For low temperatures Q has been measured to be about 10,000 cal. (gm. mol.)⁻¹ for several steels (46) and since R is 1.987 cal. deg.⁻¹ mol.⁻¹, the exponent becomes roughly 5000/T. The parameter P then has the value

$$P = \dot{\epsilon} e^{5000/T} \quad (9)$$

Here P is a strain-rate modified by a coefficient which is a function of temperature, or P is an "equivalent strain-rate". Using Q as 10,000 this concept was tested with the present data for SAE 1018 steel and found to give too little weight to the effect of temperature. For elevated temperatures, however, Q is probably not a constant but depends on stress and temperature as well. By trial and error selection a magnitude can be found for Q to cause the data to fall along a fairly smooth curve. Fig. 77 shows the torque corresponding to a shearing strain of 0.50 in./in. for SAE 1018 steel plotted to log scale against the parameter P based on $Q/R = 40,000$.

Since a small variation in temperature produces a larger effect than a fairly large increment of strain-rate it appears that if the combined effects are to be expressed in terms of only one parameter, this parameter should be more closely associated with temperature with an appropriate factor to account for strain-rate effects. One attempt to develop such a parameter is discussed in Appendix III and in Section 9-d.

c. General Equation for Flow: The general expression for flow stress as a function of strain, strain-rate and temperature proposed by Hollomon and Lubahn, (Eq. B4 in Appendix II) is:

Contrails

$$\sigma = C_0^{T_R} \left(\frac{\dot{\epsilon}}{\dot{\epsilon}_0} \right)^{D_{TR}} \epsilon \left(E - F_{TR} \ln \frac{\dot{\epsilon}}{\dot{\epsilon}_0} \right) \quad (10)$$

Correlation of the effects of rate of strain and temperature with the present data can be examined by use of equations B11, B12, and B13 of Appendix B. Of these, Eqs. B12 and B13 can be modified by the simplification for shearing stress in the torsion test given in Eq. 7. Written in logarithmic form and calling the constants C_1 to C_6 we have

$$\ln \tau \Big|_{\dot{\gamma}, T_R} = C_1 + C_2 \ln \gamma \quad (11)$$

$$\ln T \Big|_{\gamma, T_R} = C_3 + C_4 \ln \dot{\gamma} \quad (12)$$

$$\ln T \Big|_{\gamma, \dot{\gamma}} = C_5 + C_6 T_R \quad (13)$$

Constant Strain-Rate and Temperature: Equation 11 is the conventional true stress-strain equation for plastic flow, $\tau = a\epsilon^b$ and can be verified by construction of the torsional stress-strain curves to log scale for the individual specimens. These curves for at least one specimen of each material are shown in Fig. 76. These curves are considered to be typical except as indicated below and can therefore be accepted as checking the theory except for the following excluded cases:

1. For tests in which a yield point was observed, analysis by means of Eq. A20 of Appendix I for the region of initial yielding was not attempted so that for this portion of the plastic strain, Eq. 11 was not verified.
2. In no case was the relation verified for the portion of the deformation after the maximum torque had been reached. This occurred relatively late in the test for each metal except at the higher temperatures.

3. In RC-70 titanium it was observed that in the torsional testing there was a tendency for considerable strain after the maximum resisting torque had been developed. This was not the case for RC-130-B titanium alloy. The proportion of the total strain that occurred during the period of decreasing torque for RC-70 was larger for the higher temperatures and for the lower rates of strain. The flow equation (Eq. 11) was applicable only to the increasing portion of the curve.
4. For RC-130-B the stress determined by use of Eq. A20 seems to increase slightly more rapidly with respect to strain than predicted by Eq. 11 for the specimens for which these curves were drawn.

Constant Strain and Temperature: Equation 12 relates the effect of strain-rate $\dot{\gamma}$ to the flow stress or torque for a constant shearing strain γ and at constant temperature T_R . This equation indicates a linear relationship to exist between $\ln T$ and $\ln \dot{\gamma}$. Hence, if $\ln T$ for constant γ and constant T_R is plotted vs. $\ln \dot{\gamma}$ and the experimental values fall on a straight line, Eq. 12 is satisfied. Since the speeds employed in the present tests differed by factors of 50 to 1, the speed numbers can be used to represent the logarithm of the strain-rate.

In Figs. 78 to 84 the torque is plotted to a log scale versus the speed. Each point represents the results obtained from one specimen. Data are shown for two values of shearing strain for each material (that is, γ equals 5 per cent and 50 per cent for steel and titanium, and 2 per cent and 20 per cent for the aluminum alloy). Several other strains were also studied with results similar to those shown.

The curves obtained are nearly straight for all temperatures for the values of γ checked. Therefore, it can be concluded that the function which

expresses the variation of the logarithm of stress or torque with the logarithm of strain-rate is very nearly linear for all seven metals tested. Although the graphs for specimens which were given the 200-hour aging treatment have not been included here, these data were studied and the variation of $\ln T$ with speed was also found to be linear, even for the aluminum alloys tested at temperatures at which the effects of the aging treatment on the strength and ductility were large.

These data indicate then that although the effect of strain-rate is not large in general, the variations in strength with changes in strain-rate can be predicted fairly well by the relation:

$$T \Big|_{\gamma, T_R} = c_1 \dot{\gamma}^{c_2} \quad (14)$$

for all seven metals at all temperatures investigated. In this expression c_1 and c_2 depend on the strain, temperature and material. It will be noted that particularly close agreement was observed for the SAE 4340 steel Fig. 79.

Constant Strain and Strain-Rate: Equation 13 relates the torque or stress to the temperature for constant strain and strain-rate. The logarithm of the torque T is expressed as a linear function of the absolute (Rankine) temperature T_R . This can be checked readily by plotting the torque to a log scale versus T_R or, more conveniently, versus the Fahrenheit temperature T_F since $T_R = T_F + 459.6^\circ$, with the difference between T_F and T_R included in the constant c_5 in Eq. 13.

Some of the data which have been plotted in this manner are included as Figs. 85 to 91. The trends of the points in general appear to form rather definite curves which can not be considered linear. Therefore it must be concluded that Eq. 13 is inaccurate in expressing the variations of strength properties caused by temperature changes. For the two titaniums the trends were more nearly linear, particularly at the faster speeds. However, consid-

erable variations from the straight lines were observed at the slower speeds. For SAE 4340 steel the trends were essentially linear up to 700F but wide differences were evident for higher temperatures. The patterns in which test points fall for aged specimens were similar to those shown for the unaged specimens.

These data indicate that (with the possible exception of titanium) the effect of temperature for the ranges of variables studied here did not conform well with the theoretical relation expressed in Eq. 13. The reason for this inaccuracy may be attributed to such actions as precipitation and coalescence of solute atoms at certain temperatures and strain-aging. In other words, the properties of these metals changed somewhat during the progress of the test and could not be expressed by a single simple equation that is independent of the parameter of time.

The behavior of titanium was more nearly predicted by the theory; this is further evidence that the types of aging phenomena observed in the other two metals were not present (or were less significant) in the titanium.

d. Velocity-Modified Temperature Parameter: The velocity-modified temperature proposed by MacGregor and Fisher (70-72) is briefly discussed in Appendix III. The data with which this concept was originally tested (70, 71) seemed to support the hypothesis even for some instances in which ultimate stresses or yield stresses were used instead of the flow stress as expressed by the theory.

On the basis of the simplification discussed previously in Eq. 7, this concept may be expressed here in the form:

$$T \Big|_{\gamma} = f(T_m) \quad (15)$$

where: T = torque at given shearing strain γ

T_m = velocity-modified temperature.

Contrails

The defining equation for the velocity-modified temperature is:

$$T_m = T_R \left(1 - k \ln \frac{\dot{\gamma}}{\dot{\gamma}_0} \right) \quad (16)$$

In this relation the slowest strain-rate was selected as the reference strain-rate for this investigation so that $\dot{\gamma}_0 = 0.0001$ in./in./sec. The k values chosen to fit the data to the smoothest possible curves were found to be:

$k = 0.010$ for SAE 1018 steel

$k = 0.010$ for SAE 4340 steel

$k = 0.010$ for 24S-T aluminum alloy

$k = 0.015$ for 75S-T aluminum alloy

$k = 0.020$ for FS-1 magnesium alloy

$k = 0.030$ for RC-70 titanium

$k = 0.015$ for RC-130-B titanium alloy

For each metal the data were examined by plotting the torque vs. T_m for at least three values of strain. One of these charts for each metal is included in Figs. 92 - 98. From these graphs it can be seen that there is general agreement with the theory since the points group fairly well around a relatively smooth curve that has been sketched in to follow the average trend. The shapes of the curves thus obtained are not the same for different metals, but no attempt is made by the theory to predict the shape of the curve.

Correlation was noticeably poorer when the yield strength or the modulus of rupture was plotted instead of flow stress or torque at constant strain. A very broad band was required to envelope the points thus obtained although the general course followed by the band was similar to that for the curves shown in Figs. 92 - 98.

These data indicate that for all metals studied it is possible to

approximate the effects of both strain-rate and temperature in terms of a single parameter, the so-called velocity-modified temperature, for the range of variables investigated. No simple relationship resulted however between this parameter and the flow stress or torque for a given twist.

10. Correlation with Other States of Stress.

In the opening section of this report it was pointed out that one of the problems encountered in utilizing the results obtained in any series of experiments is to know how to interpret the data for applications involving somewhat different conditions. Results of the torsion tests reported here, in which the state of stress was biaxial, would not be expected to conform exactly with data from uniaxial tension or bending tests or from triaxial stressing.

It is beyond the already broad scope of this project to develop means of applying the results obtained here to cases for which other conditions are encountered. However, it seems worthwhile to point out some of the tools already available which might contribute to more general application of these data.

One method for correlation of properties of materials subjected to different states of stress is on the basis of stress-strain characteristics. In order to make this type of correlation, the generalized, effective or significant true stresses and strains must be computed for the given stress conditions. Assuming that the corresponding principal stresses and strains are known or can be determined, the generalized stresses $\bar{\sigma}$ and strains $\bar{\epsilon}$ are defined as follows:

$$\bar{\sigma} = \sqrt{\frac{1}{2} \left[(\sigma_1 - \sigma_2)^2 + (\sigma_2 - \sigma_3)^2 + (\sigma_3 - \sigma_1)^2 \right]} \quad (17)$$

and

$$\bar{\epsilon} = \sqrt{\frac{2}{3} (\epsilon_1^2 + \epsilon_2^2 + \epsilon_3^2)} \quad (18)$$

Contrails

where σ_1 , σ_2 and σ_3 are the three true normal principal stresses and ϵ_1 , ϵ_2 and ϵ_3 are the true normal principal strains.

For pure tension $\sigma_2 = \sigma_3 = 0$ and $\epsilon_2 = \epsilon_3 = -\mu\epsilon_1$. Using poissons ratio μ as $1/2$, the expressions for generalized stress and strain, Eqs. 17 and 18 reduce to:

$$\bar{\sigma} = \sigma_1 \quad (19)$$

$$\bar{\epsilon} = \epsilon_1 \quad (20)$$

For pure shear in torsion, $\sigma_1 = -\sigma_3 = \tau$, and $\sigma_2 = 0$, where τ is the shearing stress. The generalized stress for this case reduces to:

$$\bar{\sigma} = \sqrt{3} \tau \quad (21)$$

The strains for torsion are related in the same manner, i.e. $\epsilon_1 = -\epsilon_3$, $\epsilon_2 = 0$, and $\gamma = \epsilon_1 - \epsilon_3$. γ is the shearing strain computed by the relation $\frac{c\theta}{\rho}$ as discussed in Section 7a. Making these substitutions the equation for generalized strain reduces to:

$$\bar{\epsilon} = \frac{2}{\sqrt{3}} \epsilon_1 = \frac{1}{\sqrt{3}} \gamma \quad (22)$$

Equations 21 and 22 may be used for correlation of the torsion test data with the stresses and strains for a uniaxial stress condition. Somewhat more complex relationships may also be derived from Eqs. 17 and 18 for other combinations of principal stresses encountered in a service condition. For these, the values of the effective or generalized stresses and strains ($\bar{\sigma}$ and $\bar{\epsilon}$) may be predicted from the torsion test data by means of Eqs. 21 and 22.

IV SUMMARY AND CONCLUSIONS

An experimental study was made to determine the effect of rate of strain and of elevated temperatures on the mechanical properties of seven different structural metals in pure torsion. Prepared samples were tested at four constant rates of strain in the range from 0.0001 to 12.5 in./in./sec. and at four temperatures ranging from room temperature to various maximum temperatures up to 1200F depending on the type of alloy studied. Values of the torque, angle of twist and time were continuously recorded automatically to provide data from which the usual torsional properties were computed.

The experimental data were analyzed in terms of the basic mechanisms controlling the behavior, and the effects of the two parameters were compared with mathematical theories in the literature. From the results of this study the following conclusions are summarized:

1. Increasing the temperature caused the yield strength and modulus of rupture to decrease and caused the angle of twist to fracture to increase for all materials and for all rates of strain except (a) in the blue-brittleness temperature range for steel, and (b) in the temperature range for aging of aluminum.
2. Increasing the rate of strain usually caused some increase in strength but to a lesser degree than that caused by decreasing the temperature. However, increasing the rate of strain had a pronounced effect on ductility. The greatest ductility was observed at the highest temperature and slowest rate of strain except as noted in items 7, 15 and 16 below.
3. The rate of increase of flow stress τ (or torque T) at a given strain-rate $\dot{\gamma}$, can be expressed with a good degree of accuracy by the equation

Contrails

$$\tau \Big|_{\gamma, T_R} = c_1 \dot{\gamma}^{c_2}$$

where c_1 and c_2 are constants which depend on the material, the temperature and the amount of strain.

4. The rate of increase of flow stress τ (or torque) at a given strain with increase in temperature for titanium can be expressed approximately by the equation

$$\tau \Big|_{\dot{\gamma}, \gamma} = j e^{h T_R} \quad (23)$$

for $\dot{\gamma} \geq 0.005$ in./in./sec. where j and h are constants which depend on the material, strain and strain-rate.

5. The rate of decrease of flow stress τ (or torque T) for a given strain with increase in temperature for the other metals at all speeds and for titanium at $\dot{\gamma} = 0.0001$ did not conform with the behavior predicted by the Eq. 23. The shape of the curve ($\ln T$ vs temperature) was different for each different temperature.
6. It is possible to express the effects of both strain-rate and temperature in terms of a single parameter such as the velocity-modified temperature T_m and get a smooth curve for flow stress or torque at a given strain when plotted versus T_m . The shape of the curve obtained was different for each metal studied and did not appear to be readily expressible in mathematical form.
7. At certain elevated temperatures beginning at about 400F a reduction of ductility and a slight increase in strength were observed for SAE 1018 steel. This is usually referred to as blue-brittleness.

Conclusions

8. The absolute (Rankine) blue-brittleness temperature T_R for SAE 1018 steel was a function of the rate of shearing strain which can be expressed roughly by the equation

$$T_R = \frac{32,500}{28.2 + \ln \dot{\gamma}}$$

for the present data and for that of two other investigators.

9. The torque-time records obtained in the blue-brittleness range exhibited the jagged or erratic contours typical of the variations in flow stress developed by the strain-aging phenomenon.
10. The specimens of SAE 1018 steel tested at room temperature exhibited a yield point in the ordinary tension test, and a sharp yield point was observed in the more rapid torsion tests at the lower temperatures. The ratio of the upper to lower yield point torques observed was found to decrease with an increase in temperature, and decreased or disappeared at the lower strain rates.
11. The specimens of RC-70 and RC-130-B titanium tested at room temperature exhibited a definite yield point in the ordinary tension test. A pronounced yield point was also observed in the rapid torsion tests of RC-70 at elevated temperatures. The ratio of the upper to lower yield point torques observed at the highest strain-rate increased with an increase in temperature and decreased or disappeared at the lower strain-rates. The yield point observed in torsion tests of RC-130-B was less pronounced than for RC-70 titanium and not as consistent.
12. The properties of the titanium were more sensitive to changes in strain-rate than were the properties of the other metals.

Contrails

13. Specimens of steel, aluminum and magnesium remained cylindrical when deformed and there was no appreciable change in their dimensions. The titanium specimens however, tended to deform in such a manner that ridges formed on the surface and wound like screw threads around the circumference at large strains.
14. Very large strains were developed before fracture in the specimens of 1018 steel, magnesium and titanium in tests at 0.0001 in./in./sec. strain-rate at the highest test temperatures. These strains and temperatures were:
 - 1000 per cent at 1000F for SAE 1018 steel
 - 800 per cent at 600F for FS-1 magnesium alloy
 - 1200 per cent at 1000F for RC-70 titanium
 - 3750 per cent at 1000F for RC-130-B titanium
15. The largest strains in SAE 4340 steel (800 to 1000 per cent) were developed at 1200F in tests at 0.005 in./in./sec.
16. The greatest ductility for the two aluminum alloys was about 800 per cent and occurred at 600F at a strain-rate of 0.25 in./in./sec. (not at the slowest speed as for the metals listed in item 14). Marked decreases in total angle of twist were observed for both higher and lower rates of strain.
17. The two-hundred hour aging treatment (at the test temperature) in advance of the test had no appreciable effect on the strength or ductility of steel or titanium for any temperature up to 1000F or any strain-rate studied here.
18. Two-hundred hours at 1200F produced some increase in strain and some decrease in strength of SAE 4340 steel as compared with unaged specimens.

Contrails

19. The two-hundred hour aging treatment produced a decrease in strength and an increase in ductility for all speeds of testing of 75S-T aluminum alloy at 400F, and for 24S-T at 400F and 600F, but had no appreciable effects at other temperatures.

BIBLIOGRAPHY

1. Barksdale, L., Titanium, Ronald Press Co., N. Y., 1949.
2. Barrett, P. F., "Compressive Properties of Titanium Sheet at Elevated Temperatures", NACA TN 2038, February 1950.
3. Beeuwkes, R., "Concerning the Effect of Strain and Rate of Strain on Tensile Tests at Normal and Elevated Temperatures", Journ. Applied Physics, Vol. 5, pp. 135-139, 1934.
4. Bogardus, K. O., G. W. Stickley, and F. M. Howell, "A Review of Information on the Mechanical Properties of Aluminum Alloys at Low Temperatures", NACA TN 2082, 1950.
5. Bradford, C. I., J. P. Catlin, and E. L. Wemple, "Physical and Mechanical Properties of Commercially Pure Titanium", Ref. A2, pp. 49-59.
6. Bregowsky, I. M., and L. W. Spring, "The Effect of High Temperature on the Physical Properties of Some Alloys", Proc. Int. Assoc. Testing Mats., Sixth Congress, New York, Vol. II, Part 2, First Section VII.
7. Bridgman, P. W., "The Stress Distribution at the Neck of a Tension Specimen", Trans. Amer. Soc. Metals, Vol. 32, pp. 553-572, 1944.
8. Brown, A. F. C., and N. D. G. Vincent, "The Relationship Between Stress and Strain in the Tensile Impact Test", Proc. Inst. Mech. Engrs., Vol. 145, pp. 126-134, 1941.
9. Clark, D. S., "Influence of Impact Velocity on the Tensile Characteristics of Some Aircraft Metals and Alloys", NACA TN 868, Oct. 1942.
10. Clark, D. S., and G. Datwyler, "Stress-Strain Relations under Tension Impact Loading", Proc. Am. Soc. Testing Mats., Vol. 38, Part II, pp. 98-111, 1938.
11. Clark, D. S., and P. E. Duwez, "The Influence of Strain-Rate on Some Tensile Properties of Steel", Proc. Am. Soc. Testing Mats., Vol. 50, pp. 560-576, 1950.
12. Clark, D. S., and D. S. Wood, "The Tensile Impact Properties of Some Metals and Alloys", Trans. Am. Soc. Metals, Vol. 42, pp. 45-74, 1950.
13. Clark, D. S., and D. S. Wood, "The Time Delay for the Initiation of Plastic Deformation at Rapidly Applied Constant Stress", Proc. Am. Soc. Testing Mats., Vol. 49, pp. 717-737, 1949.
14. Cottrell, A. H., and B. A. Bilby, "Dislocation Theory of Yielding and Strain Aging of Iron", Proc. Phys. Soc. of London, Vol. 62, pp. 49-62, 1949.
15. Davidenkov, N. N., and N. I. Spiridonova, "Analysis of Tensile Stress in the Neck of an Elongated Test Specimen", Proc. Am. Soc. Testing Mats., Vol. 46, pp. 1147-1158, 1946.

Contrails

6. Davis, E. A., "The Effect of Speed of Stretching and the Rate of Loading on Mild Steel", Journ. Applied Mechs., Vol. 5, Trans. Am. Soc. Mechanical Engrs., Vol. 60, pp. A137-A140, 1938.
17. Davis, E. A., "Yielding and Fracture of Medium-Carbon Steel under Combined Stress", Journ. Applied Mechs., Vol. 12, Trans. Am. Soc. Mech. Engrs., Vol. 67, pp. A13-A25, 1945.
18. Dean, R. S., and B. Silkes, "Metallic Titanium and Its Alloys", U. S. Dept. Int., Bur. Mines, I. C. 7381, November, 1946.
19. Dolan, T. J., and O. M. Sidebottom, "Raised (?) Yield Point in Bend Tests", Metals Progress, Vol. 50, No. 4, pp. 653-657, October, 1946.
20. Dorn, J. E., A. Goldberg, and T. E. Tietz, "The Effect of Thermal-Mechanical History on the Strain Hardening of Metals", Am. Inst. Min. Metallurgical Engrs., Vol. 180, Metals Technology, September, 1948. (21 Refs.), Tech. Pub. No. 2445. Disc. Trans. Journ. of Mets. pp. 325, May, 1949.
21. Du Mont, C. S., Bibliography on the Production and Properties of Titanium, Metal Progress, Vol. 55, p. 368, 1949. (114 Refs.)
22. Elam, C. F., "The Influence of Rate of Deformation on the Tensile Test with Special Reference to the Yield Point in Iron and Steel", Proc. Roy. Soc., London (A), Vol. 165, pp. 568-592, 1938.
23. Everhart, J. L., "Titanium and Its Alloys", Materials and Methods, pp. 117-132, May, 1952.
24. Eyring, H., "Viscosity, Plasticity and Diffusion as Examples of Absolute Reaction Rates", Journ. of Chemical Physics, Vol. 4, p. 283, 1936.
25. Faupel, J. H., and Joseph Marin, "Tension-Compression Biaxial Plastic Stress-Strain Relations for Aluminum Alloys 24S-T and 25-O, Am. Soc. Metals, Preprint 35, (October 27, 1950).
26. Fehr, R. O., E. R. Parker, and D. J. DeMicheal, "Measurement of Dynamic Stress and Strain in Tensile Test Specimens", Journ. Applied Mech., Vol. II, Trans. Am. Soc. Mechanical Engrs., Vol. 66, pp. A65-A71, 1944.
27. Fettweiss, F., "Über die Blaubruchigkeit und das Altern des Eisens", Stahl und Eisen, Vol. 39, pp. 1-7 and 34-41, (Jan. 1919).
28. Fetzer, M. C., "Torsional Versus Tensile Properties of Steels", Steel, Vol. 118, n 25, pp. 92-94, 118-123, June 24, 1946.
29. Fontana, M. G., "Mechanical Properties and Physical Metallurgy of Aircraft Alloys at Very Low Temperatures", Ohio State University Research Foundation Dept., Nos. 40-43, 1951-52.
30. French, H. J., "Effect of Temperature, Deformation, and Rate of Loading on the Tensile Properties of low-Carbon steel Below the Thermal Critical Range", U.S. Bur. Stds. Tech. Paper, Vol. 16, pp. 679-725, 1922.
31. French, H. J., and W. A. Tucker, "Available Data on the Properties of Irons and Steels at Various Temperatures", Ref. 221, pp. 52-83, 1924.

Contrails

32. Fry, L. H., "Speed in Tension Testing and Its Influence on Yield Point Values", Proc. Am. Soc. Testing Mats., Vol. 40, pp. 625-636, 1940.
33. Fuller, F. B., "Some New Data on the Properties of Wrought Titanium", Metal Progress, Vol. 56, No. 3, pp. 348-350, September, 1949.
34. Gee, E. A., J. B. Sutton, and W. J. Barth, "Effect of Carbon in Titanium Metal Ingots", Ind. and Eng. Chem., Vol. 42, pp. 243-249, 1950.
35. Gensamer, M., "The Yield Point in Metals", Trans. Am. Inst. Mining Metallurgical Engrs., Vol. 128, pp. 104-117, 1938.
36. Gonser, B. W., "Titanium", Journ. of Metals, Am. Inst. Mining Metallurgical Engrs., No. 12, pp. 6-9, January, 1949.
37. Greaves, R. H., and J. A. Jones, "The Effect of Temperature on the Behavior of Iron and Steel in the Notched Bar Impact Test", Journ., Iron and Steel Inst., Vol. 112, No. II, pp. 123-162, 1925.
38. Greene, O. V., and R. D. Stout, "Stress-Strain Characteristics of the Torsion Impact Test", Trans. Am. Soc. Metals, pp. 277-305, June, 1940.
39. Gruschka, G., "Zugfestigkeit und Verlauf der Festigkeitskurven von Stählen bei Tief Temperaturen", Diss. der Tech-Hochsch., Berlin 28, February, 1933.
40. Gulbransen, E. A., and K. F. Andrew, "Kinetics of the Reactions of Titanium with O_2 , N_2 , and H_2 ", Trans. Am. Inst. Mining Metallurgical Engrs., Vol. 185, pp. 741-48, 1949.
41. Hall, E. O., "The Deformation and Aging of Mild Steel", Proc. Phys. Soc. Vol. 64, Sect. B, pp. 742-747, 747-751, 1951.
42. Hall, E. O., "The Deformation of Low-Carbon Steel in the Blue Brittle Range", Journ. of the Iron and Steel Institute, pp. 331-336, April, 1952.
43. Hanink, H. H., "A Realistic Approach to the Use of Titanium", Product Engineering, pp. 164-171, November, 1951.
44. Hazlett, T. H., A. T. Robinson, and J. E. Dorn, "An Evaluation of a Theory for Plastic Flow in Anisotropic Sheet Metals", Trans. Am. Soc. Metals, Vol. 42, pp. 1326-1356, 1950.
45. Heimerl, G. J., and P. F. Barrett, "A Structural-Efficiency Evaluation of Titanium at Normal and Elevated Temperatures", NACA TN 2269, January, 1951.
46. Hollomon, J. H. and L. D. Jaffe, Ferrous Metallurgical Design, John Wiley and Sons, New York, 1947.
47. Hollomon, J. H., and J. D. Lubahn, "The Flow of Metals at Elevated Temperatures", Gen. Elec. Rev., Vol. 50, No. 2, pp. 44-50, 1947.
48. Hollomon, J. H., and J. D. Lubahn, "Plastic Flow of Metals", The Physical Rev., Vol. 70, p. 775, 1946.
49. Hollomon, J. H., and C. Zener, "High Speed Testing of Mild Steel", Trans. Am. Soc. Metals, Vol. 32, pp. 111-122, 1944.

Contrails

50. Honda, Kotaro, "A Comparison of Static and Dynamic Tensile and Notched Bar Tests", Journ. Inst. Metals, Vol. 36, No. 2, pp. 27-37, 1926.
51. Hoyt, S. L., "Discussion to High Temperature Properties of the Refractory Metals", 1942.
52. Itihara, Mititosi, "Impact Torsion Test", Technology Reports of the Tohoku Imperial University, Vol. 11, pp. 16-50, 489-581, 1933-35, Vol. 12, pp. 63-118, 1936-38, Reviewed in Metallurgist, Vol. 10, pp. 141-143, June, 1936.
53. Jackson, L. R., "Work-Hardening and Rupture in Metals", Am. Inst. Mining Metallurgical Engrs., Tech. Publ No. 2072, October, 1946, (26 refs.).
54. Jeffries, Z., and R. S. Archer, "Overstrain, Internal Stresses and Creep", Chem. and Met. Engrs., Vol. 27, pp. 833-837, 1922.
55. Jones, P. G., and H. F. Moore, "An Investigation of the Effect of Rate of Strain on the Results of Tension Tests of Metals", Proc. Am. Soc. Testing Mats., Vol. 40, pp. 610-624, 1940.
56. Jones, P. G. and W. J. Worley, "An Experimental Study of the Influence of Various Factors on the Mode of Fracture of Metals", Proc. Am. Soc. Testing Mats., Vol. 48, pp. 648-663, 1948. (11 refs.).
57. Kahn, N. A., and E. A. Imbenbo, "A Study of the Geometry of the Tension-Impact Specimen", Proc. Am. Soc. Testing Mats., Vol. 46, pp. 1179-1197, 1946.
58. Kauzmann, W., "Flow of Solid Metals From the Standpoint of Chemical-Rate Theory", Trans. Am. Inst. Mining Metallurgical Engrs., Vol. 143, pp. 57-81, 1941.
59. Kenyon, R. L., and R. S. Burns, "Aging in Iron and Steel", Symposium on Age Hardening of Metals, Am. Soc. for Metals, pp. 262-296, 1940.
60. Klinger, R. F., "Tensile Properties of Some Aircraft Structural Materials at Various Rates of Loading", Proc. Am. Soc. Testing Mats., Vol. 50, pp. 1035-1050, 1950.
61. Korber, F., and R. H. Sacks, "Vergleichende Statische und Dynamische Zugversuche".
62. Kurth, A., "Untersuchungen über den Einfluss der Wärme auf die Härte der Metalle", Zeitschrift, Verein deutsche Ingenieure, Vol. 53, pp. 85, 209, 1909.
63. Larson, H., and E. P. Klier, "Strain Hardening of Mild Steel in the Torsion Test as a Function of Temperature", Trans. Am. Soc. Metals, Vol. 43, pp. 1033-1050, 1951.
64. Leighly, H. P., "Recrystallization and Grain Growth in Commercial Titanium", Doctoral Thesis, Dept. of Metallurgy, Univ. of Illinois, 1952.
65. Long, J. R., and E. T. Hayes, "Sheath Working of Metal Powders", U. S. Dept. of Int., Bur. Mines, R. I. 4464, February, 1949.

Contrails

66. Low, J. R., Jr., and M. Gensamer, "Aging and the Yield Point in Steel", Trans. Am. Inst. Mining Metallurgical Engrs., Vol. 158, pp. 207-249, Iron and Steel Division, 1944.
67. Labahn, J. D., "Derivation of Stress, Strain, Temperature Strain-Rate Relation for Plastic Deformation", Journ. Applied Mechs., Vol. 14, Trans. Am. Soc. Mech. Engrs., Vol. 69, pp. A229-A230, 1947.
68. Ludwik, P., Elemente der Technologischen Mechanik, Julius Springer, Berlin, 1909.
69. Ludwik, P., and R. Schen, "Vergleichende Zug, Druck, Dreh, und Walzversuche", Stahl und Eisen, pp. 373-381, March, 1925.
70. MacGregor, G. W., and J. C. Fisher, "A Velocity-Modified Temperature for Plastic Flow of Metals", Journ. Applied Mechs., Vol. 13, Trans. Am. Soc. Mechanical Engrs., Vol. 68, pp. A11-A16, 1946.
71. MacGregor, G. W., and J. C. Fisher, "Tension Tests at Constant True Strain Rates", Journ. Applied Mechs., Vol. 12, Trans. Am. Soc. Mech. Engrs., Vol. 67, pp. A217-A227, 1945.
72. MacGregor, G. W., and L. E. Welch, "True Stress-Strain Relations at High Temperatures by the Two-Load Method", Trans. Am. Inst. Mining Metallurgical Engrs., Vol. 154, pp. 423-437, 1943.
73. Manjoine, M. J., "Influence of Rate of Strain and Temperature on Yield Stresses of Mild Steel", Journ. Applied Mechs., Vol. 11, Trans. Am. Soc. Mechanical Engrs., Vol. 66, pp. A211-A218, 1944.
74. Manjoine, M. J., and A. Nadai, "High-Speed Tension Tests at Elevated Temperatures", Proc. Am. Soc. Testing Mats., Vol. 40, pp. 823-839, 1940.
75. Mann, H. G., "The Relation Between Tension Static and Dynamic Tests", Proc. Am. Soc. Testing Mat., Vol. 35, Part II, pp. 323-340, 1935.
76. Marin, J., "A Method of Defining Failure in Members Subjected to Combined Stresses", Trans. Am. Soc. Metals. Vol. 40, No. 6, pp. 1013-1021, December, 1941.
77. Marin, J., "Stress-Strain Relations in the Plastic Range for Biaxial Stresses", Journ., Franklin Institute, Vol. 248, pp. 231-249, 1949.
78. Marin, J., J. H. Faupel, V. L. Dutton, and M. W. Brossman, "Biaxial Plastic Stress-Strain Relations for 24S-T Aluminum Alloy", NACA TN 1536, May, 1948.
79. Marin, J., and B. J. Kotalik, "Plastic Biaxial Stress-Strain Relations for Alcoa 24S-T Subjected to Variable-Stress Ratios", Journ. Applied Mechs., Trans. Am. Soc. Mech. Engrs., Vol. 72, pp. 372-376, 1950.
80. Marshall, E. R., and M. C. Shaw, "The Determination of Flow Stress From a Tensile Specimen", Trans., Am. Soc. Metals, Vol. 44, pp. 705-720, 1952.

Contrails

81. McAdam, D. J., Jr., G. W. Geil, and R. W. Møbs, "The Effect of Combined Stresses on the Mechanical Properties of Steels Between Room Temperature and -188°C ", Proc. Am. Soc. Testing Mats., Vol. 45, pp. 448-485, 1945.
82. Moore, H. F., B. B. Betty and C. W. Dollins, "The Creep and Fracture of Lead and Lead Alloys", Univ. of Ill, Eng. Exp. Sta. Bull. No. 272, 1935.
83. Morrison, J. L. M., "The Influence of Rate of Strain in Tension Tests", Engineer, Vol. 158, pp. 183-185, 1934.
84. Murphy, G., "Stress-Strain-Time Characteristics of Materials", Am. Soc. Testing Mats., Bulletin, December, 1939.
85. Nadai, A., and M. J. Manjoine, "High-Speed Tension Tests at Elevated Temperatures, II and III, Pt. I, Proc. ASTM, Vol. 40, pp. 822-837, Journ. Applied Mechs., Vol. 8, Trans. Am. Soc. Mechanical Engrs., Vol. 63, pp. A77-A91, 1941.
86. Osgood, W. R., "Combined-Stress Tests on 24S-T Aluminum-Alloy Tubes", Journ. Applied Mechs., Trans. Am. Soc. Mechanical Engrs., Vol. 69, pp. A147-153, 1947.
87. Parker, E. R., "High Temperature Properties of the Refractory Metals", Trans. Am. Soc. Metals, Vol. 42, pp. 399-404, 1950.
88. Parker, E. R., and C. Ferguson, "The Effect of Strain Rate Upon the Tensile Yield Impact Strength of Some Metals", Trans. Am. Soc. Metals, Vol. 30, pp. 68-85, 1942.
89. Piper, T. E., "Hot Forming of Aluminum and Magnesium Alloy", Am. Soc. Metals, Vol. 43, pp. 1013-1030, 1951.
90. Quinney, H., "Further Tests on the Effect of Time in Testing", Engineer, Vol. 161, pp. 669-673, 1936.
91. Quinney, H., "Time Effect in Testing of Metals", Engineer, Vol. 157, pp. 332-334, 1934.
92. Roberts, W. M., and G. J. Heimerl, "Elevated-Temperature Compressive Stress-Strain Data for 24S-T3 Aluminum Alloy Sheet and Comparisons with Extruded 75S-T6 Aluminum Alloy, NACA TN 1837, March, 1949.
93. Robin, F., "The Resistance of Steels to Crushing at all Temperatures", Carnegie Scholarship Memoirs (Iron and Steel Inst.), Vol. 2, p. 70.
94. Sauveur, A., "Notes on the Aging of Metals and Alloys", Trans. Am. Soc. Metals, Vol. 22, p. 97, 1934.
95. Sauveur, A., "Steel at Elevated Temperatures", Trans. Am. Soc. Steel Treat., Vol. 17, p. 410, 1931.
96. Seely, F. B., and W. J. Putnam, "Torsion, Tension and Compression Relations of Elastic Strengths", Univ. of Ill., Eng. Exp. Sta. Bul. No. 115, 1919.
97. Seigle, L., and R. M. Brick, "Mechanical Properties of Metals at Low Temperatures; a Survey", Trans. Am. Soc. Metals, Vol. 40 pp. 813-861, 1948. (95 Refs)

Contrails

98. Siebel, E., and A. Pomp, "Einfluss der Formänderungsgeschwindigkeit auf den Verlauf der Fließkurve von Metallen", Mitteilungen Kaiser Wilhelm Institut Eisenforschung, Vol. 10, pp. 63-69, 1928.
99. Smith, G. V., Properties of Metals at Elevated Temperatures, Metallurgical Eng. Series, McGraw-Hill Book Co., N.Y., 1950.
100. Sunatami, Chido, "Laws of Failure of Solid Bodies Due to Stress", Tech. Reports, Tohoku Imp. Univ (Sendai, Japan), Vol. VII, No. 1, 1922.
101. Sylwestrowicz, W., and E. O. Hall, Proc. Phys. Soc. Vol. 64, Section B, pp. 495-501, 1951.
102. Tapsell, H. J., and W. J. Clenshaw, "Results of Hardness Tests of Armco Iron", "The Metal-Iron", Alloys of Iron Research, Monograph Series, McGraw-Hill Book Company, Inc., New York, N. Y., p. 376, 1935.
103. Templin, R. L., "The Determination and Significance of the Proportional Limit in the Testing of Metals", Proc. Am. Soc. Testing Metals, Vol. 29, pp. 523-534, 1929.
104. Thomsen, E. G., and J. E. Dorn, "The Effect of Combined Stresses on the Ductility and Rupture Strength of Magnesium-Alloy Extrusions", Journ. Aero. Sci., Vol. II, No. 2, pp. 125-136, April, 1944.
105. Warnock, F. V., and D. B. C. Taylor, "The Yield Phenomena of a Medium Carbon Steel Under Dynamic Loading", Inst. Mech. Engrs., Applied Mech. Proc. Vol. 161, pp. 165-175, 1949.
106. Wartman, F. S., J. P. Walker, H. C. Fuller, M. A. Cook, and E. L. Anderson, "Production of Ductile Titanium at Boulder City, Nevada", U. S. Dept. Int., Bur. Mines, R. I. 4519.
107. Welter, G., and S. Morski, "Dynamic Tensile Properties and Stress-Strain Diagrams, of Some Constructional Materials", Journ. Inst. of Metals, Vol. 66, pp. 97-107, April, 1940.
108. Williams, W. L., "Elevated Temperature Properties of Titanium and Titanium Alloys", U. S. Naval Eng. Exp. Sta. Report No. 4A006876, March 14, 1951.
109. Williams, W. L., "The Properties of Titanium Metal", U. S. Naval Eng. Exp. Sta. Report No. C-3395-B, C-3501-C, August 2, 1950.
110. Winlock, J., and R. W. E. Leiter, "Some Factors Affecting Plastic Deformation of Sheet and Strip Steel and Their Relation to Deep Drawing Properties", Trans. Am. Soc. Metals, Vol. 25, pp. 163-205, 1937.
111. Winlock, J., and R. W. E. Leiter, "Some Observations on the Yield Point of Low-Carbon Steel", Trans. Am. Soc. Mech. Engrs. Vol. 61, pp. 581-587, 1939.
112. Zener, C., and J. H. Hollomon, "Effect of Strain Rate on the Plastic Flow of Steel", Journ. Applied Phys., Vol. 15, pp. 22-32, 1944.
113. Zener, C., and J. H. Hollomon, "Plastic Flow and Rupture of Metals", Trans. Am. Soc. Metals, Vol. 39, pp. 163-235, 1944.

Contrails

114. Zener, C., and J. H. Hollomon, "Problems in Non-Elastic Deformation of Metals", Journ. Applied Phys., Vol. 17, No. 2, pp. 69-82, 1946.
115. "The Effect of Temperature upon the Properties of Metals", Joint Symposium, Am. Soc. Mech. Engrs., and Am. Soc. Testing Mats., p. 184, May 29, 1924. (216 Refs.).
116. "Symposium on Effect of Temperature on the Properties of Metals", Published jointly by the Am. Soc. Testing Mats., and Am. Soc. Mech. Engrs., pp. 829, 1932. (615 Refs.).
117. "Our Next Major Metal - Titanium", Special Progress Report, Product Engineering, pp. 129-152, November, 1949.
118. "Titanium", Report of Symposium on Titanium, Office of Naval Research, March, 1949.
119. "Investigation of Fabrication Characteristics of Titanium and Titanium Base Alloys", ONR Progress Reports 9 and 11, Chance Vought Aircraft, August 15 and October 15.
120. "Titanium Metal", Technical Bulletin of Pigments Dept., E. I. DuPont de Nemours and Co., Inc., Wilmington, Del.
121. "Titanium Alloys", Technical Information Bulletin, P. R. Mallory Company, Indianapolis, Ind.
122. "Titanium and Titanium-Base Alloys", Rand Report R-131, The Rand Corporation, Santa Monica, California, March 15, 1949. (80 Refs.).
123. "Technical Information on Titanium Metal", Bulletin of Rem-Cru Titanium, Inc., Bridgeport, Conn.
124. "Handbook on Titanium Metal", Titanium Metals Corp., New York, N. Y., 102 p., 1950.
125. Biezeno, C. E. and Koch, J. J. "Concerning the Experimental Determination of $\tau - \gamma$ Diagrams at Constant Deformation Rates and Concerning the Effect which the Deformation Rate has on the Shape of these Diagrams", Ingenieur, Vol. 51, pp. w23-w29.
126. Bishop, S. M., J. W. Spretnak and M. C. Fontana, "Mechanical Properties, Including Fatigue of Titanium-Base Alloys RC-130-B and Ti-150-A at Very Low Temperatures", Am. Soc. Metals, Preprint No. 31 for Nat'l Metal Congress, October, 1952.
127. Puttick, D. E. and M. W. Thring, "The Dynamic Theory of Yield", Iron and Steel, Vol. 25, pp. 155-159, May, 1952.
128. Rosi, F. D. and R. C. Perkins, "Mechanical Properties and Strain Aging Effects in Titanium", Am. Soc. Metals Preprint, No. 29 for Nat'l Metal Congress, October, 1952.
129. Herbert, H., "Über den Zusammenhang der Biegeelastizität des Gusseisens mit seiner Zug- und Druckelastizität", Mitt. u. Forschungsber., Ver. deut. Ing., Vol. 89, 1910, pp. 42-44.

Contrails

130. Bragg, W. L., "A Theory of the Strength of Metals", Nature, Vol. 49, p. 511, May 9, 1942.
131. Wood, W. A., and W. A. Rachinger, "Crystallite Theory of Strength of Metals", Journal, Institute of Metals, p. 571, March, 1949.
132. Freudenthal, A. M., "General Law of Work Hardening", Journal, Franklin Institute, 1949.

Contrails

APPENDIX I.

Derivation of the Equation for Shearing Stress in Torsion

Computation of the actual shearing stress at any point in a member subjected to torsion can be made using the well known $\tau = \frac{Tc}{J}$ relationship for only stresses which remain proportional to the corresponding strains. When this equation is used for torques exceeding the limit of proportionality the so-called stress resulting is not real but merely represents the torque converted to stress units by dividing by the factor $\frac{J}{c}$ which is a function of the cross-sectional area.

It is possible however to develop a relationship expressing the true shearing stress at the surface of a cylindrical bar subjected to pure torsion as a function of the twisting moment, the angle of twist or shearing strain, and the rate of increase in moment with respect to twist or strain. This relation for torsion is similar to the equation for bending developed by Herbert (129). It is based on the assumptions of homogeneity and isotropy of the material and applied to a bar of uniform circular cross-section at a point sufficiently removed from the point of application of the load so that stress is not a function of axial position.

The bar is subjected to a twisting moment or torque T acting in a plane perpendicular to the longitudinal axis of the bar (See Fig. 99). For equilibrium the resisting moment on any normal cross-section must be equal to the applied twisting moment

$$T = \int \rho \tau_p dA \quad (A 1)$$

But by choosing dA as a ring of radius ρ and width $d\rho$ the element of area is $dA = 2\pi\rho d\rho$ and we obtain

$$T = 2\pi \int_0^c \tau_p \rho^2 d\rho \quad (A 2)$$

If the assumption is made that the shearing strain γ_p in each element of the cross section is proportional to the distance of the element from the central

Contrails

longitudinal axis for both elastic and inelastic shearing strains then ρ and $d\rho$ may be expressed in terms of shearing strain γ_ρ :

$$\frac{\rho}{c} = \frac{\gamma_\rho}{\gamma} \quad (\text{A } 3)$$

where: γ_ρ is the shearing strain at a radius ρ

γ is the shearing strain at the surface where $\rho = c$

$$\text{then } d\rho = \frac{c}{\gamma} d\gamma_\rho \quad (\text{A } 4)$$

$$\text{and } \rho^2 = \left(\frac{c}{\gamma}\right)^2 \gamma_\rho^2 \quad (\text{A } 5)$$

Substituting these values of ρ and $d\rho$ in Eq. A2 and applying the corresponding limits to γ_ρ we obtain the relation:

$$T = 2\pi \int_0^\gamma \tau_\rho \left(\frac{c}{\gamma}\right)^3 \gamma_\rho^2 d\gamma_\rho \quad (\text{A } 6)$$

Since γ and c may be treated as constants in the integration with respect to γ_ρ , Eq. A6 may be rewritten as follows:

$$\frac{\gamma^3 T}{2\pi c^3} = \int_0^\gamma \tau_\rho \gamma_\rho^2 d\gamma_\rho \quad (\text{A } 7)$$

But if it can be assumed that the shearing stress is some function of the shearing strain (and angle of twist to which the strain is proportional), then

$$\tau_\rho = f(\gamma_\rho) \quad (\text{A } 8)$$

There is no need to assume what that functional relationship is, but by using Eq. A8 and letting

$$F(\gamma_\rho) = \gamma_\rho^2 f(\gamma_\rho) = \gamma_\rho^2 \tau_\rho \quad (\text{A } 9)$$

Eq. A7 may be written as follows:

$$\frac{\gamma^3 T}{2\pi c^3} = \int_0^\gamma F(\gamma_\rho) d\gamma_\rho \quad (\text{A } 10)$$

Here the function $F(\gamma_\rho)$ is not known, so the integral cannot be evaluated directly. However by taking the partial derivative with respect to γ we obtain:

$$\frac{\delta}{\delta\gamma} \int_0^\gamma F(\gamma_\rho) d\gamma_\rho = \frac{\delta}{\delta\gamma} \left(\frac{\gamma^3 T}{2\pi c^3}\right) \quad (\text{A } 11)$$

Contrails

or if we let $\int F(\gamma_\rho) d\gamma_\rho = G(\gamma_\rho)$ (A12)

it results that

$$\frac{\delta}{\delta Y} \left[G(\gamma_\rho) \right]_0^Y = \frac{1}{2\pi c^3} (3Y^2 T + Y^3 \frac{\delta T}{\delta Y}) \quad (A13)$$

Evaluating the left side of the equation for the limits given we have

$$\frac{\delta}{\delta Y} \left[G(Y) \right] = F(Y) = \tau Y^3 \quad (A14)$$

and

$$\frac{\delta}{\delta Y} \left[G(0) \right] = F(0) = 0 \quad (A15)$$

so that

$$\tau Y^3 = \frac{1}{2\pi c^3} (3Y^2 T + Y^3 \frac{\delta T}{\delta Y}) \quad (A16)$$

or

$$\tau = \frac{1}{2\pi c^3} (3T + Y \frac{\delta T}{\delta Y}) \quad (A17)$$

Equation A17 provides us with an expression from which we can determine the shearing stress τ in the outer fibers for any Y if we have test data from which to draw the curve giving the relation between the twisting moment T and the shearing strain Y in the outer fibers.

By noting that $\frac{\delta T}{\delta Y}$ is the slope of the T vs Y curve and hence for any point P on the T - Y curve

$$\frac{\delta T}{\delta Y} = \frac{T - T_0}{Y} \quad (A18)$$

where T_0 is the intercept of the tangent on the T axis, (see Fig. 100), we can substitute this relation in Eq. A17 and obtain

$$\tau = \frac{1}{2\pi c^3} (3T + Y \frac{T - T_0}{Y}) \quad (A19)$$

or

$$\tau = \frac{1}{2\pi c^3} (4T - T_0) \quad (A20)$$

Equation A20 gives the relationships in the most convenient form for use in determining τ from the T vs Y curve. However $Y = c\theta/\rho$ where: θ' is the

Contrails

angle of twist in radians in a length l . $\theta' = \theta/57.3$ where θ is expressed in degrees so that $\gamma = c\theta/57.3l = K\theta$ where K is a constant for a given specimen if the dimensions do not change during twisting. Since plots of T vs θ were made as a part of routine calculations of data, true stresses computed were determined from the T vs. θ curves available rather than replotting T versus γ .

In application of Eq. A20 to actual curves obtained experimentally it should be pointed out that difficulties are frequently encountered. In the case of the metals which exhibit a sharp drop in the torque at the yield point the stress at the circumference as calculated by Eq. A20 would have an unreasonably large negative value due to the very high T_0 for the falling portion of the curve. This is evidence of non-homogeneous yielding. Strain-aging which depends upon a function of time, temperature, and strain would lead to an inhomogeneity across the section which is a function of the strain.

If the T vs. γ (or T vs. θ) curve does not continue to increase all the way to fracture but passes through a maximum, the slope of the tangent, horizontal at this maximum point, would be zero. Hence, the term $\frac{\delta T}{\delta \gamma}$ in Eq. A17 would go to zero giving the maximum stress:

$$\tau_{\max} = \frac{3 T_{\max}}{2\pi c^3} \quad (A21)$$

The modulus of rupture was defined earlier in terms of the same T and c as:

$$\text{Modulus of rupture} = \frac{T_{\max} c}{J} = \frac{2 T_{\max}}{\pi c^3} \quad (A22)$$

By comparison of Eqs. A21 and A22 it can be seen that, for specimens for which a horizontal tangent was observed in the T vs θ diagram, the actual maximum shearing stress is equal to three-fourths of the modulus of rupture.

Contrails

APPENDIX II.

Discussion of a General Equation for Flow.

A general expression relating stress, strain, temperature and strain-rate for plastic deformation has been proposed by Hollomon and Lubahn (47, 48, 67) and is based on a series of simple relationships among different pairs of these variables obtained by holding other pairs constant. These relationships are:

$$\sigma = A \epsilon^m \left| \dot{\epsilon}, T_R \right. \quad (B 1)$$

$$\sigma = B \dot{\epsilon}^n \left| \epsilon, T_R \right. \quad (B 2)$$

$$Q/R = T_R \left(\ln P - \ln \dot{\epsilon} / \dot{\epsilon}_0 \right) \left| \sigma, \epsilon \right. \quad (B 3)$$

Equation B3 expresses the same relationships as the expression for the parameter P which is defined and discussed briefly in Section 9b. From these three relationships (Eqs. B1, B2 and B3) Lubahn (67) shows how the equation

$$\sigma = CG^{T_R} \left(\frac{\dot{\epsilon}}{\dot{\epsilon}_0} \right)^{DT_R} e^{(E - FT_R) \ln \frac{\dot{\epsilon}}{\dot{\epsilon}_0}} \quad (B 4)$$

can be developed. In this equation C, D, E, F, G and $\dot{\epsilon}_0$ are constants of the material. T_R is the absolute temperature, ϵ is the true strain and $\dot{\epsilon}$, the true strain-rate. The term G^{T_R} is added to the equation as presented earlier (47, 48).

For constant $\dot{\epsilon}$, Eq. 4 becomes

$$\sigma = CG^{T_R(H)} e^{DT_R(E + IT_R)} \quad (B 5)$$

where H and I are new constants. However

$$(H)^{DT_R} = (H^D)^{T_R} = L^{T_R} \quad (B 6)$$

where L is another constant. Combining the two constants, G and L which have the exponent T_R , we have the constant N and thus

$$\sigma = GN^{T_R} e^{(E + IT_R)} \quad (B 7)$$

Contrails

Written in logarithmic form this becomes

$$\ln \sigma = \ln C + T_R \ln N + (E + IT_R) \ln \epsilon \quad (B 8)$$

which in terms of simplified constants W and M is

$$\ln \sigma = W + MT_R + (E + IT_R) \ln \epsilon \quad (B 9)$$

For constant ϵ we have

$$\ln \sigma = W + MT_R + X + ST_R = U + VT_R \quad (B10)$$

with simplified constants.

For application directly to torsion the two-dimensional relation expressed in Equations B1, B2, and B10 can be written as follows:

$$\tau \Big|_{\dot{\gamma}, T_R} = a \dot{\gamma}^b \quad (B11)$$

$$\tau \Big|_{\gamma, T_R} = d \dot{\gamma}^n \quad (B12)$$

$$\ln \tau \Big|_{\dot{\gamma}, \gamma} = g + h T_R \quad (B13)$$

where a, b, d, g, h and n are material constants.

APPENDIX III.

Discussion of the Velocity-Modified Temperature Parameter

In order to simplify the study of the influence of temperature and time (or rate of strain) on the flow stress or stress at a given inelastic strain it has been proposed that the number of significant variables may be reduced. Since the effects of temperature and rate of strain are believed to be inter-related, MacGregor and Fisher (70, 71) have proposed that instead of expressing the flow stress as a function of three variables, absolute temperature, strain-rate and strain, as:

$$\sigma = f(T_R, \dot{\epsilon}, \epsilon) \quad (C 1)$$

the first two could be combined in a "velocity-modified temperature" T_m leaving

$$\sigma = f(T_m, \epsilon) \quad (C 2)$$

An expression for determining T_m was also proposed:

$$T_m = T_R \left(1 - k \ln \frac{\dot{\epsilon}}{\dot{\epsilon}_0} \right) \quad (C 3)$$

where: $\dot{\epsilon}_0$ is an arbitrary reference strain-rate and k is a constant for the material selected (presumably by trial and error) so that when stress is plotted versus T_m a smooth curve results. This expression was developed from a theory proposed earlier by Eyring (24) based on an absolute reaction-rate and an expression of secondary creep developed by Kauzmann (58).

This concept was examined by MacGregor and Fisher in terms of tensile data, some of which was original and some borrowed from the literature, and general agreement was observed for the materials and ranges of variables reported.

For torsional test data the shearing strain-rate may be used and the absolute temperature T_R selected for use here is in terms of the Rankine scale. Thus, the shearing stress in torsion, according to this concept

Contrails

would be

$$\tau = f(T_m, \gamma) \quad (C 4)$$

and because of the approximate relationship of torque T to shearing stress τ , and of the shearing strain γ to the angle of twist θ , this function can be rewritten as

$$T = f(T_m, \theta) \quad (C 5)$$

Contrails

APPENDIX IV

Tables of Individual Test Results

Table 1. Torsion Properties of SAE 1018 Steel at Room Temperature.

FIRST SPEED	Specimen No.	1-2	1-34	1-66			Average
Proportional Limit, 1000 psi		20.3	26.7	28.4			25.1
Yield Strength, 1000 psi							
Yield Point (Upper), 1000 psi		27.0	26.7	28.4			27.4
Yield Point (Lower), 1000 psi		25.4	25.8	24.9			25.4
Modulus of Rupture, 1000 psi		60.5	69.2	70.8			66.8
Shearing Strain, in/in		2.00	2.26	2.76			2.34
Energy Absorbed, in-lb		2,690	3,350	4,080			3,370

SECOND SPEED	Specimen No.	1-1	1-18	1-49	1-65		Average
Proportional Limit, 1000 psi		29.9	30.2	28.8	14.7		25.9
Yield Strength, 1000 psi							
Yield Point (Upper), 1000 psi		31.5	30.2	29.4	30.0		30.3
Yield Point (Lower), 1000 psi		25.3	24.5	24.8	24.4		24.8
Modulus of Rupture, 1000 psi			70.4	69.3	70.0		69.9
Shearing Strain, in/in			2.84	2.58	2.84		2.75
Energy Absorbed, in-lb			4,310	3,870	4,320		4,170

THIRD SPEED	Specimen No.	1-3	1-17	1-35	1-67	1-85	Average
Proportional Limit, 1000 psi		37.9	39.2		24.8	33.2	33.8
Yield Strength, 1000 psi							
Yield Point (Upper), 1000 psi		39.4	39.2	38.1	35.3	39.2	38.2
Yield Point (Lower), 1000 psi		30.3	32.0	29.9	28.4	33.7	30.9
Modulus of Rupture, 1000 psi			67.5		65.4	73.1	68.7
Shearing Strain, in/in			2.61	2.96	2.78	2.22	2.64
Energy Absorbed, in-lb			3,890	4,410	4,040	3,470	3,950

FOURTH SPEED	Specimen No.	1-14	1-42	1-52	1-68	1-36	Average
Proportional Limit, 1000 psi		51.0	50.5	41.3			47.6
Yield Strength, 1000 psi							
Yield Point (Upper), 1000 psi		51.0	50.5	41.3			47.6
Yield Point (Lower), 1000 psi		36.4	36.5	37.3			36.7
Modulus of Rupture, 1000 psi		67.0	67.3	68.8			67.7
Shearing Strain, in/in		2.22	2.17	2.13	2.38	2.23	2.25
Energy Absorbed, in-lb		3,540	3,310	3,450			3,430

Contrails

Table 2. Torsion Properties of SAE 1018 Steel at 400°F (Not Aged)

FIRST SPEED	Specimen No.	1-9	1-64	1-125			Average
Proportional Limit, 1000 psi		26.7	14.7	27.7			23.0
Yield Strength, 1000 psi							
Yield Point (Upper), 1000 psi		26.7	26.5	28.0			27.1
Yield Point (Lower), 1000 psi		24.3	20.2	27.4			24.0
Modulus of Rupture, 1000 psi		73.1	72.1	83.2			76.1
Shearing Strain, in/in		0.90	0.94	0.83			0.89
Energy Absorbed, in-lb		1,378	1,410	1,420			1,400

SECOND SPEED	Specimen No.	1-13	1-69	1-126			Average
Proportional Limit, 1000 psi		25.7	26.6	27.4			26.6
Yield Strength, 1000 psi							
Yield Point (Upper), 1000 psi		25.7	26.6	27.4			26.6
Yield Point (Lower), 1000 psi		22.8	25.5	24.7			24.3
Modulus of Rupture, 1000 psi		68.6	74.4	76.3			73.1
Shearing Strain, in/in		1.37	1.21	1.29			1.29
Energy Absorbed, in-lb		1,920	1,880	2,030			1,940

THIRD SPEED	Specimen No.	1-29	1-73	1-129			Average
Proportional Limit, 1000 psi		27.5	30.1	28.0			28.5
Yield Strength, 1000 psi							
Yield Point (Upper), 1000 psi		27.5	30.1	28.0			28.5
Yield Point (Lower), 1000 psi		22.6	27.7	26.2			25.5
Modulus of Rupture, 1000 psi		70.9	74.5	74.0			73.1
Shearing Strain, in/in		2.03	1.50	1.62			1.72
Energy Absorbed, in-lb		2,910	2,380	2,480			2,590

FOURTH SPEED	Specimen No.	1-30	1-94	1-130			Average
Proportional Limit, 1000 psi		25.1	44.8	38.2			36.0
Yield Strength, 1000 psi							
Yield Point (Upper), 1000 psi		44.3	44.8	38.2			42.4
Yield Point (Lower), 1000 psi		23.4	26.7	27.1			25.7
Modulus of Rupture, 1000 psi		73.1	77.8	72.5			74.5
Shearing Strain, in/in		2.24	1.96	1.85			2.02
Energy Absorbed, in-lb		3,490	3,120	2,750			3,120

Contrails

Table 3. Torsion Properties of SAE 1018 Steel at 400°F (Aged)

FIRST SPEED	Specimen No.	1-53	1-55	1-84	1-87	Average
Proportional Limit, 1000 psi		27.0	23.9	27.4	28.5	26.7
Yield Strength, 1000 psi						
Yield Point (Upper), 1000 psi		27.0	23.9	27.4	28.5	26.7
Yield Point (Lower), 1000 psi		25.0	21.5	25.8	27.6	25.0
Modulus of Rupture, 1000 psi		68.7	68.0	81.5	82.0	75.1
Shearing Strain, in/in		0.87	0.98	0.89	0.85	0.90
Energy Absorbed, in-lb		1,260	1,420	1,480	1,480	1,410

SECOND SPEED	Specimen No.	1-22	1-56	1-88	Average
Proportional Limit, 1000 psi		25.4	27.0	28.1	26.8
Yield Strength, 1000 psi					
Yield Point (Upper), 1000 psi		25.4	27.0	28.1	26.8
Yield Point (Lower), 1000 psi		22.6	22.1	25.0	23.2
Modulus of Rupture, 1000 psi		68.9	68.6	76.6	71.4
Shearing Strain, in/in		1.52	1.49	1.32	1.44
Energy Absorbed, in-lb		2,170	2,130	2,110	2,140

THIRD SPEED	Specimen No.	1-21	1-57	Average
Proportional Limit, 1000 psi		27.3	29.7	28.5
Yield Strength, 1000 psi				
Yield Point (Upper), 1000 psi		27.3	29.7	28.5
Yield Point (Lower), 1000 psi		22.1	22.6	22.4
Modulus of Rupture, 1000 psi		70.8	70.2	70.5
Shearing Strain, in/in		2.16	1.95	2.06
Energy Absorbed, in-lb		3,160	2,860	3,010

FOURTH SPEED	Specimen No.	1-24	1-54	1-90	Average
Proportional Limit, 1000 psi		35.4	35.9	37.3	36.2
Yield Strength, 1000 psi					
Yield Point (Upper), 1000 psi		35.4	35.9	37.3	36.2
Yield Point (Lower), 1000 psi		21.4	25.2	30.0	25.5
Modulus of Rupture, 1000 psi		67.8	69.4	78.9	72.0
Shearing Strain, in/in		2.65	2.28	2.27	2.40
Energy Absorbed, in-lb		4,080	3,160	3,730	3,660

Contrails

Table 4. Torsion Properties of SAE 1018 Steel at 700°F (Not Aged)

FIRST SPEED	Specimen No.	1-31	1-93	1-133			Average
Proportional Limit, 1000 psi		13.2	14.0	15.7			14.3
Yield Strength, 1000 psi		16.6	17.4	20.7			18.2
Yield Point (Upper), 1000 psi							
Yield Point (Lower), 1000 psi							
Modulus of Rupture, 1000 psi		57.3	60.3	66.9			61.5
Shearing Strain, in/in		3.18	3.08	3.24			3.17
Energy Absorbed, in-lb		4,190	4,260	4,900			4,450
SECOND SPEED	Specimen No.	1-45	1-95	1-134			Average
Proportional Limit, 1000 psi		13.9	16.4				15.2
Yield Strength, 1000 psi		17.6	19.7				18.7
Yield Point (Upper), 1000 psi							
Yield Point (Lower), 1000 psi							
Modulus of Rupture, 1000 psi		60.6	69.5	71.0			67.0
Shearing Strain, in/in		2.18	2.40	2.13			2.24
Energy Absorbed, in-lb		2,940	3,580	3,220			3,250
THIRD SPEED	Specimen No.	1-41	1-111	1-135			Average
Proportional Limit, 1000 psi		19.9	22.8	22.5			21.7
Yield Strength, 1000 psi							
Yield Point (Upper), 1000 psi		19.9	22.8	22.5			21.7
Yield Point (Lower), 1000 psi		19.1	22.0	21.6			20.9
Modulus of Rupture, 1000 psi		60.4	66.8	68.8			65.3
Shearing Strain, in/in		1.44	1.34	1.31			1.36
Energy Absorbed, in-lb		1,910	1,930	1,940			1,930
FOURTH SPEED	Specimen No.	1-40	1-96	1-152			Average
Proportional Limit, 1000 psi		29.0	29.6	18.4			25.7
Yield Strength, 1000 psi							
Yield Point (Upper), 1000 psi		29.0	29.6	25.4			28.0
Yield Point (Lower), 1000 psi		22.8	25.8	21.6			23.4
Modulus of Rupture, 1000 psi		67.6	74.0	67.4			69.7
Shearing Strain, in/in		1.70	1.38	1.55			1.54
Energy Absorbed, in-lb		2,420	2,150	2,120			2,230

Contrails

Table 5. Torsion Properties of SAE 1018 Steel at 700°F (Aged)

FIRST SPEED	Specimen No.	1-25	1-89	1-109			Average
Proportional Limit, 1000 psi		11.1	15.4	13.4			13.3
Yield Strength, 1000 psi		16.5	21.0	16.6			18.0
Yield Point (Upper), 1000 psi							
Yield Point (Lower), 1000 psi							
Modulus of Rupture, 1000 psi		61.8	62.9	61.5			62.1
Shearing Strain, in/in		3.30	2.76	2.67			2.91
Energy Absorbed, in-lb		4,340	4,110	3,290			3,910

SECOND SPEED	Specimen No.	1-26	1-91	1-117			Average
Proportional Limit, 1000 psi		16.9	18.9	17.8			17.9
Yield Strength, 1000 psi		17.7	19.5	19.8			19.0
Yield Point (Upper), 1000 psi							
Yield Point (Lower), 1000 psi							
Modulus of Rupture, 1000 psi		62.5	67.6	68.3			66.1
Shearing Strain, in/in		2.46	2.55	1.91			2.31
Energy Absorbed, in-lb		3,390	3,950	2,920			3,420

THIRD SPEED	Specimen No.	1-27	1-59	1-121			Average
Proportional Limit, 1000 psi		18.2	21.0	23.0			20.7
Yield Strength, 1000 psi							
Yield Point (Upper), 1000 psi		20.9	21.0	23.0			21.6
Yield Point (Lower), 1000 psi		19.1	19.0	22.4			20.2
Modulus of Rupture, 1000 psi		60.9	60.6	68.6			63.4
Shearing Strain, in/in		1.51	1.39	1.14			1.35
Energy Absorbed, in-lb		2,020	1,880	1,720			1,870

FOURTH SPEED	Specimen No.	1-28	1-60	1-92			Average
Proportional Limit, 1000 psi		25.6	26.2	26.2			26.0
Yield Strength, 1000 psi							
Yield Point (Upper), 1000 psi		25.6	26.2	26.2			26.0
Yield Point (Lower), 1000 psi		22.0	20.6	20.6			21.1
Modulus of Rupture, 1000 psi		65.7	65.5	73.2			68.1
Shearing Strain, in/in		1.57	1.54	1.28			1.46
Energy Absorbed, in-lb		2,090	2,040	1,860			2,000

Contrails

**Table 6 . Torsion Properties of SAE 1018 Steel at 1000°F
(Not Aged)**

FIRST SPEED	Specimen No.	1-74	1-113	1-147		Average
Proportional Limit, 1000 psi		10.40	3.64	2.98		5.7
Yield Strength, 1000 psi		14.0	8.27	7.72		10.0
Yield Point (Upper), 1000 psi						
Yield Point (Lower), 1000 psi						
Modulus of Rupture, 1000 psi		23.3	24.1	21.7		23.0
Shearing Strain, in/in		7.67	5.55	17.00		10.07
Energy Absorbed, in-lb		3,130	2,840	6,530		4,170

SECOND SPEED	Specimen No.	1-61	1-114	1-148		Average
Proportional Limit, 1000 psi		15.1	16.1	10.2		13.8
Yield Strength, 1000 psi		16.0	18.5	14.0		16.2
Yield Point (Upper), 1000 psi						
Yield Point (Lower), 1000 psi						
Modulus of Rupture, 1000 psi		31.5	34.1	30.5		32.0
Shearing Strain, in/in		7.38	5.02	8.48		6.96
Energy Absorbed, in-lb		5,250	3,870	5,770		4,960

THIRD SPEED	Specimen No.	1-63	1-115	1-119	1-143	Average
Proportional Limit, 1000 psi		8.7	15.0	19.0	14.5	14.3
Yield Strength, 1000 psi		13.6	19.4	21.2	17.2	17.9
Yield Point (Upper), 1000 psi						
Yield Point (Lower), 1000 psi						
Modulus of Rupture, 1000 psi		36.2	41.0	40.4	36.2	38.5
Shearing Strain, in/in		4.42	3.48	3.81	4.52	4.06
Energy Absorbed, in-lb			2,810	2,860	3,310	2,990

FOURTH SPEED	Specimen No.	1-62	1-116	1-142	1-146	Average
Proportional Limit, 1000 psi		22.2	22.4	21.3	22.6	22.1
Yield Strength, 1000 psi		24.3	25.5	21.8	23.2	23.7
Yield Point (Upper), 1000 psi						
Yield Point (Lower), 1000 psi						
Modulus of Rupture, 1000 psi		52.6	55.0	45.2	48.8	50.4
Shearing Strain, in/in		3.05	2.73	3.06	3.34	3.05
Energy Absorbed, in-lb		3,030	2,620	2,550	3,050	2,810

Contrails

Table 7. Torsion Properties of SAE 1018 Steel at 1000°F (Aged)

FIRST SPEED	Specimen No.	1-123	1-131	1-151		Average
Proportional Limit, 1000 psi		12.3	12.1	12.5		12.3
Yield Strength, 1000 psi		14.4	14.8	13.7		14.3
Yield Point (Upper), 1000 psi						
Yield Point (Lower), 1000 psi						
Modulus of Rupture, 1000 psi		22.9	19.9	19.1		21.6
Shearing Strain, in/in		6.64	7.53	9.18		7.78
Energy Absorbed, in-lb		3,240	3,400	3,130		3,260

SECOND SPEED	Specimen No.	1-124	1-136	1-150		Average
Proportional Limit, 1000 psi		15.6	13.1	13.7		14.1
Yield Strength, 1000 psi		17.8	15.2	15.7		16.2
Yield Point (Upper), 1000 psi						
Yield Point (Lower), 1000 psi						
Modulus of Rupture, 1000 psi		32.6	30.8	29.4		30.9
Shearing Strain, in/in		5.97	8.08	9.11		7.72
Energy Absorbed, in-lb		4,440	5,550	6,020		5,340

THIRD SPEED	Specimen No.	1-127	1-137	1-155		Average
Proportional Limit, 1000 psi		13.5	12.1	11.5		12.4
Yield Strength, 1000 psi		15.0	13.2	13.2		13.8
Yield Point (Upper), 1000 psi						
Yield Point (Lower), 1000 psi						
Modulus of Rupture, 1000 psi		29.0	26.6	26.2		27.3
Shearing Strain, in/in		3.87	4.85	4.76		4.49
Energy Absorbed, in-lb		2,270	2,290	2,520		2,360

FOURTH SPEED	Specimen No.	1-128	1-140	1-154		Average
Proportional Limit, 1000 psi		18.2	20.8	17.3		18.8
Yield Strength, 1000 psi		20.4	21.3	18.2		20.0
Yield Point (Upper), 1000 psi						
Yield Point (Lower), 1000 psi						
Modulus of Rupture, 1000 psi		53.3	48.5	49.0		50.3
Shearing Strain, in/in		3.03	3.23	3.06		3.11
Energy Absorbed, in-lb		3,070	3,010	2,800		2,960

Contrails

Table 8. Torsion Properties of SAE 4340 Steel at Room Temperature.

FIRST SPEED	Specimen No.	2-85	2-88	2-100			Average
Proportional Limit, 1000 psi		91.5	97.7	100.0			96.4
Yield Strength, 1000 psi		113.0	108.0	110.0			110.3
Yield Point (Upper), 1000 psi							
Yield Point (Lower), 1000 psi							
Modulus of Rupture, 1000 psi		138.0	135.0	139.0			137.3
Shearing Strain, in/in		0.88	0.81	0.92			0.87
Energy Absorbed, in-lb		2,900	2,550	2,900			2,780

SECOND SPEED	Specimen No.	2-40	2-92	2-113			Average
Proportional Limit, 1000 psi		85.6	92.4	97.0			91.7
Yield Strength, 1000 psi		103.0	105.0	108.0			105.3
Yield Point (Upper), 1000 psi							
Yield Point (Lower), 1000 psi							
Modulus of Rupture, 1000 psi		137.0	134.6	139.0			136.9
Shearing Strain, in/in		0.87	1.05	0.99			0.97
Energy Absorbed, in-lb		2,760	3,310	3,160			3,080

THIRD SPEED	Specimen No.	2-93	2-99	2-109	2-121	2-123	Average
Proportional Limit, 1000 psi		106.3	90.0	84.0	82.5	100.0	92.6
Yield Strength, 1000 psi		118.5	109.0	98.0	98.5	110.0	106.8
Yield Point (Upper), 1000 psi							
Yield Point (Lower), 1000 psi							
Modulus of Rupture, 1000 psi		143.8	136.0	125.0	135.2	136.0	133.2
Shearing Strain, in/in		0.80	1.23	1.09	0.61	0.63	0.87
Energy Absorbed, in-lb		2,660	3,880	3,130	1,980	1,960	

FOURTH SPEED	Specimen No.	2-68	2-104	2-110	2-122		Average
Proportional Limit, 1000 psi		118.0	106.8	96.5	110.0		107.8
Yield Strength, 1000 psi		119.0		111.0	115.0		115.0
Yield Point (Upper), 1000 psi							
Yield Point (Lower), 1000 psi							
Modulus of Rupture, 1000 psi		137.7	140.5	137.0	141.0		139.1
Shearing Strain, in/in		0.36	0.38	0.52	0.44		0.43
Energy Absorbed, in-lb		1,220	1,240	1,590	1,340		1,350

Contrails

**Table 9. Torsion Properties of SAE 4340 Steel at 400°F
(Not Aged)**

FIRST SPEED	Specimen No.					Average
	2-42	2-95	2-111			
Proportional Limit, 1000 psi	69.4	69.2	66.0			68.2
Yield Strength, 1000 psi	85.7	90.7	81.9			86.1
Yield Point (Upper), 1000 psi						
Yield Point (Lower), 1000 psi						
Modulus of Rupture, 1000 psi	138.6	140.4	147.0			142.0
Shearing Strain, in/in	0.96	0.97	0.88			0.94
Energy Absorbed, in-lb	3040	3,030	2,790			2,950

SECOND SPEED	Specimen No.					Average
	2-36	2-112	2-126			
Proportional Limit, 1000 psi	80.5	82.4	79.1			80.6
Yield Strength, 1000 psi	90.0	94.0	91.5			91.8
Yield Point (Upper), 1000 psi						
Yield Point (Lower), 1000 psi						
Modulus of Rupture, 1000 psi	131.5	133.7	132.2			132.5
Shearing Strain, in/in	0.85	0.87	0.77			0.83
Energy Absorbed, in-lb	2,500	2,580	2,270			2,450

THIRD SPEED	Specimen No.					Average
	2-35	2-89	2-127			
Proportional Limit, 1000 psi	77.8	68.3	74.5			73.5
Yield Strength, 1000 psi	92.5	85.8	91.3			89.9
Yield Point (Upper), 1000 psi						
Yield Point (Lower), 1000 psi						
Modulus of Rupture, 1000 psi	122.5	122.8	125.1			123.5
Shearing Strain, in/in	0.98	1.13	1.09			1.07
Energy Absorbed, in-lb	2,750	3,180	3,050			2,990

FOURTH SPEED	Specimen No.					Average
	2-86	2-90	2-114			
Proportional Limit, 1000 psi	95.0	83.8	96.0			91.6
Yield Strength, 1000 psi	99.7	98.6	98.7			99.0
Yield Point (Upper), 1000 psi						
Yield Point (Lower), 1000 psi						
Modulus of Rupture, 1000 psi	119.0	116.4	119.0			118.1
Shearing Strain, in/in	0.52	0.48	0.48			0.49
Energy Absorbed, in-lb	1,360	1,280	1,230			1,290

**Table 10. Torsion Properties of SAE 4340 Steel at 400°F
(Aged)**

FIRST SPEED	Specimen No.	2-55	2-57	2-67	2-75	Average
Proportional Limit, 1000 psi		75.0	70.5	50.5	70.2	66.6
Yield Strength, 1000 psi		84.6	89.3	62.4	77.2	78.4
Yield Point (Upper), 1000 psi						
Yield Point (Lower), 1000 psi						
Modulus of Rupture, 1000 psi		116.1	153.0	140.4	147.0	139.1
Shearing Strain, in/in		0.82	0.70	0.95	0.85	0.83
Energy Absorbed, in-lb		2,130	2,290	2,704	2,590	2,430
SECOND SPEED	Specimen No.	2-28	2-58	2-76		Average
Proportional Limit, 1000 psi		76.0	77.0	77.1		76.7
Yield Strength, 1000 psi		89.6	90.4	89.7		89.9
Yield Point (Upper), 1000 psi						
Yield Point (Lower), 1000 psi						
Modulus of Rupture, 1000 psi		117.2	132.3	128.5		126.0
Shearing Strain, in/in		0.86	0.84	0.74		0.81
Energy Absorbed, in-lb		2,480	2,480	2,110		2,360
THIRD SPEED	Specimen No.	2-51	2-65	2-77		Average
Proportional Limit, 1000 psi		71.2	77.9	72.1		73.7
Yield Strength, 1000 psi		85.2	93.1	86.4		88.2
Yield Point (Upper), 1000 psi						
Yield Point (Lower), 1000 psi						
Modulus of Rupture, 1000 psi		118.3	126.2	122.1		122.2
Shearing Strain, in/in		1.03	0.70	0.99		0.91
Energy Absorbed, in-lb		2,840	2,000	2,720		2,520
FOURTH SPEED	Specimen No.	2-64	2-78	2-136		Average
Proportional Limit, 1000 psi		100.5	101.2	106.1		102.6
Yield Strength, 1000 psi		100.7	101.4	106.7		102.9
Yield Point (Upper), 1000 psi						
Yield Point (Lower), 1000 psi						
Modulus of Rupture, 1000 psi		120.2	118.0	124.0		120.7
Shearing Strain, in/in		0.57	0.57	0.59		0.58
Energy Absorbed, in-lb		1,530	1,480	1,630		1,550

Contrails

**Table 11. Torsion Properties of SAE 4340 Steel at 700°F
(Not Aged)**

FIRST SPEED	Specimen No.	2-39	2-115	2-129		Average
Proportional Limit, 1000 psi		57.0	57.0	50.2		54.7
Yield Strength, 1000 psi		76.2	77.0	77.4		76.9
Yield Point (Upper), 1000 psi						
Yield Point (Lower), 1000 psi						
Modulus of Rupture, 1000 psi		111.1	110.0	113.6		111.6
Shearing Strain, in/in		1.49	1.83	1.73		1.68
Energy Absorbed, in-lb		3,890	4,750	4,560		4,400
SECOND SPEED	Specimen No.	2-43	2-116	2-130		Average
Proportional Limit, 1000 psi		57.4	70.5	66.7		64.9
Yield Strength, 1000 psi		83.5	80.5	82.1		82.0
Yield Point (Upper), 1000 psi						
Yield Point (Lower), 1000 psi						
Modulus of Rupture, 1000 psi		115.2	116.4	115.3		115.6
Shearing Strain, in/in		1.23	1.41	1.49		1.38
Energy Absorbed, in-lb		3,380	3,810	4,060		3,750
THIRD SPEED	Specimen No.	2-41	2-103	2-117		Average
Proportional Limit, 1000 psi		74.5	66.1	65.1		68.6
Yield Strength, 1000 psi		89.8	80.1	83.4		84.4
Yield Point (Upper), 1000 psi						
Yield Point (Lower), 1000 psi						
Modulus of Rupture, 1000 psi		126.0	118.2	117.5		120.6
Shearing Strain, in/in		0.82	0.88	0.77		0.82
Energy Absorbed, in-lb		2,090	2,190	1,920		2,070
FOURTH SPEED	Specimen No.	2-102	2-118	2-132		Average
Proportional Limit, 1000 psi		82.0	89.5	85.5		85.7
Yield Strength, 1000 psi		88.5	98.5	91.3		92.8
Yield Point (Upper), 1000 psi						
Yield Point (Lower), 1000 psi						
Modulus of Rupture, 1000 psi		114.0	120.3	119.7		118.0
Shearing Strain, in/in		0.78	0.72	0.65		0.72
Energy Absorbed, in-lb		1,750	1,780	1,620		1,720

Contrails

Table 12. Torsion Properties of SAE 4340 at 700°F (Aged)

FIRST SPEED	Specimen No.	2-53	2-63	2-79		Average
Proportional Limit, 1000 psi		62.6	72.3	61.0		65.3
Yield Strength, 1000 psi		71.5	88.4	69.0		76.3
Yield Point (Upper), 1000 psi						
Yield Point (Lower), 1000 psi						
Modulus of Rupture, 1000 psi		105.0	116.0	115.1		112.0
Shearing Strain, in/in		1.37	1.34	1.30		1.34
Energy Absorbed, in-lb		3,340	3,550	3,320		3,400

SECOND SPEED	Specimen No.	2-32	2-54	2-80		Average
Proportional Limit, 1000 psi		65.4	62.5	61.3		63.1
Yield Strength, 1000 psi		78.5	82.5	78.5		79.8
Yield Point (Upper), 1000 psi						
Yield Point (Lower), 1000 psi						
Modulus of Rupture, 1000 psi		114.0	117.6	117.0		116.2
Shearing Strain, in/in		1.34	1.16	1.25		1.25
Energy Absorbed, in-lb		3,650	3,180	3,460		3,430

THIRD SPEED	Specimen No.	2-33	2-61	2-83		Average
Proportional Limit, 1000 psi		74.0	64.9	65.1		68.0
Yield Strength, 1000 psi		85.0	83.6	79.0		82.5
Yield Point (Upper), 1000 psi						
Yield Point (Lower), 1000 psi						
Modulus of Rupture, 1000 psi		117.6	118.6	115.2		117.1
Shearing Strain, in/in		0.81	0.70	0.80		0.77
Energy Absorbed, in-lb		2,140	1,850	1,960		1,980

FOURTH SPEED	Specimen No.	2-52	2-62	2-82		Average
Proportional Limit, 1000 psi		98.0	91.2	85.5		91.6
Yield Strength, 1000 psi		100.0	91.4	87.4		92.9
Yield Point (Upper), 1000 psi						
Yield Point (Lower), 1000 psi						
Modulus of Rupture, 1000 psi		113.8	117.9	114.5		115.4
Shearing Strain, in/in		0.71	0.64	0.70		0.68
Energy Absorbed, in-lb		1,800	1,620	1,720		1,710

Contrails

Table 13. Torsion Properties of SAE 4340 Steel at 1000°F
(Not Aged)

FIRST SPEED	Specimen No.	2-38	2-44	2-49	2-105	2-133	Average
Proportional Limit, 1000 psi		31.6		34.8	35.1	37.8	34.8
Yield Strength, 1000 psi		43.8		46.7	44.5	49.1	46.0
Yield Point (Upper), 1000 psi							
Yield Point (Lower), 1000 psi							
Modulus of Rupture, 1000 psi		54.5		56.1		58.6	56.4
Shearing Strain, in/in		4.97	3.68	4.40		3.94	4.25
Energy Absorbed, in-lb		4,750		4,460		4,170	4,460

SECOND SPEED	Specimen No.	2-34	2-87	2-106			Average
Proportional Limit, 1000 psi		47.8	50.6	49.1			49.2
Yield Strength, 1000 psi		61.5	62.0	60.6			61.4
Yield Point (Upper), 1000 psi							
Yield Point (Lower), 1000 psi							
Modulus of Rupture, 1000 psi		71.3	72.5	71.0			71.6
Shearing Strain, in/in		2.69	2.64	2.97			2.77
Energy Absorbed, in-lb		3,920	3,720	4,170			3,940

THIRD SPEED	Specimen No.	2-37	2-107	2-135			Average
Proportional Limit, 1000 psi		56.9	56.6	57.6			57.0
Yield Strength, 1000 psi		69.8	71.4	69.5			70.2
Yield Point (Upper), 1000 psi							
Yield Point (Lower), 1000 psi							
Modulus of Rupture, 1000 psi		85.1	88.9	86.6			86.9
Shearing Strain, in/in		1.30	1.04	1.19			1.18
Energy Absorbed, in-lb		1,790	1,600	1,680			1,690

FOURTH SPEED	Specimen No.	2-108	2-120	2-134			Average
Proportional Limit, 1000 psi		67.2	78.8	77.5			74.5
Yield Strength, 1000 psi		71.9	83.5	84.4			79.9
Yield Point (Upper), 1000 psi							
Yield Point (Lower), 1000 psi							
Modulus of Rupture, 1000 psi		93.5	99.5	103.4			98.8
Shearing Strain, in/in		1.10	1.29	1.19			1.19
Energy Absorbed, in-lb		1,680	1,970	1,810			1,820

Contrails

Table 14. Torsion Properties of SAE 4340 Steel at 1000°F (Aged)

FIRST SPEED	Specimen No.	2-1	2-9	2-19	Average
Proportional Limit, 1000 psi		37.0	30.0	38.5	35.2
Yield Strength, 1000 psi		48.0	43.5	47.8	46.4
Yield Point (Upper), 1000 psi					
Yield Point (Lower), 1000 psi					
Modulus of Rupture, 1000 psi		57.5	53.2	57.5	56.1
Shearing Strain, in/in		5.18	5.00	4.78	4.99
Energy Absorbed, in-lb		5,280	4,750	4,410	4,810
SECOND SPEED	Specimen No.	2-2	2-10	2-20	Average
Proportional Limit, 1000 psi		46.6	50.0	44.1	46.9
Yield Strength, 1000 psi		61.1	59.1	58.9	59.7
Yield Point (Upper), 1000 psi					
Yield Point (Lower), 1000 psi					
Modulus of Rupture, 1000 psi		69.0	68.3	69.4	68.9
Shearing Strain, in/in		3.29	3.31	3.04	3.21
Energy Absorbed, in-lb		4,510	4,550	4,190	4,420
THIRD SPEED	Specimen No.	2-3	2-11	2-21	Average
Proportional Limit, 1000 psi		60.8	59.2	59.1	59.7
Yield Strength, 1000 psi		69.0	67.1	66.2	67.4
Yield Point (Upper), 1000 psi					
Yield Point (Lower), 1000 psi					
Modulus of Rupture, 1000 psi		84.5	79.5	79.6	81.2
Shearing Strain, in/in		1.15	1.26	1.14	1.18
Energy Absorbed, in-lb		1,690	1,740	1,570	1,670
FOURTH SPEED	Specimen No.	2-4	2-12	2-22	Average
Proportional Limit, 1000 psi		80.5	79.8	80.4	80.2
Yield Strength, 1000 psi		81.2	80.8	81.1	81.0
Yield Point (Upper), 1000 psi					
Yield Point (Lower), 1000 psi					
Modulus of Rupture, 1000 psi		96.5	98.0	97.9	97.5
Shearing Strain, in/in		1.59	1.25	1.24	1.36
Energy Absorbed, in-lb		2,170	1,950	1,800	1,970

Contrails

Table 15. Torsion Properties of SAE 4340 Steel at 1200°F (Not Aged)

FIRST SPEED	Specimen No.	2-45	2-69	2-101		Average
Proportional Limit, 1000 psi		2.6	3.5	3.8		3.3
Yield Strength, 1000 psi		4.7	6.7	7.7		6.3
Yield Point (Upper), 1000 psi						
Yield Point (Lower), 1000 psi						
Modulus of Rupture, 1000 psi		12.1	12.4	13.0		12.5
Shearing Strain, in/in		5.68	7.80	8.25		7.31
Energy Absorbed, in-lb		1280	2020	2130		1810

SECOND SPEED	Specimen No.	2-46	2-72	2-119		Average
Proportional Limit, 1000 psi		24.6	21.8	20.7		22.4
Yield Strength, 1000 psi		27.6	24.7	23.0		25.1
Yield Point (Upper), 1000 psi						
Yield Point (Lower), 1000 psi						
Modulus of Rupture, 1000 psi		33.9	30.0	27.2		30.4
Shearing Strain, in/in		8.10	9.87	6.15		8.03
Energy Absorbed, in-lb		4,970	5,280	2,920		4,390

THIRD SPEED	Specimen No.	2-47	2-73	2-125		Average
Proportional Limit, 1000 psi		34.8	36.8	31.3		34.3
Yield Strength, 1000 psi		42.9	42.1	40.4		41.8
Yield Point (Upper), 1000 psi						
Yield Point (Lower), 1000 psi						
Modulus of Rupture, 1000 psi		49.3	49.3	47.7		48.8
Shearing Strain, in/in		3.97	3.37	3.65		3.66
Energy Absorbed, in-lb		3,030	2,640	2,660		2,710

FOURTH SPEED	Specimen No.	2-56	2-74	2-96		Average
Proportional Limit, 1000 psi		66.3	58.6	75.5		66.8
Yield Strength, 1000 psi		67.3	64.0	78.6		70.0
Yield Point (Upper), 1000 psi						
Yield Point (Lower), 1000 psi						
Modulus of Rupture, 1000 psi		71.0	72.0	87.4		76.8
Shearing Strain, in/in		4.33	2.51	2.10		2.98
Energy Absorbed, in-lb		4,200	2,660	2,820		3,230

Contrails

Table 16. Torsion Properties of SAE 4340 Steel at 1200°F (Aged)

FIRST SPEED	Specimen No.					Average
Proportional Limit, 1000 psi	2-141 1.6	2-143 1.3	2-147 0.9			1.3
Yield Strength, 1000 psi	3.7	4.3	6.2			4.7
Yield Point (Upper), 1000 psi						
Yield Point (Lower), 1000 psi						
Modulus of Rupture, 1000 psi	11.5	12.8	9.4			11.2
Shearing Strain, in/in	8.71	7.99	9.45			8.72
Energy Absorbed, in-lb	2,200	1280	1,900			1,730
SECOND SPEED	Specimen No.					Average
Proportional Limit, 1000 psi	23.6	20.6	22.0			22.1
Yield Strength, 1000 psi	25.8	24.2	25.3			25.1
Yield Point (Upper), 1000 psi						
Yield Point (Lower), 1000 psi						
Modulus of Rupture, 1000 psi	28.9	26.7	28.9			28.2
Shearing Strain, in/in	10.80	9.28	11.59			10.58
Energy Absorbed, in-lb	5,450	4,400	5,720			5,190
THIRD SPEED	Specimen No.					Average
Proportional Limit, 1000 psi	24.2	19.7	26.0			23.3
Yield Strength, 1000 psi	29.4	25.6	30.0			28.3
Yield Point (Upper), 1000 psi						
Yield Point (Lower), 1000 psi						
Modulus of Rupture, 1000 psi	35.0	30.0	37.7			34.2
Shearing Strain, in/in	4.48	5.02	4.84			4.78
Energy Absorbed, in-lb	2,850	2,710	3,290			2,950
FOURTH SPEED	Specimen No.					Average
Proportional Limit, 1000 psi	42.5	45.7	38.2			42.1
Yield Strength, 1000 psi	43.1	46.5	40.0			43.2
Yield Point (Upper), 1000 psi						
Yield Point (Lower), 1000 psi						
Modulus of Rupture, 1000 psi	49.6	53.2	48.5			50.4
Shearing Strain, in/in	3.92	4.25	4.00			4.06
Energy Absorbed, in-lb	3,350	4,030	3,450			3,610

Table 17. Torsion Properties of 24S-T Aluminum Alloy at Room Temperature

FIRST SPEED	Specimen No.	3-2	3-34	3-66		Average
Proportional Limit, 1000 psi		24.7	24.0	22.6		23.8
Yield Strength, 1000 psi		27.5	30.2	29.8		29.2
Yield Point (Upper), 1000 psi						
Yield Point (Lower), 1000 psi						
Modulus of Rupture, 1000 psi		59.7	59.5	59.2		59.5
Shearing Strain, in/in		0.51	0.52	0.57		0.53
Energy Absorbed, in-lb		660	660	730		680

SECOND SPEED	Specimen No.	3-1	3-31	3-65		Average
Proportional Limit, 1000 psi		18.4	23.5	18.3		20.1
Yield Strength, 1000 psi		29.7	26.0	29.5		28.4
Yield Point (Upper), 1000 psi						
Yield Point (Lower), 1000 psi						
Modulus of Rupture, 1000 psi		58.4	57.4	55.9		57.2
Shearing Strain, in/in		0.55	0.58	0.51		0.55
Energy Absorbed, in-lb		690	710	520		640

THIRD SPEED	Specimen No.	3-3	3-35	3-67		Average
Proportional Limit, 1000 psi		21.9	19.0	23.9		21.6
Yield Strength, 1000 psi		30.6	29.9	30.7		30.4
Yield Point (Upper), 1000 psi						
Yield Point (Lower), 1000 psi						
Modulus of Rupture, 1000 psi		56.5	57.2	56.2		56.6
Shearing Strain, in/in		0.52	0.54	0.52		0.53
Energy Absorbed, in-lb		650	660	620		640

FOURTH SPEED	Specimen No.	3-52	3-58	3-98		Average
Proportional Limit, 1000 psi		38.5	37.1	33.1		36.2
Yield Strength, 1000 psi		38.8	38.4	35.4		37.5
Yield Point (Upper), 1000 psi						
Yield Point (Lower), 1000 psi						
Modulus of Rupture, 1000 psi		57.5	56.7	56.4		56.9
Shearing Strain, in/in		0.52	0.52	0.50		0.51
Energy Absorbed, in-lb		610	630	600		610

Contrails

Table 18. Torsion Properties of 24S-T Aluminum Alloy at 200°F
(Not Aged)

FIRST SPEED	Specimen No.	3-113	3-119	3-155			Average
Proportional Limit, 1000 psi		26.6	26.0	28.5			27.0
Yield Strength, 1000 psi		34.8	32.5	34.7			34.0
Yield Point (Upper), 1000 psi							
Yield Point (Lower), 1000 psi							
Modulus of Rupture, 1000 psi		61.1	59.7	64.2			61.7
Shearing Strain, in/in		0.89	0.93	0.82			0.88
Energy Absorbed, in-lb		1,240	1,240	1,080			1,190

SECOND SPEED	Specimen No.	3-73	3-120	3-149			Average
Proportional Limit, 1000 psi		24.0	26.8	27.0			25.9
Yield Strength, 1000 psi		33.6	32.2	32.8			32.9
Yield Point (Upper), 1000 psi							
Yield Point (Lower), 1000 psi							
Modulus of Rupture, 1000 psi		57.8	57.7	58.9			58.1
Shearing Strain, in/in		0.57	0.54	0.51			0.54
Energy Absorbed, in-lb		710	660	630			670

THIRD SPEED	Specimen No.	3-37	3-69	3-121			Average
Proportional Limit, 1000 psi		27.4	28.0	22.1			25.8
Yield Strength, 1000 psi		32.7	33.2	31.6			32.5
Yield Point (Upper), 1000 psi							
Yield Point (Lower), 1000 psi							
Modulus of Rupture, 1000 psi		53.8	55.2	54.4			54.5
Shearing Strain, in/in		0.51	0.51	0.47			0.50
Energy Absorbed, in-lb		600	600	550			580

FOURTH SPEED	Specimen No.	3-112	3-114	3-122			Average
Proportional Limit, 1000 psi		36.3	25.4	32.2			31.3
Yield Strength, 1000 psi		39.3	29.7	37.5			35.5
Yield Point (Upper), 1000 psi							
Yield Point (Lower), 1000 psi							
Modulus of Rupture, 1000 psi		61.2	64.2	60.0			61.8
Shearing Strain, in/in		0.45	0.45	0.47			0.46
Energy Absorbed, in-lb		600	630	600			610

Contrails

Table 19. Torsion Properties of 24S-T Aluminum Alloy at 200°F (Aged)

FIRST SPEED	Specimen No.	3-19	3-21	3-132		Average
Proportional Limit, 1000 psi		25.9	21.7	23.6		23.7
Yield Strength, 1000 psi		35.7	29.2	28.3		31.1
Yield Point (Upper), 1000 psi						
Yield Point (Lower), 1000 psi						
Modulus of Rupture, 1000 psi		63.8	58.8	62.8		61.8
Shearing Strain, in/in		1.17	1.00	0.84		1.00
Energy Absorbed, in-lb		1,730	1,320	1,030		1,360

SECOND SPEED	Specimen No.	3-54	3-84	3-86		Average
Proportional Limit, 1000 psi		24.2	23.2	26.3		24.6
Yield Strength, 1000 psi		31.4	32.6	32.9		32.3
Yield Point (Upper), 1000 psi						
Yield Point (Lower), 1000 psi						
Modulus of Rupture, 1000 psi		56.4	58.6	59.5		58.2
Shearing Strain, in/in		0.62	0.62	0.63		0.62
Energy Absorbed, in-lb		880	780	820		830

THIRD SPEED	Specimen No.	3-53	3-85	3-133		Average
Proportional Limit, 1000 psi		30.0	28.8	22.0		26.9
Yield Strength, 1000 psi		33.2	34.0	30.2		32.5
Yield Point (Upper), 1000 psi						
Yield Point (Lower), 1000 psi						
Modulus of Rupture, 1000 psi		56.9	56.4	55.6		56.3
Shearing Strain, in/in		0.49	0.51	0.50		0.50
Energy Absorbed, in-lb		590	610	590		600

FOURTH SPEED	Specimen No.	3-24	3-56	3-88		Average
Proportional Limit, 1000 psi		28.0	27.8	38.9		31.6
Yield Strength, 1000 psi		36.3	40.9	41.5		39.6
Yield Point (Upper), 1000 psi						
Yield Point (Lower), 1000 psi						
Modulus of Rupture, 1000 psi		61.8	62.3	62.8		62.3
Shearing Strain, in/in		0.50	0.42	0.49		0.47
Energy Absorbed, in-lb		630	560	640		610

Contrails

**Table 20. Torsion Properties of 24S-T Aluminum Alloy at 400°F
(Not Aged)**

FIRST SPEED	Specimen No.	3-105	3-123	3-143			Average
Proportional Limit, 1000 psi		24.9	26.4	29.5			26.9
Yield Strength, 1000 psi		35.5	30.5	34.7			33.6
Yield Point (Upper), 1000 psi							
Yield Point (Lower), 1000 psi							
Modulus of Rupture, 1000 psi		44.5	37.2	43.2			41.6
Shearing Strain, in/in		0.45	0.49	0.46			0.47
Energy Absorbed, in-lb		420	380	460			420

SECOND SPEED	Specimen No.	3-115	3-126	3-150			Average
Proportional Limit, 1000 psi		21.0	21.8	28.1			23.6
Yield Strength, 1000 psi		30.0	29.2	34.9			31.4
Yield Point (Upper), 1000 psi							
Yield Point (Lower), 1000 psi							
Modulus of Rupture, 1000 psi		48.3	50.0	46.9			48.4
Shearing Strain, in/in		0.76	0.76	0.62			0.71
Energy Absorbed, in-lb		820	850	670			780

THIRD SPEED	Specimen No.	3-45	3-109	3-125			Average
Proportional Limit, 1000 psi		30.8	33.0	29.2			31.0
Yield Strength, 1000 psi		36.8	38.5	30.9			35.4
Yield Point (Upper), 1000 psi							
Yield Point (Lower), 1000 psi							
Modulus of Rupture, 1000 psi		46.2	44.2	45.5			45.3
Shearing Strain, in/in		0.62	0.50	0.60			0.57
Energy Absorbed, in-lb		550	490	620			550

FOURTH SPEED	Specimen No.	3-72	3-106	3-110			Average
Proportional Limit, 1000 psi		24.1	29.9	29.8			27.9
Yield Strength, 1000 psi		32.1	26.2	32.7			35.3
Yield Point (Upper), 1000 psi							
Yield Point (Lower), 1000 psi							
Modulus of Rupture, 1000 psi		49.8	49.8	48.2			49.3
Shearing Strain, in/in		0.38	0.22	0.40			0.33
Energy Absorbed, in-lb		430	240	470			380

Contrails

Table 21. Torsion Properties of 24S-T Aluminum Alloy at 400°F (Aged)

FIRST SPEED	Specimen No.	3-25	3-83	3-134		Average
Proportional Limit, 1000 psi		21.0	24.0	19.8		21.6
Yield Strength, 1000 psi		25.6	28.2	22.6		25.5
Yield Point (Upper), 1000 psi						
Yield Point (Lower), 1000 psi						
Modulus of Rupture, 1000 psi		28.4	28.9	26.0		27.8
Shearing Strain, in/in		0.54	0.52	0.77		0.61
Energy Absorbed, in-lb		310	310	390		340

SECOND SPEED	Specimen No.	3-90	3-136	3-156		Average
Proportional Limit, 1000 psi		26.0	22.5	14.4		21.0
Yield Strength, 1000 psi		32.2	27.4	21.5		27.0
Yield Point (Upper), 1000 psi						
Yield Point (Lower), 1000 psi						
Modulus of Rupture, 1000 psi		38.3	33.4	28.7		33.5
Shearing Strain, in/in		0.83	1.04	1.38		1.08
Energy Absorbed, in-lb		700	740	880		770

THIRD SPEED	Specimen No.	3-57	3-89	3-137		Average
Proportional Limit, 1000 psi		29.8	28.2	16.7		24.9
Yield Strength, 1000 psi		32.5	36.5	23.8		30.9
Yield Point (Upper), 1000 psi						
Yield Point (Lower), 1000 psi						
Modulus of Rupture, 1000 psi		38.9	43.7	34.0		38.9
Shearing Strain, in/in		0.77	0.71	1.04		0.84
Energy Absorbed, in-lb		640	660	750		680

FOURTH SPEED	Specimen No.	3-28	3-60	3-92		Average
Proportional Limit, 1000 psi		34.1	27.2	32.1		31.1
Yield Strength, 1000 psi		38.3	32.1	36.6		35.7
Yield Point (Upper), 1000 psi						
Yield Point (Lower), 1000 psi						
Modulus of Rupture, 1000 psi		48.1	47.7	46.5		47.4
Shearing Strain, in/in		0.29	0.32	0.27		0.29
Energy Absorbed, in-lb		300	340	270		300

Contrails

Table 22. Torsion Properties of 24S-T Aluminum Alloy at 600°F
(Not Aged)

FIRST SPEED	Specimen No.	3-116	3-127	3-151		Average
Proportional Limit, 1000 psi		5.9	6.3	7.3		6.5
Yield Strength, 1000 psi		7.7	7.9	10.5		8.7
Yield Point (Upper), 1000 psi						
Yield Point (Lower), 1000 psi						
Modulus of Rupture, 1000 psi		8.3	8.8	12.3		9.8
Shearing Strain, in/in		1.42	1.83	1.67		1.64
Energy Absorbed, in-lb		180	290	290		250

SECOND SPEED	Specimen No.	3-41	3-111	3-128		Average
Proportional Limit, 1000 psi		10.2	12.1	10.6		11.0
Yield Strength, 1000 psi		12.8	13.1	14.1		13.3
Yield Point (Upper), 1000 psi						
Yield Point (Lower), 1000 psi						
Modulus of Rupture, 1000 psi		14.9	14.5	16.2		15.2
Shearing Strain, in/in		1.42	1.55	1.47		1.48
Energy Absorbed, in-lb		420	410	460		430

THIRD SPEED	Specimen No.	3-13	3-107	3-129	3-153	Average
Proportional Limit, 1000 psi		16.4	17.2	15.2	16.2	16.3
Yield Strength, 1000 psi		17.7	18.0	18.0	17.0	17.7
Yield Point (Upper), 1000 psi						
Yield Point (Lower), 1000 psi						
Modulus of Rupture, 1000 psi		20.3	22.7	23.0	19.7	21.4
Shearing Strain, in/in		1.67	2.07	1.76	1.37	1.72
Energy Absorbed, in-lb		690	840	750	510	700

FOURTH SPEED	Specimen No.	3-20	3-130	3-154		Average
Proportional Limit, 1000 psi		21.1	15.4	25.0		20.6
Yield Strength, 1000 psi		21.4	18.9	21.5		20.6
Yield Point (Upper), 1000 psi						
Yield Point (Lower), 1000 psi						
Modulus of Rupture, 1000 psi		25.7	28.4	27.8		27.3
Shearing Strain, in/in		0.75	1.14	0.94		0.94
Energy Absorbed, in-lb		390	680	480		520

Contrails

Table 23. Torsion Properties of 24S-T Aluminum Alloy at 600°F (Aged)

FIRST SPEED	Specimen No.	3-140	3-142	3-157		Average
Proportional Limit, 1000 psi		2.6	3.3	1.6		2.5
Yield Strength, 1000 psi		4.9	5.3	2.9		4.4
Yield Point (Upper), 1000 psi						
Yield Point (Lower), 1000 psi						
Modulus of Rupture, 1000 psi		5.5	6.2	3.3		5.0
Shearing Strain, in/in		2.86	2.13	4.33		3.11
Energy Absorbed, in-lb		330	270	290		300

SECOND SPEED	Specimen No.	3-18	3-94	3-158		Average
Proportional Limit, 1000 psi		4.1	5.1	5.9		5.0
Yield Strength, 1000 psi		6.5	5.9	6.5		6.3
Yield Point (Upper), 1000 psi						
Yield Point (Lower), 1000 psi						
Modulus of Rupture, 1000 psi		8.7	7.5	7.6		7.9
Shearing Strain, in/in		6.51	6.25	7.34		6.70
Energy Absorbed, in-lb		1,030	990	1,010		1,010

THIRD SPEED	Specimen No.	3-117	3-139	3-159		Average
Proportional Limit, 1000 psi		7.5	7.9	7.5		7.6
Yield Strength, 1000 psi		8.7	9.0	8.6		8.8
Yield Point (Upper), 1000 psi						
Yield Point (Lower), 1000 psi						
Modulus of Rupture, 1000 psi		13.0	13.5	12.5		13.0
Shearing Strain, in/in		6.73	7.20	11.0		8.31
Energy Absorbed, in-lb		1,620	1,780	2,550		1,980

FOURTH SPEED	Specimen No.	3-32	3-64	3-100		Average
Proportional Limit, 1000 psi		7.0	10.8	9.0		8.9
Yield Strength, 1000 psi		8.6	12.3	10.7		10.5
Yield Point (Upper), 1000 psi						
Yield Point (Lower), 1000 psi						
Modulus of Rupture, 1000 psi		14.4	19.4	18.6		17.5
Shearing Strain, in/in		2.30	2.31	2.28		2.30
Energy Absorbed, in-lb		710	940	900		850

Contrails

Table 24. Torsion Properties of 75S-T Aluminum Alloy at Room Temperature

FIRST SPEED	Specimen No.	4-1	4-3	4-74	4-80	4-103	Average
Proportional Limit, 1000 psi		35.8	40.3	29.6	33.9	35.0	34.9
Yield Strength, 1000 psi		46.7	47.7	41.8	43.0	48.2	45.5
Yield Point (Upper), 1000 psi							
Yield Point (Lower), 1000 psi							
Modulus of Rupture, 1000 psi		64.3	67.5	63.7	64.5	71.3	66.3
Shearing Strain, in/in		0.45	0.37	0.46	0.50	0.45	0.45
Energy Absorbed, in-lb		670	560	670	740	730	670

SECOND SPEED	Specimen No.	4-11	4-17	4-19			Average
Proportional Limit, 1000 psi		39.4	37.4	33.4			36.7
Yield Strength, 1000 psi		45.6	49.2	44.6			46.5
Yield Point (Upper), 1000 psi							
Yield Point (Lower), 1000 psi							
Modulus of Rupture, 1000 psi		63.5	68.9	63.3			65.2
Shearing Strain, in/in		0.31	0.34	0.38			0.34
Energy Absorbed, in-lb		460	530	540			510

THIRD SPEED	Specimen No.	4-23	4-31	4-39			Average
Proportional Limit, 1000 psi		33.8	47.5	43.0			41.4
Yield Strength, 1000 psi		44.5	55.1	51.0			50.2
Yield Point (Upper), 1000 psi							
Yield Point (Lower), 1000 psi							
Modulus of Rupture, 1000 psi		65.0	74.1	72.0			70.4
Shearing Strain, in/in		0.31	0.27	0.30			0.29
Energy Absorbed, in-lb		450	450	480			460

FOURTH SPEED	Specimen No.	4-6	4-34	4-46	4-60	4-98	Average
Proportional Limit, 1000 psi		50.9	52.5	46.0	49.4	50.0	49.8
Yield Strength, 1000 psi		55.6	57.8	54.4	54.6	55.7	55.6
Yield Point (Upper), 1000 psi							
Yield Point (Lower), 1000 psi							
Modulus of Rupture, 1000 psi		72.3	71.0	71.0	72.4	70.6	71.5
Shearing Strain, in/in		0.30	0.27	0.30	0.26	0.30	0.29
Energy Absorbed, in-lb		470	420	450	430	470	450

Contrails

**Table 25. Torsion Properties of 75S-T Aluminum Alloy
at 200 F (Not Aged)**

FIRST SPEED	Specimen No.	4-10	4-48	4-75			Average
Proportional Limit, 1000 psi		36.7	36.2	33.0			35.3
Yield Strength, 1000 psi		45.6	42.8	37.9			42.1
Yield Point (Upper), 1000 psi							
Yield Point (Lower), 1000 psi							
Modulus of Rupture, 1000 psi		60.3	56.4	50.7			55.8
Shearing Strain, in/in		0.67	0.65	0.74			0.69
Energy Absorbed, in-lb		1030	870	850			920

SECOND SPEED	Specimen No.	4-12	4-51	4-76			Average
Proportional Limit, 1000 psi		38.2	44.9	32.1			38.4
Yield Strength, 1000 psi		45.7	48.8	41.9			45.5
Yield Point (Upper), 1000 psi							
Yield Point (Lower), 1000 psi							
Modulus of Rupture, 1000 psi		64.1	64.9	65.6			64.9
Shearing Strain, in/in		0.50	0.50	0.57			0.52
Energy Absorbed, in-lb		720	750	850			770

THIRD SPEED	Specimen No.	4-16	4-65	4-77			Average
Proportional Limit, 1000 psi		43.3	45.0	37.5			41.9
Yield Strength, 1000 psi		49.0	50.6	48.0			49.2
Yield Point (Upper), 1000 psi							
Yield Point (Lower), 1000 psi							
Modulus of Rupture, 1000 psi		65.4	64.7	65.8			65.3
Shearing Strain, in/in		0.34	0.37	0.34			0.35
Energy Absorbed, in-lb		500	550	500			520

FOURTH SPEED	Specimen No.	4-26	4-66	4-78			Average
Proportional Limit, 1000 psi		52.3	46.8	44.9			48.0
Yield Strength, 1000 psi		55.0	54.7	58.0			55.9
Yield Point (Upper), 1000 psi							
Yield Point (Lower), 1000 psi							
Modulus of Rupture, 1000 psi		70.5	71.8	71.1			71.1
Shearing Strain, in/in		0.28	0.26	0.27			0.27
Energy Absorbed, in-lb		440	430	430			430

Contrails

**Table 26. Torsion Properties of 75S-T Aluminum Alloy
at 200°F (Aged)**

FIRST SPEED	Specimen No.	4-4	4-38	4-64			Average
Proportional Limit, 1000 psi		38.4	43.2	46.2			42.6
Yield Strength, 1000 psi		49.1	49.5	51.2			49.9
Yield Point (Upper), 1000 psi							
Yield Point (Lower), 1000 psi							
Modulus of Rupture, 1000 psi		61.9	60.4	66.8			63.0
Shearing Strain, in/in		0.67	0.72	0.73			0.71
Energy Absorbed, in-lb		1,050	1,000	1,100			1,050

SECOND SPEED	Specimen No.	4-2	4-22	4-62			Average
Proportional Limit, 1000 psi		39.2	37.2	35.7			37.4
Yield Strength, 1000 psi		49.6	47.8	46.9			48.1
Yield Point (Upper), 1000 psi							
Yield Point (Lower), 1000 psi							
Modulus of Rupture, 1000 psi		64.3	63.0	65.9			64.4
Shearing Strain, in/in		0.53	0.45	0.46			0.48
Energy Absorbed, in-lb		830	640	670			710

THIRD SPEED	Specimen No.	4-16	4-55	4-61			Average
Proportional Limit, 1000 psi		38.1	41.9	40.0			40.0
Yield Strength, 1000 psi		48.1	48.2	48.5			48.3
Yield Point (Upper), 1000 psi							
Yield Point (Lower), 1000 psi							
Modulus of Rupture, 1000 psi		65.0	65.4	66.0			65.5
Shearing Strain, in/in		0.34	0.35	0.33			0.34
Energy Absorbed, in-lb		470	510	560			510

FOURTH SPEED	Specimen No.	4-18	4-32	4-36			Average
Proportional Limit, 1000 psi		47.0	49.8	40.8			45.9
Yield Strength, 1000 psi		59.8	56.4	50.2			55.5
Yield Point (Upper), 1000 psi							
Yield Point (Lower), 1000 psi							
Modulus of Rupture, 1000 psi		70.0	70.1	66.2			68.8
Shearing Strain, in/in		0.24	0.25	0.24			0.24
Energy Absorbed, in-lb		370	390	330			360

Contrails

**Table 27. Tension Properties of 75S-T Aluminum Alloy
at 400° F (Not Aged)**

FIRST SPEED	Specimen No.	4-35	4-67	4-79			Average
Proportional Limit, 1000 psi		10.6	22.4	19.4			17.5
Yield Strength, 1000 psi		22.3	25.6	24.4			24.1
Yield Point (Upper), 1000 psi							
Yield Point (Lower), 1000 psi							
Modulus of Rupture, 1000 psi		26.8	28.0	27.5			27.4
Shearing Strain, in/in		1.18	1.23	1.35			1.25
Energy Absorbed, in-lb		510	560	690			590
SECOND SPEED	Specimen No.	4-30	4-82	4-102			Average
Proportional Limit, 1000 psi		18.1	29.0	29.4			25.5
Yield Strength, 1000 psi		30.3	32.7	33.8			32.3
Yield Point (Upper), 1000 psi							
Yield Point (Lower), 1000 psi							
Modulus of Rupture, 1000 psi		35.7	37.5	38.3			37.2
Shearing Strain, in/in		0.88	1.05	0.95			0.96
Energy Absorbed, in-lb		700	870	750			770
THIRD SPEED	Specimen No.	4-37	4-69	4-85			Average
Proportional Limit, 1000 psi		30.5	30.0	29.0			29.8
Yield Strength, 1000 psi		33.8	33.4	32.6			33.3
Yield Point (Upper), 1000 psi							
Yield Point (Lower), 1000 psi							
Modulus of Rupture, 1000 psi		38.3	39.4	36.4			38.0
Shearing Strain, in/in		0.97	0.83	0.87			0.89
Energy Absorbed, in-lb		960	700	700			790
FOURTH SPEED	Specimen No.	4-40	4-70	4-86			Average
Proportional Limit, 1000 psi		30.4	35.0	38.3			34.6
Yield Strength, 1000 psi		40.0	46.5	42.4			43.0
Yield Point (Upper), 1000 psi							
Yield Point (Lower), 1000 psi							
Modulus of Rupture, 1000 psi		45.7	56.3	50.1			50.7
Shearing Strain, in/in		0.34	0.31	0.31			0.32
Energy Absorbed, in-lb		420	400	350			390

Contrails

**Table 28. Tension Properties of 75S-T Aluminum Alloy
at 400°F (Aged)**

FIRST SPEED	Specimen No.	4-7	4-49	4-96			Average
Proportional Limit, 1000 psi		13.5	4.5	6.6			8.2
Yield Strength, 1000 psi		16.2	6.0	13.3			11.8
Yield Point (Upper), 1000 psi							
Yield Point (Lower), 1000 psi							
Modulus of Rupture, 1000 psi		17.0	17.0	15.0			16.3
Shearing Strain, in/in		2.64	3.50	2.93			3.02
Energy Absorbed, in-lb		870	990	880			910

SECOND SPEED	Specimen No.	4-27	4-59	4-63			Average
Proportional Limit, 1000 psi		14.6	12.0	14.7			13.8
Yield Strength, 1000 psi		16.5	15.6	16.8			16.3
Yield Point (Upper), 1000 psi							
Yield Point (Lower), 1000 psi							
Modulus of Rupture, 1000 psi		17.3	19.0	19.0			18.4
Shearing Strain, in/in		5.74	4.89	4.87			5.17
Energy Absorbed, in-lb		2,290	2,050	2,030			2,120

THIRD SPEED	Specimen No.	4-9	4-53	4-71			Average
Proportional Limit, 1000 psi		11.7	14.0	9.9			11.9
Yield Strength, 1000 psi		14.4	16.8	16.1			15.8
Yield Point (Upper), 1000 psi							
Yield Point (Lower), 1000 psi							
Modulus of Rupture, 1000 psi		21.7	22.8	22.8			22.4
Shearing Strain, in/in		4.87	4.89	4.32			4.69
Energy Absorbed, in-lb		2,160	2,100	2,040			2,100

FOURTH SPEED	Specimen No.	4-88	4-90	4-104			Average
Proportional Limit, 1000 psi		21.2	19.0	18.4			19.5
Yield Strength, 1000 psi		22.8	21.9	21.4			22.0
Yield Point (Upper), 1000 psi							
Yield Point (Lower), 1000 psi							
Modulus of Rupture, 1000 psi		34.5	29.7	32.6			32.3
Shearing Strain, in/in		0.88	0.83	0.88			0.86
Energy Absorbed, in-lb		590	550	540			560

Contrails

Table 29. Torsion Properties of 75S-T Aluminum Alloy at 600°F
(Not Aged)

FIRST SPEED	Specimen No.	4-20	4-41	4-91	Average
Proportional Limit, 1000 psi		2.0	2.2	1.9	2.0
Yield Strength, 1000 psi		6.2	3.5	3.9	4.5
Yield Point (Upper), 1000 psi					
Yield Point (Lower), 1000 psi					
Modulus of Rupture, 1000 psi		7.5	5.0	5.7	6.1
Shearing Strain, in/in		2.61	2.63	2.77	2.67
Energy Absorbed, in-lb		370	280	280	310

SECOND SPEED	Specimen No.	4-87	4-95	4-101	Average
Proportional Limit, 1000 psi		4.0	3.6	6.1	4.6
Yield Strength, 1000 psi		5.5	7.7	7.5	6.9
Yield Point (Upper), 1000 psi					
Yield Point (Lower), 1000 psi					
Modulus of Rupture, 1000 psi		6.7	8.8	7.6	7.7
Shearing Strain, in/in		5.45	5.14	6.30	5.63
Energy Absorbed, in-lb		780	860	940	860

THIRD SPEED	Specimen No.	4-43	4-73	4-89	Average
Proportional Limit, 1000 psi		9.4	9.0	10.0	9.5
Yield Strength, 1000 psi		10.2	10.3	10.7	10.4
Yield Point (Upper), 1000 psi					
Yield Point (Lower), 1000 psi					
Modulus of Rupture, 1000 psi		11.1	12.4	11.8	11.8
Shearing Strain, in/in		7.77	8.70	7.44	7.97
Energy Absorbed, in-lb		1,810	2,190	1,850	1,950

FOURTH SPEED	Specimen No.	4-44	4-72	4-100	Average
Proportional Limit, 1000 psi		9.0	10.0	9.7	9.6
Yield Strength, 1000 psi		10.6	11.7	10.8	11.0
Yield Point (Upper), 1000 psi					
Yield Point (Lower), 1000 psi					
Modulus of Rupture, 1000 psi		16.5	15.4	15.9	15.9
Shearing Strain, in/in		2.63	2.31	2.42	2.45
Energy Absorbed, in-lb		830	770	830	810

Contrails

**Table 3Q Torsion Properties of 75S-T Aluminum Alloy at 600°F
(Aged)**

FIRST SPEED	Specimen No.	4-14	4-45	4-99	Average
Proportional Limit, 1000 psi		1.7	2.7	0.9	1.8
Yield Strength, 1000 psi		4.2	3.9	2.7	3.6
Yield Point (Upper), 1000 psi					
Yield Point (Lower), 1000 psi					
Modulus of Rupture, 1000 psi		4.9	4.3	4.3	4.5
Shearing Strain, in/in		2.66	2.44	2.69	2.60
Energy Absorbed, in-lb		290	230	240	250
SECOND SPEED	Specimen No.	4-8	4-33	4-68	Average
Proportional Limit, 1000 psi		2.7	5.3	5.9	4.6
Yield Strength, 1000 psi		7.3	6.5	6.9	6.9
Yield Point (Upper), 1000 psi					
Yield Point (Lower), 1000 psi					
Modulus of Rupture, 1000 psi		7.3	6.8	6.9	7.0
Shearing Strain, in/in		6.56	5.78	6.16	6.17
Energy Absorbed, in-lb		880	830	860	860
THIRD SPEED	Specimen No.	4-15	4-57	4-83	Average
Proportional Limit, 1000 psi		7.4	8.4	7.7	7.8
Yield Strength, 1000 psi		9.5	9.0	8.5	9.0
Yield Point (Upper), 1000 psi					
Yield Point (Lower), 1000 psi					
Modulus of Rupture, 1000 psi		12.4	12.4	11.0	11.9
Shearing Strain, in/in		7.14	5.94		6.54
Energy Absorbed, in-lb		1,900	1,500		1,700
FOURTH SPEED	Specimen No.	4-28	4-54	4-84	Average
Proportional Limit, 1000 psi		8.3	7.4	11.5	9.1
Yield Strength, 1000 psi		9.1	9.7	12.3	10.4
Yield Point (Upper), 1000 psi					
Yield Point (Lower), 1000 psi					
Modulus of Rupture, 1000 psi		16.0	15.8	15.7	15.8
Shearing Strain, in/in		2.57	2.35	3.22	2.71
Energy Absorbed, in-lb		810	770	1,120	900

Table 31. Torsion Properties of FS-1 Magnesium at Room Temperature

FIRST SPEED	Specimen No.	5-35	5-49	5-7		Average
Proportional Limit, 1000 psi		6.8	4.2	3.5		4.8
Yield Strength, 1000 psi		9.5	8.1	6.6		8.1
Yield Point (Upper), 1000 psi						
Yield Point (Lower), 1000 psi						
Modulus of Rupture, 1000 psi		36.0	34.0	35.6		35.2
Shearing Strain, in/in		0.51	0.51	0.54		0.52
Energy Absorbed, in-lb		320	310	330		320

SECOND SPEED	Specimen No.	5-2	5-34	5-66	5-70A	Average
Proportional Limit, 1000 psi		5.3	4.6	4.9	4.7	4.9
Yield Strength, 1000 psi		9.0	7.9	9.0	8.6	8.6
Yield Point (Upper), 1000 psi						
Yield Point (Lower), 1000 psi						
Modulus of Rupture, 1000 psi			31.7	31.8	29.6	31.0
Shearing Strain, in/in			0.47	0.57	0.47	0.50
Energy Absorbed, in-lb			270	290	270	280

THIRD SPEED	Specimen No.	5-19	5-23	5-37		Average
Proportional Limit, 1000 psi		5.1	6.0	7.8		6.3
Yield Strength, 1000 psi		9.1	10.4	11.5		10.3
Yield Point (Upper), 1000 psi						
Yield Point (Lower), 1000 psi						
Modulus of Rupture, 1000 psi		22.8	30.6	33.0		32.1
Shearing Strain, in/in		0.42	0.31	0.37		0.37
Energy Absorbed, in-lb		260	180	230		220

FOURTH SPEED	Specimen No.	5-28	5-58	5-84	5-86	Average
Proportional Limit, 1000 psi		13.8	15.8	11.4	15.4	14.1
Yield Strength, 1000 psi		16.3	15.9	14.0	16.5	15.7
Yield Point (Upper), 1000 psi						
Yield Point (Lower), 1000 psi						
Modulus of Rupture, 1000 psi		40.4	39.6	36.8	36.8	39.4
Shearing Strain, in/in		0.35	0.36	0.41	0.38	0.38
Energy Absorbed, in-lb		260	260	280	250	260

Contrails

**Table 32. Torsion Properties of PS-1 Magnesium at 200°F
(Not Aged)**

FIRST SPEED	Specimen No.	5-71	5-100	5-102			Average
Proportional Limit, 1000 psi		4.2	4.9	3.6			4.2
Yield Strength, 1000 psi		6.9	7.1	5.3			6.4
Yield Point (Upper), 1000 psi							
Yield Point (Lower), 1000 psi							
Modulus of Rupture, 1000 psi		35.6	32.9	32.6			33.7
Shearing Strain, in/in		1.08	1.17	1.09			1.11
Energy Absorbed, in-lb		600	700	610			640
SECOND SPEED	Specimen No.	5-1	5-11	5-29			Average
Proportional Limit, 1000 psi		4.3	2.9	6.6			4.6
Yield Strength, 1000 psi		6.2	7.2	9.5			7.6
Yield Point (Upper), 1000 psi							
Yield Point (Lower), 1000 psi							
Modulus of Rupture, 1000 psi		34.0	34.6	35.2			34.6
Shearing Strain, in/in		0.94	0.79	0.87			0.87
Energy Absorbed, in-lb		480	500	580			520
THIRD SPEED	Specimen No.	5-75	5-99	5-117			Average
Proportional Limit, 1000 psi		4.8	4.5	5.1			4.8
Yield Strength, 1000 psi		7.9	7.3	7.9			7.7
Yield Point (Upper), 1000 psi							
Yield Point (Lower), 1000 psi							
Modulus of Rupture, 1000 psi		29.3	29.7	30.8			29.9
Shearing Strain, in/in		0.53	0.53	0.56			0.54
Energy Absorbed, in-lb		280	280	310			290
FOURTH SPEED	Specimen No.	5-60	5-62	5-74			Average
Proportional Limit, 1000 psi		8.3	6.6	6.9			7.3
Yield Strength, 1000 psi		9.6	8.7	8.3			8.9
Yield Point (Upper), 1000 psi							
Yield Point (Lower), 1000 psi							
Modulus of Rupture, 1000 psi		24.7	23.8	23.2			23.9
Shearing Strain, in/in		0.44	0.48	0.42			0.45
Energy Absorbed, in-lb		200	240	170			200

Contrails

Table 33. Torsion Properties of FS-1 Magnesium at 200°F (Aged)

FIRST SPEED	Specimen No.	5-3	5-7	5-83			Average
Proportional Limit, 1000 psi		2.6	4.6	2.6			3.3
Yield Strength, 1000 psi		5.9	7.9	7.4			7.1
Yield Point (Upper), 1000 psi							
Yield Point (Lower), 1000 psi							
Modulus of Rupture, 1000 psi		32.5	31.5	32.6			32.2
Shearing Strain, in/in		1.43	1.40	1.34			1.39
Energy Absorbed, in-lb		920	850	830			870

SECOND SPEED	Specimen No.	5-68	5-88	5-90			Average
Proportional Limit, 1000 psi		4.0	5.1	2.6			3.9
Yield Strength, 1000 psi		7.4	7.1	4.6			6.4
Yield Point (Upper), 1000 psi							
Yield Point (Lower), 1000 psi							
Modulus of Rupture, 1000 psi		30.4	33.4	33.0			32.3
Shearing Strain, in/in		0.72	0.94	0.84			0.83
Energy Absorbed, in-lb		420	590	540			520

THIRD SPEED	Specimen No.	5-69	5-93	5-95			Average
Proportional Limit, 1000 psi		6.0	6.4	4.9			5.8
Yield Strength, 1000 psi		8.4	8.6	7.4			8.1
Yield Point (Upper), 1000 psi							
Yield Point (Lower), 1000 psi							
Modulus of Rupture, 1000 psi		33.8	34.4	33.5			33.9
Shearing Strain, in/in		0.63	0.60	0.56			0.60
Energy Absorbed, in-lb		390	380	350			370

FOURTH SPEED	Specimen No.	5-12	5-26	5-78			Average
Proportional Limit, 1000 psi		10.1	9.4	8.0			9.2
Yield Strength, 1000 psi		11.4	12.2	11.3			11.6
Yield Point (Upper), 1000 psi							
Yield Point (Lower), 1000 psi							
Modulus of Rupture, 1000 psi		25.1	27.8	23.9			25.6
Shearing Strain, in/in		0.45	0.45	0.45			0.45
Energy Absorbed, in-lb		220	230	200			220

Contrails

**Table 34. Torsion Properties of FS-1 Magnesium at 400°F
(Not Aged)**

FIRST SPEED	Specimen No.	5-81	5-110	5-115	Average
Proportional Limit, 1000 psi		1.7		1.3	1.5
Yield Strength, 1000 psi		3.7		3.9	3.8
Yield Point (Upper), 1000 psi					
Yield Point (Lower), 1000 psi					
Modulus of Rupture, 1000 psi		8.3	9.5	11.2	9.7
Shearing Strain, in/in		3.25	3.16	2.51	2.97
Energy Absorbed, in-lb		510	560	460	510
SECOND SPEED	Specimen No.	5-52	5-70B	5-87	Average
Proportional Limit, 1000 psi		2.9	3.0	3.4	3.1
Yield Strength, 1000 psi		4.8	4.4	5.5	4.9
Yield Point (Upper), 1000 psi					
Yield Point (Lower), 1000 psi					
Modulus of Rupture, 1000 psi		16.6	16.9	14.8	16.1
Shearing Strain, in/in		1.64	1.69	2.12	1.82
Energy Absorbed, in-lb		550	590	660	600
THIRD SPEED	Specimen No.	5-5	5-105	5-111	Average
Proportional Limit, 1000 psi		1.9	4.3	3.9	3.4
Yield Strength, 1000 psi		5.2	5.9	6.5	5.9
Yield Point (Upper), 1000 psi					
Yield Point (Lower), 1000 psi					
Modulus of Rupture, 1000 psi		22.6	24.2	22.2	23.0
Shearing Strain, in/in		1.55	1.31	1.27	1.38
Energy Absorbed, in-lb		680	630	550	620
FOURTH SPEED	Specimen No.	5-16	5-36	5-80	Average
Proportional Limit, 1000 psi		6.6	5.8	6.6	6.3
Yield Strength, 1000 psi		8.0	7.5	7.2	7.6
Yield Point (Upper), 1000 psi					
Yield Point (Lower), 1000 psi					
Modulus of Rupture, 1000 psi		22.3	21.8	21.4	21.8
Shearing Strain, in/in		1.00	0.95	0.98	0.98
Energy Absorbed, in-lb		450	420	420	430

Contrails

Table 35. Torsion Properties of RS-1 Magnesium at 400°F (Aged)

FIRST SPEED	Specimen No.	5-4	5-47	5-53	Average	
Proportional Limit, 1000 psi			1.7	1.3		1.5
Yield Strength, 1000 psi			3.6	3.5		3.6
Yield Point (Upper), 1000 psi						
Yield Point (Lower), 1000 psi						
Modulus of Rupture, 1000 psi		8.2	9.4	8.8		8.8
Shearing Strain, in/in		3.40	2.65	2.69		2.91
Energy Absorbed, in-lb		480	470	440		460

SECOND SPEED	Specimen No.	5-22	5-42	5-61	Average	
Proportional Limit, 1000 psi		3.7	2.8	3.2		3.2
Yield Strength, 1000 psi		5.4	6.0	5.3		5.6
Yield Point (Upper), 1000 psi						
Yield Point (Lower), 1000 psi						
Modulus of Rupture, 1000 psi		14.6	16.4	17.1		16.0
Shearing Strain, in/in		2.03	1.69	1.62		1.78
Energy Absorbed, in-lb		670	580	570		610

THIRD SPEED	Specimen No.	5-15	5-43	5-107	Average	
Proportional Limit, 1000 psi		5.0	3.0	3.2		3.7
Yield Strength, 1000 psi		6.6	5.5	5.2		5.8
Yield Point (Upper), 1000 psi						
Yield Point (Lower), 1000 psi						
Modulus of Rupture, 1000 psi		24.0	25.0	22.6		23.9
Shearing Strain, in/in		1.43	1.40	1.37		1.40
Energy Absorbed, in-lb		660	630	610		630

FOURTH SPEED	Specimen No.	5-32	5-44	5-82	Average	
Proportional Limit, 1000 psi		5.4	5.3	6.3		5.7
Yield Strength, 1000 psi		9.3	6.8	7.7		7.9
Yield Point (Upper), 1000 psi						
Yield Point (Lower), 1000 psi						
Modulus of Rupture, 1000 psi		22.8	22.2	22.4		22.5
Shearing Strain, in/in		1.05	0.99	0.99		1.01
Energy Absorbed, in-lb		460	440	420		440

Contrails

**Table 36. Torsion Properties of FS-1 Magnesium at 600°F
(Not Aged)**

FIRST SPEED	Specimen No.	5-13	5-101	5-119	Average
Proportional Limit, 1000 psi		0.4	0.6	0.7	0.6
Yield Strength, 1000 psi		1.1	1.5	1.4	1.3
Yield Point (Upper), 1000 psi					
Yield Point (Lower), 1000 psi					
Modulus of Rupture, 1000 psi		2.6	3.6	2.4	2.9
Shearing Strain, in/in		7.14	5.84	6.89	6.62
Energy Absorbed, in-lb		340	320	280	310

SECOND SPEED	Specimen No.	5-25	5-65	5-89	Average
Proportional Limit, 1000 psi		2.4	2.9	2.8	2.7
Yield Strength, 1000 psi		3.1	3.4	3.1	3.2
Yield Point (Upper), 1000 psi					
Yield Point (Lower), 1000 psi					
Modulus of Rupture, 1000 psi		5.3	6.0	5.4	5.6
Shearing Strain, in/in		3.80	3.18	4.27	3.75
Energy Absorbed, in-lb		430	390	430	420

THIRD SPEED	Specimen No.	5-57	5-103	5-113	Average
Proportional Limit, 1000 psi		3.4	3.7	4.1	3.7
Yield Strength, 1000 psi		4.7	4.5	4.9	4.7
Yield Point (Upper), 1000 psi					
Yield Point (Lower), 1000 psi					
Modulus of Rupture, 1000 psi		11.0	11.4	11.5	11.3
Shearing Strain, in/in		1.92	1.99	1.79	1.90
Energy Absorbed, in-lb		430	450	410	430

FOURTH SPEED	Specimen No.	5-20	5-24	5-56	Average
Proportional Limit, 1000 psi		5.2	5.8	5.4	5.5
Yield Strength, 1000 psi		5.4	6.8	5.7	6.0
Yield Point (Upper), 1000 psi					
Yield Point (Lower), 1000 psi		13			
Modulus of Rupture, 1000 psi		13.6	16.0	14.4	14.7
Shearing Strain, in/in		1.77	1.77	1.57	1.70
Energy Absorbed, in-lb		490	530	450	490

Contrails

Table 37. Torsion Properties of FS-1 Magnesium at 600°F (Aged)

FIRST SPEED	Specimen No.	5-21	5-31	5-92	Average	
Proportional Limit, 1000 psi		0.5	0.6	0.4		0.5
Yield Strength, 1000 psi		0.9	1.2	1.0		1.0
Yield Point (Upper), 1000 psi						
Yield Point (Lower), 1000 psi						
Modulus of Rupture, 1000 psi		1.9	2.7	2.2		2.3
Shearing Strain, in/in		6.61	8.41	7.11		7.38
Energy Absorbed, in-lb		220	410	310		310

SECOND SPEED	Specimen No.	5-10	5-36	5-94	Average	
Proportional Limit, 1000 psi		2.4	2.0	2.4		2.3
Yield Strength, 1000 psi		3.1	2.9	3.2		3.1
Yield Point (Upper), 1000 psi						
Yield Point (Lower), 1000 psi						
Modulus of Rupture, 1000 psi		4.4	5.4	5.8		5.2
Shearing Strain, in/in		4.04	3.49	3.83		3.79
Energy Absorbed, in-lb		340	380	410		380

THIRD SPEED	Specimen No.	5-51	5-97	Average	
Proportional Limit, 1000 psi		2.6	2.3		2.5
Yield Strength, 1000 psi		4.3	4.4		4.3
Yield Point (Upper), 1000 psi					
Yield Point (Lower), 1000 psi					
Modulus of Rupture, 1000 psi		11.8	11.1		11.5
Shearing Strain, in/in		1.72	2.06		1.89
Energy Absorbed, in-lb		410	450		430

FOURTH SPEED	Specimen No.	5-18	5-48	5-98	Average	
Proportional Limit, 1000 psi		3.5	4.0	4.8		4.1
Yield Strength, 1000 psi		5.6	4.8	6.0		5.5
Yield Point (Upper), 1000 psi						
Yield Point (Lower), 1000 psi						
Modulus of Rupture, 1000 psi		14.5	14.8	14.2		14.5
Shearing Strain, in/in		1.63	1.51	1.55		1.56
Energy Absorbed, in-lb		460	410	430		430

Table 38. Torsion Properties of RC-70 Titanium at Room Temperature

FIRST SPEED	Specimen No.	6-1	6-33	6-65			Average
Proportional Limit, 1000 psi		41.4	36.0	54.0			43.8
Yield Strength, 1000 psi		56.7	61.5	62.5			60.2
Yield Point (Upper), 1000 psi							
Yield Point (Lower), 1000 psi							
Modulus of Rupture, 1000 psi		110.7	111.5	107.7			110.0
Shearing Strain, in/in		1.35	1.34	1.28			1.32
Energy Absorbed, in-lb		3,100	3,210	2,960			3,090

SECOND SPEED	Specimen No.	6-2	6-34	6-66	6-100			Average
Proportional Limit, 1000 psi		68.7	32.7	65.2	58.6			56.3
Yield Strength, 1000 psi		83.5	65.3	72.0	68.4			72.3
Yield Point (Upper), 1000 psi								
Yield Point (Lower), 1000 psi								
Modulus of Rupture, 1000 psi		111.0	112.4	116.0	109.7			113.0
Shearing Strain, in/in		1.27	1.27	1.16	1.20			1.23
Energy Absorbed, in-lb		2,940	3,180	2,880	2,910			2,980

THIRD SPEED	Specimen No.	6-35	6-67	6-99			Average
Proportional Limit, 1000 psi		63.0	63.5	57.4			61.3
Yield Strength, 1000 psi		80.6	76.9	105.0			87.5
Yield Point (Upper), 1000 psi							
Yield Point (Lower), 1000 psi							
Modulus of Rupture, 1000 psi		104.0	100.2	131.7			112.0
Shearing Strain, in/in		1.04	0.98	1.06			1.03
Energy Absorbed, in-lb		2,480	2,240	3,310			2,680

FOURTH SPEED	Specimen No.	6-13	6-14	6-36	6-68			Average
Proportional Limit, 1000 psi		94.5	80.5	91.7	94.5			90.3
Yield Strength, 1000 psi		95.5	92.0	94.1	101.0			95.5
Yield Point (Upper), 1000 psi								
Yield Point (Lower), 1000 psi								
Modulus of Rupture, 1000 psi		108.6	110.0	109.0	114.7			110.6
Shearing Strain, in/in		0.97	0.84	1.08	0.86			0.94
Energy Absorbed, in-lb		2,510	2,180	2,750	2,440			2,470

Contrails

**Table 39. Tension Properties of RC-70 Titanium at 400°F
(Not Aged.)**

FIRST SPEED	Specimen No.	6-5	6-37	6-69			Average
Proportional Limit, 1000 psi		24.2	23.4	27.5			25.0
Yield Strength, 1000 psi							
Yield Point (Upper), 1000 psi		30.5	27.4	29.3			29.1
Yield Point (Lower), 1000 psi		29.2	26.7	28.7			28.2
Modulus of Rupture, 1000 psi		74.6	68.1	73.5			72.1
Shearing Strain, in/in		1.28	1.33	1.36			1.32
Energy Absorbed, in-lb		1,910	1,810	1,970			1,900

SECOND SPEED	Specimen No.	6-6	6-38	6-70			Average
Proportional Limit, 1000 psi		34.2	30.4	30.4			31.7
Yield Strength, 1000 psi							
Yield Point (Upper), 1000 psi		37.8	34.6	37.3			36.6
Yield Point (Lower), 1000 psi		37.2	33.3	36.0			35.5
Modulus of Rupture, 1000 psi		75.2	73.8	74.9			74.6
Shearing Strain, in/in		1.34	1.35	1.22			1.30
Energy Absorbed, in-lb		2,170	2,010	1,840			2,010

THIRD SPEED	Specimen No.	6-7	6-39	6-71			Average
Proportional Limit, 1000 psi		43.7	45.8	48.8			46.1
Yield Strength, 1000 psi							
Yield Point (Upper), 1000 psi		48.1	45.8	48.8			47.6
Yield Point (Lower), 1000 psi		46.4	43.2	46.6			44.7
Modulus of Rupture, 1000 psi		76.2	74.8	75.6			75.9
Shearing Strain, in/in		1.22	1.22	1.15			1.20
Energy Absorbed, in-lb		1,970	1,910	1,750			1,880

FOURTH SPEED	Specimen No.	6-8	6-40	6-72			Average
Proportional Limit, 1000 psi		61.2	58.5	64.9			61.5
Yield Strength, 1000 psi							
Yield Point (Upper), 1000 psi		68.4	62.4	68.7			66.5
Yield Point (Lower), 1000 psi		61.2	57.8	63.9			61.0
Modulus of Rupture, 1000 psi		83.0	82.5	89.1			84.9
Shearing Strain, in/in		1.11	1.16	1.10			1.12
Energy Absorbed, in-lb		2,150	2,090	2,120			2,120

Contrails

**Table 40. Tension Properties of RC-70 Titanium at 400°F
(Aged)**

FIRST SPEED	Specimen No.	6-17	6-49	6-109			Average
Proportional Limit, 1000 psi		21.8	21.6	30.1			24.5
Yield Strength, 1000 psi		24.6	26.0	32.0			27.5
Yield Point (Upper), 1000 psi							
Yield Point (Lower), 1000 psi							
Modulus of Rupture, 1000 psi		64.3	64.4	66.5			65.1
Shearing Strain, in/in		1.27	1.33	1.26			1.29
Energy Absorbed, in-lb		1,630	1,790	1,750			1,720

SECOND SPEED	Specimen No.	6-18	6-84	6-110			Average
Proportional Limit, 1000 psi		32.7	34.1	34.7			33.8
Yield Strength, 1000 psi							
Yield Point (Upper), 1000 psi		36.2	38.2	36.9			37.1
Yield Point (Lower), 1000 psi		35.0	37.1	35.5			35.9
Modulus of Rupture, 1000 psi		76.0	77.5	76.5			76.7
Shearing Strain, in/in		1.30	1.27	1.27			1.28
Energy Absorbed, in-lb		1,990	2,000	1,940			1,980

THIRD SPEED	Specimen No.	6-19	6-51	6-111			Average
Proportional Limit, 1000 psi		42.8	47.4	46.2			45.5
Yield Strength, 1000 psi							
Yield Point (Upper), 1000 psi		46.0	47.4	46.2			46.9
Yield Point (Lower), 1000 psi		44.5	46.4	44.2			45.0
Modulus of Rupture, 1000 psi		73.6	76.9	74.6			75.0
Shearing Strain, in/in		1.18	1.19	1.12			1.16
Energy Absorbed, in-lb		1,820	1,890	1,710			1,810

FOURTH SPEED	Specimen No.	6-20	6-52	6-82			Average
Proportional Limit, 1000 psi		67.9	75.5	72.3			71.9
Yield Strength, 1000 psi							
Yield Point (Upper), 1000 psi		67.9	75.5	72.3			71.9
Yield Point (Lower), 1000 psi		61.4	66.0	64.5			64.0
Modulus of Rupture, 1000 psi		86.3	98.3	87.9			90.8
Shearing Strain, in/in		1.18	1.13	1.23			1.18
Energy Absorbed, in-lb		2,230	2,540	2,440			2,400

Contrails

**Table 41. Torsion Properties of RC-70 Titanium at 700°F
(Not Aged)**

FIRST SPEED	Specimen No.	6-9	6-41	6-74		Average
Proportional Limit, 1000 psi		9.6	17.6	17.0		14.7
Yield Strength, 1000 psi		19.7	20.2	19.6		19.8
Yield Point (Upper), 1000 psi						
Yield Point (Lower), 1000 psi						
Modulus of Rupture, 1000 psi		54.2	51.6	51.6		52.5
Shearing Strain, in/in		1.24	1.06	1.13		1.14
Energy Absorbed, in-lb		1,350	1,100	1,170		1,210
SECOND SPEED	Specimen No.	6-10	6-42	6-74		Average
Proportional Limit, 1000 psi		14.6	19.6	17.1		17.1
Yield Strength, 1000 psi						
Yield Point (Upper), 1000 psi		20.2	22.0	21.7		21.3
Yield Point (Lower), 1000 psi		20.2	22.0	21.7		21.3
Modulus of Rupture, 1000 psi		49.1	54.7	52.4		52.1
Shearing Strain, in/in		1.42	1.21	1.36		1.33
Energy Absorbed, in-lb		1,450	1,310	1,440		1,400
THIRD SPEED	Specimen No.	6-11	6-43	6-75		Average
Proportional Limit, 1000 psi		24.4	28.5	27.8		26.9
Yield Strength, 1000 psi						
Yield Point (Upper), 1000 psi		27.9	28.5	27.8		28.1
Yield Point (Lower), 1000 psi		25.3	23.8	24.9		24.7
Modulus of Rupture, 1000 psi		51.8	49.7	50.1		50.5
Shearing Strain, in/in		1.32	1.27	1.36		1.32
Energy Absorbed, in-lb		1,370	1,240	1,390		1,330
FOURTH SPEED	Specimen No.	6-12	6-44	6-76		Average
Proportional Limit, 1000 psi		50.0	46.7	49.2		48.6
Yield Strength, 1000 psi						
Yield Point (Upper), 1000 psi		50.0	46.7	49.2		48.6
Yield Point (Lower), 1000 psi		39.1	38.0	37.1		38.1
Modulus of Rupture, 1000 psi		68.3	66.6	65.1		66.7
Shearing Strain, in/in		1.31	1.21	1.31		1.28
Energy Absorbed, in-lb		1,850	1,740	1,830		1,810

**Table 42. Tension Properties of RC-70 Titanium at 700°F
(Aged)**

FIRST SPEED	Specimen No.	6-21	6-53	6-85			Average
Proportional Limit, 1000 psi		16.4	16.2	18.9			17.2
Yield Strength, 1000 psi		19.0	19.3	21.0			19.8
Yield Point (Upper), 1000 psi							
Yield Point (Lower), 1000 psi							
Modulus of Rupture, 1000 psi		56.5	52.5	57.8			55.6
Shearing Strain, in/in		1.30	1.16	1.04			1.17
Energy Absorbed, in-lb		1,490	1,280	1,220			1,330

SECOND SPEED	Specimen No.	6-22	6-54	6-86	6-107		Average
Proportional Limit, 1000 psi		20.7	18.1	18.6	16.6		18.5
Yield Strength, 1000 psi			21.0				21.0
Yield Point (Upper), 1000 psi		21.9		23.3	22.7		22.6
Yield Point (Lower), 1000 psi		21.9		23.0	22.4		22.4
Modulus of Rupture, 1000 psi		56.2	54.0	53.6	53.3		54.3
Shearing Strain, in/in		1.40	1.45	1.38	1.35		1.40
Energy Absorbed, in-lb		1,640	1,660	1,580	1,520		1,600

THIRD SPEED	Specimen No.	6-23	6-55	6-87			Average
Proportional Limit, 1000 psi		20.9	23.5	22.8			22.4
Yield Strength, 1000 psi							
Yield Point (Upper), 1000 psi		26.3	27.9	27.8			27.3
Yield Point (Lower), 1000 psi		24.5	26.4	25.2			25.4
Modulus of Rupture, 1000 psi		51.4	54.4	52.6			52.8
Shearing Strain, in/in		1.37	1.38	1.30			1.35
Energy Absorbed, in-lb		1,440	1,550	1,400			1,460

FOURTH SPEED	Specimen No.	6-24	6-56	6-88			Average
Proportional Limit, 1000 psi		42.0	42.5	44.0			42.8
Yield Strength, 1000 psi							
Yield Point (Upper), 1000 psi		42.0	42.5	44.0			42.8
Yield Point (Lower), 1000 psi		35.6	36.0	34.7			35.4
Modulus of Rupture, 1000 psi		60.1	60.3	60.7			60.4
Shearing Strain, in/in		1.38	1.36	1.36			1.37
Energy Absorbed, in-lb		1,750	1,730	1,740			1,740

Contrails

**Table 43. Torsion Properties of RC-70 Titanium at 1000°F
(Not Aged)**

FIRST SPEED	Specimen No.	6-45	6-77	6-102			Average
Proportional Limit, 1000 psi		10.4	8.8	10.1			9.8
Yield Strength, 1000 psi		10.9	10.2	11.3			10.8
Yield Point (Upper), 1000 psi							
Yield Point (Lower), 1000 psi							
Modulus of Rupture, 1000 psi		12.1	12.3	12.2			12.2
Shearing Strain, in/in		11.34	15.50	9.11			11.98
Energy Absorbed, in-lb		2,090	2,490	1,550			2,040
SECOND SPEED	Specimen No.	6-46	6-78	6-104			Average
Proportional Limit, 1000 psi		13.0	12.0	8.3			11.1
Yield Strength, 1000 psi		14.3	13.1	13.4			13.6
Yield Point (Upper), 1000 psi							
Yield Point (Lower), 1000 psi							
Modulus of Rupture, 1000 psi		29.1	28.0	27.0			28.0
Shearing Strain, in/in		3.41	2.96	4.38			3.58
Energy Absorbed, in-lb		2,080	1,790	2,220			2,030
THIRD SPEED	Specimen No.	6-47	6-79	6-105			Average
Proportional Limit, 1000 psi		15.7	15.7	16.3			15.9
Yield Strength, 1000 psi							
Yield Point (Upper), 1000 psi		15.7	19.0	16.3			17.0
Yield Point (Lower), 1000 psi		14.9	17.6	15.4			16.0
Modulus of Rupture, 1000 psi		30.5	38.0	33.3			33.9
Shearing Strain, in/in		1.75	1.54	1.50			1.60
Energy Absorbed, in-lb		1,540	1,210	1,020			1,260
FOURTH SPEED	Specimen No.	6-16	6-48	6-80			Average
Proportional Limit, 1000 psi		31.0	32.1	34.1			32.4
Yield Strength, 1000 psi							
Yield Point (Upper), 1000 psi		31.0	32.1	34.1			32.4
Yield Point (Lower), 1000 psi		23.2	24.2	23.9			23.8
Modulus of Rupture, 1000 psi		43.3	43.9	42.6			43.3
Shearing Strain, in/in		1.65	1.68	1.61			1.65
Energy Absorbed, in-lb		1,540	1,570	1,530			1,550

Contrails

Table 44. Torsion Properties of RC-70 Titanium at 1000°F (Aged)

FIRST SPEED	Specimen No.	6-25	6-89	6-93		Average
Proportional Limit, 1000 psi		6.15	7.05	5.33		6.18
Yield Strength, 1000 psi		8.37	8.45	8.44		8.42
Yield Point (Upper), 1000 psi						
Yield Point (Lower), 1000 psi						
Modulus of Rupture, 1000 psi		10.9	11.4	11.7		11.3
Shearing Strain, in/in		11.0	13.4	12.2		12.2
Energy Absorbed, in-lb		1740	1680	2140		1850

SECOND SPEED	Specimen No.	6-26	6-58	6-90		Average
Proportional Limit, 1000 psi		9.7	10.0	10.6		10.1
Yield Strength, 1000 psi		10.5	10.7	11.5		10.9
Yield Point (Upper), 1000 psi						
Yield Point (Lower), 1000 psi						
Modulus of Rupture, 1000 psi		23.0	24.1	24.6		23.9
Shearing Strain, in/in		2.66	2.52	2.76		2.65
Energy Absorbed, in-lb		1,330	1,300	1,420		1,350

THIRD SPEED	Specimen No.	6-27	6-59	6-91		Average
Proportional Limit, 1000 psi		10.5	10.8	10.5		10.6
Yield Strength, 1000 psi						
Yield Point (Upper), 1000 psi		11.6	12.2	11.9		11.9
Yield Point (Lower), 1000 psi		11.2	11.7	11.7		11.5
Modulus of Rupture, 1000 psi		29.4	29.4	29.2		29.3
Shearing Strain, in/in		1.93	1.77	1.77		1.82
Energy Absorbed, in-lb		1,180	1,070	1,100		1,120

FOURTH SPEED	Specimen No.	6-28	6-60	6-92		Average
Proportional Limit, 1000 psi		24.7	26.8	23.4		25.0
Yield Strength, 1000 psi						
Yield Point (Upper), 1000 psi		24.7	26.8	23.4		25.0
Yield Point (Lower), 1000 psi		19.3	18.0	16.8		18.0
Modulus of Rupture, 1000 psi		37.2	37.4	36.3		37.0
Shearing Strain, in/in		1.87	1.82	1.79		1.83
Energy Absorbed, in-lb		1,410	1,430	1,390		1,410

Contrails

**Table 45. Torsion Properties of RC-130B Titanium Alloy
at Room Temperature**

FIRST SPEED	Specimen No.	7-13	7-57	7-77		Average
Proportional Limit, 1000 psi		65.6	82.8	80.3		76.2
Yield Strength, 1000 psi		96.8	97.4	98.2		97.5
Yield Point (Upper), 1000 psi						
Yield Point (Lower), 1000 psi						
Modulus of Rupture, 1000 psi		139.0	145.0	155.0		146.3
Shearing Strain, in/in		0.70	0.76	0.80		0.75
Energy Absorbed, in-lb		2,070	2,280	2,470		2,270

SECOND SPEED	Specimen No.	7-14	7-58	7-78		Average
Proportional Limit, 1000 psi		79.8	65.6	72.1		72.5
Yield Strength, 1000 psi		98.0	106.5	89.5		98.0
Yield Point (Upper), 1000 psi						
Yield Point (Lower), 1000 psi						
Modulus of Rupture, 1000 psi		138.0	153.5	130.0		140.5
Shearing Strain, in/in		0.84	0.84	0.77		0.82
Energy Absorbed, in-lb		2,440	2,510	2,100		2,350

THIRD SPEED	Specimen No.	7-15	7-59	7-61		Average
Proportional Limit, 1000 psi		92.6	79.9	94.0		88.8
Yield Strength, 1000 psi		104.0	102.3	110.0		102.1
Yield Point (Upper), 1000 psi						
Yield Point (Lower), 1000 psi						
Modulus of Rupture, 1000 psi		131.0	127.1			129.0
Shearing Strain, in/in		0.74	0.75	0.79		0.77
Energy Absorbed, in-lb		2,290	2,210			2,250

FOURTH SPEED	Specimen No.	7-16	7-80	7-82		Average
Proportional Limit, 1000 psi		117.0	123.6	112.7		117.8
Yield Strength, 1000 psi		126.5	130.0	122.0		126.2
Yield Point (Upper), 1000 psi						
Yield Point (Lower), 1000 psi						
Modulus of Rupture, 1000 psi		143.6	144.0	135.7		141.1
Shearing Strain, in/in		0.79	0.76	0.76		0.77
Energy Absorbed, in-lb		2,790	2,600	2,610		2,670

**Table 46. Torsion Properties of RC-130B Titanium Alloy
at 400 F (Not Aged)**

FIRST SPEED	Specimen No.	7-63	7-83	7-95		Average
Proportional Limit, 1000 psi		58.6	62.0	60.5		60.4
Yield Strength, 1000 psi		68.5	69.3	67.6		68.5
Yield Point (Upper), 1000 psi						
Yield Point (Lower), 1000 psi						
Modulus of Rupture, 1000 psi		120.0	125.2	119.1		121.4
Shearing Strain, in/in		0.80	0.85	0.75		0.80
Energy Absorbed, in-lb		1,910	2,040	1,770		1,910
SECOND SPEED	Specimen No.	7-30	7-64	7-84		Average
Proportional Limit, 1000 psi		61.8	65.9	63.9		63.9
Yield Strength, 1000 psi		71.3	72.9	72.7		72.3
Yield Point (Upper), 1000 psi						
Yield Point (Lower), 1000 psi						
Modulus of Rupture, 1000 psi		117.5	120.2	119.2		119.0
Shearing Strain, in/in		0.84	0.83	0.78		0.82
Energy Absorbed, in-lb		1,960	1,990	1,850		1,930
THIRD SPEED	Specimen No.	7-31	7-65	7-85		Average
Proportional Limit, 1000 psi		74.8	78.9	72.8		75.5
Yield Strength, 1000 psi		77.8	82.3	77.1		79.1
Yield Point (Upper), 1000 psi						
Yield Point (Lower), 1000 psi						
Modulus of Rupture, 1000 psi		118.8	118.0	114.0		116.9
Shearing Strain, in/in		0.89	0.83	0.84		0.85
Energy Absorbed, in-lb		2,230	2,060	1,940		2,080
FOURTH SPEED	Specimen No.	7-32	7-66	7-86		Average
Proportional Limit, 1000 psi		89.8	86.2	94.6		90.2
Yield Strength, 1000 psi		96.4	92.2			94.6
Yield Point (Upper), 1000 psi				97.4		
Yield Point (Lower), 1000 psi				95.3		
Modulus of Rupture, 1000 psi		124.0	119.0	125.0		122.7
Shearing Strain, in/in		0.80	0.88	0.90		0.86
Energy Absorbed, in-lb		2,220	2,300	2,410		2,310

Contrails

**Table 47. Torsion Properties of RC-130B Titanium Alloy at 400°F
(Aged)**

FIRST SPEED	Specimen No.	7-5	7-21	7-37			Average
Proportional Limit, 1000 psi		58.5	59.6	61.5			59.9
Yield Strength, 1000 psi		66.3	67.1	67.8			67.1
Yield Point (Upper), 1000 psi							
Yield Point (Lower), 1000 psi							
Modulus of Rupture, 1000 psi		127.2	117.0	121.3			121.8
Shearing Strain, in/in		0.86	0.73	0.79			0.79
Energy Absorbed, in-lb		2,110	1,680	1,920			1,900
SECOND SPEED	Specimen No.	7-6	7-22	7-38			Average
Proportional Limit, 1000 psi		65.5	66.9	67.9			66.8
Yield Strength, 1000 psi		74.0	73.8	71.8			73.2
Yield Point (Upper), 1000 psi							
Yield Point (Lower), 1000 psi							
Modulus of Rupture, 1000 psi		120.0	120.0	122.2			120.7
Shearing Strain, in/in		0.90	0.89	0.84			0.88
Energy Absorbed, in-lb		2,180	2,180	2,090			2,150
THIRD SPEED	Specimen No.	7-7	7-23	7-39			Average
Proportional Limit, 1000 psi		75.2	66.0	78.5			73.2
Yield Strength, 1000 psi		78.9	78.5	82.5			80.0
Yield Point (Upper), 1000 psi							
Yield Point (Lower), 1000 psi							
Modulus of Rupture, 1000 psi		116.5	117.3	124.5			119.4
Shearing Strain, in/in		0.93	0.93	0.85			0.90
Energy Absorbed, in-lb		2,220	2,220	2,190			2,210
FOURTH SPEED	Specimen No.	7-24	7-103	7-104			Average
Proportional Limit, 1000 psi		92.6	99.5	103.5			98.5
Yield Strength, 1000 psi		94.8					97.1
Yield Point (Upper), 1000 psi			99.5	103.5			
Yield Point (Lower), 1000 psi			95.2	101.2			
Modulus of Rupture, 1000 psi		126.0	125.0	131.0			127.0
Shearing Strain, in/in		0.94	1.00	0.95			0.96
Energy Absorbed, in-lb		2,330	2,690	2,660			2,560

Contrails

**Table 48. Torsion Properties of RC-130B Titanium Alloy
at 700°F (Not Aged)**

FIRST SPEED	Specimen No.	7-45	7-67	7-87	Average
Proportional Limit, 1000 psi		54.8	54.4	52.6	53.9
Yield Strength, 1000 psi		61.3	56.6	58.9	58.9
Yield Point (Upper), 1000 psi					
Yield Point (Lower), 1000 psi					
Modulus of Rupture, 1000 psi		117.5	120.0	118.8	118.8
Shearing Strain, in/in		0.95	0.99	0.95	0.96
Energy Absorbed, in-lb		2,170	2,230	2,190	2,200
SECOND SPEED	Specimen No.	7-46	7-68	7-88	Average
Proportional Limit, 1000 psi		52.5	49.0	43.2	48.2
Yield Strength, 1000 psi		59.5	58.1	58.6	58.7
Yield Point (Upper), 1000 psi					
Yield Point (Lower), 1000 psi					
Modulus of Rupture, 1000 psi		106.2	106.2	105.4	105.9
Shearing Strain, in/in		0.90	0.88	0.88	0.89
Energy Absorbed, in-lb		1,900	1,860	1,860	1,870
THIRD SPEED	Specimen No.	7-47	7-69	7-89	Average
Proportional Limit, 1000 psi		47.2	52.5	48.2	49.3
Yield Strength, 1000 psi		51.8	60.8	65.6	59.4
Yield Point (Upper), 1000 psi					
Yield Point (Lower), 1000 psi					
Modulus of Rupture, 1000 psi		99.0	97.3	103.0	99.8
Shearing Strain, in/in		0.90	0.88	0.86	0.88
Energy Absorbed, in-lb		1,860	1,780	1,780	1,810
FOURTH SPEED	Specimen No.	7-48	7-70	7-90	Average
Proportional Limit, 1000 psi		71.6	70.6	73.9	72.0
Yield Strength, 1000 psi		75.0		74.1	74.7
Yield Point (Upper), 1000 psi			77.9		
Yield Point (Lower), 1000 psi			75.1		
Modulus of Rupture, 1000 psi		106.5	106.2	107.0	106.6
Shearing Strain, in/in		0.96	0.95	0.94	0.95
Energy Absorbed, in-lb		2,180	2,100	2,120	2,130

Table 49. Torsion Properties of RC-130B Titanium Alloy at 700° F
(Aged)

FIRST SPEED	Specimen No.	7-9	7-25	7-41		Average
Proportional Limit, 1000 psi		47.7	50.7	54.5		51.0
Yield Strength, 1000 psi		62.4	59.2	59.0		60.2
Yield Point (Upper), 1000 psi						
Yield Point (Lower), 1000 psi						
Modulus of Rupture, 1000 psi		115.1	115.9	112.0		114.3
Shearing Strain, in/in		0.95	1.01	0.98		0.98
Energy Absorbed, in-lb		2,200	2,300	2,180		2,230
SECOND SPEED	Specimen No.	7-10	7-26	7-42		Average
Proportional Limit, 1000 psi		51.5	51.5	51.5		51.4
Yield Strength, 1000 psi		60.1	57.3	60.0		59.1
Yield Point (Upper), 1000 psi						
Yield Point (Lower), 1000 psi						
Modulus of Rupture, 1000 psi		106.0	105.0	109.1		106.7
Shearing Strain, in/in		0.88	0.86	0.95		0.90
Energy Absorbed, in-lb		1,910	1,810	2,110		1,940
THIRD SPEED	Specimen No.	7-11	7-27	7-43		Average
Proportional Limit, 1000 psi		56.0	56.4	53.4		55.3
Yield Strength, 1000 psi		63.9	64.2	65.5		64.5
Yield Point (Upper), 1000 psi						
Yield Point (Lower), 1000 psi						
Modulus of Rupture, 1000 psi		106.4	105.3	104.7		105.5
Shearing Strain, in/in		0.92	0.87	0.87		0.89
Energy Absorbed, in-lb		2,020	1,920	1,900		1,950
FOURTH SPEED	Specimen No.	7-12	7-28	7-44		Average
Proportional Limit, 1000 psi		76.1	76.6	73.8		75.5
Yield Strength, 1000 psi			76.8			75.2
Yield Point (Upper), 1000 psi		76.1		77.1		
Yield Point (Lower), 1000 psi		74.7		74.2		
Modulus of Rupture, 1000 psi		106.9	108.2	108.2		107.8
Shearing Strain, in/in		1.01	0.93	0.98		0.97
Energy Absorbed, in-lb		2,310	2,100	2,240		2,220

Contrails

**Table 50. Tension Properties of BC-130B Titanium Alloy
at 1000 F (Not Aged)**

FIRST SPEED	Specimen No.	7-49	7-71	7-91	Average
Proportional Limit, 1000 psi		13.3	9.6	20.9	14.6
Yield Strength, 1000 psi		18.4	17.7	25.0	20.4
Yield Point (Upper), 1000 psi					
Yield Point (Lower), 1000 psi					
Modulus of Rupture, 1000 psi		23.6	23.1	28.5	25.1
Shearing Strain, in/in		31.20	35.63	33.67	33.5
Energy Absorbed, in-lb		11,000	13,400	14,870	13,100

SECOND SPEED	Specimen No.	7-53	7-72	7-92	Average
Proportional Limit, 1000 psi		32.8	35.1	32.8	33.6
Yield Strength, 1000 psi					
Yield Point (Upper), 1000 psi		43.3	43.2	43.0	43.2
Yield Point (Lower), 1000 psi		38.6	41.2	40.9	40.2
Modulus of Rupture, 1000 psi		44.5	45.9	44.8	45.1
Shearing Strain, in/in		4.41	4.40	4.11	4.31
Energy Absorbed, in-lb		3,600	3,630	3,550	3,590

THIRD SPEED	Specimen No.	7-51	7-73	7-93	Average
Proportional Limit, 1000 psi		46.1	41.4	43.7	43.7
Yield Strength, 1000 psi		47.4	47.8	49.3	48.2
Yield Point (Upper), 1000 psi					
Yield Point (Lower), 1000 psi					
Modulus of Rupture, 1000 psi		57.6	58.0	59.9	58.5
Shearing Strain, in/in		2.33	2.09	2.38	2.27
Energy Absorbed, in-lb		2,240	2,120	2,340	2,230

FOURTH SPEED	Specimen No.	7-52	7-56	7-74	Average
Proportional Limit, 1000 psi		66.0	52.6	62.5	60.4
Yield Strength, 1000 psi			53.4		57.5
Yield Point (Upper), 1000 psi		66.0		62.5	
Yield Point (Lower), 1000 psi		59.3		59.8	
Modulus of Rupture, 1000 psi		80.0	72.5	80.1	77.5
Shearing Strain, in/in		1.25	1.23	1.14	1.21
Energy Absorbed, in-lb		2,120	1,980	1,930	2,010

Contrails

Table 51. Torsion Properties of RC-130B Titanium Alloy at 1000°F (Aged)

FIRST SPEED	Specimen No.	7-1	7-17	7-33			Average
Proportional Limit, 1000 psi		12.5	12.0	18.7			14.4
Yield Strength, 1000 psi		18.6	19.0	22.0			19.9
Yield Point (Upper), 1000 psi							
Yield Point (Lower), 1000 psi							
Modulus of Rupture, 1000 psi		25.0	24.4	25.0			24.8
Shearing Strain, in/in		38.40	37.35	37.85			37.87
Energy Absorbed, in-lb			16,680				16,680

SECOND SPEED	Specimen No.	7-18	7-34				Average
Proportional Limit, 1000 psi		31.7	30.3				30.7
Yield Strength, 1000 psi							
Yield Point (Upper), 1000 psi		40.0	38.8				39.4
Yield Point (Lower), 1000 psi		39.9	38.8				39.3
Modulus of Rupture, 1000 psi		44.6	43.3				43.9
Shearing Strain, in/in		4.29	3.66				3.97
Energy Absorbed, in-lb		3,640	3,070				3,350

THIRD SPEED	Specimen No.	7-3	7-19	7-35			Average
Proportional Limit, 1000 psi		33.9	35.6	36.3			35.3
Yield Strength, 1000 psi		41.1	41.2	41.6			41.3
Yield Point (Upper), 1000 psi							
Yield Point (Lower), 1000 psi							
Modulus of Rupture, 1000 psi		56.8	55.2	57.0			56.3
Shearing Strain, in/in		2.27	2.64	1.76			2.22
Energy Absorbed, in-lb		2,350	2,510	1,810			2,220

FOURTH SPEED	Specimen No.	7-2	7-4	7-98			Average
Proportional Limit, 1000 psi		50.4	44.3	46.4			47.0
Yield Strength, 1000 psi			49.2	58.3			51.7
Yield Point (Upper), 1000 psi		50.4					
Yield Point (Lower), 1000 psi		47.5					
Modulus of Rupture, 1000 psi		67.3	71.4	74.6			71.1
Shearing Strain, in/in		1.37	1.20	1.30			1.29
Energy Absorbed, in-lb		2,040	1,850	2,120			2,000

Contrails

The following tables of data numbered 52 to 64 list information obtained in an exploratory series of tests in which a furnace was used that did not develop uniform temperature along the gage length. The temperatures listed are those measured at the center of length of the specimen. The ends of the one inch gage length were as much as 50F to 100F cooler at the highest temperatures employed. Therefore, these data have not been analyzed nor included in the report of this investigation.

Contrails

EXPLORATORY TESTS

**Table 52. Torsion Properties of SAE 1018 Steel at 400°F
(Not Aged)**

FIRST SPEED	Specimen No.					Average
Proportional Limit, 1000 psi						
Yield Strength, 1000 psi						
Yield Point (Upper), 1000 psi						
Yield Point (Lower), 1000 psi						
Modulus of Rupture, 1000 psi						
Shearing Strain, in/in						
Energy Absorbed, in-lb						
SECOND SPEED	Specimen No.	1-8	1-38	1-107		Average
Proportional Limit, 1000 psi		25.9	26.4	26.6		26.3
Yield Strength, 1000 psi						
Yield Point (Upper), 1000 psi		25.9	26.4	26.6		26.3
Yield Point (Lower), 1000 psi		22.2	21.6	25.8		23.2
Modulus of Rupture, 1000 psi		68.8	65.3	73.0		69.0
Shearing Strain, in/in		1.74	1.43	1.21		1.46
Energy Absorbed, in-lb		2,500	1,960	1,840		2,100
THIRD SPEED	Specimen No.	1-7	1-39	1-71		Average
Proportional Limit, 1000 psi		26.2	25.9	17.1		23.1
Yield Strength, 1000 psi						
Yield Point (Upper), 1000 psi		26.2	25.9	28.9		27.0
Yield Point (Lower), 1000 psi		22.4	22.3	26.6		23.8
Modulus of Rupture, 1000 psi		66.7	64.8	74.7		68.7
Shearing Strain, in/in		2.48	1.92	1.61		2.00
Energy Absorbed, in-lb		3,440	2,460	2,440		2,780
FOURTH SPEED	Specimen No.	1-5	1-12	1-72		Average
Proportional Limit, 1000 psi		34.6	30.3	33.3		32.7
Yield Strength, 1000 psi						
Yield Point (Upper), 1000 psi		34.6	30.3	33.3		32.7
Yield Point (Lower), 1000 psi		30.2	28.4	30.8		29.8
Modulus of Rupture, 1000 psi		71.1	67.2	75.3		71.2
Shearing Strain, in/in		2.79	2.52	2.40		2.57
Energy Absorbed, in-lb		4,040	3,580	3,630		3,750

EXPLORATORY TESTS

TABLE 53. Torsion Properties of SAE 1018 Steel at 400°F (Aged)

FIRST SPEED	Specimen No.						Average
Proportional Limit, 1000 psi							
Yield Strength, 1000 psi							
Yield Point (Upper), 1000 psi							
Yield Point (Lower), 1000 psi							
Modulus of Rupture, 1000 psi							
Shearing Strain, in/in							
Energy Absorbed, in-lb							

SECOND SPEED	Specimen No.						Average
Proportional Limit, 1000 psi							
Yield Strength, 1000 psi							
Yield Point (Upper), 1000 psi							
Yield Point (Lower), 1000 psi							
Modulus of Rupture, 1000 psi							
Shearing Strain, in/in							
Energy Absorbed, in-lb							

THIRD SPEED	Specimen No.	1-23					Average
Proportional Limit, 1000 psi		27.8					27.8
Yield Strength, 1000 psi							
Yield Point (Upper), 1000 psi		27.8					27.8
Yield Point (Lower), 1000 psi		23.0					23.0
Modulus of Rupture, 1000 psi		68.5					68.5
Shearing Strain, in/in		2.08					2.08
Energy Absorbed, in-lb		2,850					2,850

FOURTH SPEED	Specimen No.						Average
Proportional Limit, 1000 psi							
Yield Strength, 1000 psi							
Yield Point (Upper), 1000 psi							
Yield Point (Lower), 1000 psi							
Modulus of Rupture, 1000 psi							
Shearing Strain, in/in							
Energy Absorbed, in-lb							

EXPLORATORY TESTS

**TABLE 54. Torsion Properties of SAE 1018 Steel at 700°F
(Not Aged)**

FIRST SPEED	Specimen No.					Average
Proportional Limit, 1000 psi						
Yield Strength, 1000 psi						
Yield Point (Upper), 1000 psi						
Yield Point (Lower), 1000 psi						
Modulus of Rupture, 1000 psi						
Shearing Strain, in/in						
Energy Absorbed, in-lb						
SECOND SPEED	Specimen No.					Average
Proportional Limit, 1000 psi	1-6	1-10	1-112			22.2
Yield Strength, 1000 psi						
Yield Point (Upper), 1000 psi	25.7	19.5	21.4			22.2
Yield Point (Lower), 1000 psi	22.0	18.3	21.4			20.6
Modulus of Rupture, 1000 psi	69.0	65.0	72.4			68.8
Shearing Strain, in/in	1.27	1.39	1.27			1.31
Energy Absorbed, in-lb	1,800	1,950	2,000			1,920
THIRD SPEED	Specimen No.					Average
Proportional Limit, 1000 psi	1-11	1-43	1-75			17.3
Yield Strength, 1000 psi						
Yield Point (Upper), 1000 psi	24.2	24.2	23.6			24.0
Yield Point (Lower), 1000 psi	21.2	21.2	22.7			21.7
Modulus of Rupture, 1000 psi	66.0	64.7	72.0			67.9
Shearing Strain, in/in	1.85	1.93	0.87			1.55
Energy Absorbed, in-lb	2,470	2,440	1,210			2,040
FOURTH SPEED	Specimen No.					Average
Proportional Limit, 1000 psi	1-37	1-44	1-76			30.0
Yield Strength, 1000 psi						
Yield Point (Upper), 1000 psi	27.7	27.5	34.8			30.0
Yield Point (Lower), 1000 psi	25.2	24.8	29.0			26.3
Modulus of Rupture, 1000 psi	66.3	64.2	73.0			67.8
Shearing Strain, in/in	2.00	1.90	1.74			1.88
Energy Absorbed, in-lb	2,740	2,500	2,550			2,600

EXPLORATORY TESTS

**TABLE 55. Torsion Properties of SAE 1018 Steel at 1000°F
(Not Aged)**

FIRST SPEED	Specimen No.					Average
Proportional Limit, 1000 psi						
Yield Strength, 1000 psi						
Yield Point (Upper), 1000 psi						
Yield Point (Lower), 1000 psi						
Modulus of Rupture, 1000 psi						
Shearing Strain, in/in						
Energy Absorbed, in-lb						

SECOND SPEED	Specimen No.					Average
	1-46	1-77	1-78	1-118	1-122	
Proportional Limit, 1000 psi	11.2	15.5	14.7	15.0	13.3	13.9
Yield Strength, 1000 psi	16.4	20.0	20.0	19.0	19.7	19.0
Yield Point (Upper), 1000 psi						
Yield Point (Lower), 1000 psi						
Modulus of Rupture, 1000 psi	49.7	45.8	44.2	47.6	42.2	45.9
Shearing Strain, in/in	-	1.86	-	1.90	2.13	1.96
Energy Absorbed, in-lb	-	1,900	-	2,000	2,030	1,980

THIRD SPEED	Specimen No.					Average
	1-15	1-47	1-79			
Proportional Limit, 1000 psi	19.1	19.3	18.0			18.8
Yield Strength, 1000 psi						
Yield Point (Upper), 1000 psi	19.1	19.3	20.8			19.7
Yield Point (Lower), 1000 psi	17.9	17.9	20.8			18.9
Modulus of Rupture, 1000 psi	55.5	56.2	62.0			57.9
Shearing Strain, in/in	1.14	1.04	0.99			1.06
Energy Absorbed, in-lb	1,320	1,270	1,330			1,310

FOURTH SPEED	Specimen No.					Average
	1-16	1-48	1-80			
Proportional Limit, 1000 psi	24.4	28.0	26.1			26.2
Yield Strength, 1000 psi						
Yield Point (Upper), 1000 psi	24.4	28.0	26.1			26.2
Yield Point (Lower), 1000 psi	24.4	26.7	26.1			25.7
Modulus of Rupture, 1000 psi	62.0	66.2	68.9			65.7
Shearing Strain, in/in	1.46	1.52	1.23			1.40
Energy Absorbed, in-lb	1,730	2,100	1,730			1,850

EXPLORATORY TESTS

**TABLE 56. Torsion Properties of 24S-T Aluminum Alloy at 200°F
(Not Aged)**

FIRST SPEED	Specimen No.					Average
Proportional Limit, 1000 psi						
Yield Strength, 1000 psi						
Yield Point (Upper), 1000 psi						
Yield Point (Lower), 1000 psi						
Modulus of Rupture, 1000 psi						
Shearing Strain, in/in						
Energy Absorbed, in-lb						

SECOND SPEED	Specimen No.					Average
	3-6	3-38	3-70			
Proportional Limit, 1000 psi	28.1	26.3	28.2			27.5
Yield Strength, 1000 psi	32.0	32.2	31.8			32.0
Yield Point (Upper), 1000 psi						
Yield Point (Lower), 1000 psi						
Modulus of Rupture, 1000 psi	59.5	57.3	56.7			57.8
Shearing Strain, in/in	0.56	0.56	0.57			0.56
Energy Absorbed, in-lb	700	690	700			700

THIRD SPEED	Specimen No.					Average
	3-7	3-39	3-71			
Proportional Limit, 1000 psi	21.5	21.5	24.7			22.6
Yield Strength, 1000 psi	26.7	29.9	31.4			29.3
Yield Point (Upper), 1000 psi						
Yield Point (Lower), 1000 psi						
Modulus of Rupture, 1000 psi	50.7	53.2	52.2			52.0
Shearing Strain, in/in	0.51	0.46	0.53			0.50
Energy Absorbed, in-lb	560	520	610			560

FOURTH SPEED	Specimen No.					Average
	3-8	3-40	3-76			
Proportional Limit, 1000 psi	26.4	36.0	23.1			28.5
Yield Strength, 1000 psi						
Yield Point (Upper), 1000 psi						
Yield Point (Lower), 1000 psi						
Modulus of Rupture, 1000 psi	56.7	57.2	56.8			56.9
Shearing Strain, in/in	0.47	0.55	0.51			0.51
Energy Absorbed, in-lb	570	660	540			590

EXPLORATORY TESTS

TABLE 57. Torsion Properties of 24S-T Aluminum Alloy at 200°F (Aged)

FIRST SPEED	Specimen No.					Average
Proportional Limit, 1000 psi						
Yield Strength, 1000 psi						
Yield Point (Upper), 1000 psi						
Yield Point (Lower), 1000 psi						
Modulus of Rupture, 1000 psi						
Shearing Strain, in/in						
Energy Absorbed, in-lb						

SECOND SPEED	Specimen No. 3-22A					Average
Proportional Limit, 1000 psi	26.2					26.2
Yield Strength, 1000 psi	31.4					31.4
Yield Point (Upper), 1000 psi						
Yield Point (Lower), 1000 psi						
Modulus of Rupture, 1000 psi	56.4					56.4
Shearing Strain, in/in	0.56					0.56
Energy Absorbed, in-lb	700					700

THIRD SPEED	Specimen No. 3-23			3-55	3-87	Average
Proportional Limit, 1000 psi	30.0	27.2	15.0			24.1
Yield Strength, 1000 psi	33.8	31.8	26.7			30.8
Yield Point (Upper), 1000 psi						
Yield Point (Lower), 1000 psi						
Modulus of Rupture, 1000 psi	56.5	50.6	56.2			54.4
Shearing Strain, in/in	0.55	0.48	0.51			0.51
Energy Absorbed, in-lb	670	580	640			630

FOURTH SPEED	Specimen No.					Average
Proportional Limit, 1000 psi						
Yield Strength, 1000 psi						
Yield Point (Upper), 1000 psi						
Yield Point (Lower), 1000 psi						
Modulus of Rupture, 1000 psi						
Shearing Strain, in/in						
Energy Absorbed, in-lb						

EXPLORATORY TESTS

TABLE 58. Tension Properties of 243-T Aluminum Alloy at 400°F (Not Aged)

FIRST SPEED	Specimen No.					Average
Proportional Limit, 1000 psi						
Yield Strength, 1000 psi						
Yield Point (Upper), 1000 psi						
Yield Point (Lower), 1000 psi						
Modulus of Rupture, 1000 psi						
Shearing Strain, in/in						
Energy Absorbed, in-lb						

SECOND SPEED	Specimen No.					Average
	3-10	3-42	3-74			
Proportional Limit, 1000 psi	24.7	22.3	21.3			22.8
Yield Strength, 1000 psi	29.3	26.9	26.2			27.5
Yield Point (Upper), 1000 psi						
Yield Point (Lower), 1000 psi						
Modulus of Rupture, 1000 psi	48.0	47.9	47.2			47.7
Shearing Strain, in/in	0.64	0.74	0.69			0.69
Energy Absorbed, in-lb	700	790	740			740

THIRD SPEED	Specimen No.					Average
	3-11	3-43	3-75			
Proportional Limit, 1000 psi	15.4	23.3	12.0			16.9
Yield Strength, 1000 psi	24.6	25.9	25.7			25.4
Yield Point (Upper), 1000 psi						
Yield Point (Lower), 1000 psi						
Modulus of Rupture, 1000 psi	45.8	44.5	49.4			46.6
Shearing Strain, in/in	0.62	0.62	0.64			0.63
Energy Absorbed, in-lb	640	630	720			660

FOURTH SPEED	Specimen No.					Average
	3-9	3-12	3-82			
Proportional Limit, 1000 psi	24.5	20.3	27.0			23.9
Yield Strength, 1000 psi						
Yield Point (Upper), 1000 psi						
Yield Point (Lower), 1000 psi						
Modulus of Rupture, 1000 psi	51.8	47.7	51.7			50.4
Shearing Strain, in/in	0.43	0.38	0.44			0.42
Energy Absorbed, in-lb	470	380	490			450

Contrails

EXPLORATORY TESTS

TABLE 59. Tension Properties of 24S-T Aluminum Alloy at 400°F (Aged)

FIRST SPEED	Specimen No.						Average
Proportional Limit, 1000 psi							
Yield Strength, 1000 psi							
Yield Point (Upper), 1000 psi							
Yield Point (Lower), 1000 psi							
Modulus of Rupture, 1000 psi							
Shearing Strain, in/in							
Energy Absorbed, in-lb							
SECOND SPEED	Specimen No.	3-26	3-49	3-99			Average
Proportional Limit, 1000 psi		25.0	23.0	27.8			25.3
Yield Strength, 1000 psi		30.5	31.6	31.4			31.2
Yield Point (Upper), 1000 psi							
Yield Point (Lower), 1000 psi							
Modulus of Rupture, 1000 psi		34.9	35.6	36.4			35.6
Shearing Strain, in/in		0.74	0.72	0.80			0.75
Energy Absorbed, in-lb		550	550	600			570
THIRD SPEED	Specimen No.	3-27	3-59	3-91			Average
Proportional Limit, 1000 psi		27.4	21.4	26.9			25.2
Yield Strength, 1000 psi		33.7	35.4	30.8			33.3
Yield Point (Upper), 1000 psi							
Yield Point (Lower), 1000 psi							
Modulus of Rupture, 1000 psi		40.7	43.1	40.0			41.3
Shearing Strain, in/in		0.68	0.63	0.67			0.66
Energy Absorbed, in-lb		580	570	560			570
FOURTH SPEED	Specimen No.						Average
Proportional Limit, 1000 psi							
Yield Strength, 1000 psi							
Yield Point (Upper), 1000 psi							
Yield Point (Lower), 1000 psi							
Modulus of Rupture, 1000 psi							
Shearing Strain, in/in							
Energy Absorbed, in-lb							

EXPLORATORY TESTS

**TABLE 60. Tension Properties of 24S-T Aluminum Alloy at 600°F
(Not Aged)**

FIRST SPEED	Specimen No.					Average
Proportional Limit, 1000 psi						
Yield Strength, 1000 psi						
Yield Point (Upper), 1000 psi						
Yield Point (Lower), 1000 psi						
Modulus of Rupture, 1000 psi						
Shearing Strain, in/in						
Energy Absorbed, in-lb						
SECOND SPEED	Specimen No.					Average
	3-14	3-46	3-78			
Proportional Limit, 1000 psi	15.1	19.0	23.0			19.0
Yield Strength, 1000 psi	17.3	22.0	26.5			21.9
Yield Point (Upper), 1000 psi						
Yield Point (Lower), 1000 psi						
Modulus of Rupture, 1000 psi	19.8	24.4	28.0			24.1
Shearing Strain, in/in	0.72	0.78	0.62			0.71
Energy Absorbed, in-lb	270	370	340			330
THIRD SPEED	Specimen No.				Average	
	3-15	3-17	3-47	3-77		
Proportional Limit, 1000 psi	26.2	11.0	10.0	26.3		18.4
Yield Strength, 1000 psi	27.8	26.9	25.3	31.0		27.8
Yield Point (Upper), 1000 psi						
Yield Point (Lower), 1000 psi						
Modulus of Rupture, 1000 psi	49.1	—	45.0	35.5		43.2
Shearing Strain, in/in	0.59	—	0.62	0.72		0.64
Energy Absorbed, in-lb	640	—	640	490		590
FOURTH SPEED	Specimen No.					Average
	3-16	3-48	3-80			
Proportional Limit, 1000 psi	26.0	32.0	30.0			29.3
Yield Strength, 1000 psi						
Yield Point (Upper), 1000 psi						
Yield Point (Lower), 1000 psi						
Modulus of Rupture, 1000 psi	45.8	46.2	49.5			47.2
Shearing Strain, in/in	0.26	0.33	0.34			0.31
Energy Absorbed, in-lb	270	340	380			330

EXPLORATORY TESTS

TABLE 61. Torsion Properties of 24S-T Aluminum Alloy at 600°F (Aged)

FIRST SPEED	Specimen No.					Average
Proportional Limit, 1000 psi						
Yield Strength, 1000 psi						
Yield Point (Upper), 1000 psi						
Yield Point (Lower), 1000 psi						
Modulus of Rupture, 1000 psi						
Shearing Strain, in/in						
Energy Absorbed, in-lb						

SECOND SPEED	Specimen No.					Average
	3-30	3-62	3-96			
Proportional Limit, 1000 psi	5.3	5.1	6.5			5.6
Yield Strength, 1000 psi	6.6	6.0	7.6			6.7
Yield Point (Upper), 1000 psi						
Yield Point (Lower), 1000 psi						
Modulus of Rupture, 1000 psi	8.6	7.5	10.3			8.8
Shearing Strain, in/in	5.24	—	—			5.24
Energy Absorbed, in-lb	900	—	—			900

THIRD SPEED	Specimen No.					Average
	3-29	3-33	3-51	3-61	3-95	
Proportional Limit, 1000 psi	4.9	6.6	6.5	7.2	5.8	6.2
Yield Strength, 1000 psi	7.3	8.2	8.0	8.7	8.2	8.1
Yield Point (Upper), 1000 psi						
Yield Point (Lower), 1000 psi						
Modulus of Rupture, 1000 psi	13.2	13.8	14.4	18.5	16.8	15.3
Shearing Strain, in/in	5.57	—	5.34	2.80	—	4.57
Energy Absorbed, in-lb	1,400	—	1,460	1,050	—	1,300

FOURTH SPEED	Specimen No.					Average
Proportional Limit, 1000 psi						
Yield Strength, 1000 psi						
Yield Point (Upper), 1000 psi						
Yield Point (Lower), 1000 psi						
Modulus of Rupture, 1000 psi						
Shearing Strain, in/in						
Energy Absorbed, in-lb						

EXPLORATORY TESTS

TABLE 62. Tension Properties of PS-1 Magnesium Alloy at 200°F (Not Aged)

FIRST SPEED	Specimen No.						Average
Proportional Limit, 1000 psi							
Yield Strength, 1000 psi							
Yield Point (Upper), 1000 psi							
Yield Point (Lower), 1000 psi							
Modulus of Rupture, 1000 psi							
Shearing Strain, in/in							
Energy Absorbed, in-lb							

SECOND SPEED	Specimen No.						Average
Proportional Limit, 1000 psi							
Yield Strength, 1000 psi							
Yield Point (Upper), 1000 psi							
Yield Point (Lower), 1000 psi							
Modulus of Rupture, 1000 psi							
Shearing Strain, in/in							
Energy Absorbed, in-lb							

THIRD SPEED	Specimen No.	5-33	5-41	5-73			Average
Proportional Limit, 1000 psi		7.1	6.8	4.4			6.1
Yield Strength, 1000 psi		10.2	9.7	6.6			8.8
Yield Point (Upper), 1000 psi							
Yield Point (Lower), 1000 psi							
Modulus of Rupture, 1000 psi		31.0	20.9	28.5			30.1
Shearing Strain, in/in		0.44	0.48	0.50			0.47
Energy Absorbed, in-lb		250	250	260			250

FOURTH SPEED	Specimen No.	5-88					Average
Proportional Limit, 1000 psi		14.0					14.0
Yield Strength, 1000 psi							
Yield Point (Upper), 1000 psi							
Yield Point (Lower), 1000 psi							
Modulus of Rupture, 1000 psi		29.2					29.2
Shearing Strain, in/in		0.34					0.34
Energy Absorbed, in-lb		180					180

EXPLORATORY TESTS

**TABLE 63. Tension Properties of FS-1 Magnesium Alloy at 400°F
(Not Aged)**

FIRST SPEED	Specimen No.						Average
Proportional Limit, 1000 psi							
Yield Strength, 1000 psi							
Yield Point (Upper), 1000 psi							
Yield Point (Lower), 1000 psi							
Modulus of Rupture, 1000 psi							
Shearing Strain, in/in							
Energy Absorbed, in-lb							

SECOND SPEED	Specimen No.						Average
Proportional Limit, 1000 psi							
Yield Strength, 1000 psi							
Yield Point (Upper), 1000 psi							
Yield Point (Lower), 1000 psi							
Modulus of Rupture, 1000 psi							
Shearing Strain, in/in							
Energy Absorbed, in-lb							

THIRD SPEED	Specimen No.	5-9	5-45	5-77			Average
Proportional Limit, 1000 psi		4.1	3.0	3.6			3.6
Yield Strength, 1000 psi		6.8	5.3	6.6			6.2
Yield Point (Upper), 1000 psi							
Yield Point (Lower), 1000 psi							
Modulus of Rupture, 1000 psi		23.4	22.7	24.9			23.7
Shearing Strain, in/in		1.11	0.93	0.86			0.97
Energy Absorbed, in-lb		490	420	390			430

FOURTH SPEED	Specimen No.						Average
Proportional Limit, 1000 psi							
Yield Strength, 1000 psi							
Yield Point (Upper), 1000 psi							
Yield Point (Lower), 1000 psi							
Modulus of Rupture, 1000 psi							
Shearing Strain, in/in							
Energy Absorbed, in-lb							

EXPLORATORY TESTS

**TABLE 64. Torsion Properties of FS-1 Magnesium Alloy at 600°F
(Not Aged)**

FIRST SPEED	Specimen No.						Average
Proportional Limit, 1000 psi							
Yield Strength, 1000 psi							
Yield Point (Upper), 1000 psi							
Yield Point (Lower), 1000 psi							
Modulus of Rupture, 1000 psi							
Shearing Strain, in/in							
Energy Absorbed, in-lb							

SECOND SPEED	Specimen No.						Average
Proportional Limit, 1000 psi							
Yield Strength, 1000 psi							
Yield Point (Upper), 1000 psi							
Yield Point (Lower), 1000 psi							
Modulus of Rupture, 1000 psi							
Shearing Strain, in/in							
Energy Absorbed, in-lb							

THIRD SPEED	Specimen No.	5-27	5-63	5-91			Average
Proportional Limit, 1000 psi		3.1	2.8	2.7			2.9
Yield Strength, 1000 psi		4.8	4.7	5.0			4.8
Yield Point (Upper), 1000 psi							
Yield Point (Lower), 1000 psi							
Modulus of Rupture, 1000 psi		10.9	12.1	16.2			13.1
Shearing Strain, in/in		1.59	1.08	1.48			1.38
Energy Absorbed, in-lb		330	250	460			350

FOURTH SPEED	Specimen No.						Average
Proportional Limit, 1000 psi							
Yield Strength, 1000 psi							
Yield Point (Upper), 1000 psi							
Yield Point (Lower), 1000 psi							
Modulus of Rupture, 1000 psi							
Shearing Strain, in/in							
Energy Absorbed, in-lb							

APPENDIX V

Tables and Figures

TABLE I. CHEMICAL ANALYSIS OF METALS TO BE TESTED

	<u>Steel</u>		<u>Aluminum</u>				<u>Magnesium</u>	<u>Titanium</u>
	1016	4340	24S-T4	75S-T6	Max	Min	PS-1	RC-70 RC-130-B
Carbon	0.16	0.40					0.90	0.35 0.13
Manganese	0.75	0.71	0.9	0.3	0.30			3.9
Phosphorus	0.012	0.014					Max. 0.3	
Sulphur	0.024	0.012					Max. 0.005	
Silicon	0.04	0.31	0.50	0.50				
Nickel		1.79						
Chromium		0.83	0.10	0.40		0.18		
Molybdenum		0.24						
Iron	balance	balance	0.50	0.70			Max. 0.005	
Copper			4.9	3.9	2.0	1.2	Max. 0.05	
Zinc			0.10	6.1	5.1		1.15	
Magnesium			1.8	1.2	2.9	2.1	balance	
Titanium				6.20				balance balance
Aluminum			balance	balance			3.5	2.4
Others, each			0.05	0.05			0.3	
Others, total			0.15	0.15				

TABLE II
STATIC TENSILE PROPERTIES OF METALS TESTED

Material	Specimen Number	Yield Strength (0.2% offset) psi.	Yield Point (upper) psi.	Yield Point (lower) psi.	Ultimate Strength psi.	Elongation in one inch (4D) per cent	Reduction of area, per cent
SAE 1018 Steel	1-50	-----	34,900	34,700	57,000	38.5	72.0
	1-81	-----	41,200	39,800	68,200	35.0	67.7
	1-97	-----	38,900	38,800	65,400	34.0	68.5
	Average	-----	38,300	37,800	63,500	35.8	69.4
SAE 4340 Steel	2-50	-----	142,000	140,500	152,000	18.5	60.0
	2-81	-----	142,800	140,000	152,000	18.0	58.6
	2-97	-----	142,200	141,000	152,000	19.0	61.8
	Average	-----	142,300	140,500	152,000	18.5	60.1
24S-T Aluminum Alloy	3-50	49,000	-----	-----	68,100	19.0	31.0
	3-81	47,400	-----	-----	67,400	20.0	33.5
	3-97	45,300	-----	-----	66,600	22.0	32.0
	Average	47,200	-----	-----	67,700	20.3	32.2
75S-T Aluminum Alloy	4-50	68,200	-----	-----	78,600	14.0	32.8
	4-81	66,200	-----	-----	77,400	15.0	31.8
	4-97	67,600	-----	-----	78,100	15.0	32.4
	Average	67,300	-----	-----	78,000	14.7	32.3
FS-1 Magnesium Alloy	5-112	28,500	-----	-----	40,700	15.0	35.6
	5-113	28,500	-----	-----	40,900	15.0	34.9
	5-114	28,600	-----	-----	40,800	16.0	35.6
	Average	28,500	-----	-----	40,800	15.3	35.4
Commercially Pure Titanium RC-70	6-50	-----	84,500	80,500	95,500	27.0	45.4
	6-81	-----	82,800	82,400	95,500	26.0	48.9
	6-97	-----	77,900	77,300	91,000	27.0	52.4
	Average	-----	81,700	80,100	94,000	26.7	48.9
Titanium Alloy RC-130B	7-50	-----	132,000	130,000	141,000	20.0	52.3
	7-81	-----	134,000	131,000	144,000	20.0	50.8
	7-96	-----	133,100	132,900	143,000	20.0	48.0
	Average	-----	132,700	131,300	142,700	20.0	50.4

TABLE III. INSTRUMENTATION AND CONDITIONS FOR CONDUCTING VARIOUS TESTS

Speed	1st	2nd	3rd	4th
Driving Mechanism	Motor M_1 with Reducers R_1 , R_2 and R_3	Motor M_1 with Reducers R_2 and R_3	Motor M_1 with Reducer R_3	Auxiliary Motor M_2
Flywheel speed (rpm)	0.0104	0.52	26	1300 ⁺
Strain rate (in/in/sec)	0.0001	0.005	0.25	12.5
Oscillograph record speed (in/sec)	0.03 - 0.1 ⁺⁺	0.07 - 0.13	3 - 5.6	45
Record paper used, Kodak Linograph Paper No.	809	809	809	1127
Time interval between time marks (sec)	5 ⁺⁺⁺	5	0.1	0.01
Method of measuring over-all twist (flywheel position)	Cam on output of R_2 , 67-1/2 sig-nals per rev. of flywheel	Cam on output of R_2 , 67-1/2 sig-nals per rev. of flywheel	Magnetic pickup with 68 tooth gear on flywheel shaft	Magnetic pickup with 45 tooth gear on flywheel shaft
Angle of twist in gage length (room temperature)	C-beam bridge circuit Slide-wire pickup	C-beam bridge circuit Slide-wire pickup	C-beam bridge circuit Slide-wire pickup	Photocell apparatus Photocell apparatus
Torque	Weigh-bar bridge circuit	Weigh-bar bridge circuit	Weigh-bar bridge circuit	Weigh-bar bridge circuit

⁺ At beginning of the test, decreases slightly as energy is absorbed by the specimen.
⁺⁺ Continuous during the elastic portion of the test; intermittent for the remainder of the test.
⁺⁺⁺ During continuous portion of record only.

TABLE IV

SAMPLE CALCULATIONS

Test No. 133, 75S-T Aluminum Alloy, Spec. No. 4-19
2nd Speed (.005 shearing strain/sec.), Room Temperature

1. For converting deflections on oscillograph record to units for plotting, calibration constants are used. For example:

$$\text{Twist} = 1.26 \text{ in. (deflection)} \times 3.29 \text{ deg./in.} = 4.14^\circ$$

$$\text{Torque} = 1.21 \text{ in. (deflection)} \times 86.5 \text{ lb-in./in.} = 104.6 \text{ lb-in.}$$

2. The strength properties, proportional limit, yield strength and modulus of rupture are computed from the ordinary formula $\tau = T_c/J$; for example:

$$\tau_r = \frac{T_{\text{max}}}{J/c} = \frac{193 \text{ lb-in.}}{0.00305 \text{ in.}^3} = 63,300 \text{ psi.}$$

3. The angle of twist corresponding to a 0.2 percent shear strain offset is found from the relation: $\gamma = c\theta/R$

$$\text{Solving, } \theta = \frac{57.3 \gamma R}{c} = \frac{57.3 \times 0.002 \times 1}{0.2495/2} = 0.92^\circ$$

4. The total energy absorbed, W , in the 1-in. gage length is equal to $\int T d\theta$ represented by the area under the T vs. θ curve.

From Fig. 13, Area = 77.0 squares (by planimeter); thus

$$W = \frac{77.0 \times 20 \text{ deg.} \times 20 \text{ lb-in.}}{57.3 \text{ deg./radian}} = 538 \text{ in-lb.}$$

5. The total shearing strain is equal to $\frac{c\theta_{\text{max}}}{R}$

$$\gamma = \frac{0.2495 \times 173}{2 \times 1 \times 57.3} = 0.377 \text{ in./in.}$$

6. The strain rate (average) = $\frac{\text{total strain}}{\text{total time}} = \frac{0.377 \text{ in./in.}}{74.5 \text{ sec.}}$

$$\dot{\gamma} = 0.00507 \text{ in./in./sec.}$$

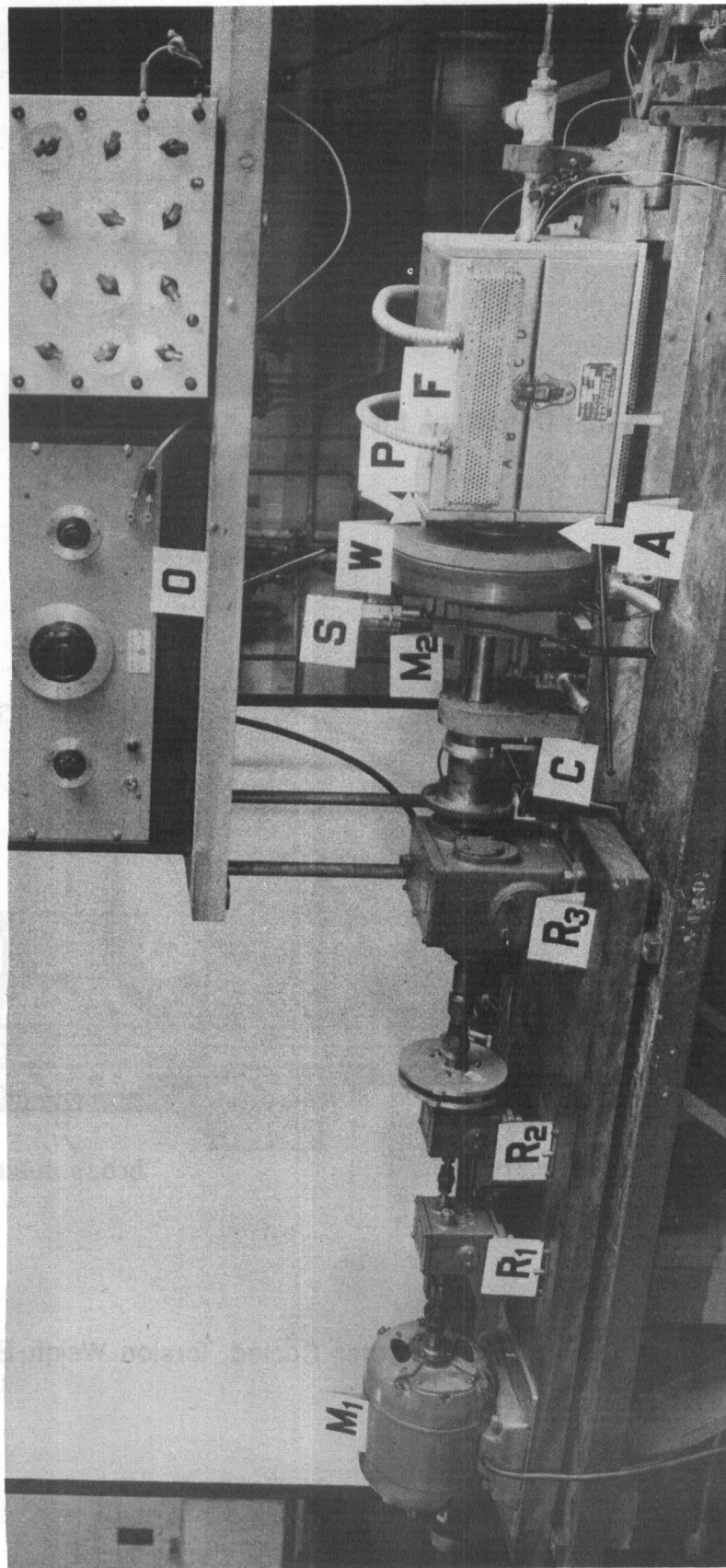


FIG. 1 Torsion Testing Machine Set Up for the Slowest Rate of Loading.

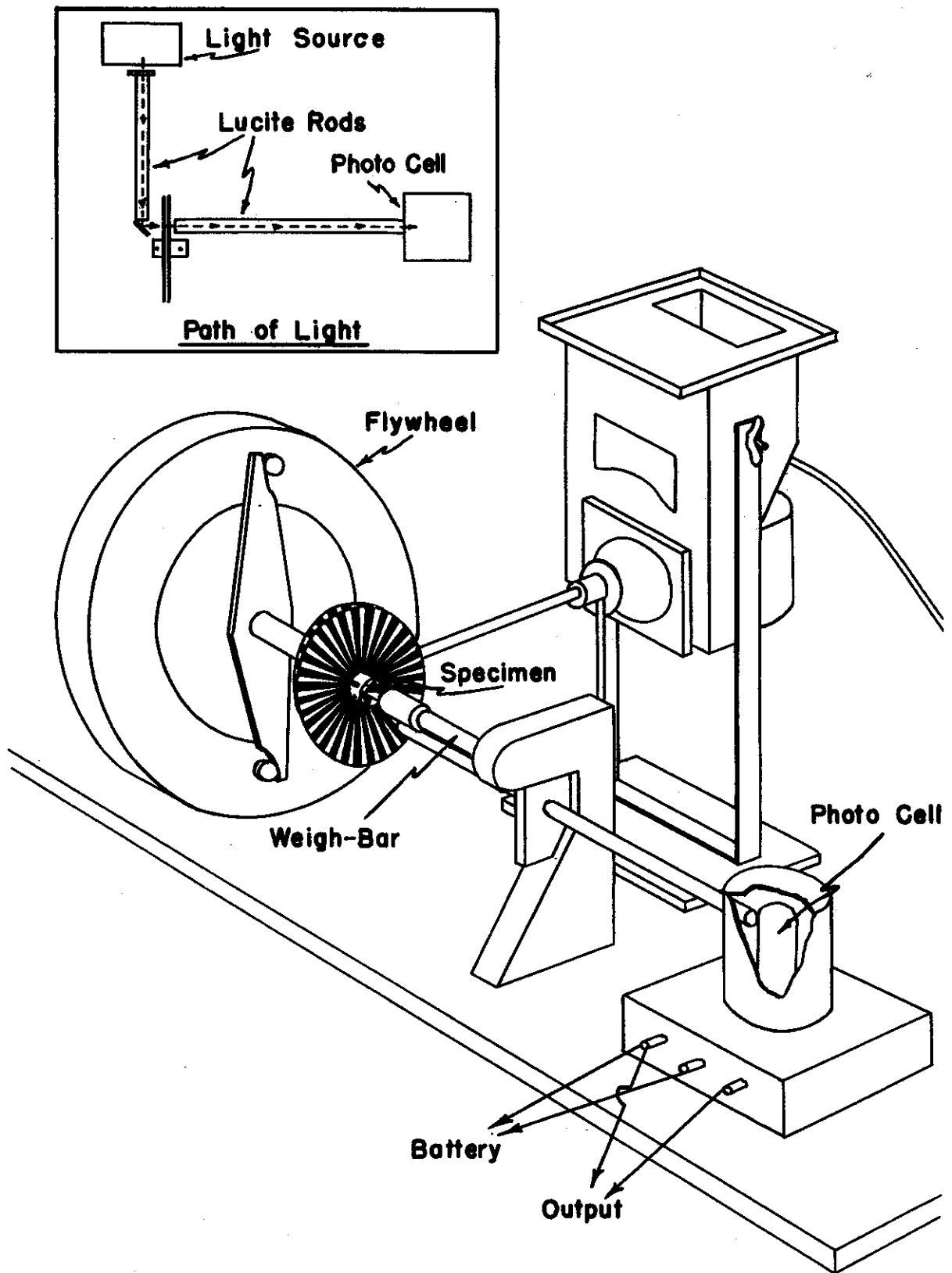


Fig. 4 Apparatus for Measurement of the Angle of Twist by Means of a Photoelectric Cell.

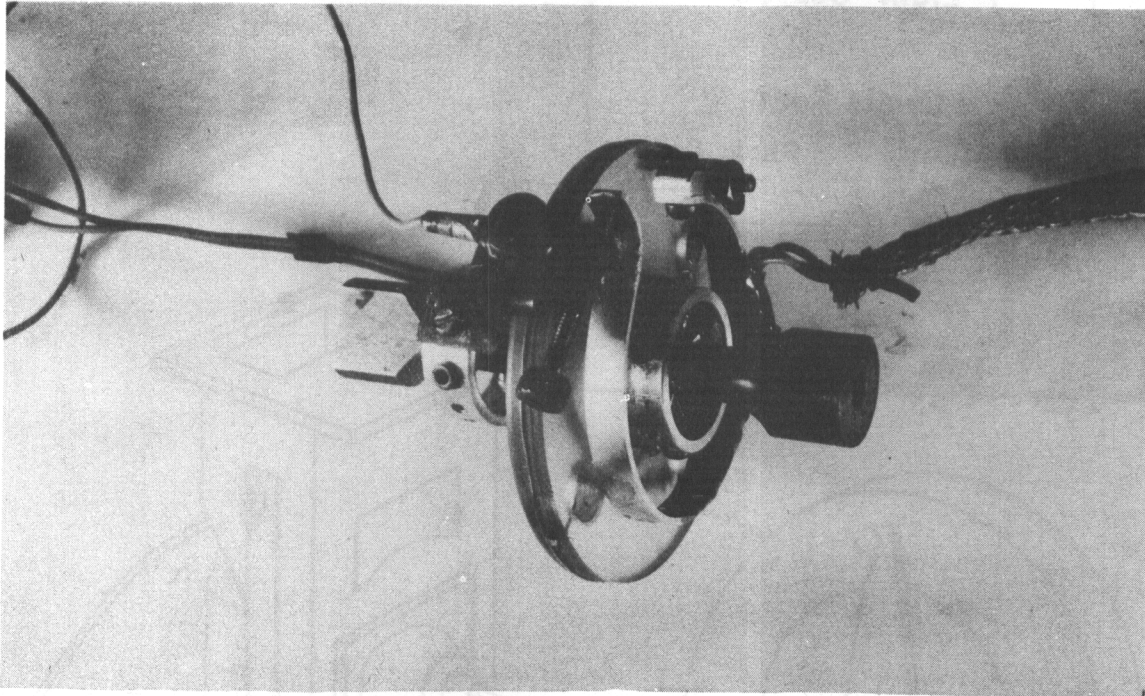


Fig. 5 Twist Measuring Apparatus for Slower Speed Tests.

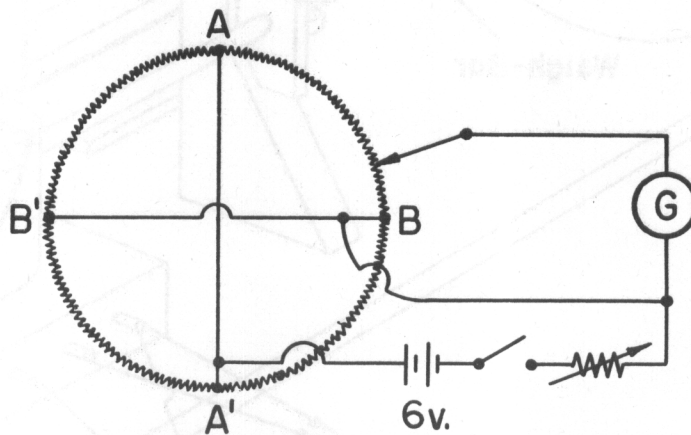


Fig. 6 Circuit Diagram for the Slide Wire Component of the Twist Indicator, Fig. 5.

WADC TR 53-10
161

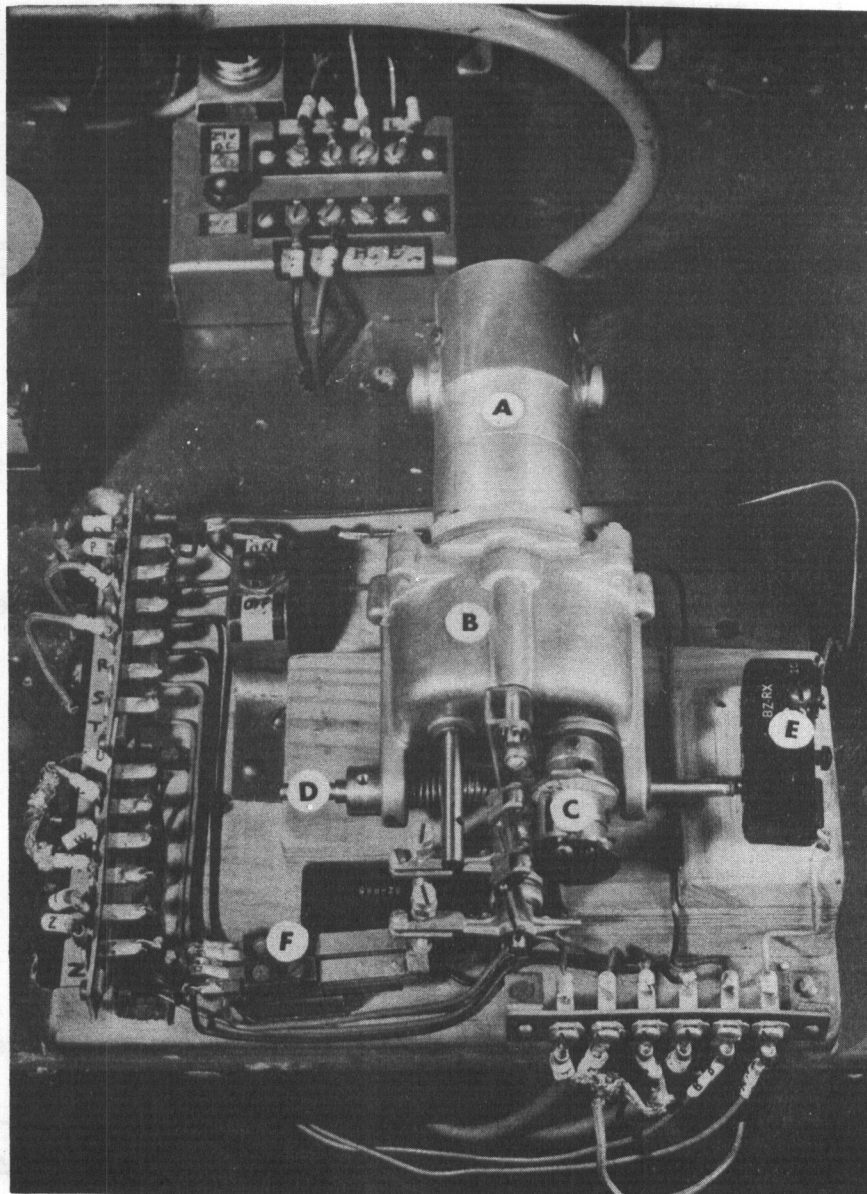


Fig. 7 Timing and Switching Mechanisms for Controlling the Sequence of Events When Testing at the High Rates of Strain.

Fig. 8 Wiring of the Timing and Control Circuit

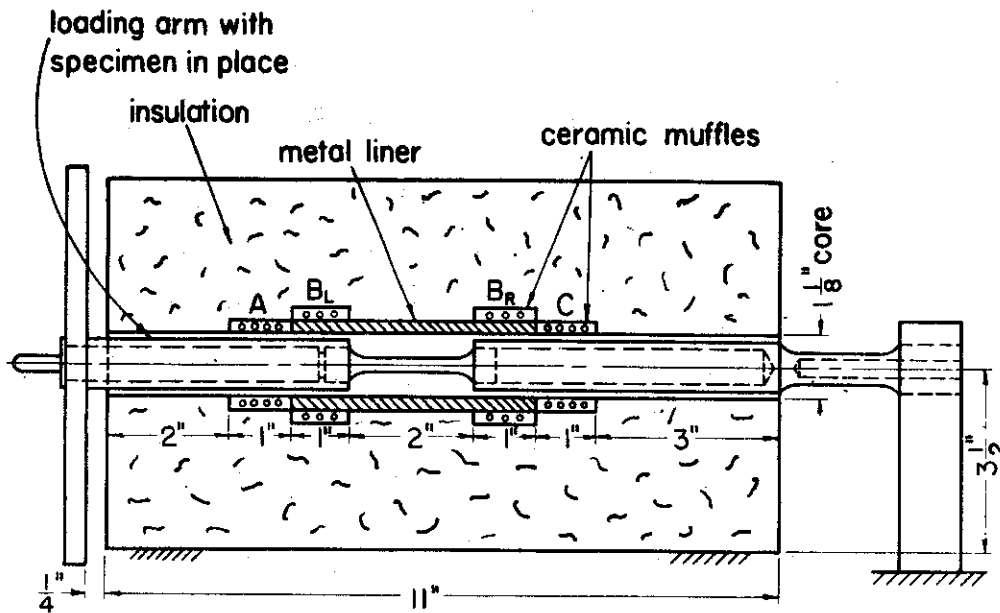


Fig.8 Sectional View of the Electric Furnace for Elevated Temperature Torsion Tests.

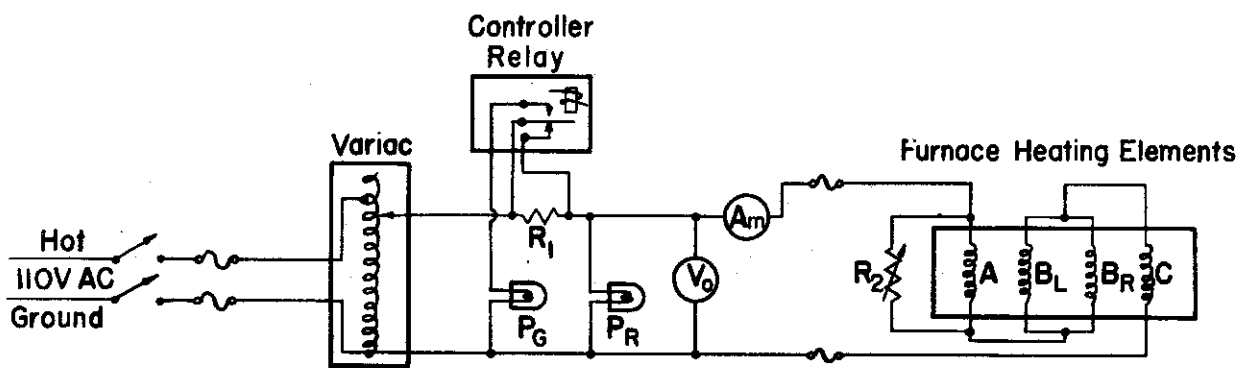


Fig.9 Wiring of the Furnace and Control Circuit.

Controls

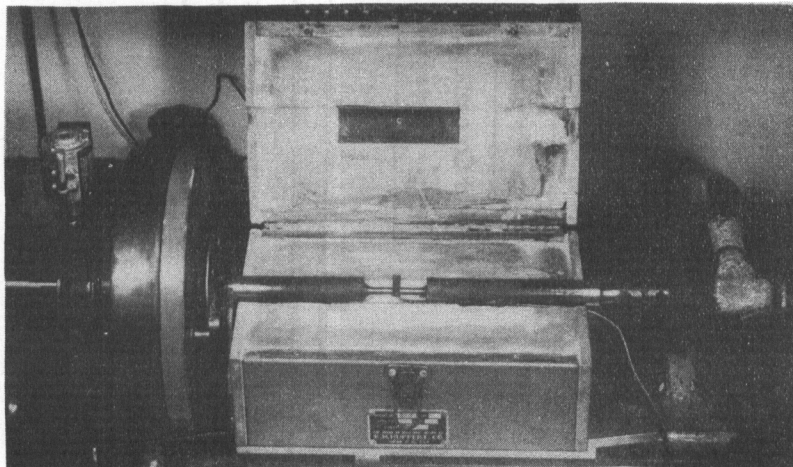
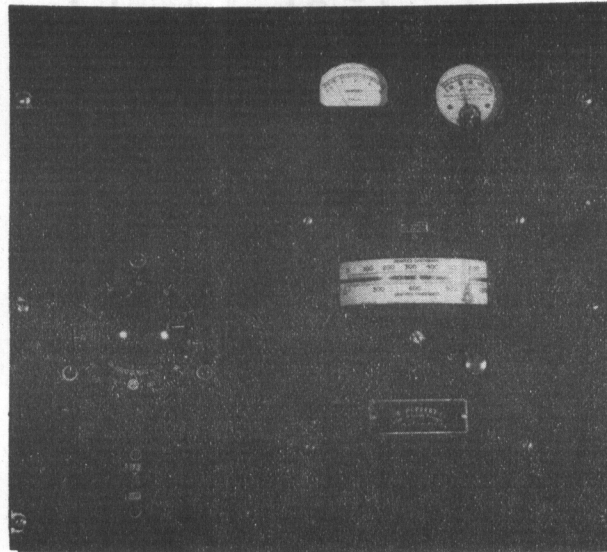


Fig. 10 Electric Furnace and Control Panel for Elevated Temperature Tests.

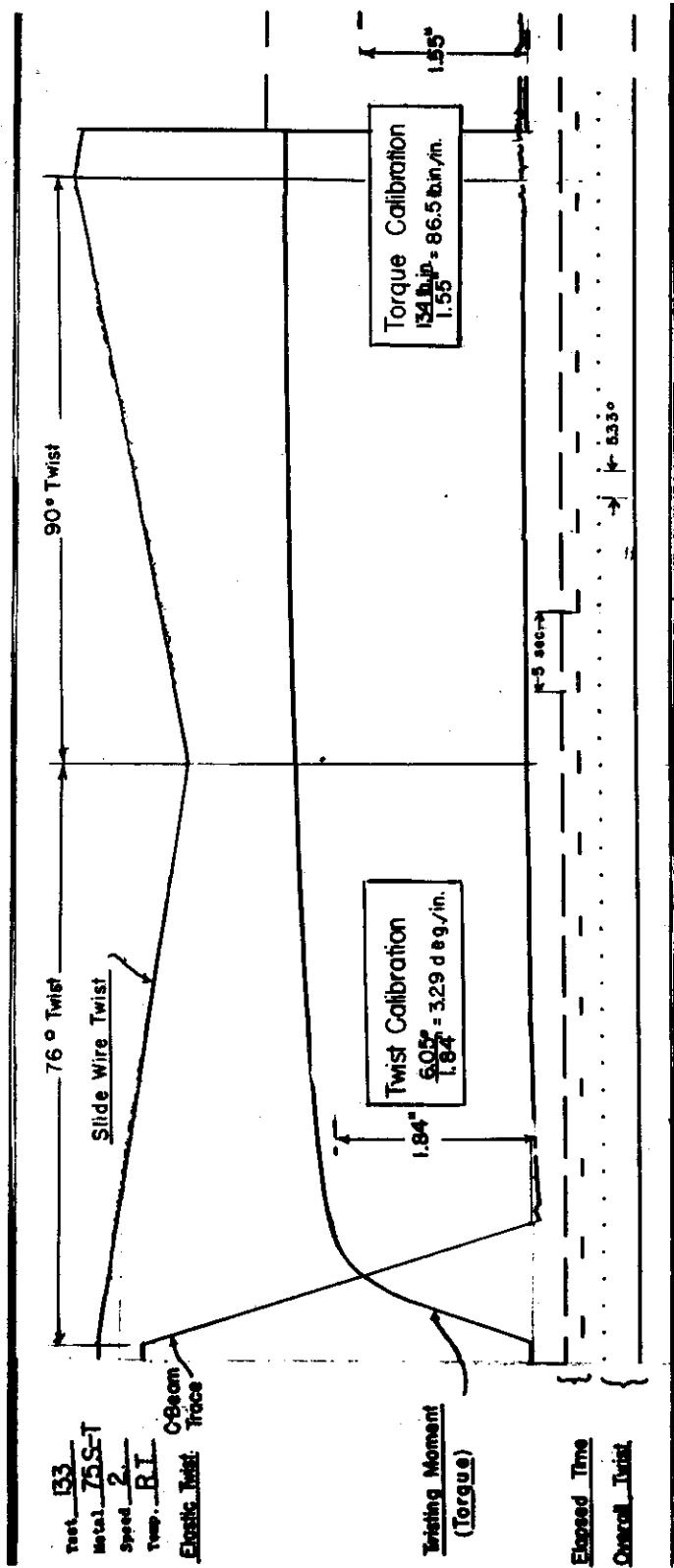


Fig.11 Typical Oscillograph Record from Torsion Test at Room Temperature and Strain Rate of 0.005 in/in/sec.

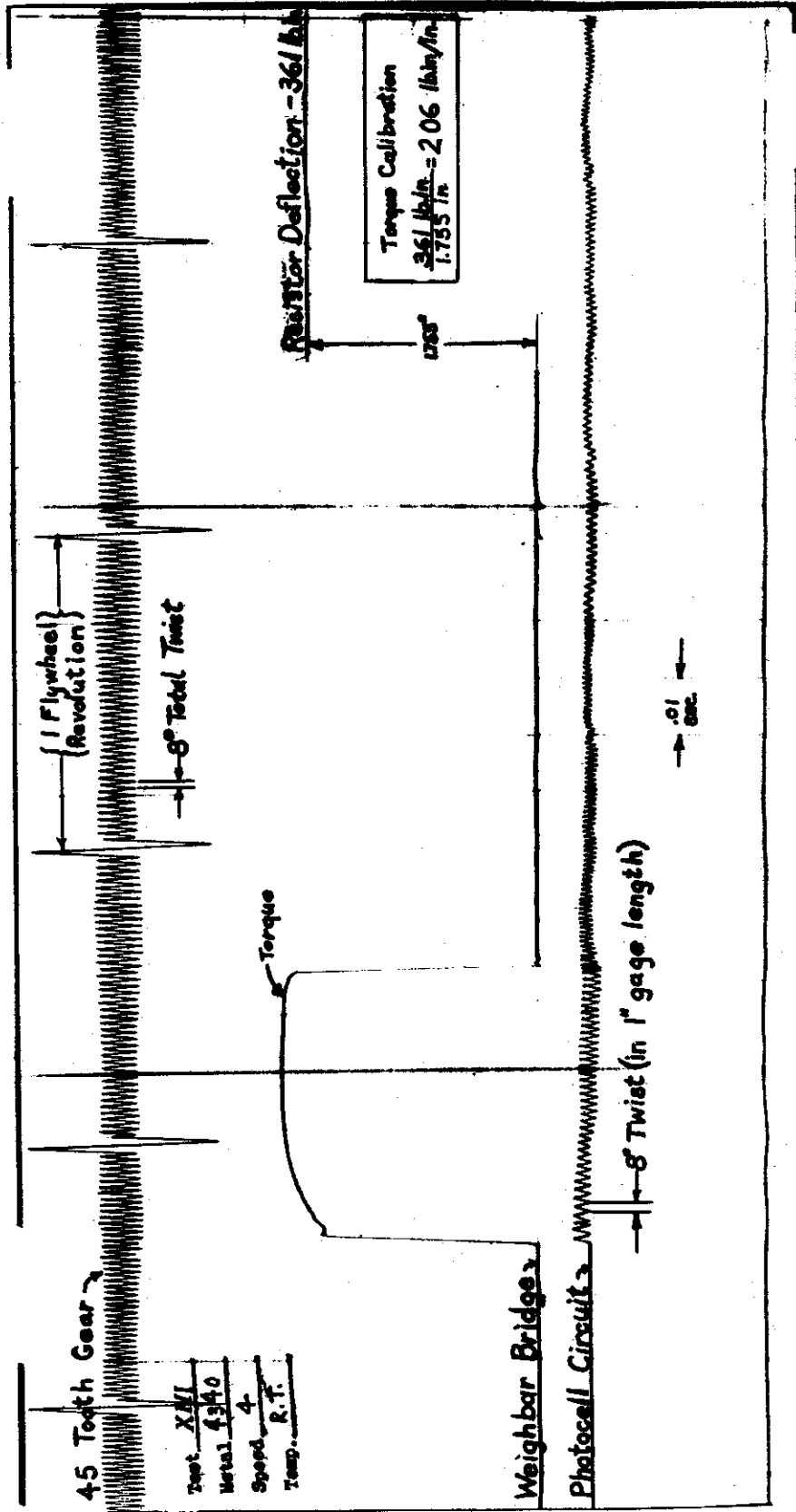


Fig. 12 Typical Oscillograph Record from Torsion Test at Room Temperature and Strain-Rate of 12.5 in./in./sec.

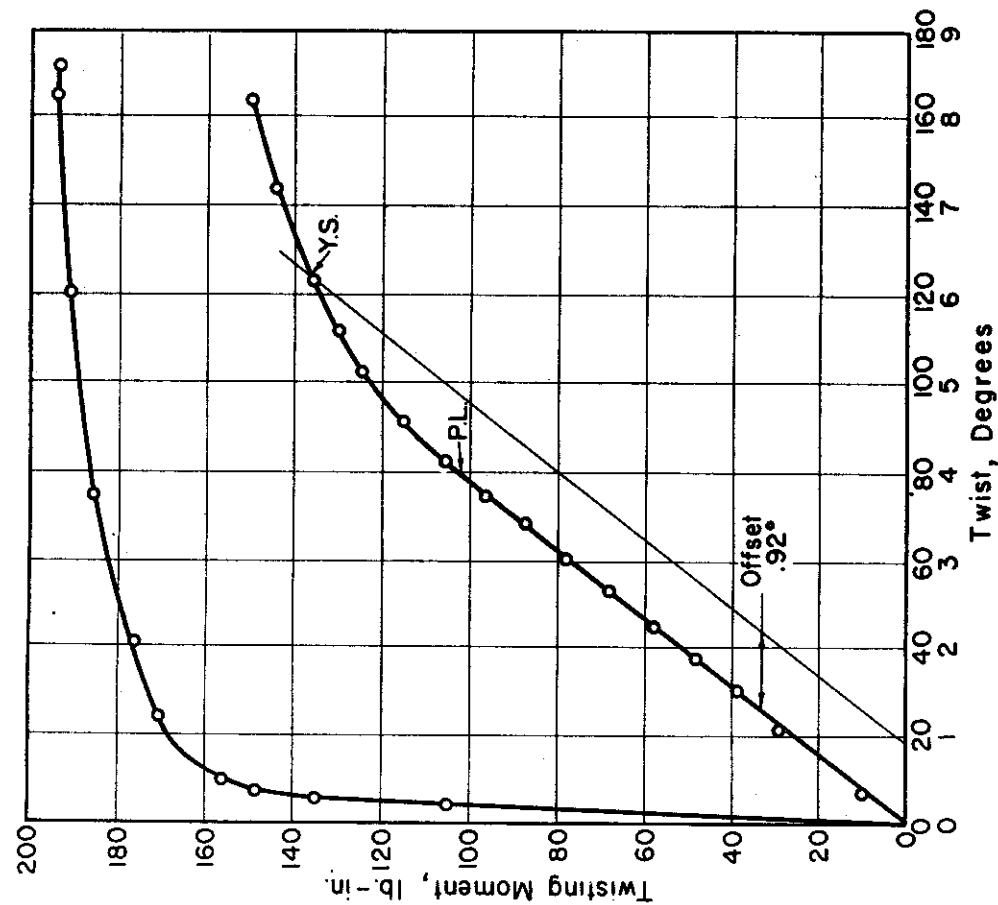


Fig.13 Torque-Twist Diagram for 75S-T Aluminum Alloy in Torsion (Test No.133, 2nd Speed, Room Temperature).

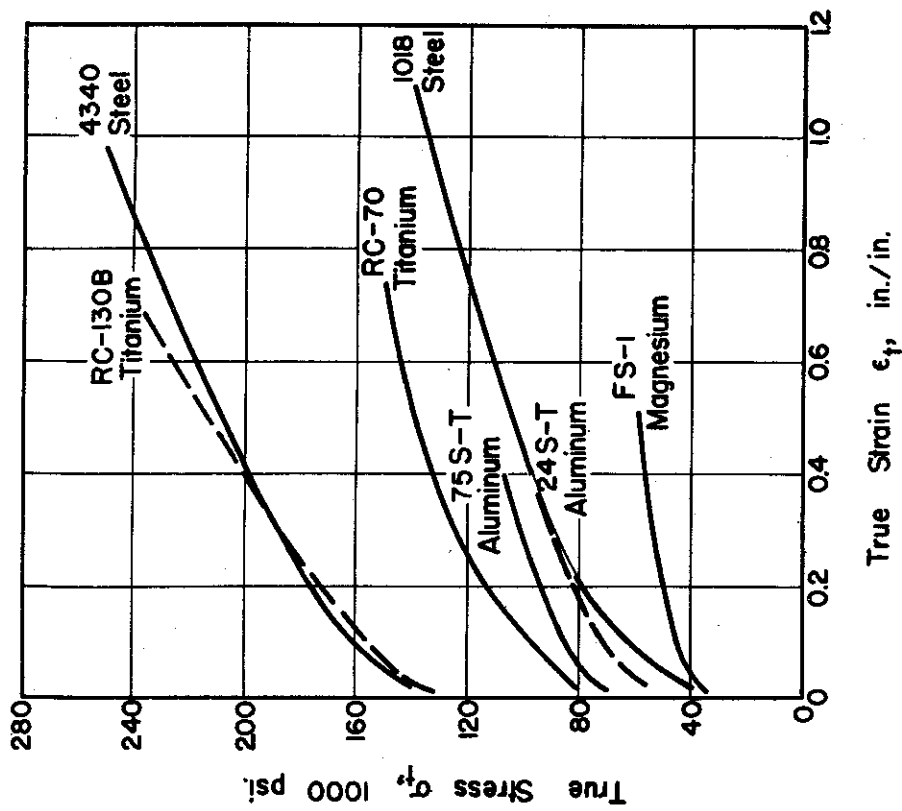


Fig.14 True Tensile Stress-Strain Curves for the Seven Metals Studied

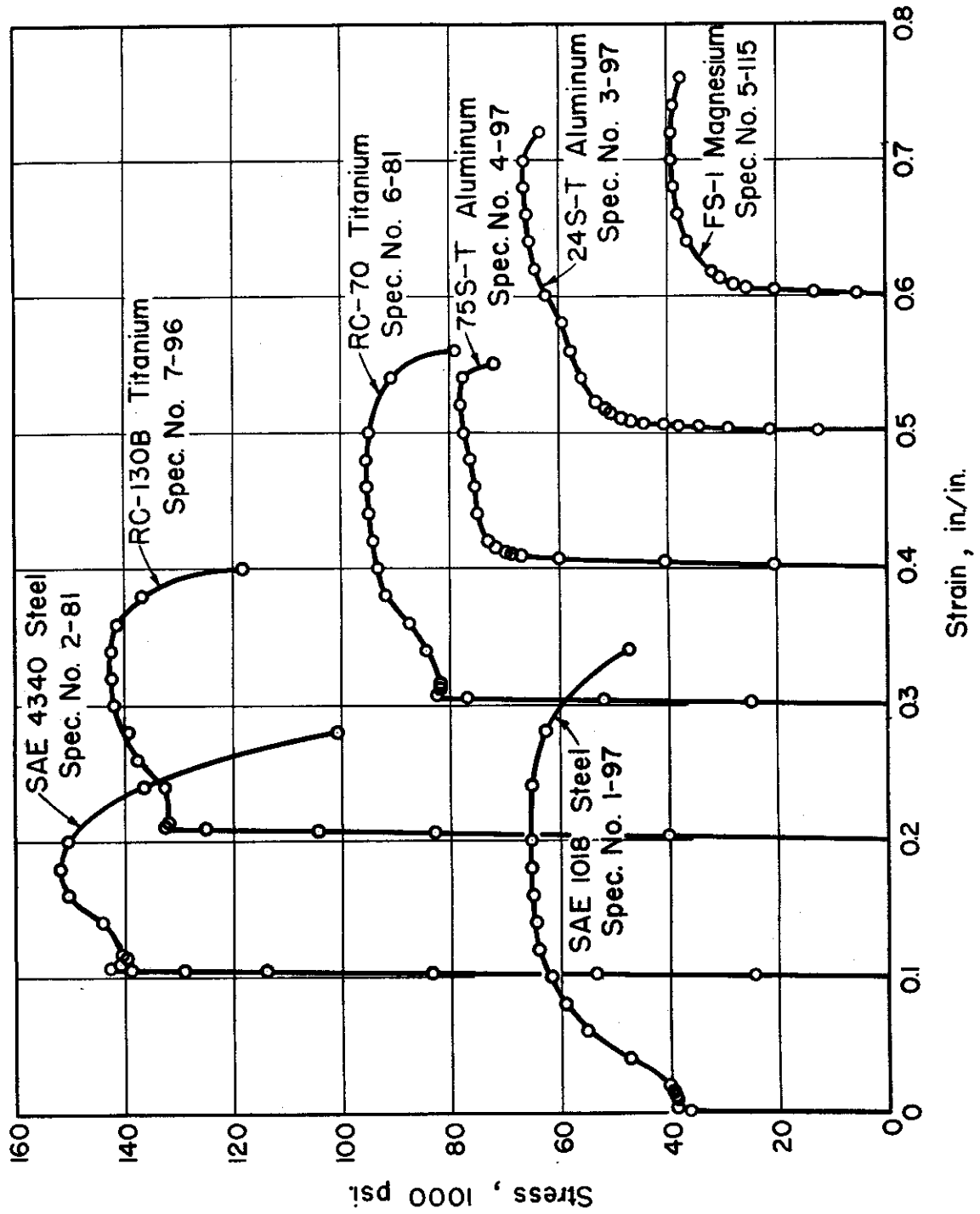


Fig.15 Ordinary Tensile Stress-Strain Curves for the Seven Metals Studied

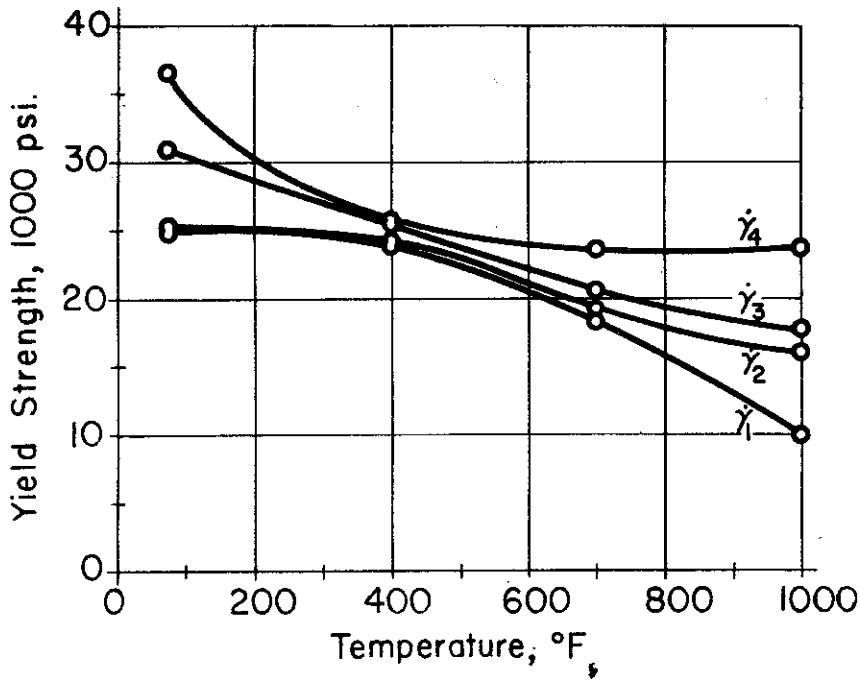


Fig. 16 Effect of Temperature on the Shearing Yield Strength of SAE 1018 Steel in Torsion.

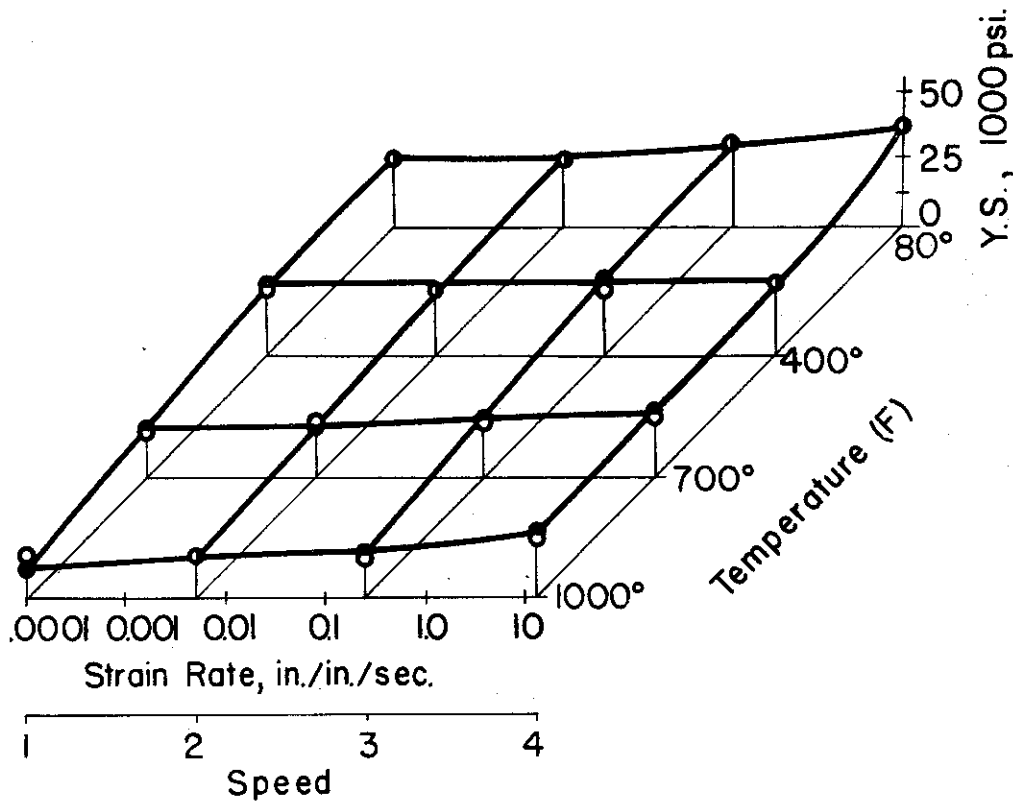


Fig. 17. Combined Effects of Rate of Strain and Temperature on the Shearing Yield Strength of SAE 1018 Steel in Torsion.

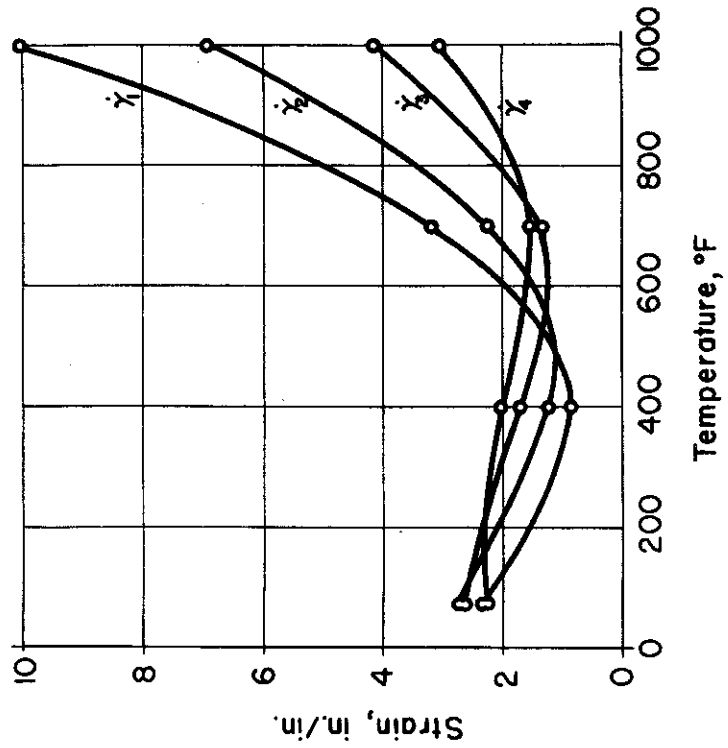


Fig.19 Effect of Temperature on the Total Shearing Strain of SAE 1018 Steel in Torsion.

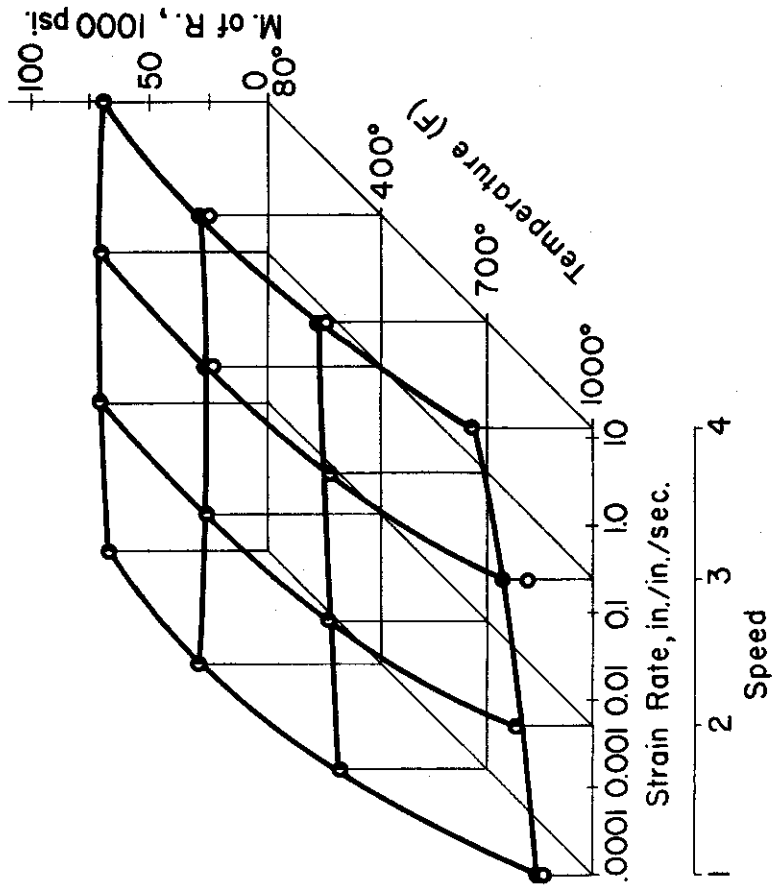


Fig. 18. Combined Effects of Rate of Strain and Temperature on the Modulus of Rupture of SAE 1018 Steel in Torsion.

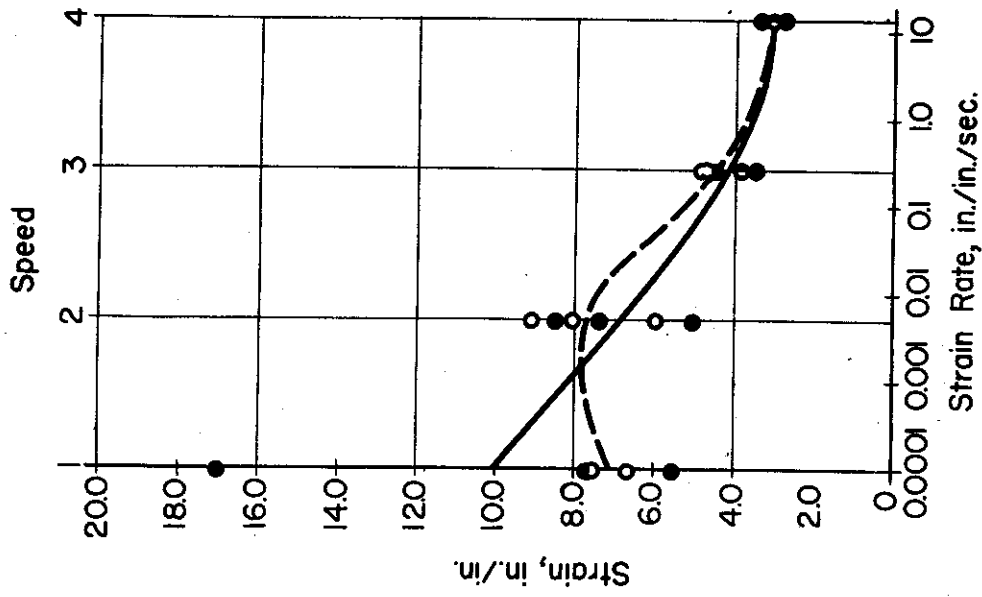


Fig.21 Effect of Rate of Strain on the Total Shearing Strain of SAE 1018 Steel at 1000°F in Torsion. (Each point represents the strain for one specimen, not an average.)

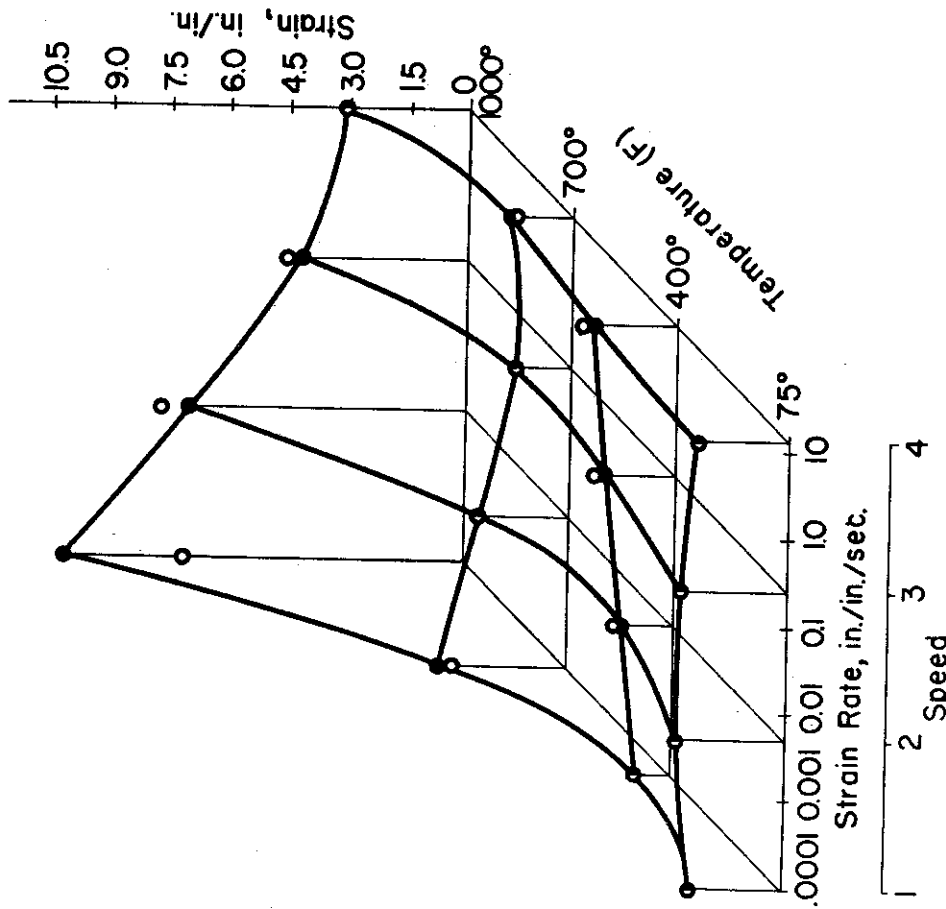


Fig. 20. Combined Effects of Rate of Strain and Temperature on the Total Shearing Strain of SAE 1018 Steel in Torsion.

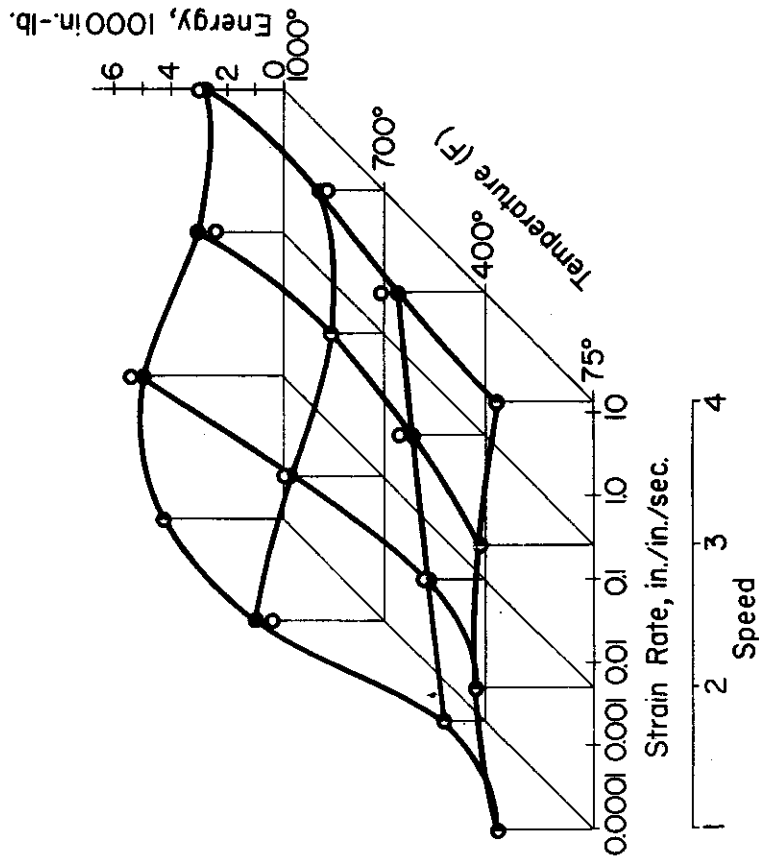


Fig.22 Combined Effects of Rate of Strain and Temperature on the Energy Absorbed in Specimens of SAE 1018 Steel in Torsion.

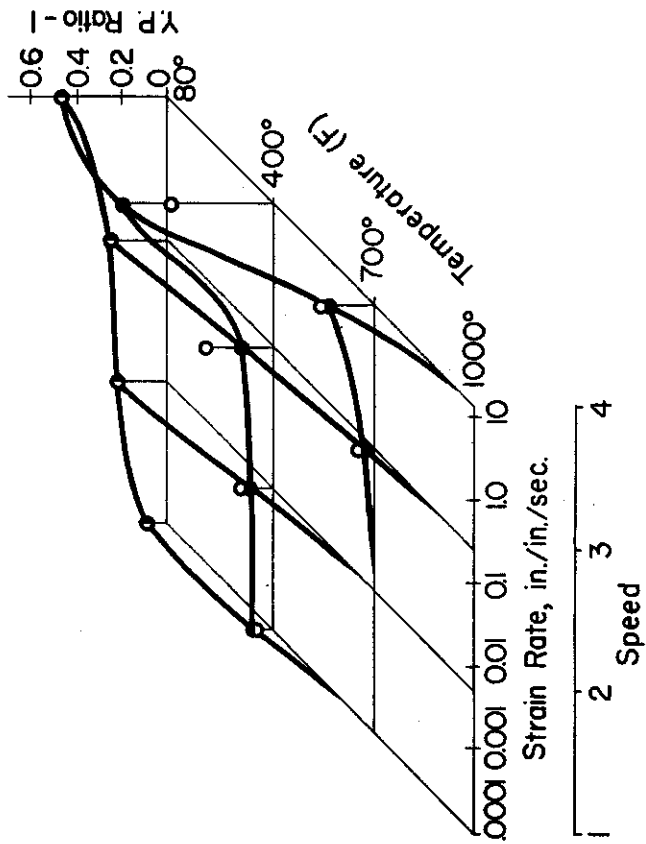


Fig.23 Combined Effects of Rate of Strain and Temperature on the Yield Point Ratio for SAE 1018 Steel in Torsion.

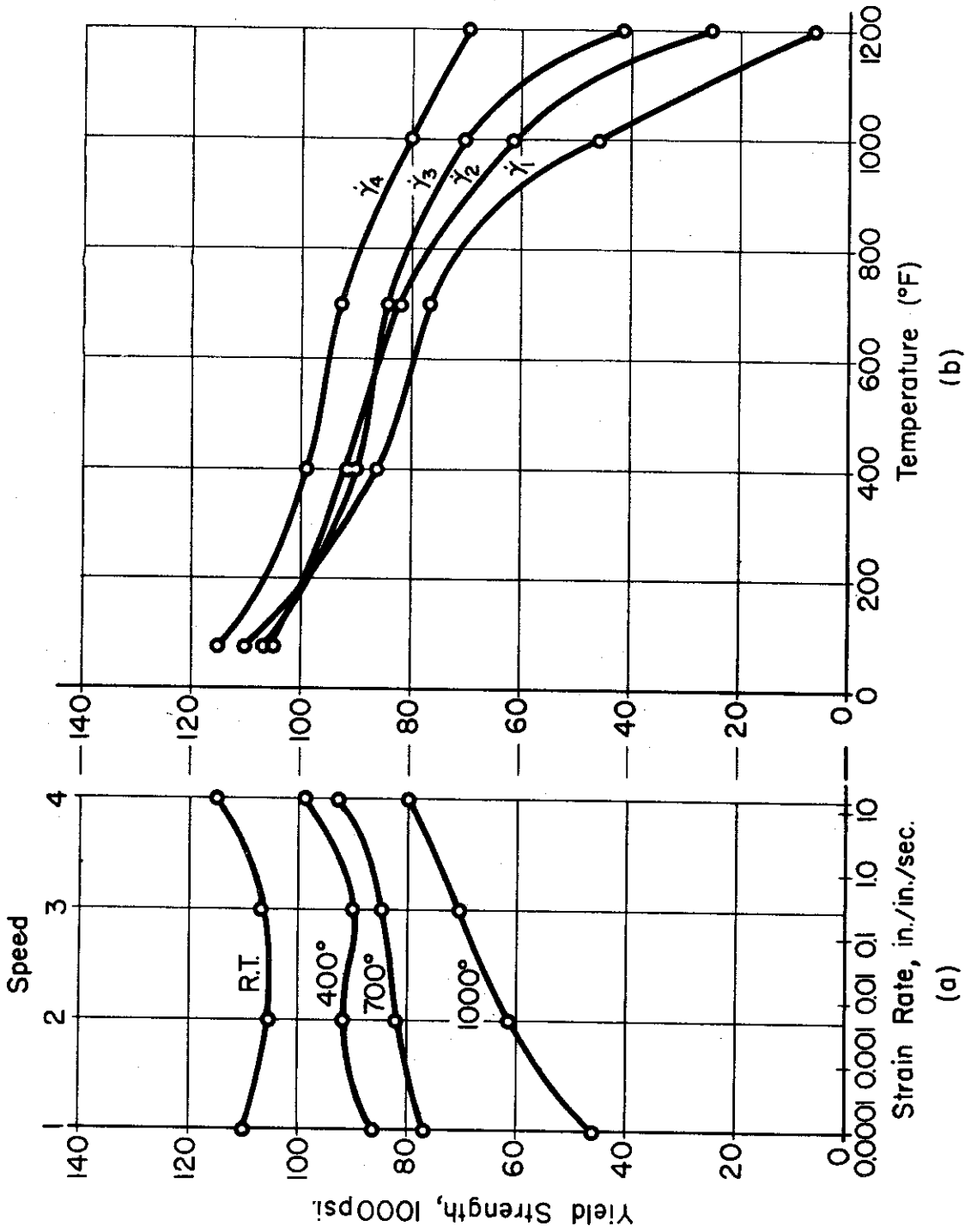


Fig.24 Effect of (a) Rate of Strain and (b) Temperature on the Shearing Yield Strength of SAE 4340 Steel in Torsion.

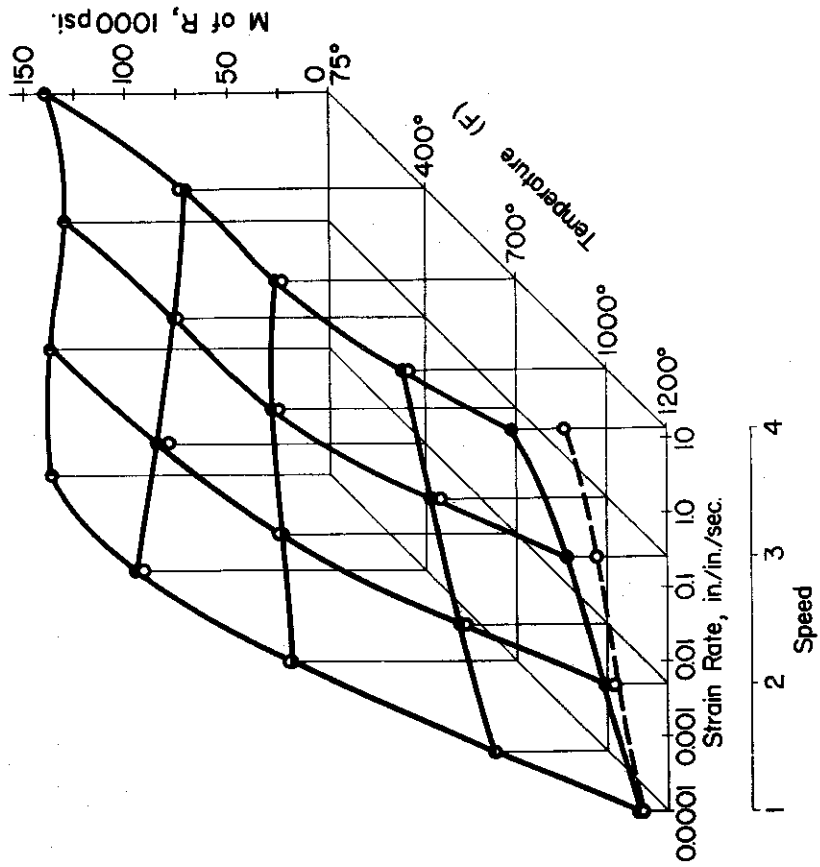


Fig.26 Combined Effects of Rate of Strain and Temperature on the Modulus of Rupture of SAE 4340 Steel in Torsion.

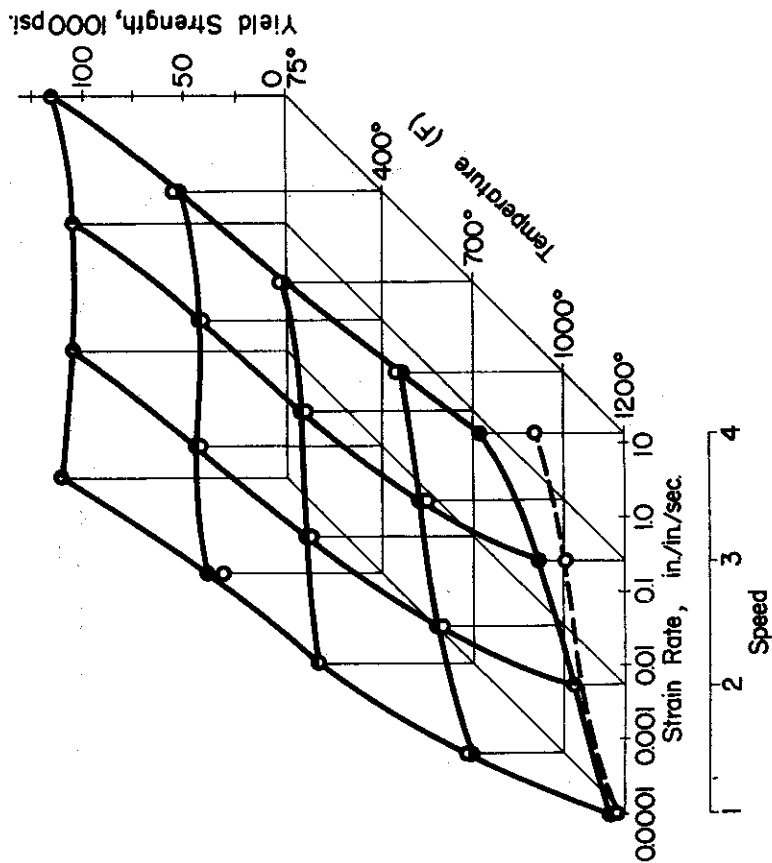


Fig.25 Combined Effects of Rate of Strain and Temperature on the Shearing Yield Strength of SAE 4340 Steel in Torsion.

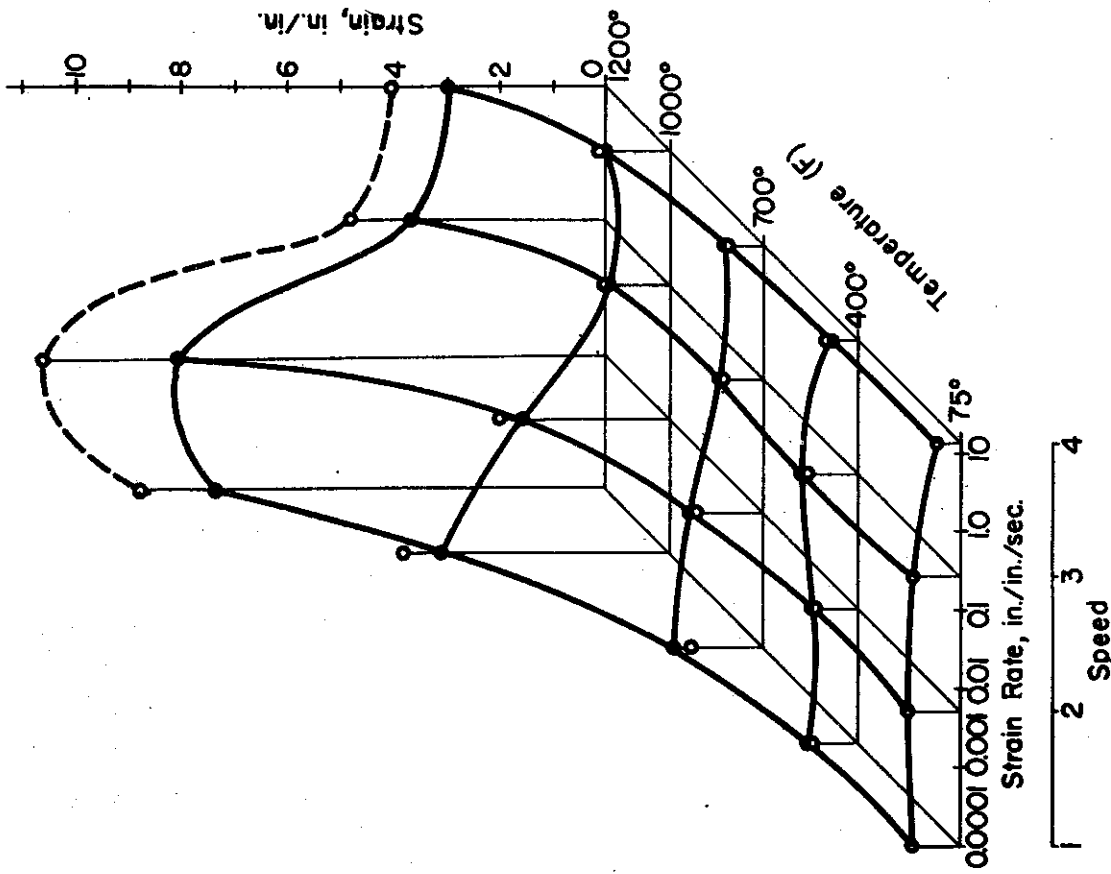


Fig.28 Combined Effects of Rate of Strain and Temperature on the Total Shearing Strain of SAE 4340 Steel in Torsion.

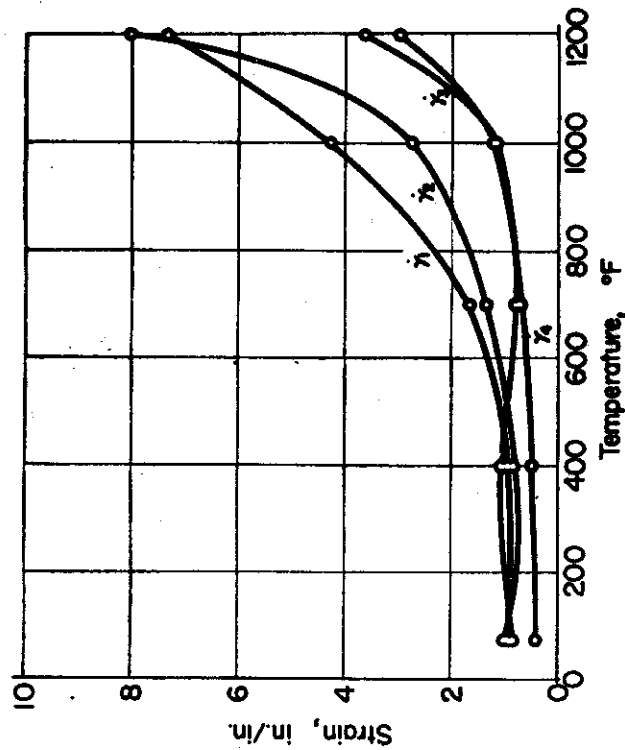


Fig.27 Effect of Temperature on the Total Shearing Strain of SAE 4340 Steel in Torsion.

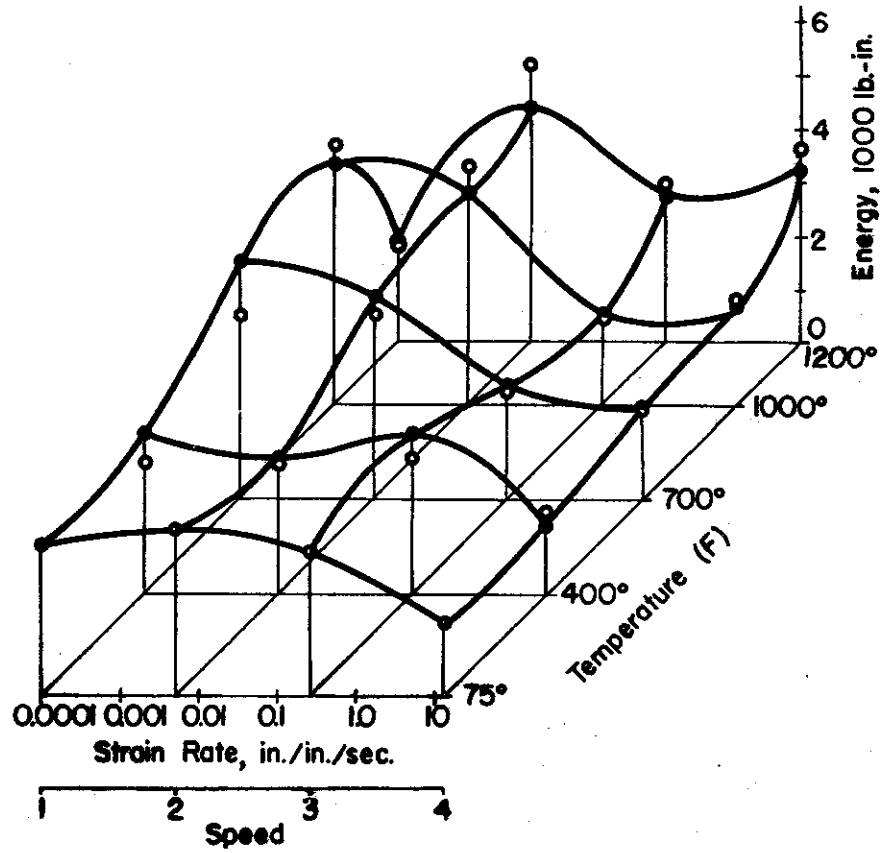


Fig.29 Combined Effects of Rate of Strain and Temperature on the Energy Absorbed in Specimens of SAE 4340 Steel in Torsion.

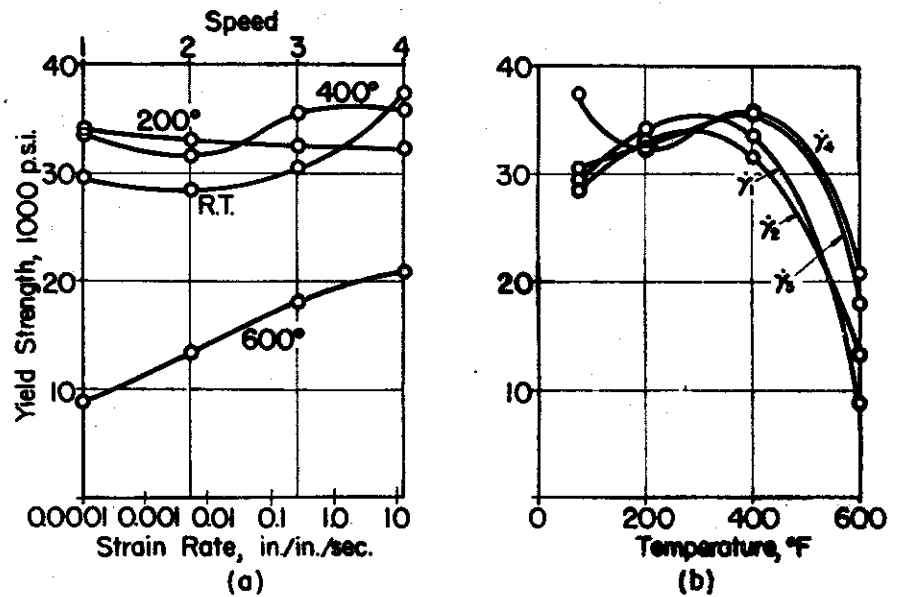


Fig. 30. Effect of (a) Rate of Strain and (b) Temperature on the Shearing Yield Strength of 24 S-T Aluminium Alloy in Torsion.

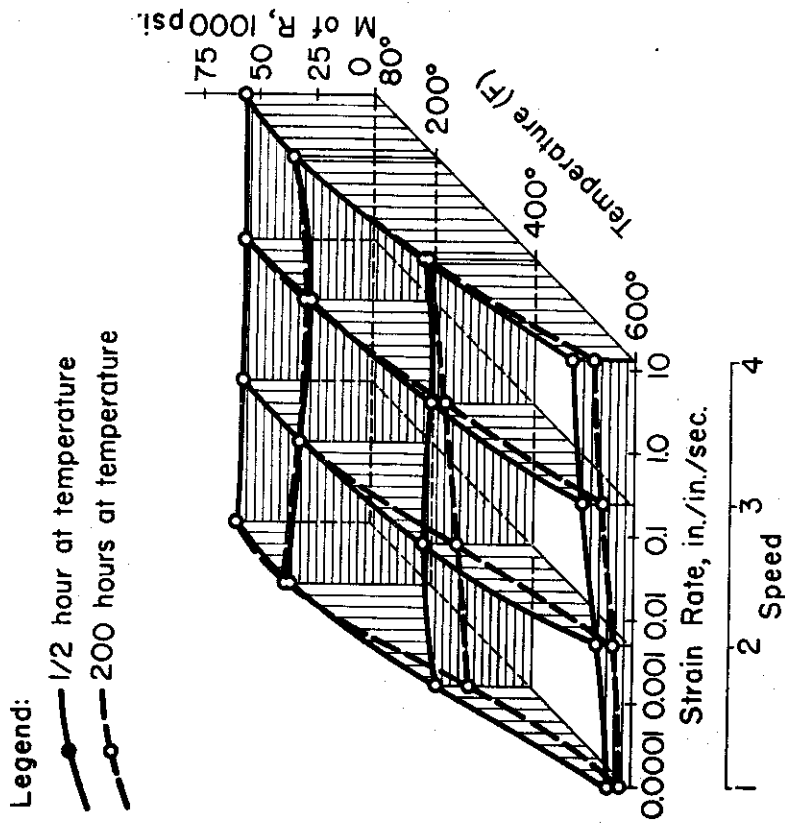


Fig.32 Combined Effects of Rate of Strain and Temperature on the Modulus of Rupture of 24S-T Aluminum Alloy in Torsion.

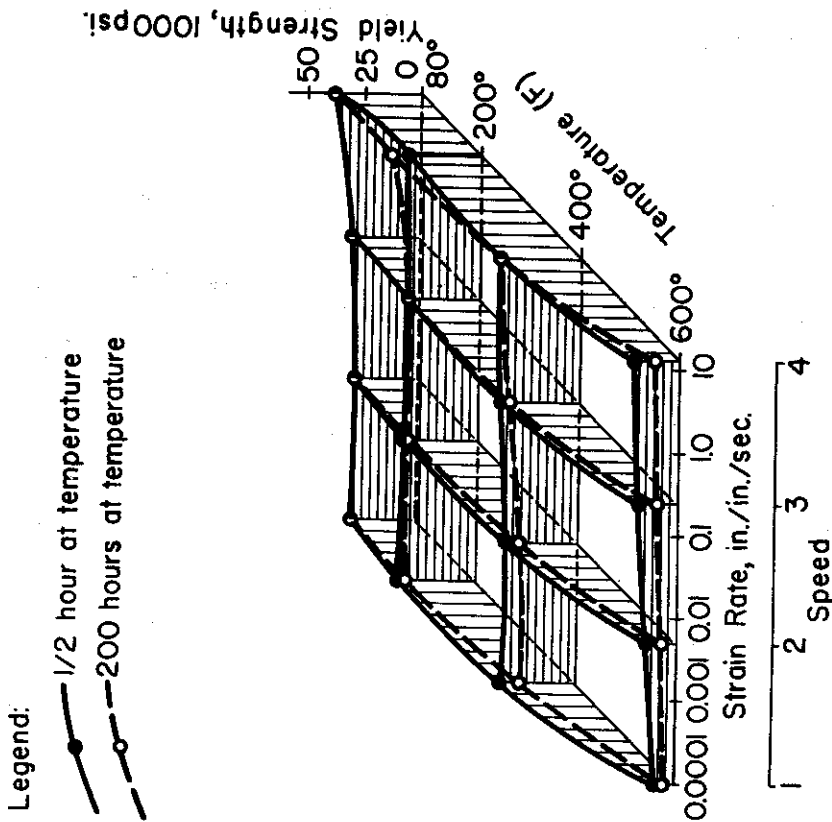


Fig.31 Combined Effects of Rate of Strain and Temperature on the Shearing Yield Strength of 24S-T Aluminum Alloy in Torsion.

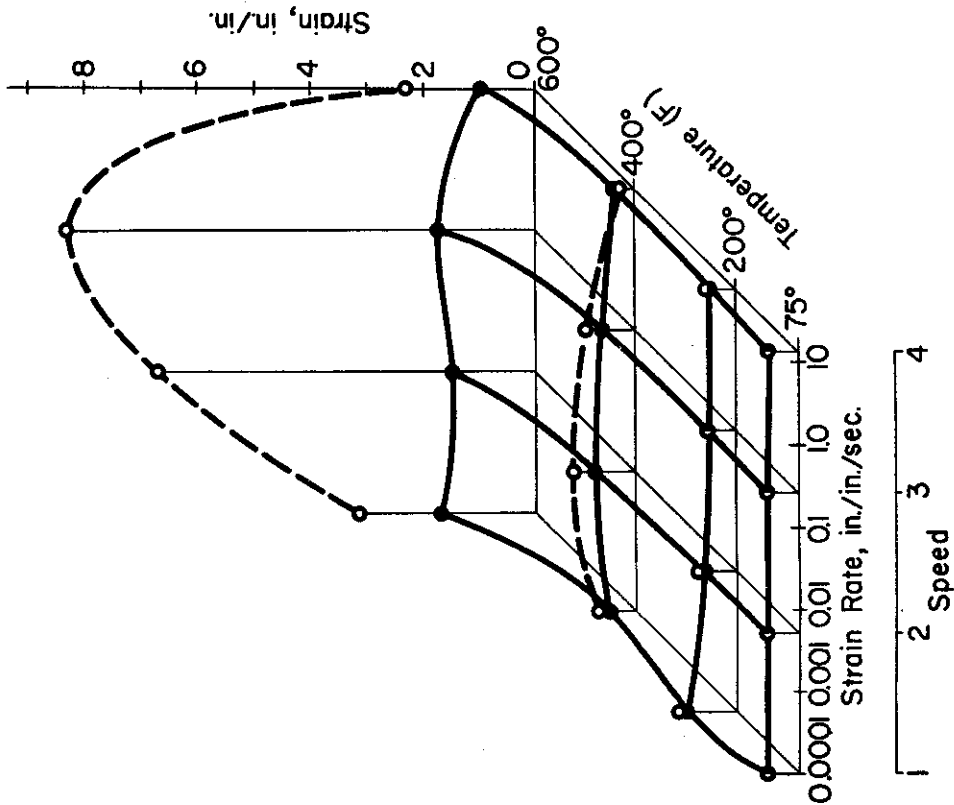


Fig.33 Combined Effects of Rate of Strain and Temperature on the Total Shearing Strain of 24S-T Aluminum Alloy in Torsion.

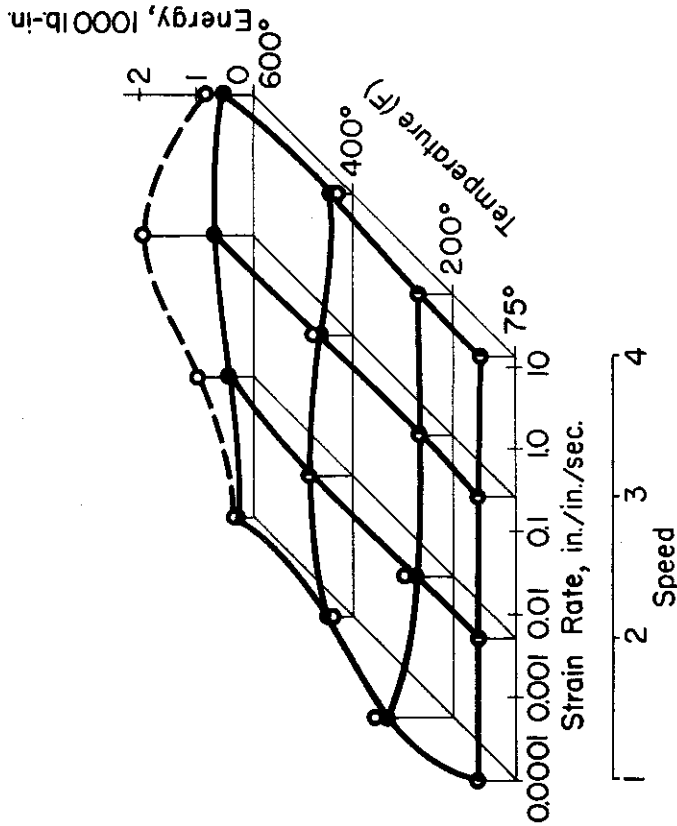


Fig.34 Combined Effects of Rate of Strain and Temperature on the Energy Absorbed in Specimens of 24S-T Aluminum Alloy in Torsion.

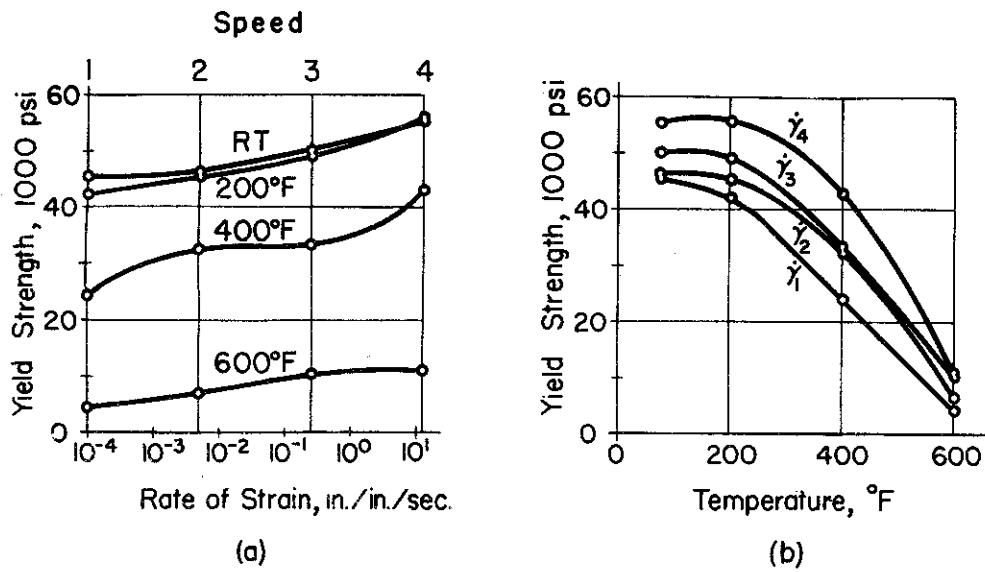


Fig.35 Effect of (a) Rate of Strain and (b) Temperature on the Shearing Yield Strength of 75S-T Aluminum Alloy in Torsion.

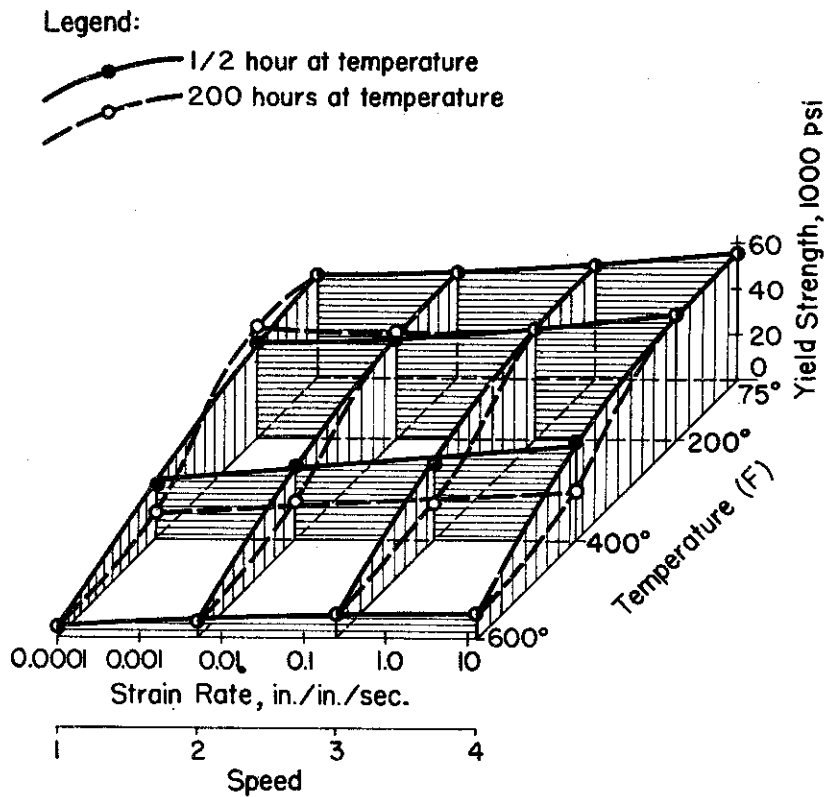




Fig.36 Combined Effects of Rate of Strain and Temperature on the Shearing Yield Strength of 75S-T Aluminum Alloy in Torsion.

Legend:

-  1/2 hour at temperature
-  200 hours at temperature

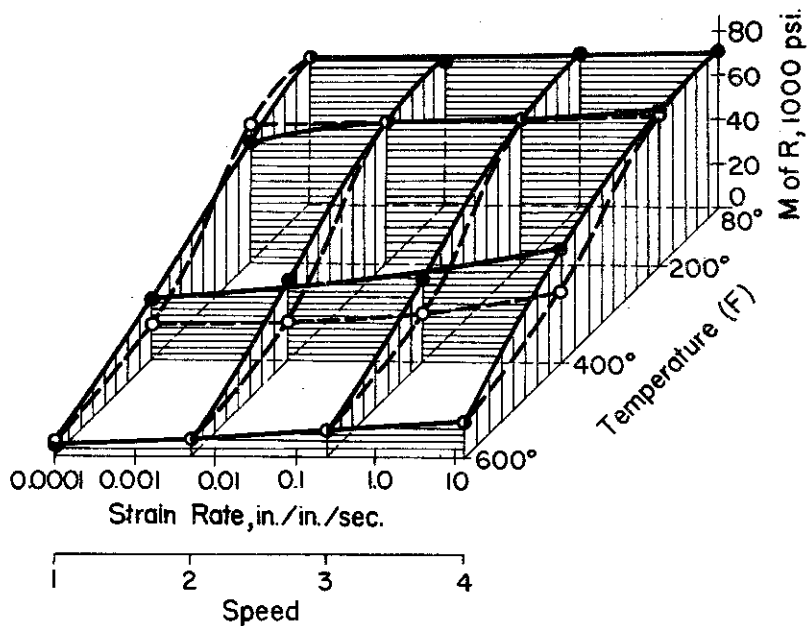


Fig.37 Combined Effects of Rate of Strain and Temperature on the Modulus of Rupture of 75S-T Aluminum Alloy in Torsion.

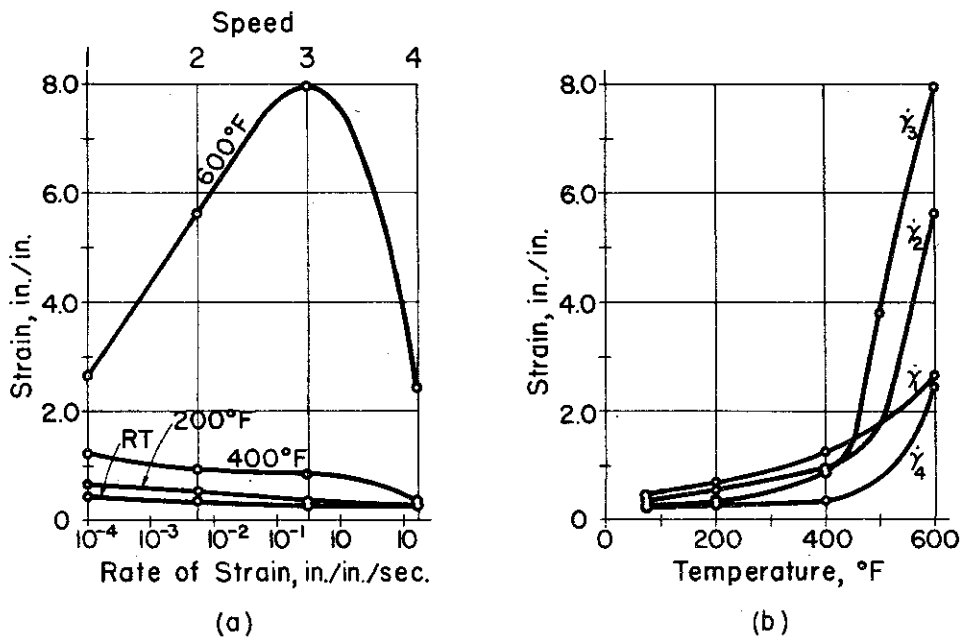


Fig.38 Effect of (a) Rate of Strain and (b) Temperature on the Total Shearing Strain of 75S-T Aluminum Alloy in Torsion.

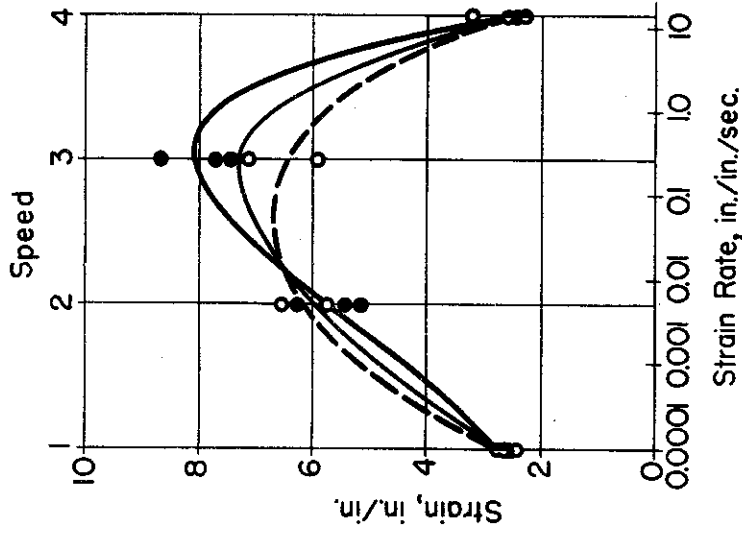


Fig.40 Effect of Rate of Strain on the Total Shearing Strain of 75S-T Aluminum Alloy at 600°F in Torsion. (Each point represents the strain for one specimen, not an average.)

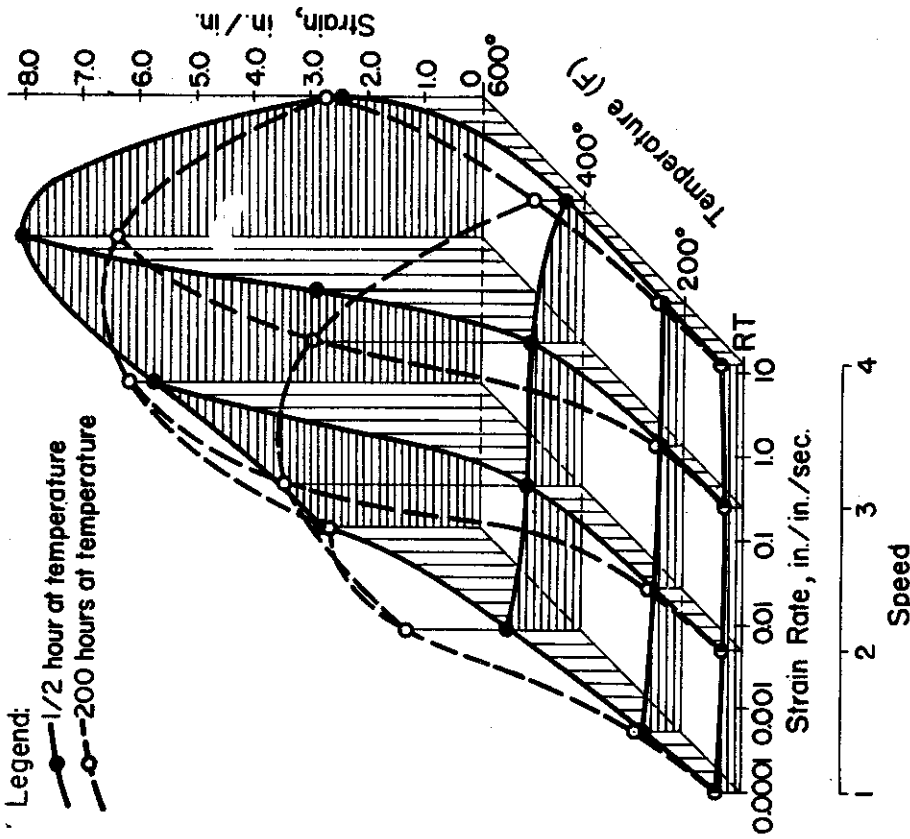


Fig.39 Combined Effects of Rate of Strain and Temperature on the Total Shearing Strain of 75S-T Aluminum Alloy in Torsion.

Legend:

—●— 1/2 hour at temperature
 -○- 200 hours at temperature

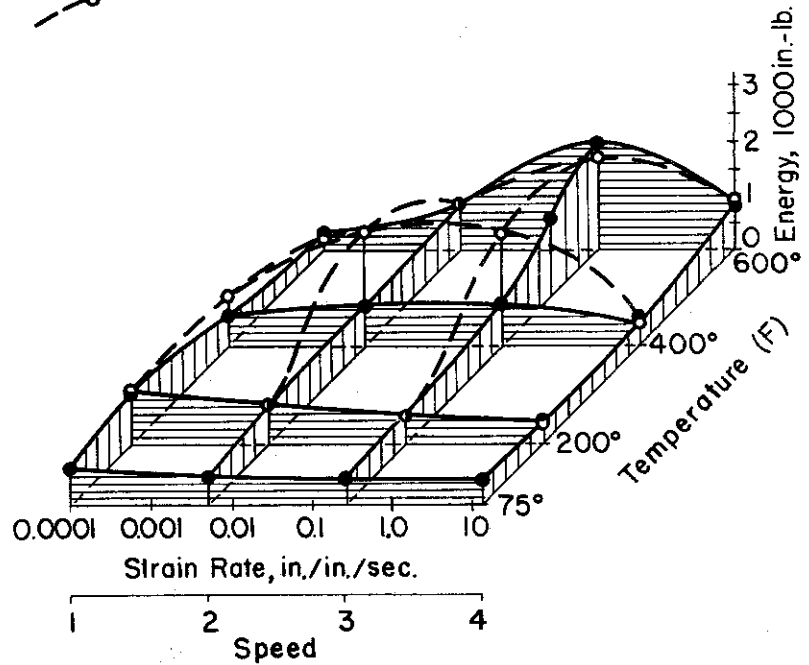


Fig. 41 Combined Effects of Rate of Strain and Temperature on the Energy Absorbed in Specimens of 75S-T Aluminum Alloy in Torsion.

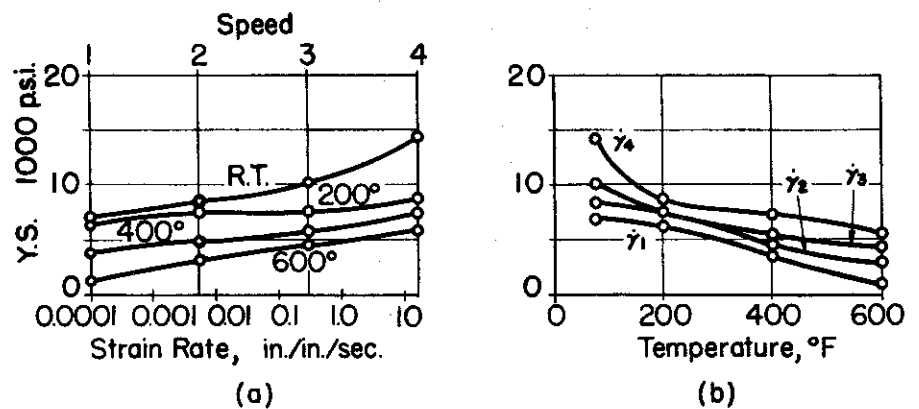


Fig. 42. Effect of (a) Rate of Strain and (b) Temperature on the Shearing Yield Strength of FS-1 Magnesium Alloy in Torsion.

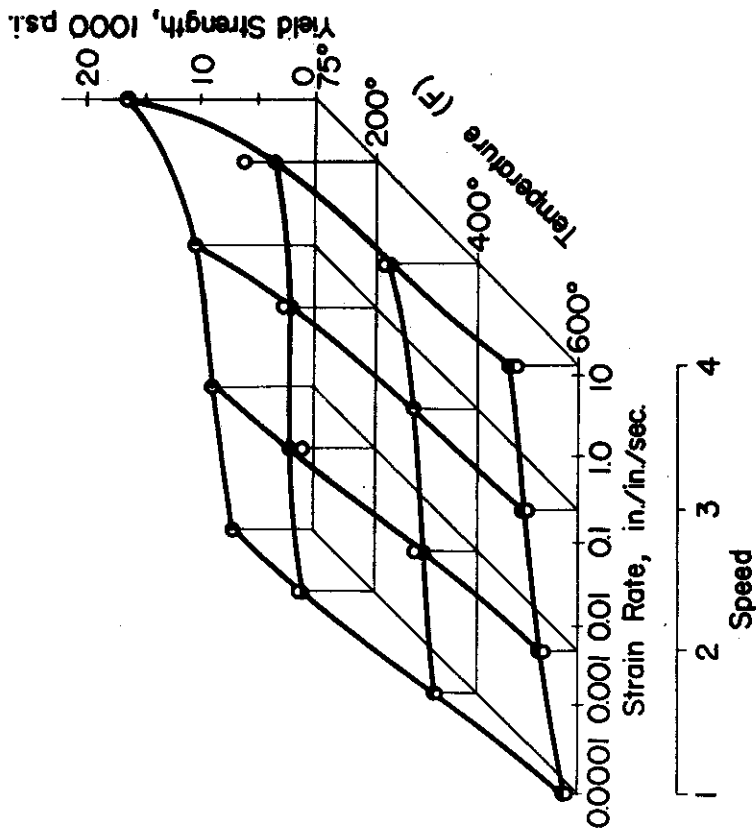


Fig.43 Combined Effects of Rate of Strain and Temperature on the Shearing Yield Strength of FS-1 Magnesium Alloy in Torsion.

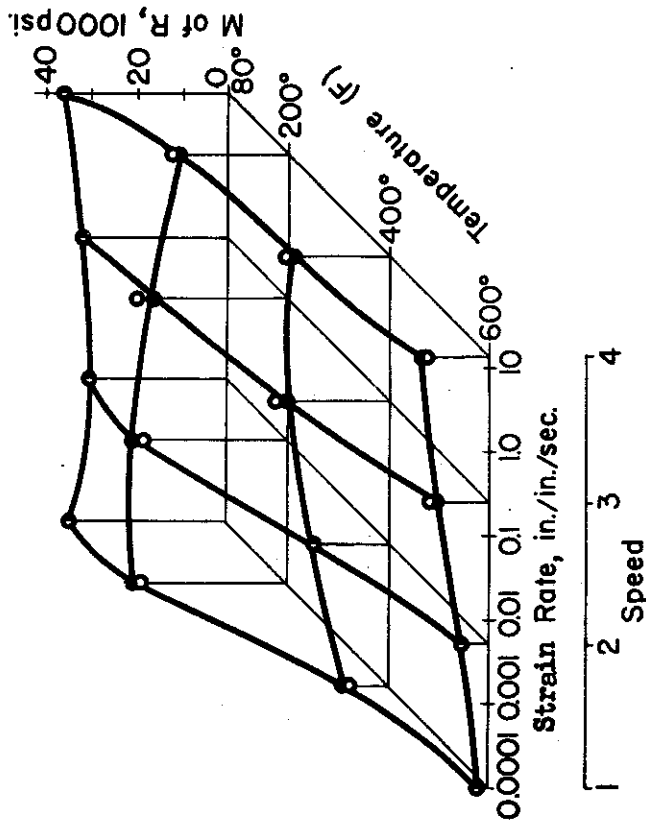


Fig.44 Combined Effects of Rate of Strain and Temperature on the Modulus of Rupture of FS-1 Magnesium Alloy in Torsion.

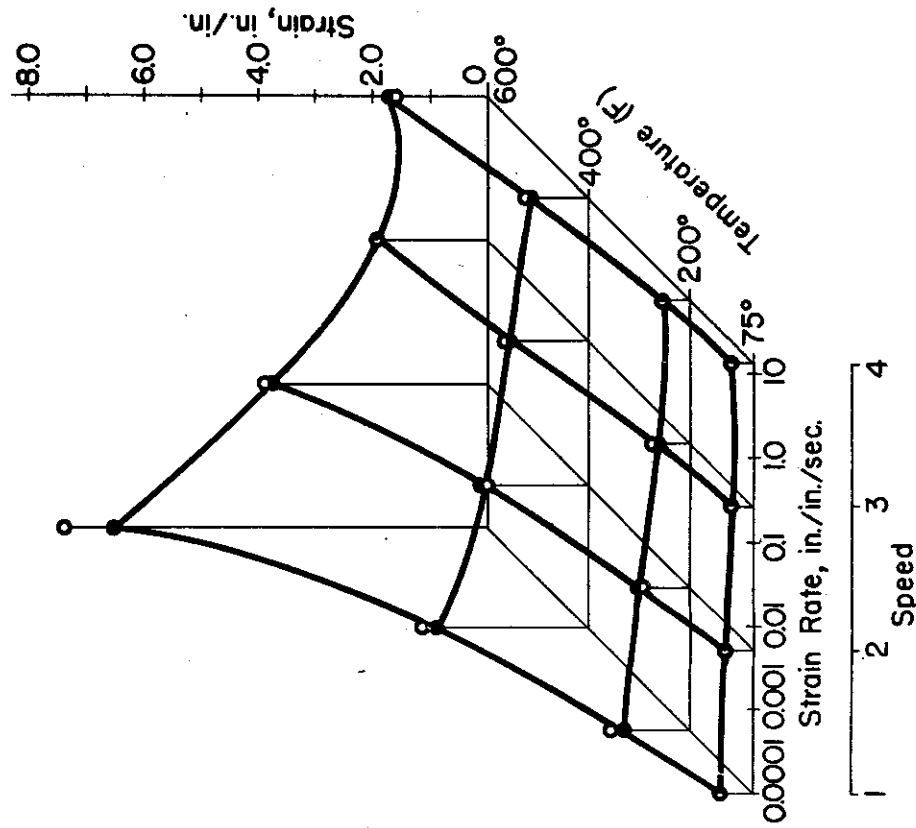


Fig.45 Combined Effects of Rate of Strain and Temperature on the Total Shearing Strain of FS-1 Magnesium Alloy in Torsion.

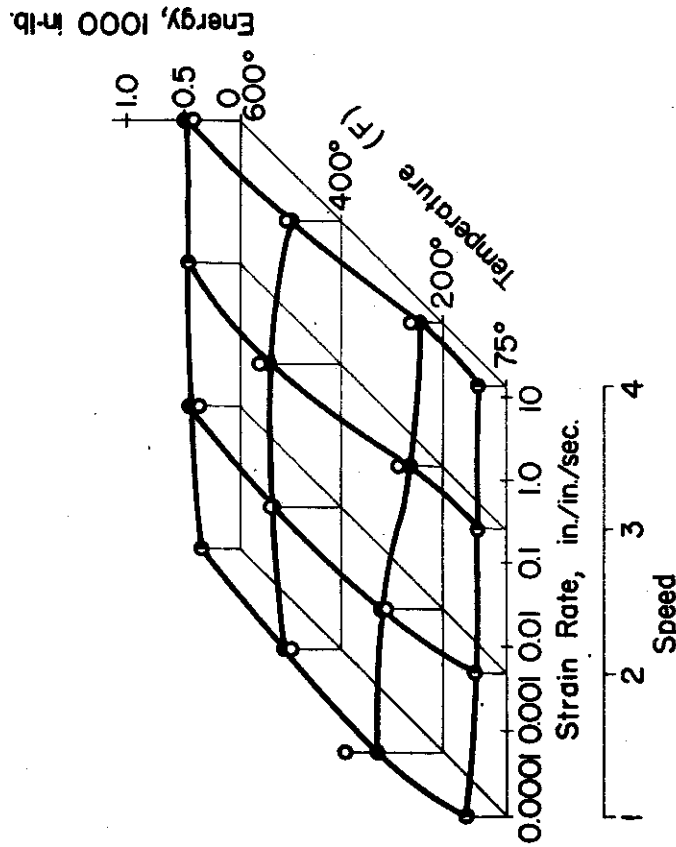


Fig.46 Combined Effects of Rate of Strain and Temperature on the Energy Absorbed in Specimens of FS-1 Magnesium Alloy in Torsion.

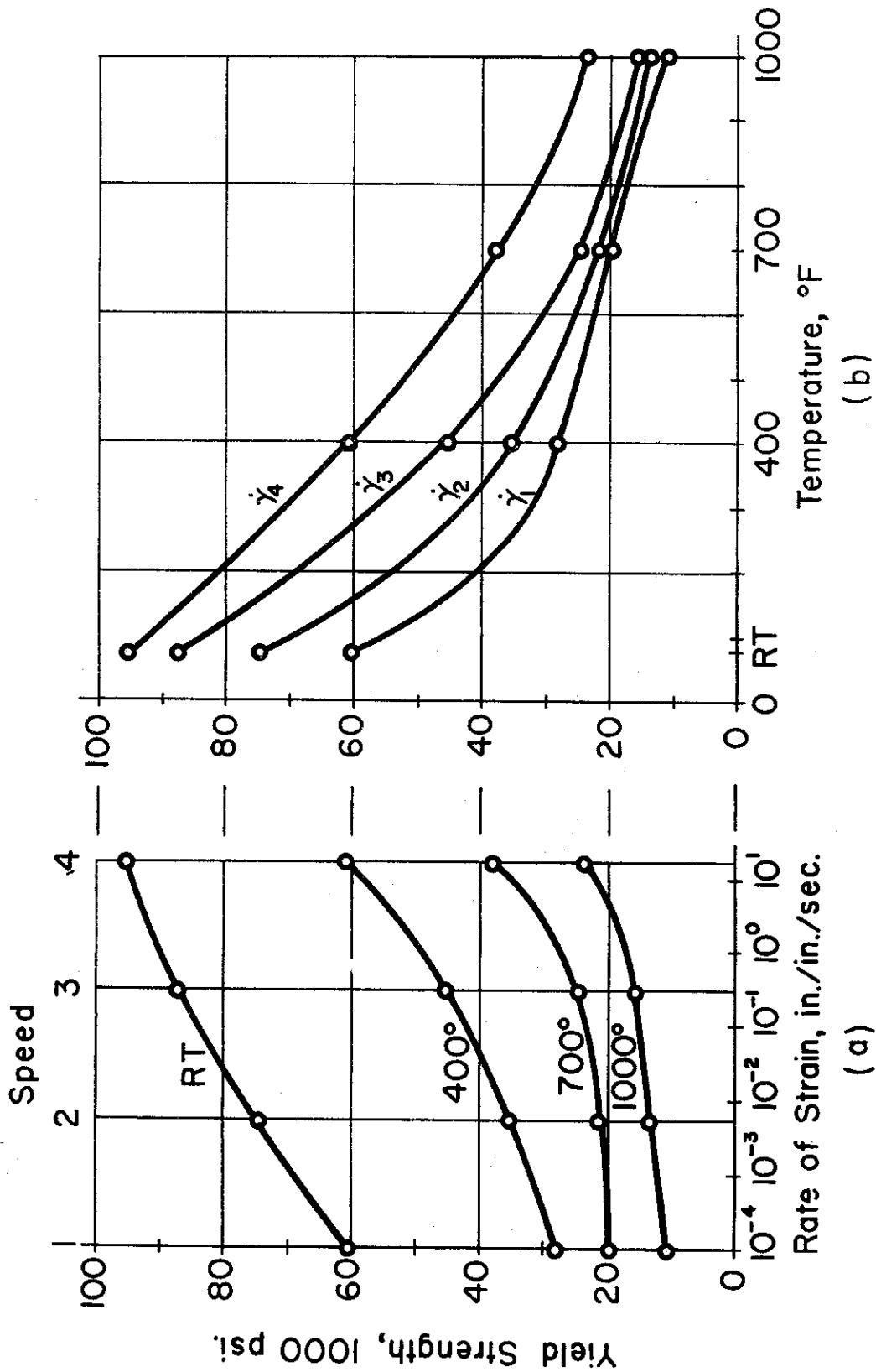


Fig. 47. Effect of (a) Rate of Strain and (b) Temperature on the Shearing Yield Strength of RC-70 Titanium in Torsion.

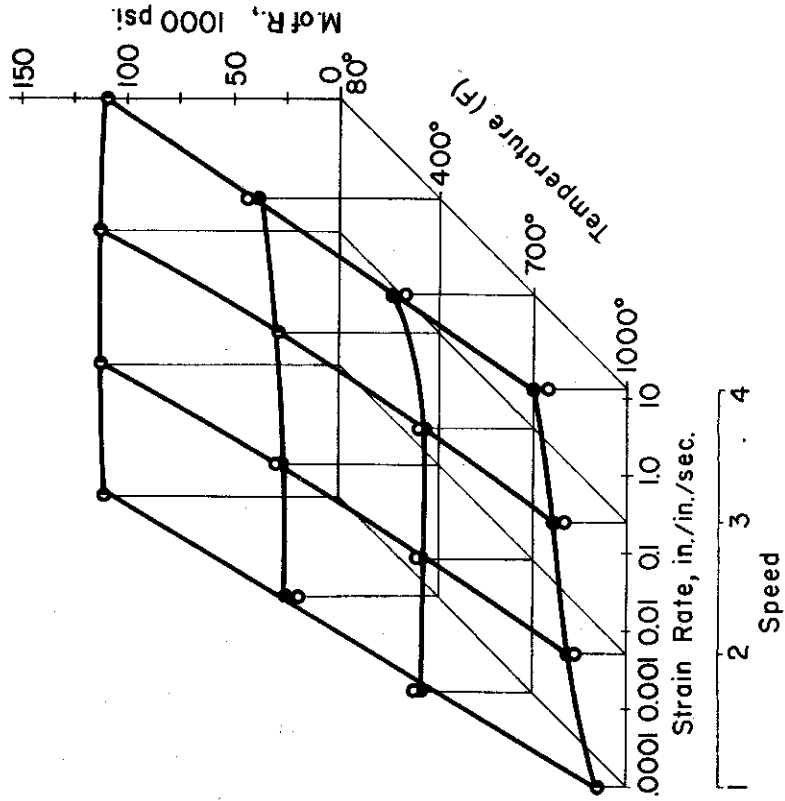


Fig. 49. Combined Effects of Rate of Strain and Temperature on the Modulus of Rupture of RC-70 Titanium in Torsion.

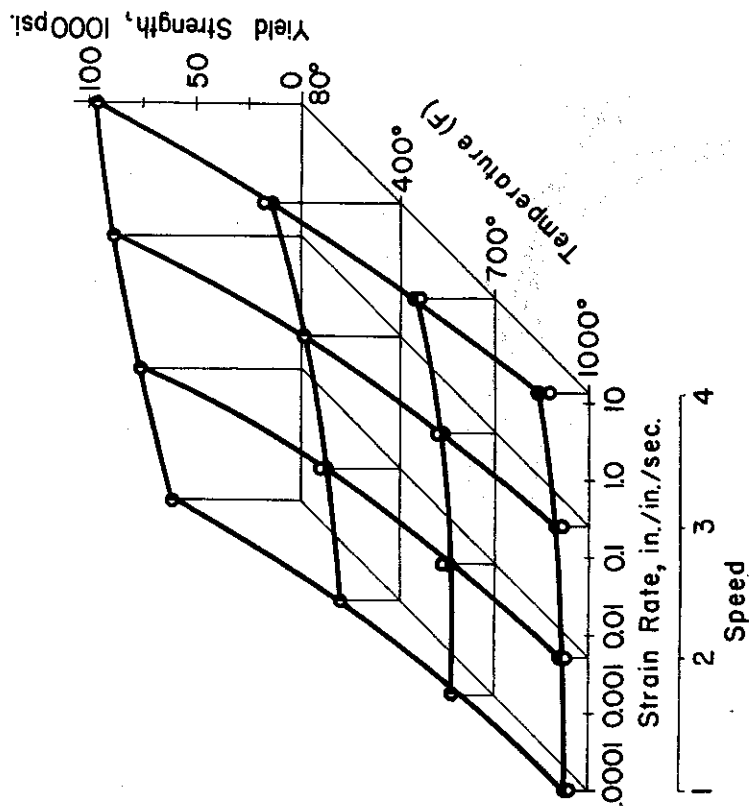


Fig. 48. Combined Effects of Rate of Strain and Temperature on the Shearing Yield Strength of RC-70 Titanium in Torsion.

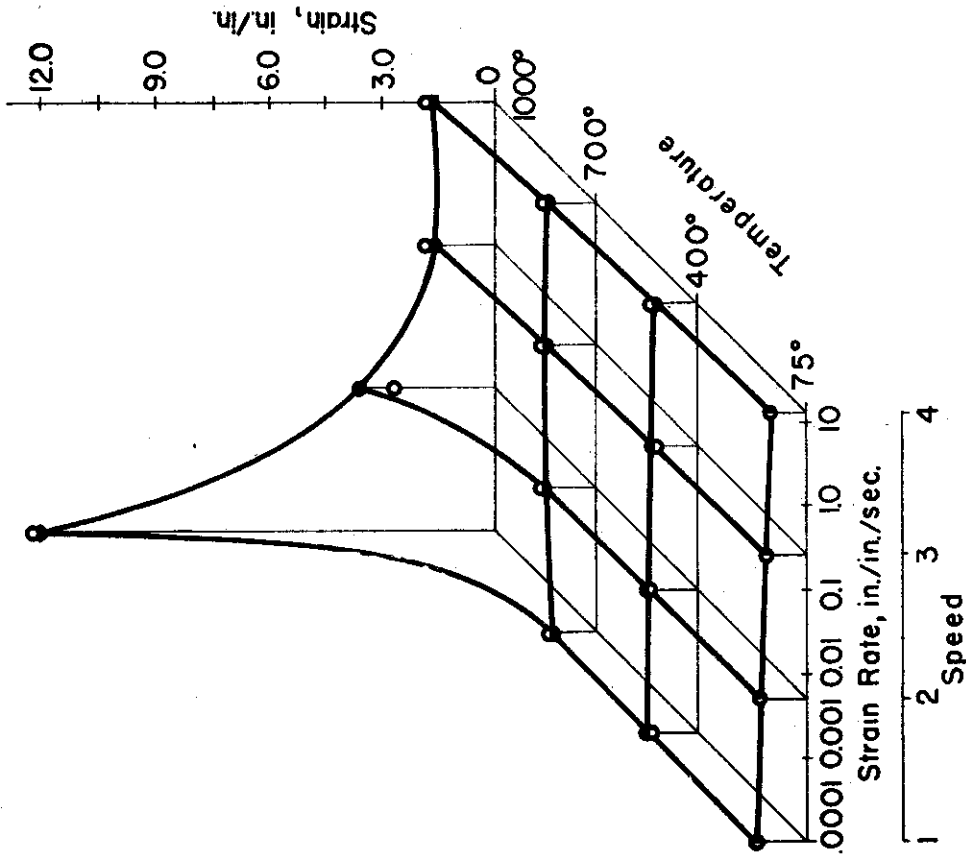


Fig.51. Combined Effects of Rate of Strain and Temperature on the Total Shearing Strain of RC-70 Titanium in Torsion.

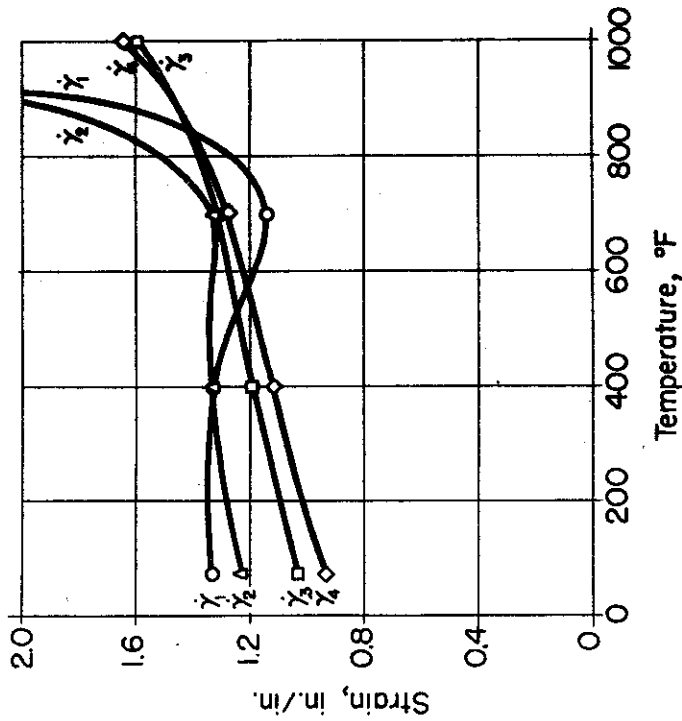


Fig.50 Effect of Temperature on the Total Shearing Strain of RC-70 Titanium in Torsion.

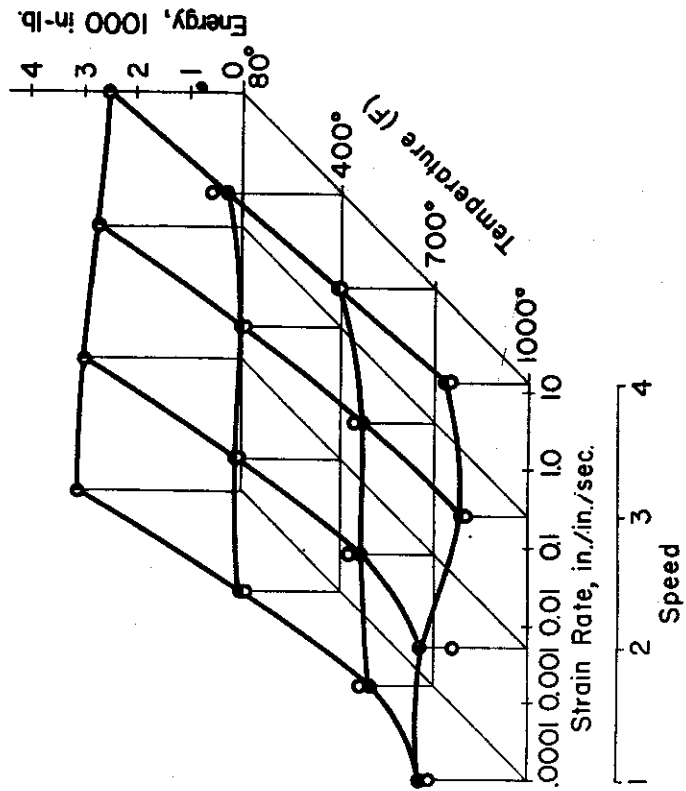


Fig.52. Combined Effects of Rate of Strain and Temperature on the Energy Absorbed in Specimens of RC-70 Titanium in Torsion.

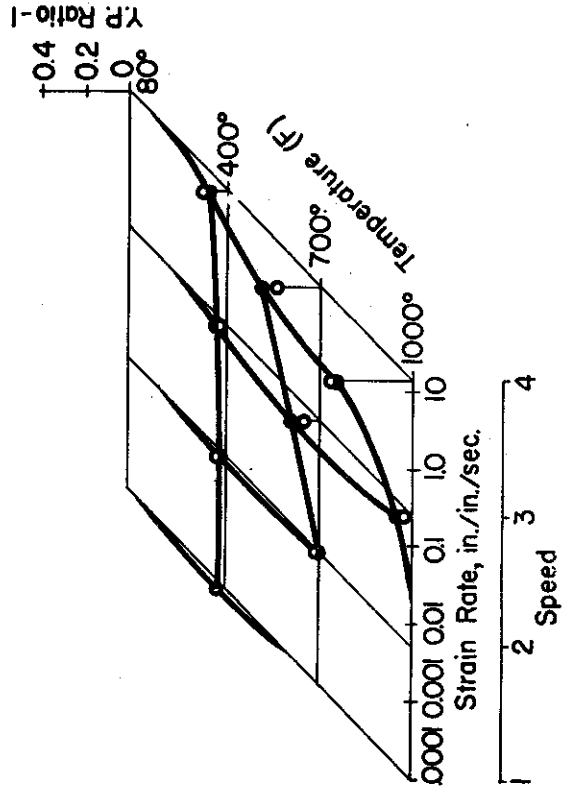


Fig.53. Combined Effects of Rate of Strain and Temperature on the Yield Point Ratio for RC-70 Titanium in Torsion.

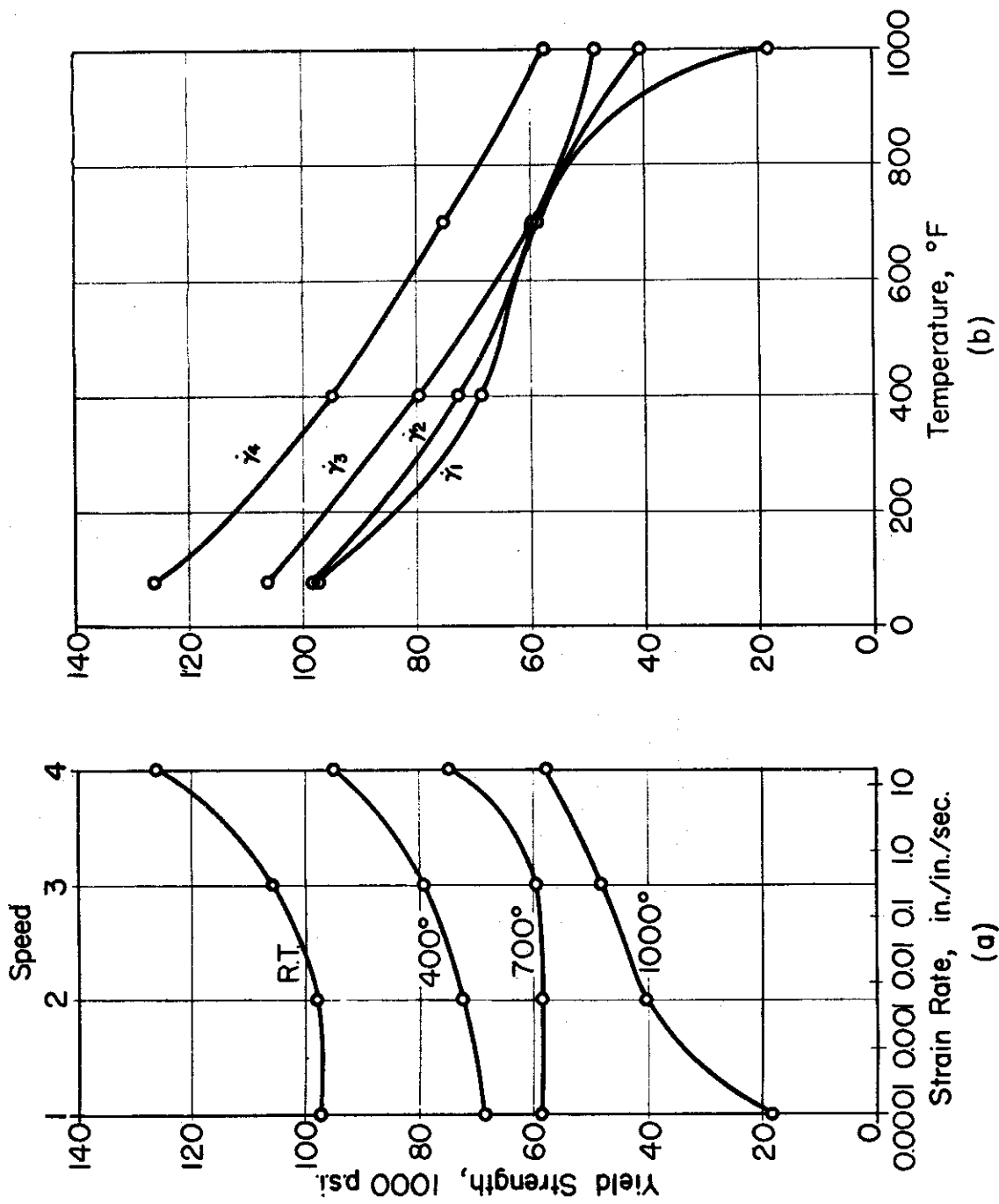


Fig. 54. Effect of (a) Rate of Strain and (b) Temperature on the Shearing Yield Strength of RC-130-B Titanium Alloy in Torsion.

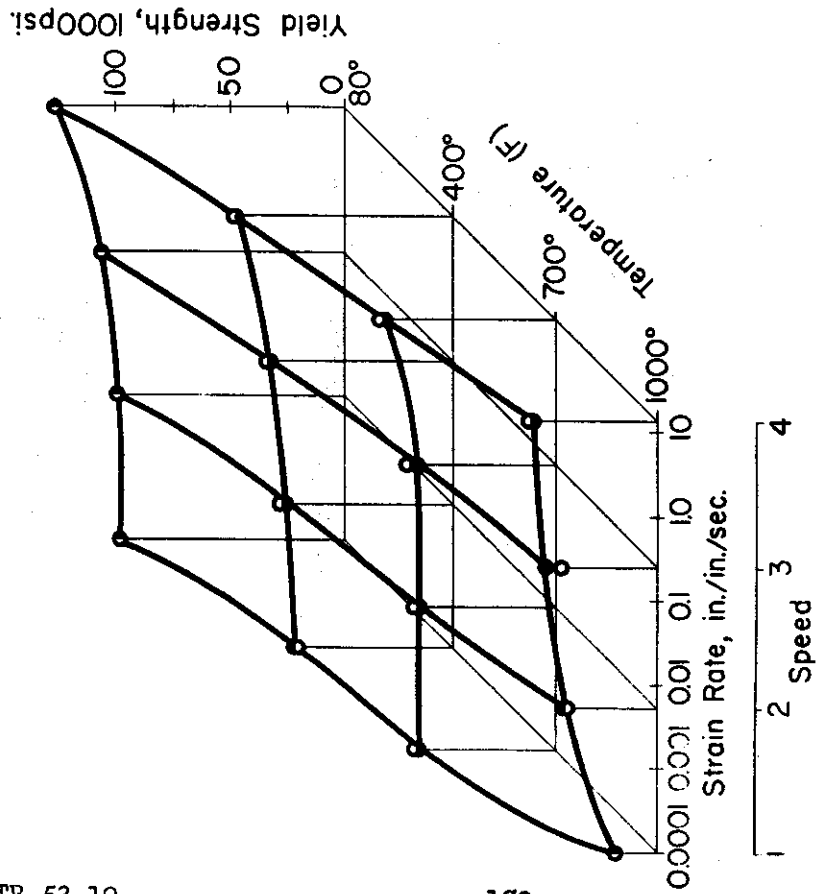


Fig.55 Combined Effects of Rate of Strain and Temperature on the Yield Strength of RC-130-B Titanium Alloy in Torsion.

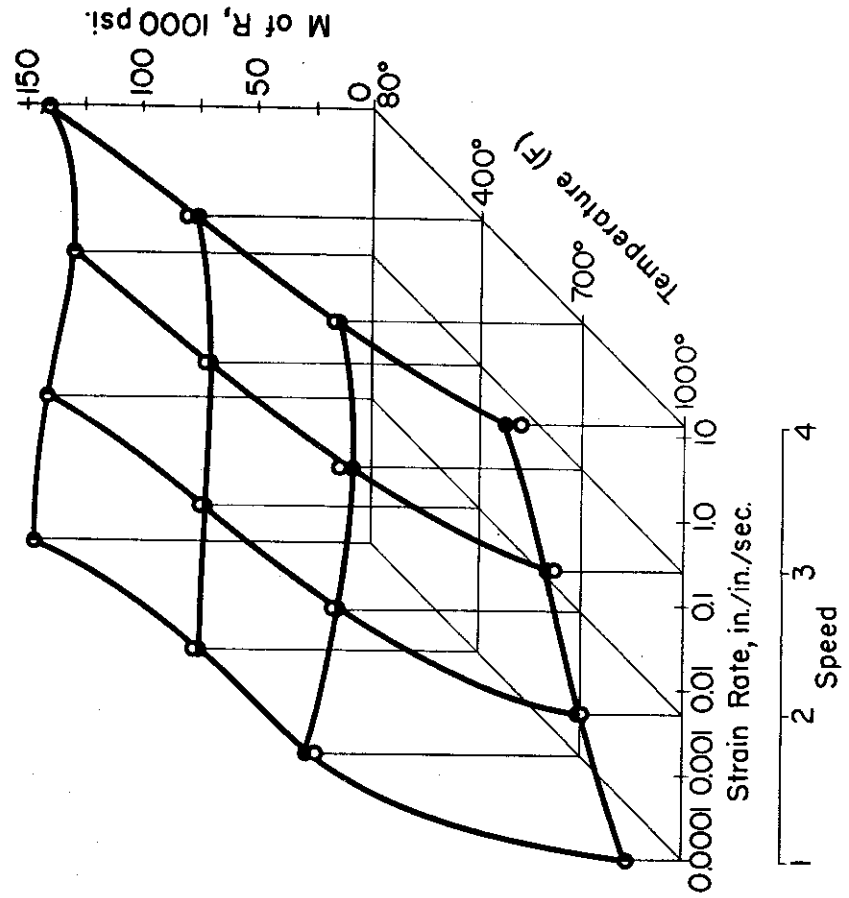


Fig.56 Combined Effects of Rate of Strain and Temperature on the Modulus of Rupture of RC-130-B Titanium Alloy in Torsion.

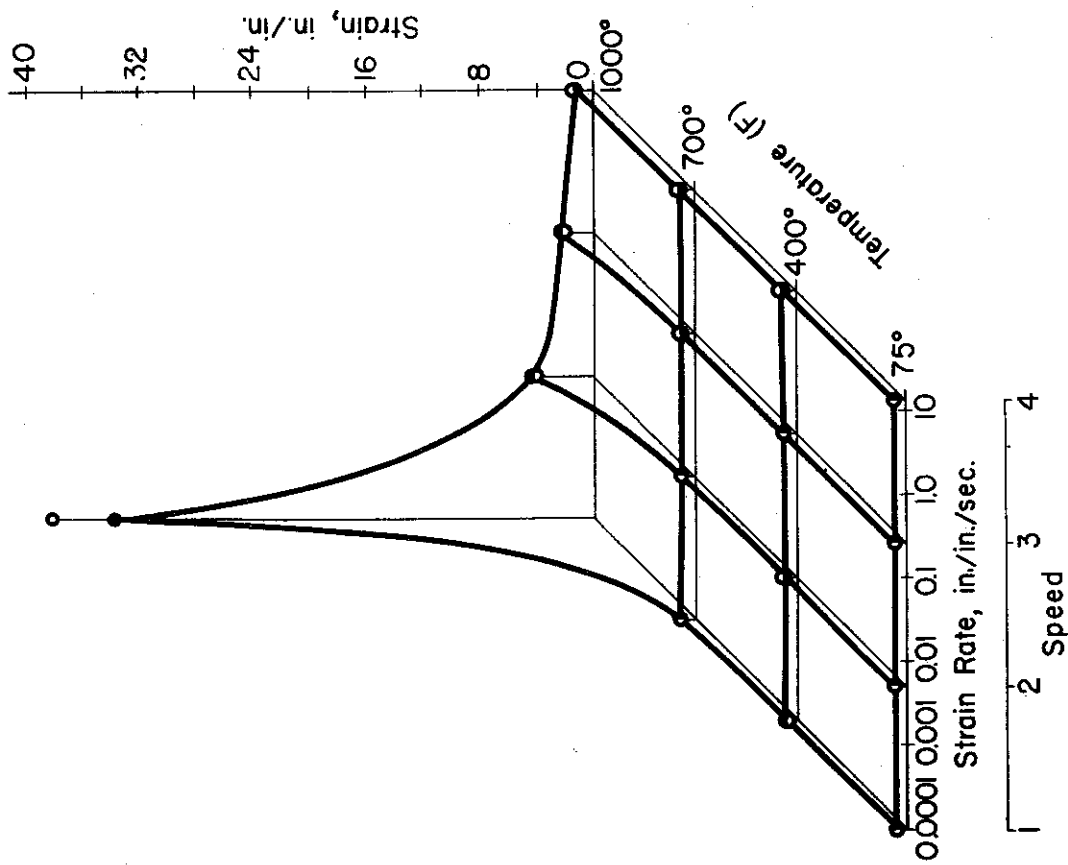


Fig.58 Combined Effects of Rate of Strain and Temperature on the Total Shearing Strain of RC-130-B Titanium Alloy in Torsion.

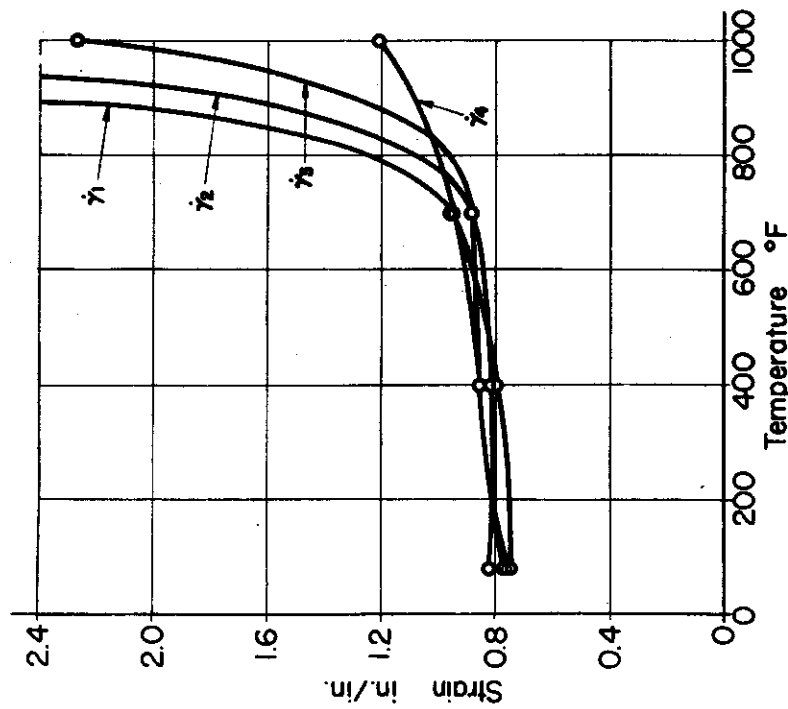


Fig.57 Effect of Temperature on the Total Shearing Strain of RC-130-B Titanium Alloy in Torsion.

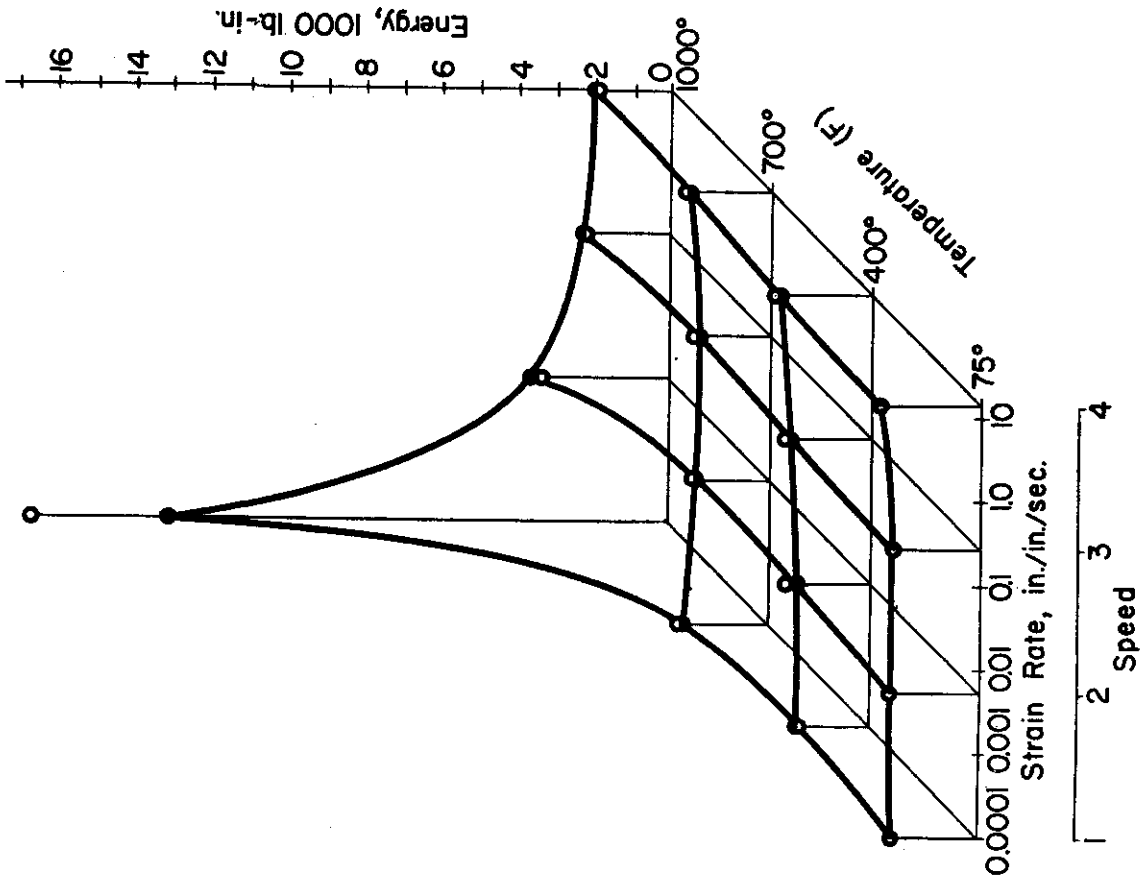


Fig.59 Combined Effects of Rate of Strain and Temperature on the Energy Absorbed in Specimens of RC-130-B Titanium Alloy in Torsion.

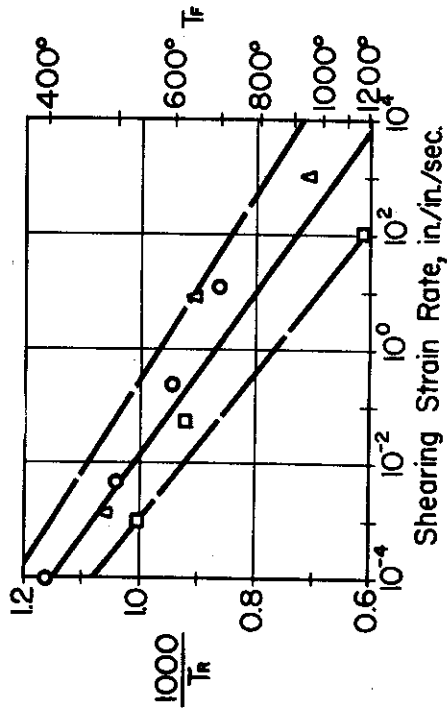
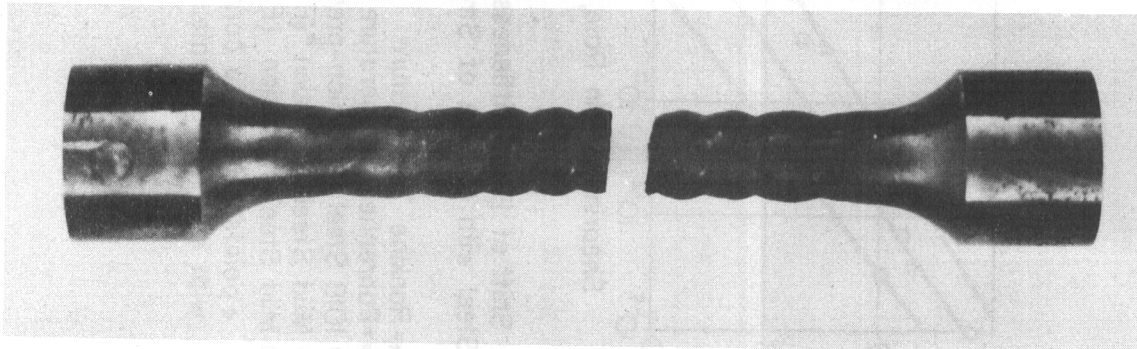
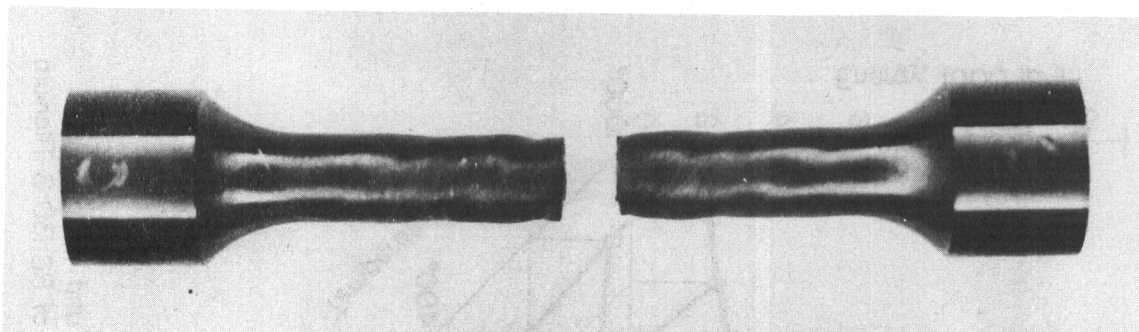


Fig.60 Shift of Blue Brittleness Temperature for Steel with Change of Strain-Rate

T_R = Rankine Temperature
 T_F = Fahrenheit Temperature
 ○ 1018 Steel in Torsion - present data
 △ Mild Steel in Tension * (Fig.14, Ref.85)
 □ Mild Steel in Torsion (Fig.63, Ref.52)
 * points off-set to correspond with shear strain rate.



TESTED AT 1000F



TESTED AT 700F

Fig. 61 RC-70 Titanium Specimens Broken in Second Speed Tests.
(Magnification X2)

Contrails

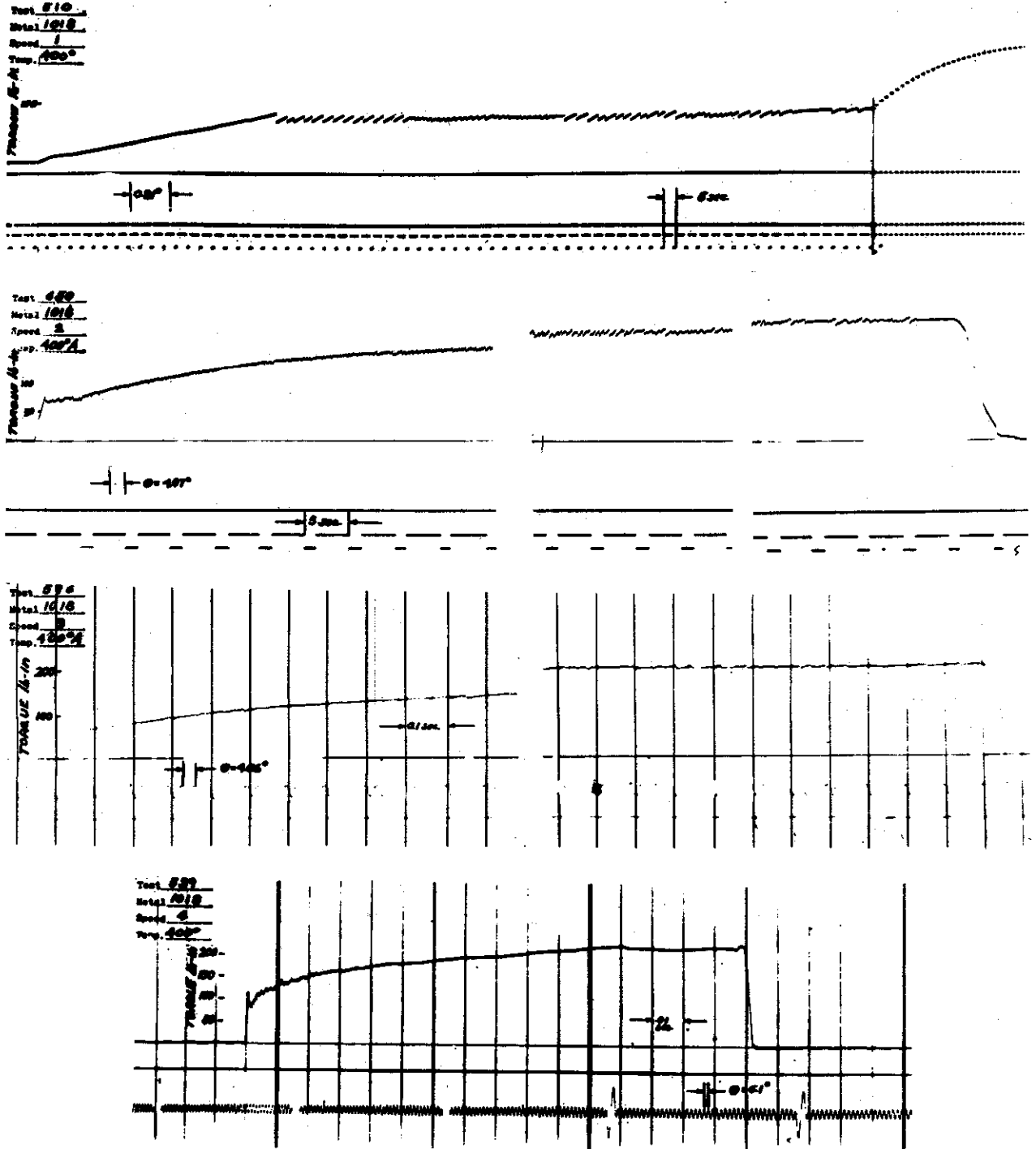


Fig. 62 Oscillograph Records for Tests of SAE 1018 Steel at 400°F

Contrails

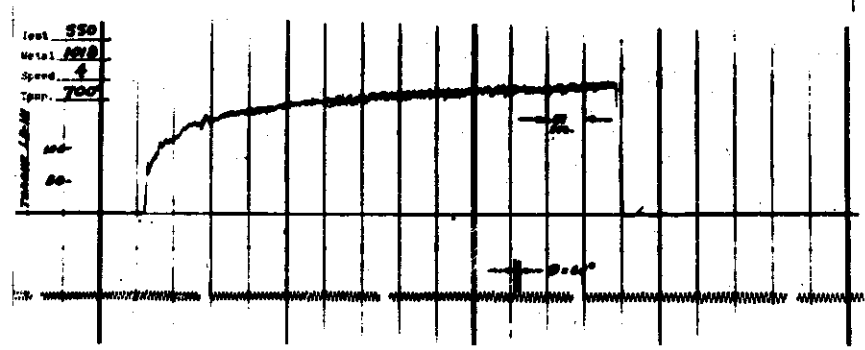
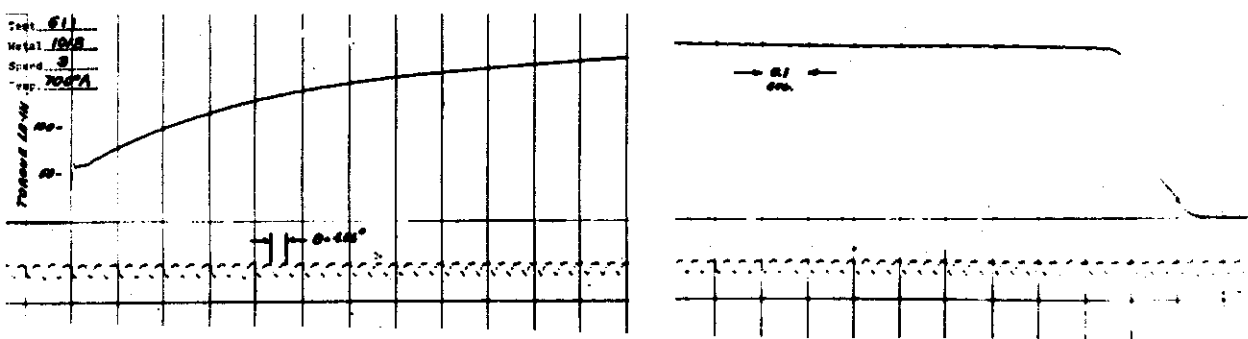
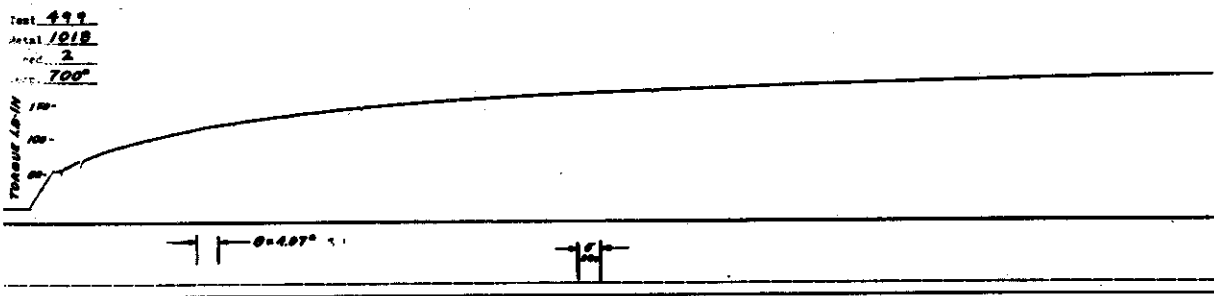
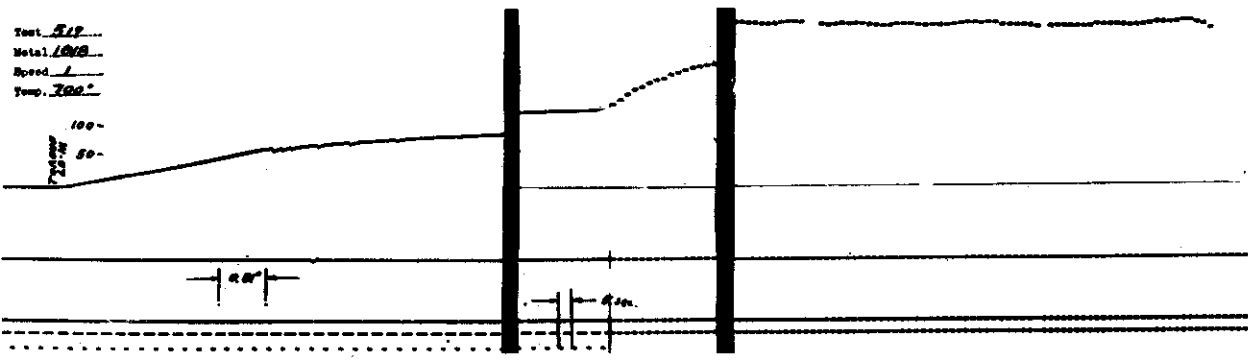


Fig. 63 Oscillograph Records for Tests of SAE 1018 Steel at 700°F

Contrails

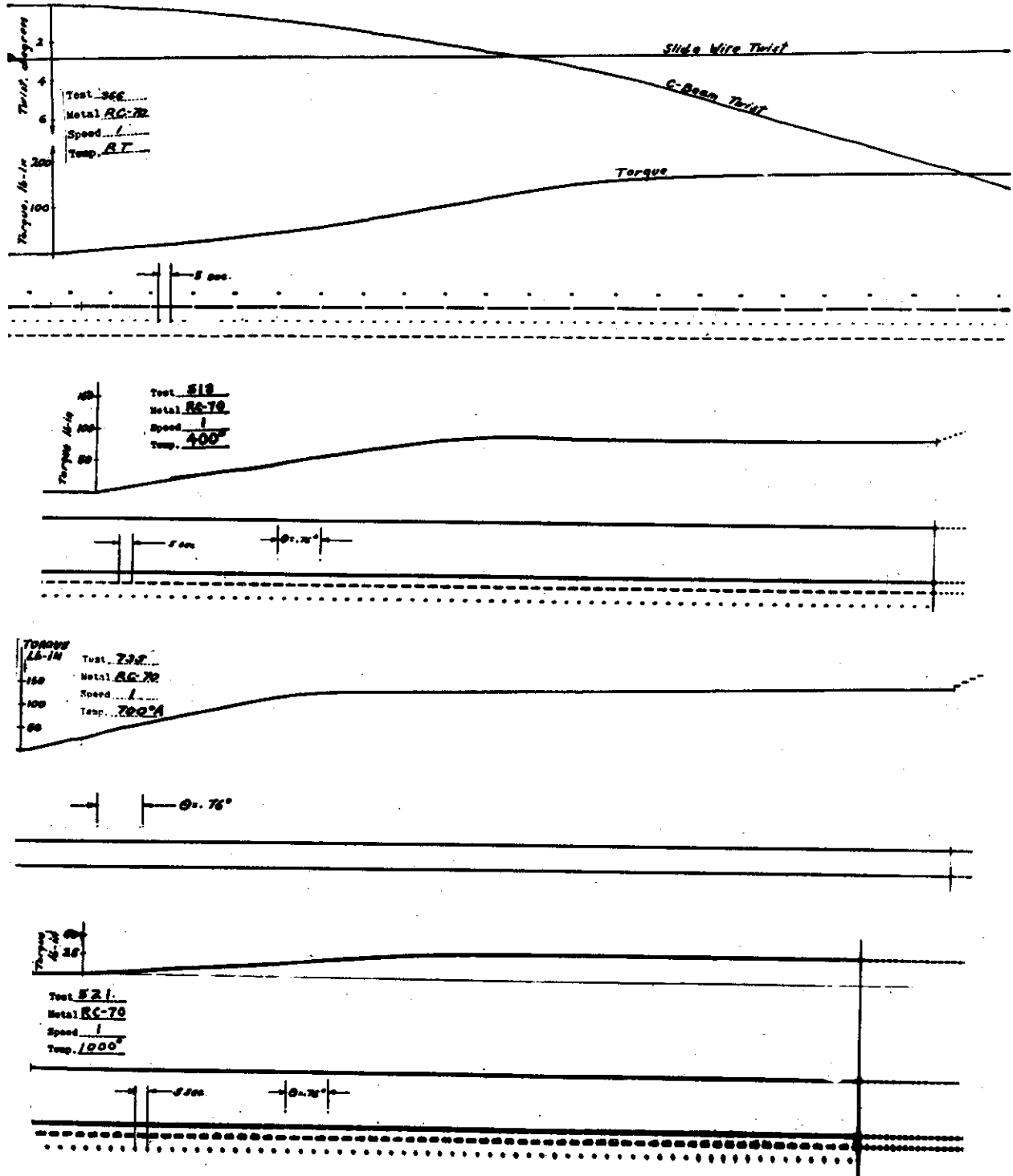


Fig. 64 Initial Portions of Oscillograph Records for First Speed Tests of RC-70 Titanium.

Contrails

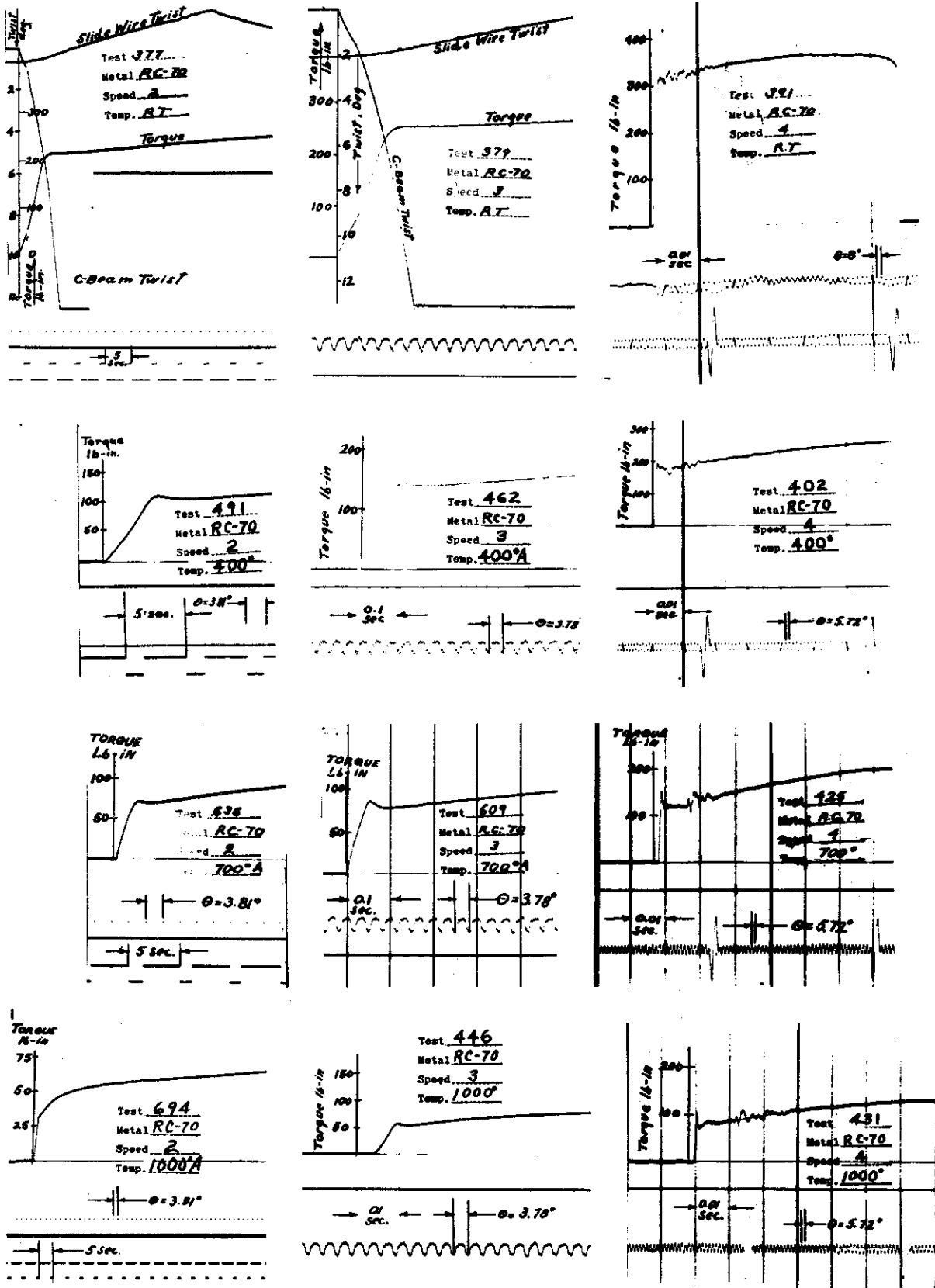


Fig. 65 Initial Portions of Oscillograph Records for Second, Third and Fourth Speed Tests of RC-70 Titanium.

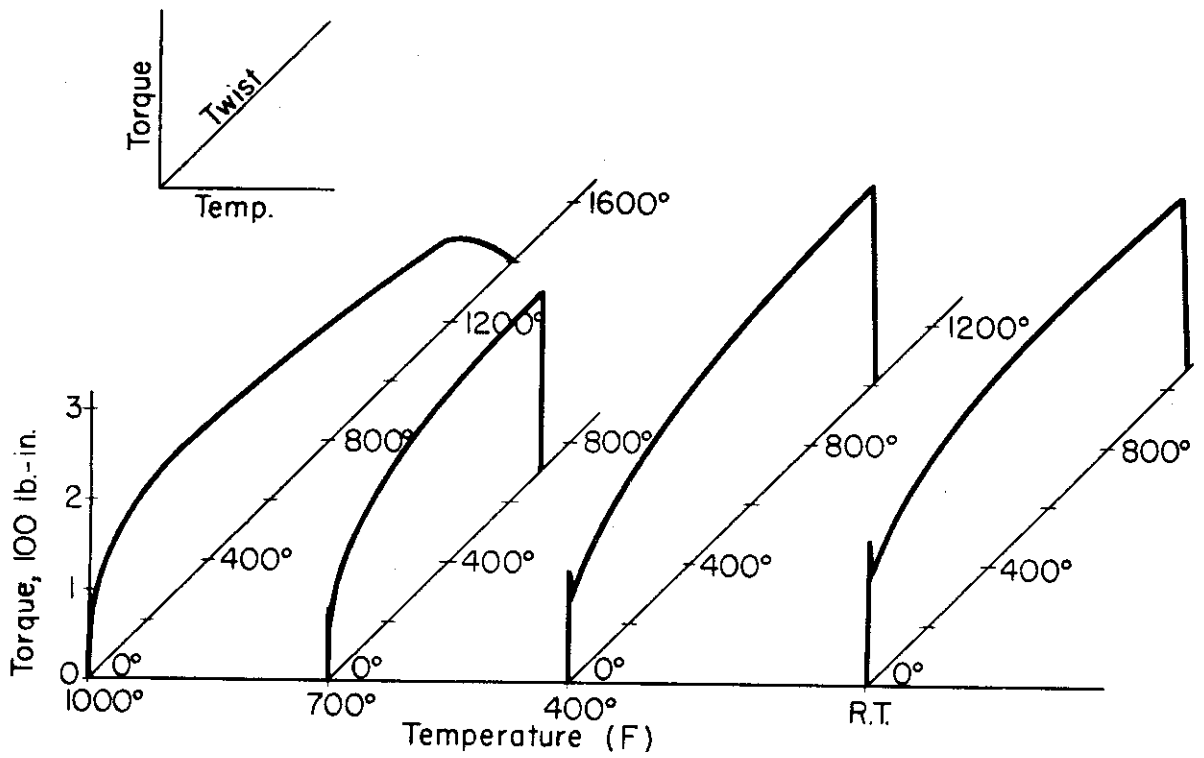


Fig.66 Torque-Twist*Curves for Fourth Speed Torsion Tests of SAE 1018 Steel at Four Temperatures.

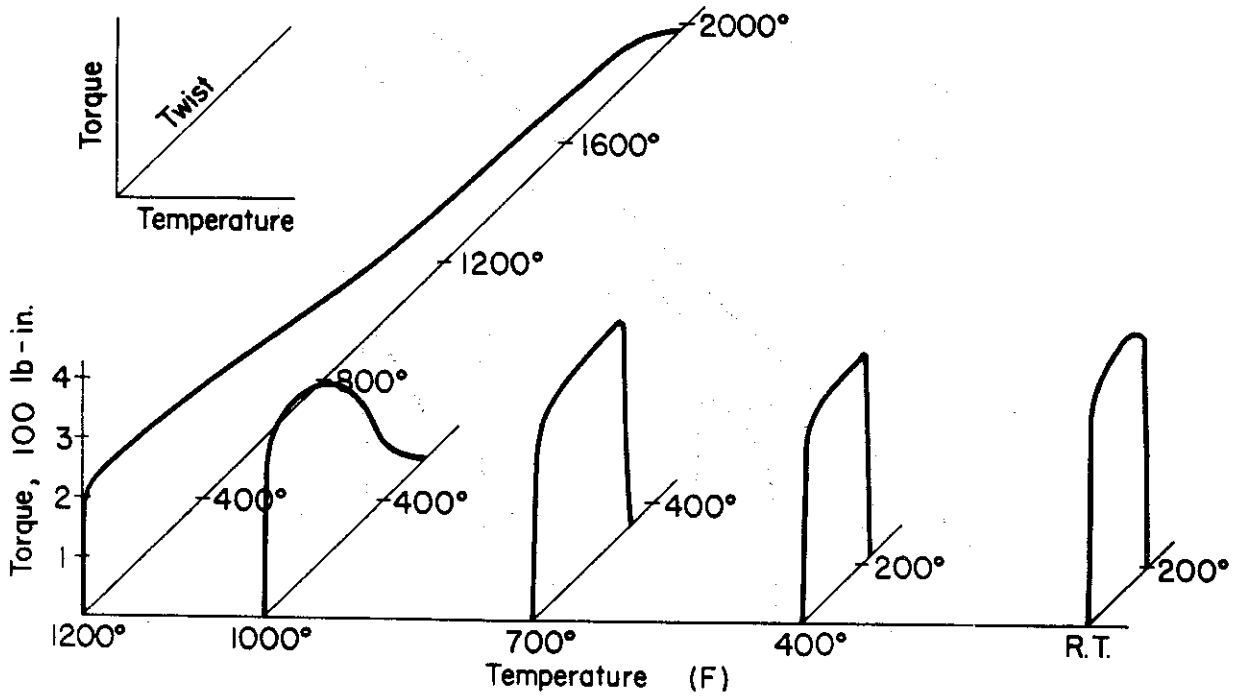


Fig.67 Torque - Twist Curves for Fourth Speed Torsion Tests of SAE 4340 Steel at Five Temperatures.

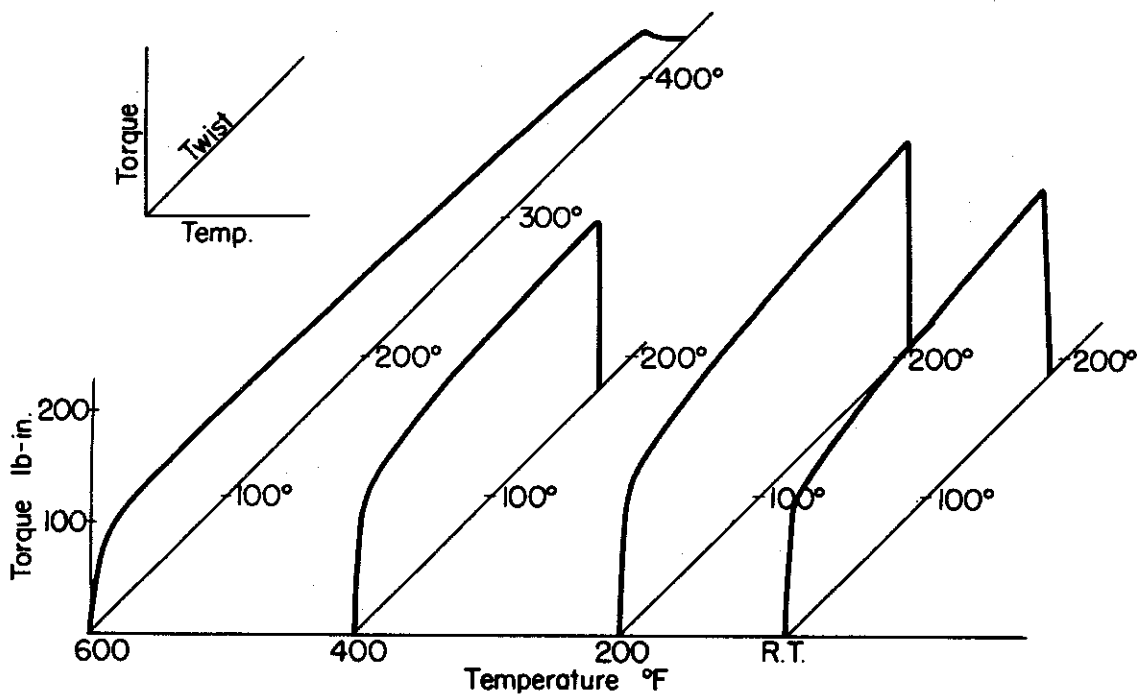


Fig.68 Torque-Twist Curves for Fourth Speed Torsion Tests of 24S-T Aluminum Alloy at Four Temperatures.

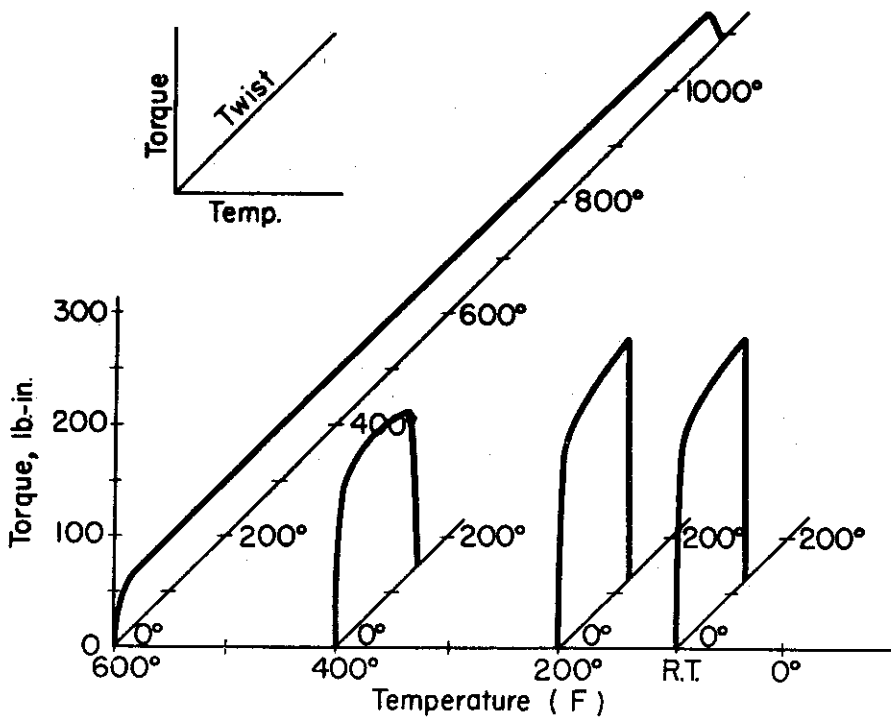


Fig.69 Torque-Twist Curves for Fourth Speed Torsion Tests of 75S-T Aluminum Alloy at Four Temperatures.

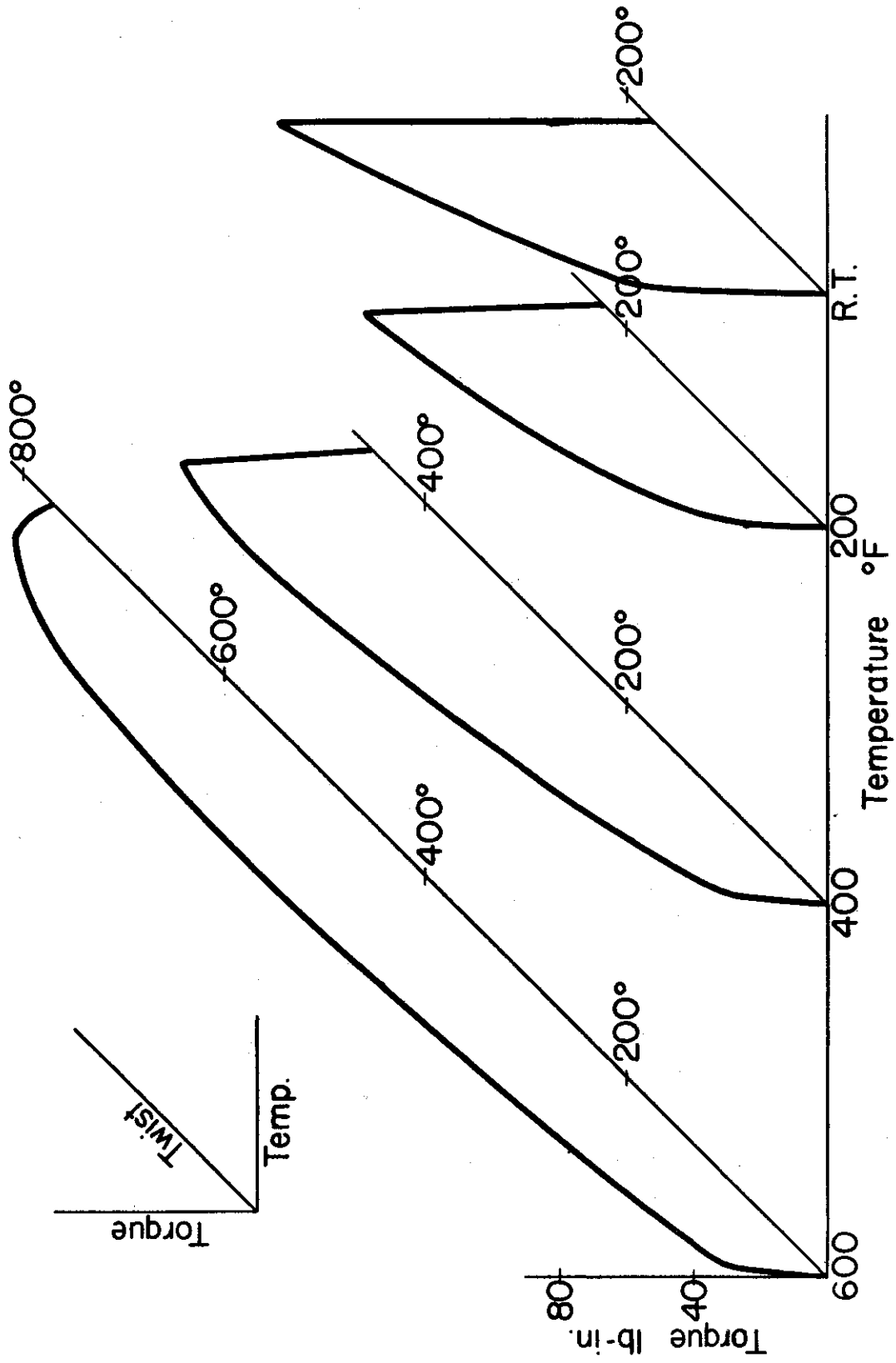


Fig.70 Torque-Twist Curves for Fourth Speed Torsion Tests of FS-1 Magnesium Alloy at Four Temperatures.

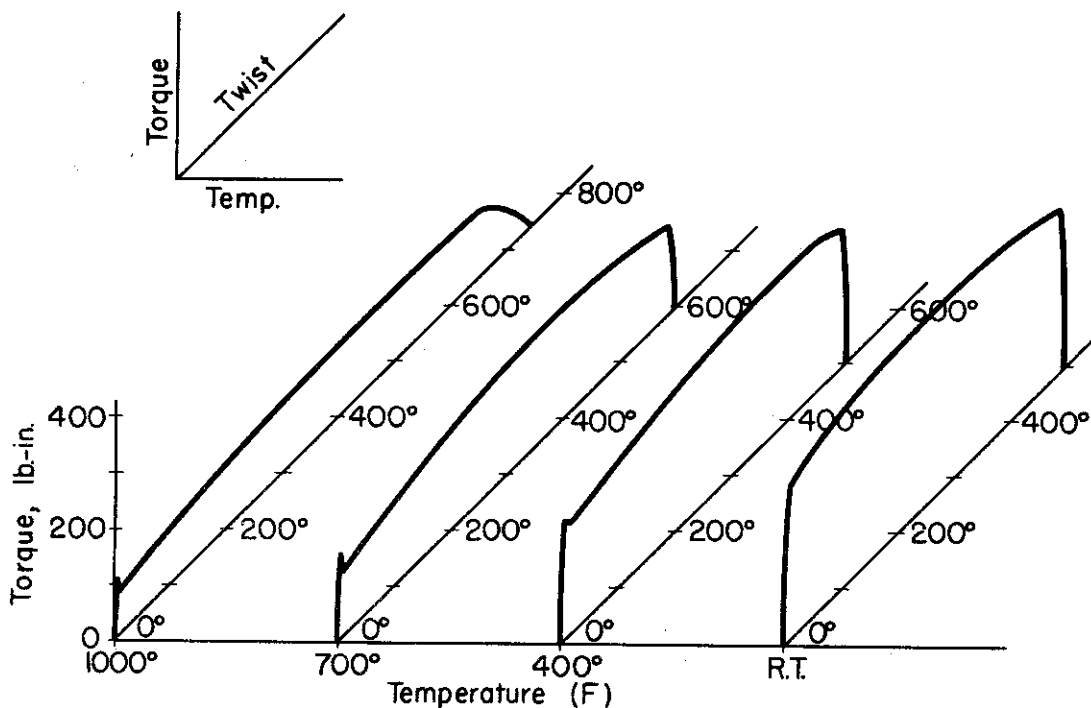


Fig.71 Torque-Twist Curves for Fourth Speed Torsion Tests of RC-70 Titanium at Four Temperatures.

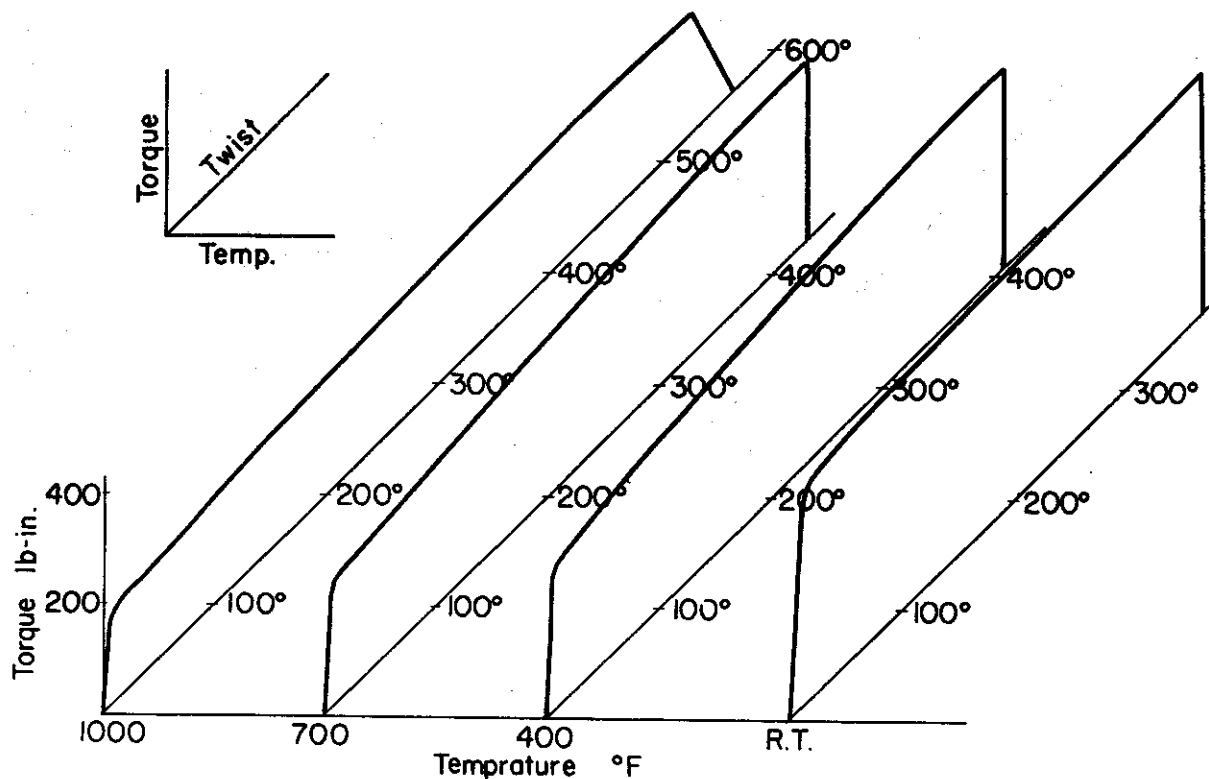
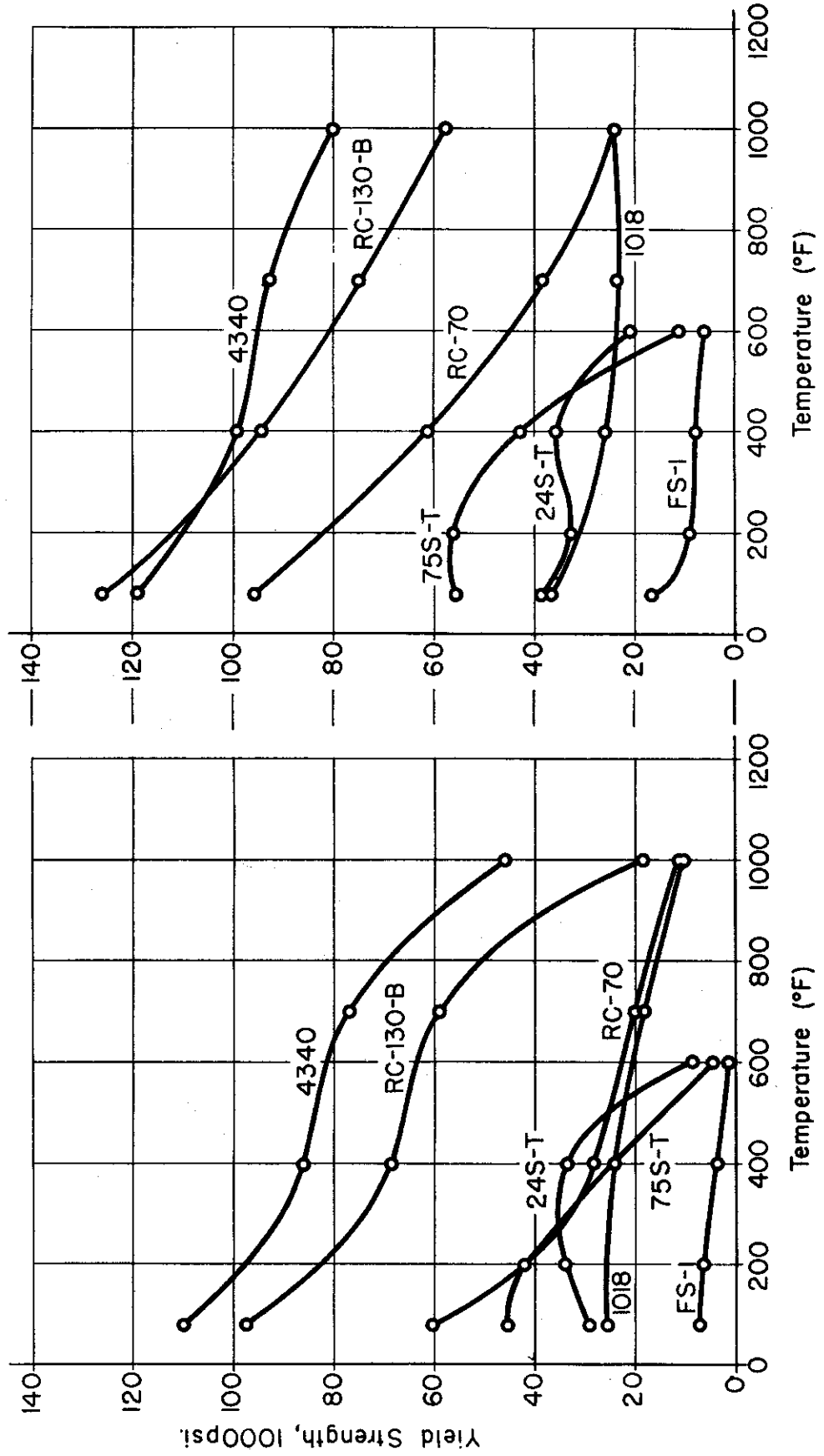


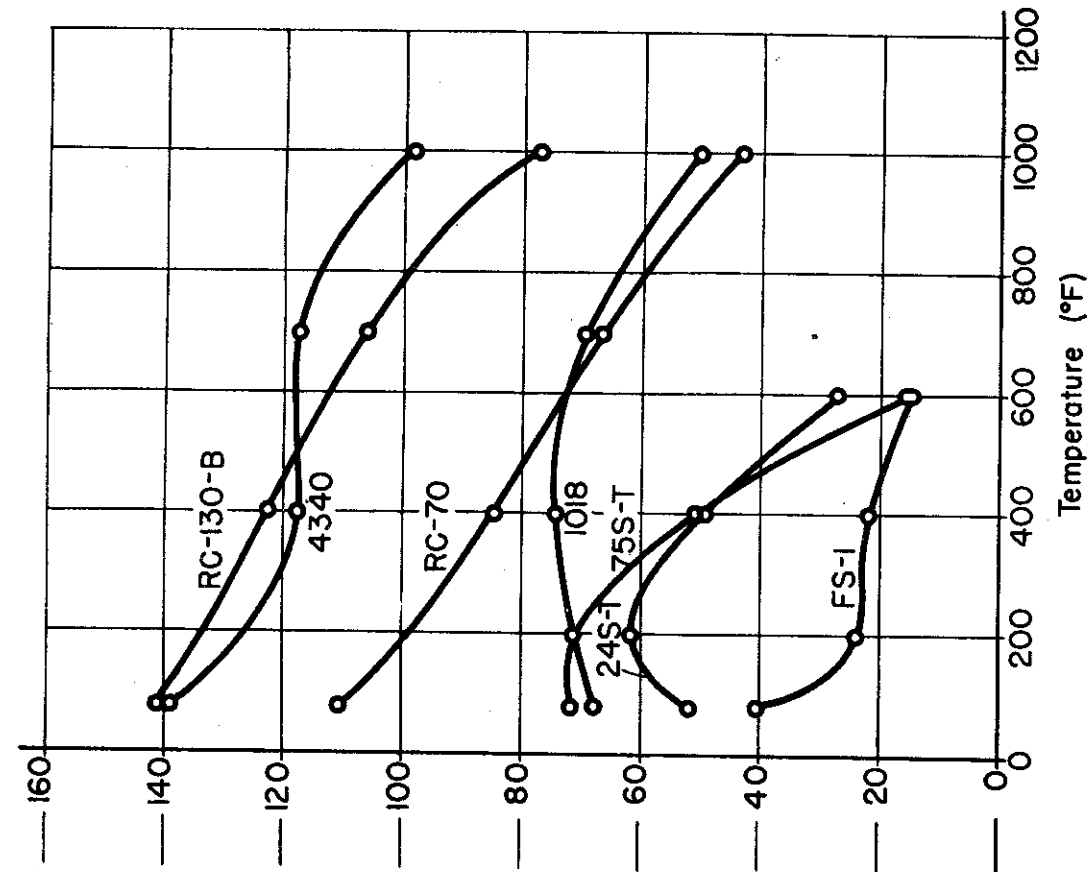
Fig.72 Torque -Twist Curves for Fourth Speed Torsion Tests of RC-130-B Titanium Alloy at Four Temperatures.



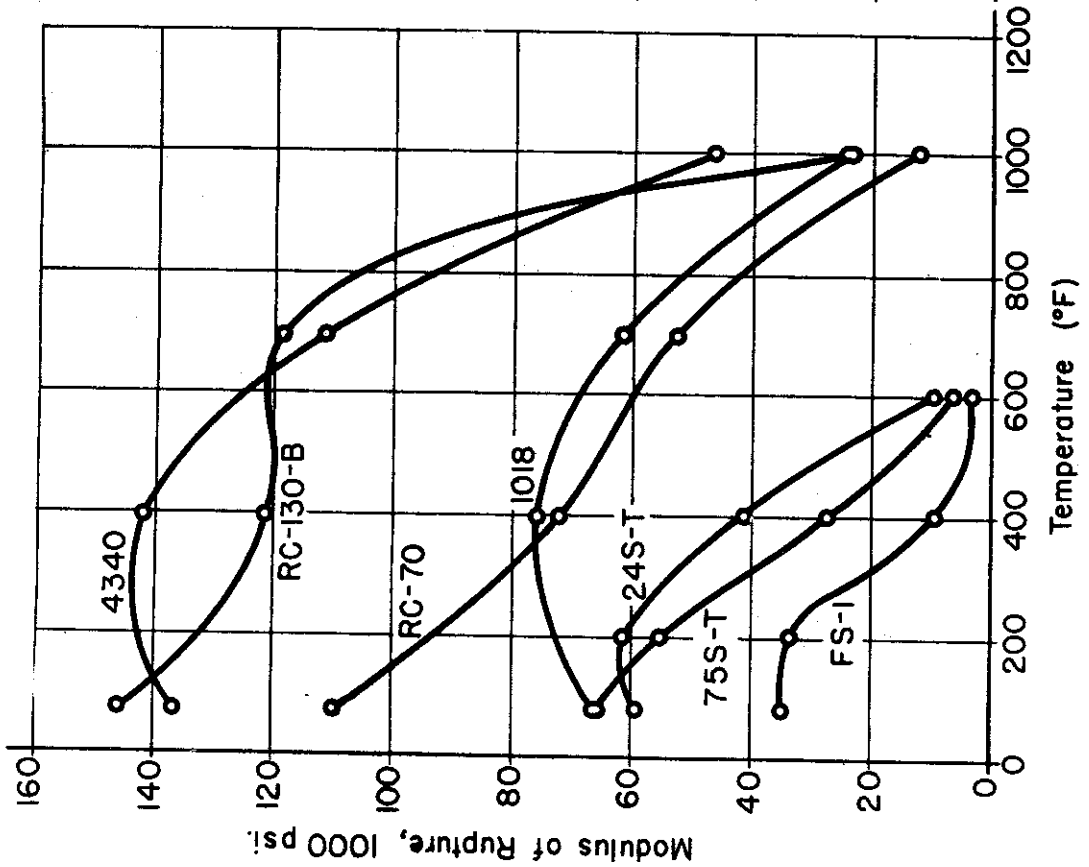
(a) $\dot{\gamma} = 0.0001$ in./in./sec.

(b) $\dot{\gamma} = 12.5$ in./in./sec.

Fig.73 Comparison of the Shearing Yield Strengths at Elevated Temperatures of Seven Metals Tested in Torsion.

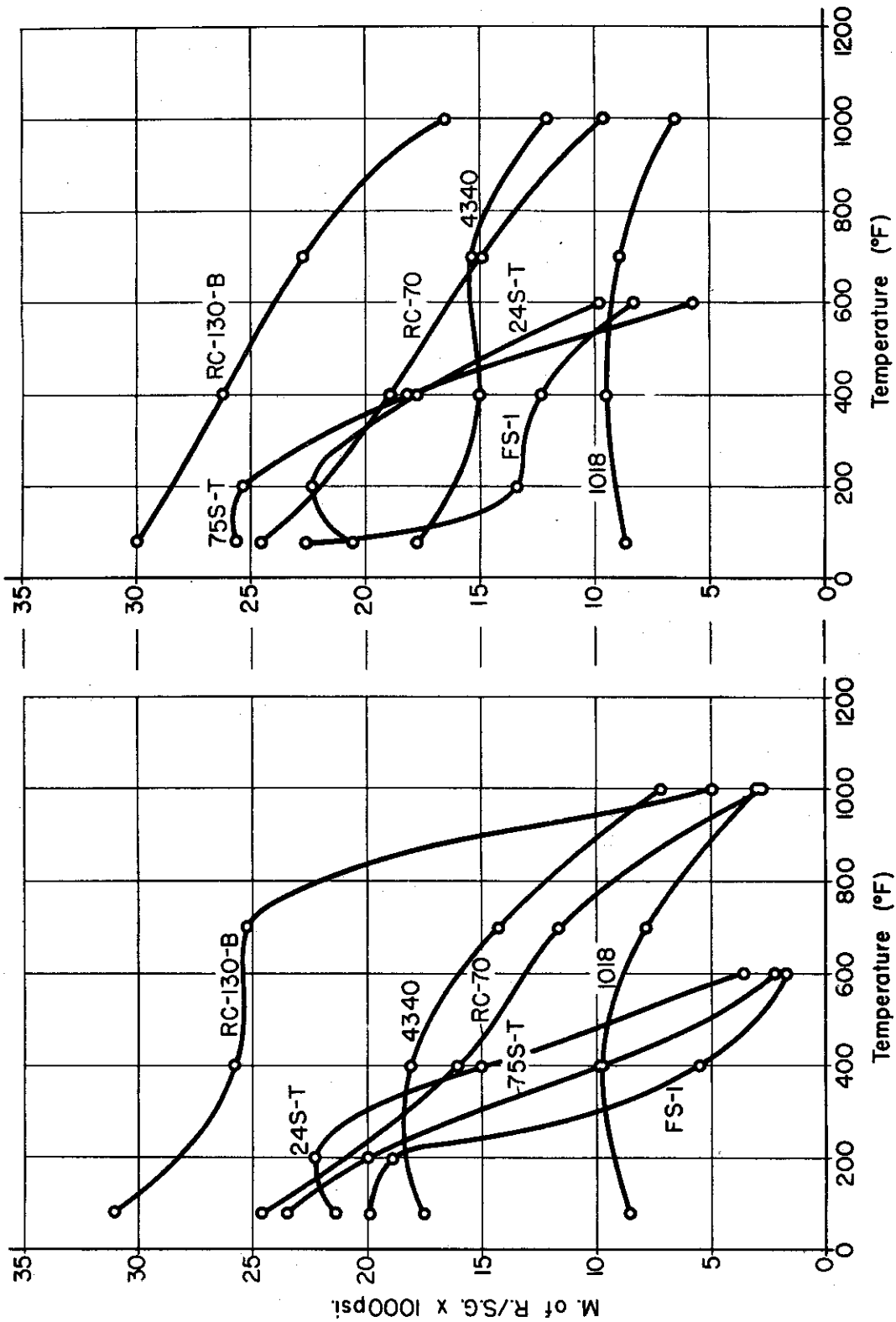


(a) $\dot{\gamma} = 0.0001$ in./in./sec.



(b) $\dot{\gamma} = 12.5$ in./in./sec.

Fig.74 Comparison of the Moduli of Rupture at Elevated Temperatures of Seven Metals Tested in Torsion.



(a) $\dot{\gamma} = 0.0001$ in./in./sec.

(b) $\dot{\gamma} = 12.5$ in./in./sec.

Fig.75 Comparison of the Torsional Strength-Weight Ratios of Seven Metals at Elevated Temperatures. (Based on Modulus of Rupture)

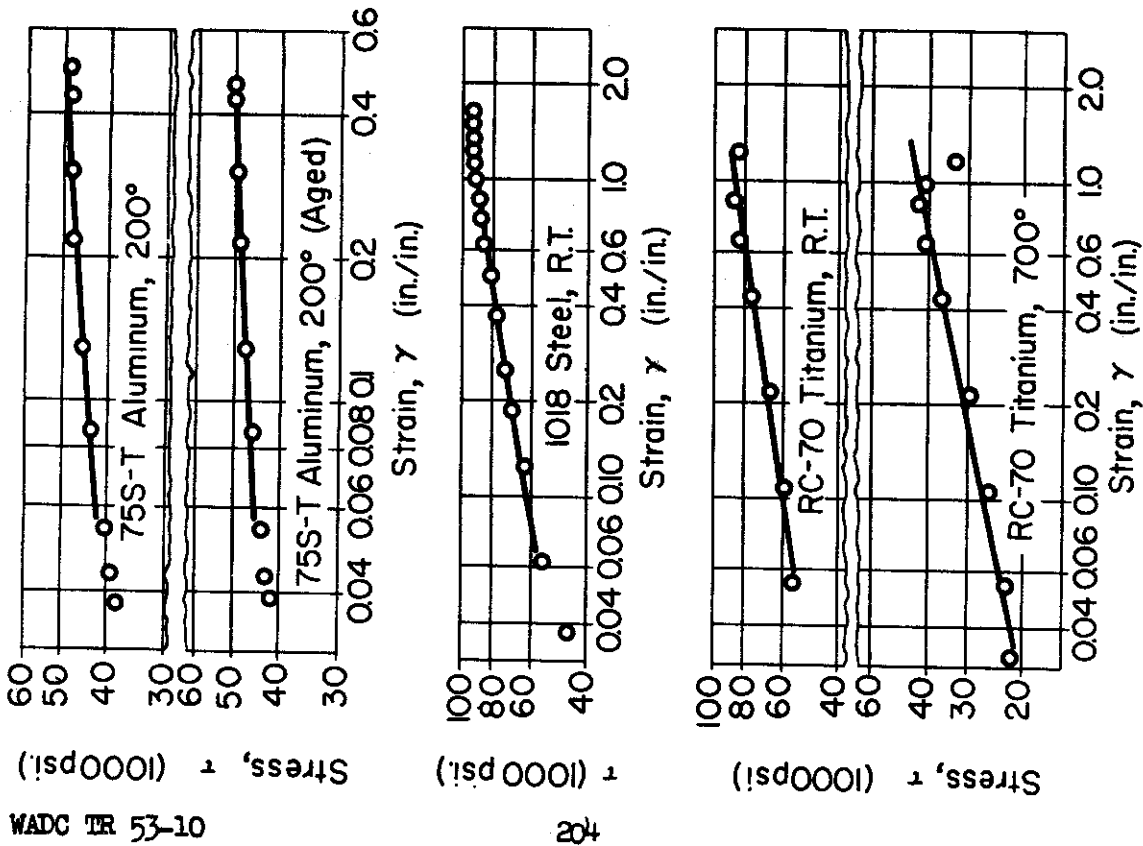
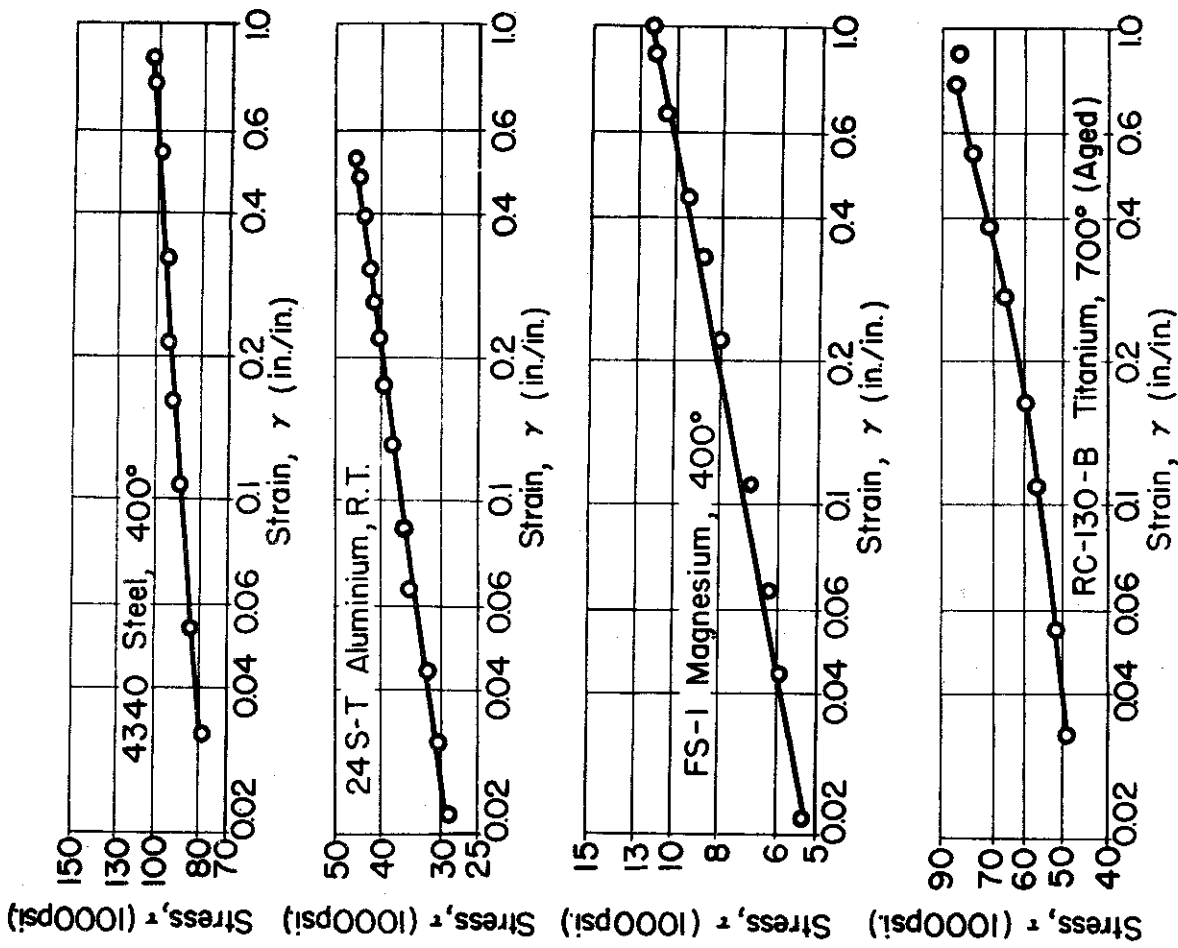


Fig. 76 Plastic True Stress-Strain Curves for Torsion. (Strain Rate 0.005 in./in./sec.)

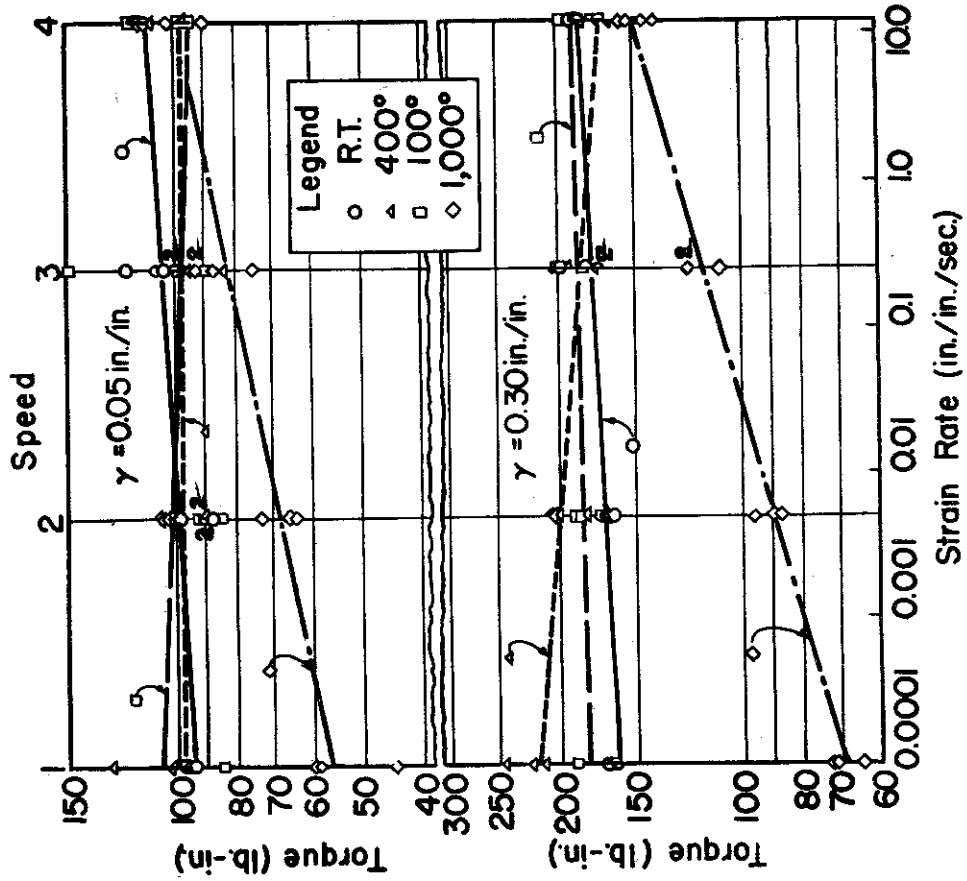


Fig.78 Effect of Rate of Strain on the Torque at Constant Shearing Strain in Torsion Tests of SAE 1018 Steel.

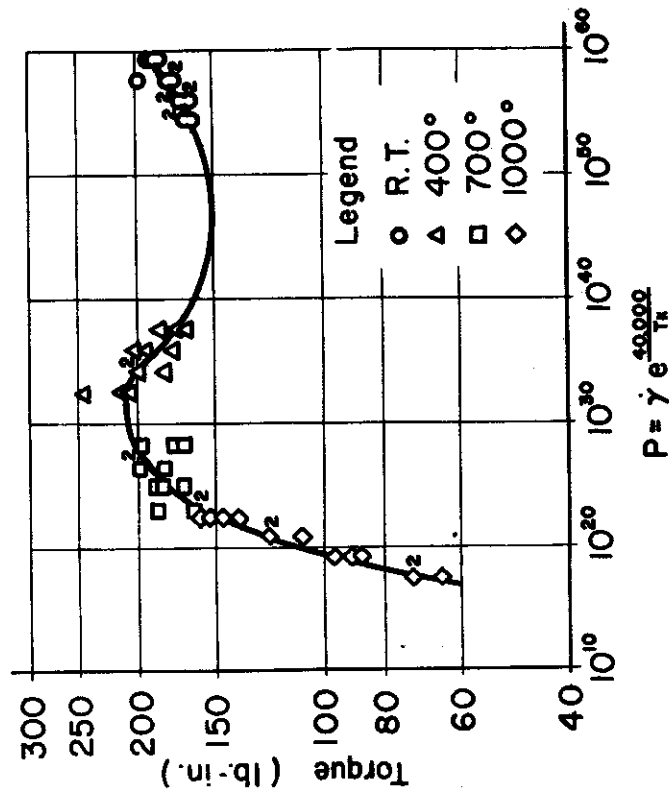


Fig.77 Variation of Torque at Shearing Strain $\gamma = 0.50$ in./in. with the Parameter P for SAE 1018 Steel in Torsion.

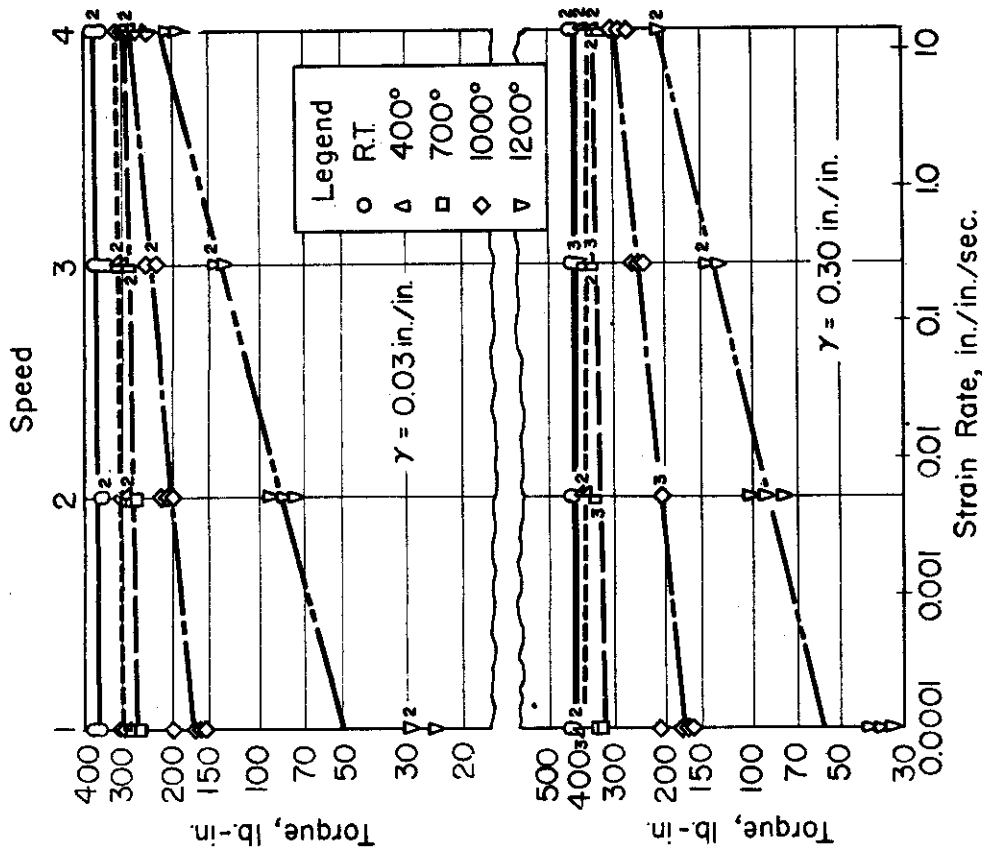


Fig.79 Effect of Rate of Strain on the Torque at Constant Shearing Strain in Torsion Tests of SAE 4340 Steel.

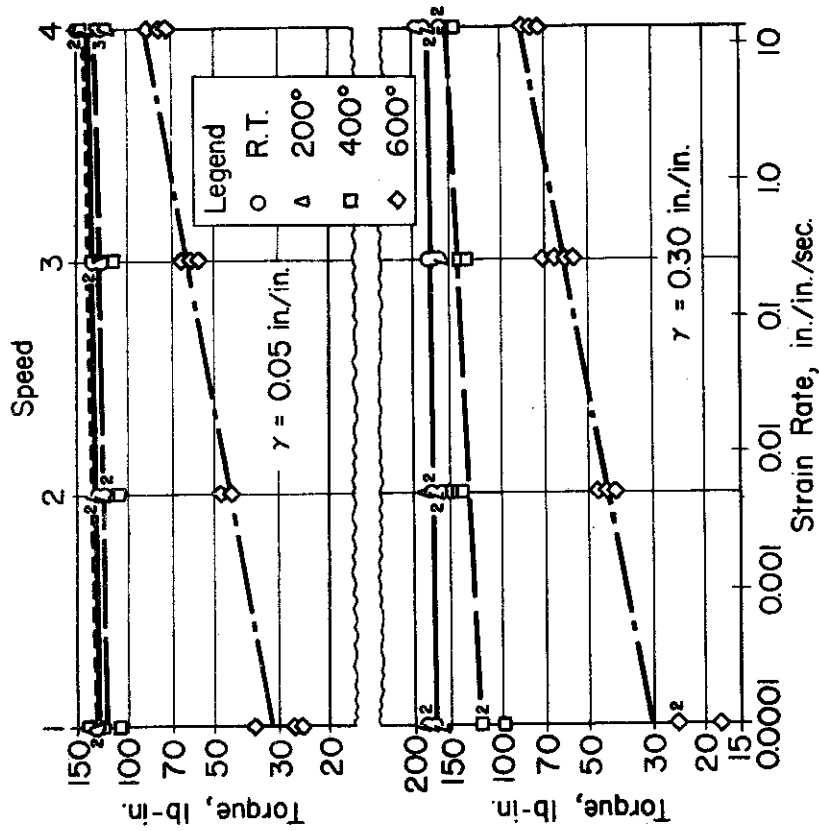


Fig.80 Effect of Rate of Strain on the Torque at Constant Shearing Strain in Torsion Tests of 24 S-T Aluminum Alloy.

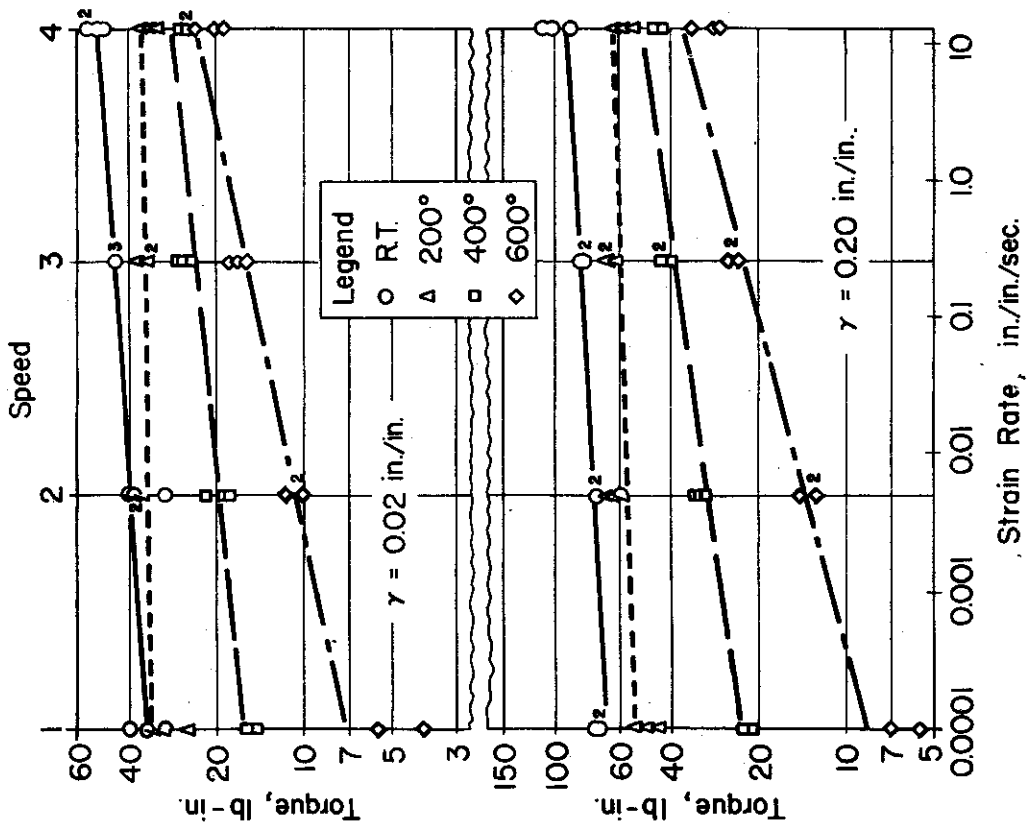


Fig.82 Effect of Rate of Strain on the Torque at Constant Shearing Strain in Torsion Tests of FS-1 Magnesium Alloy.

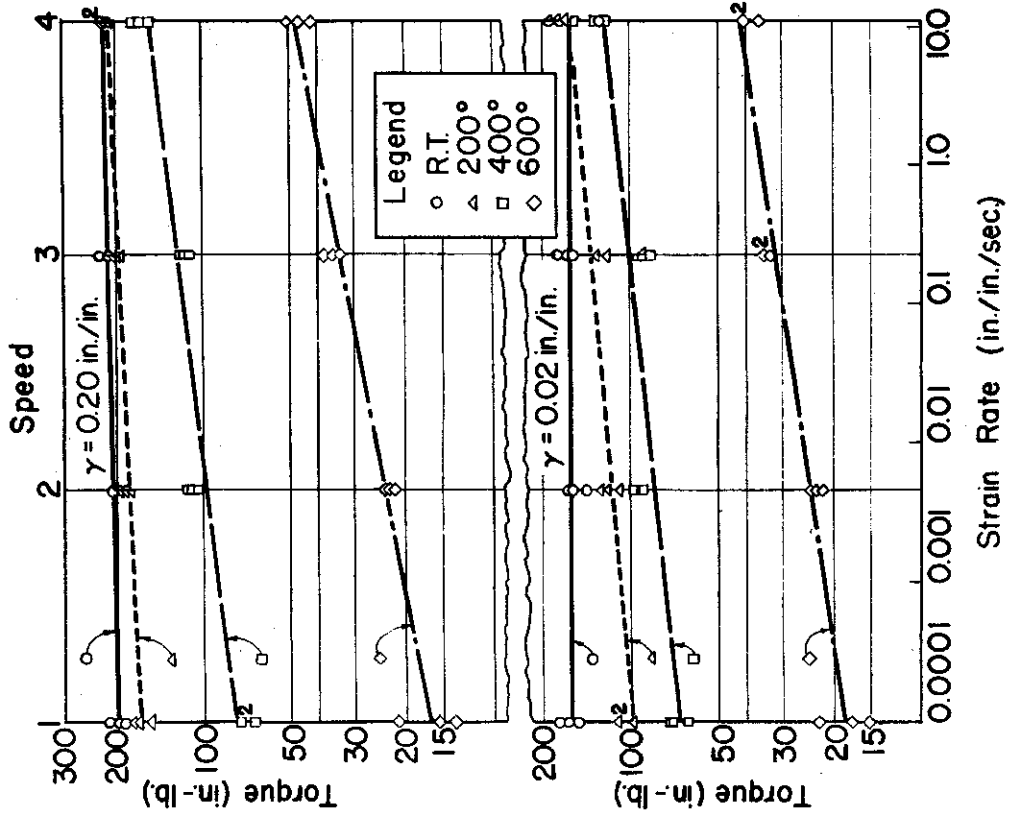


Fig.81 Effect of Rate of Strain on the Torque at Constant Shearing Strain in Torsion Tests of 75S-T Aluminum Alloy

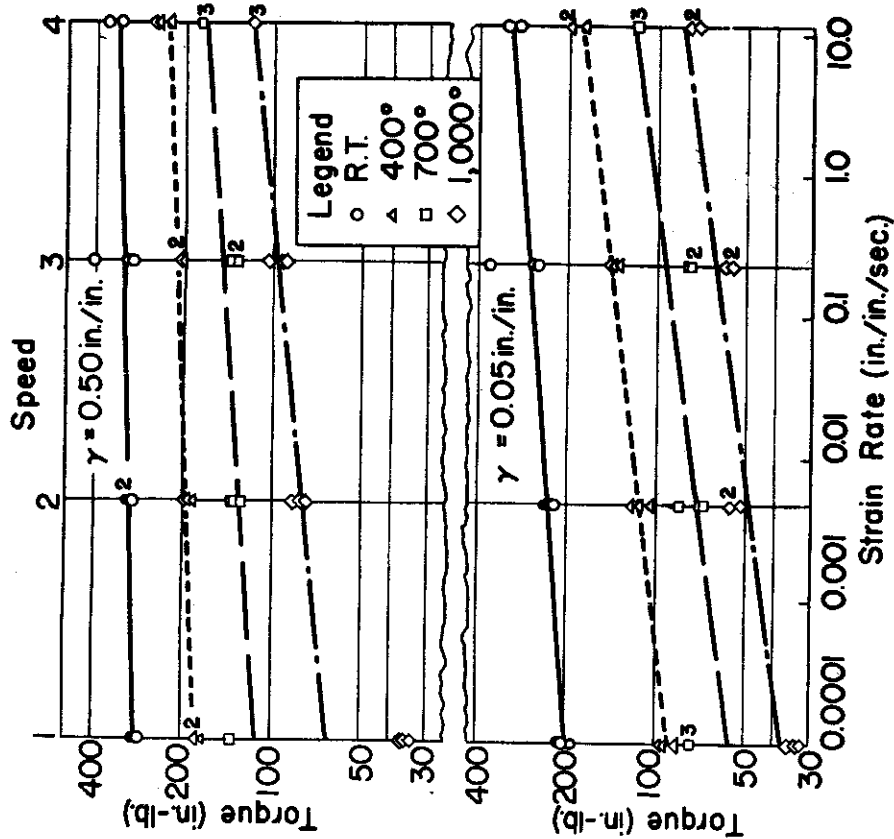


Fig.83 Effect of Rate of Strain on the Torque at Constant Shearing Strain in Torsion Tests of RC-70 Titanium.

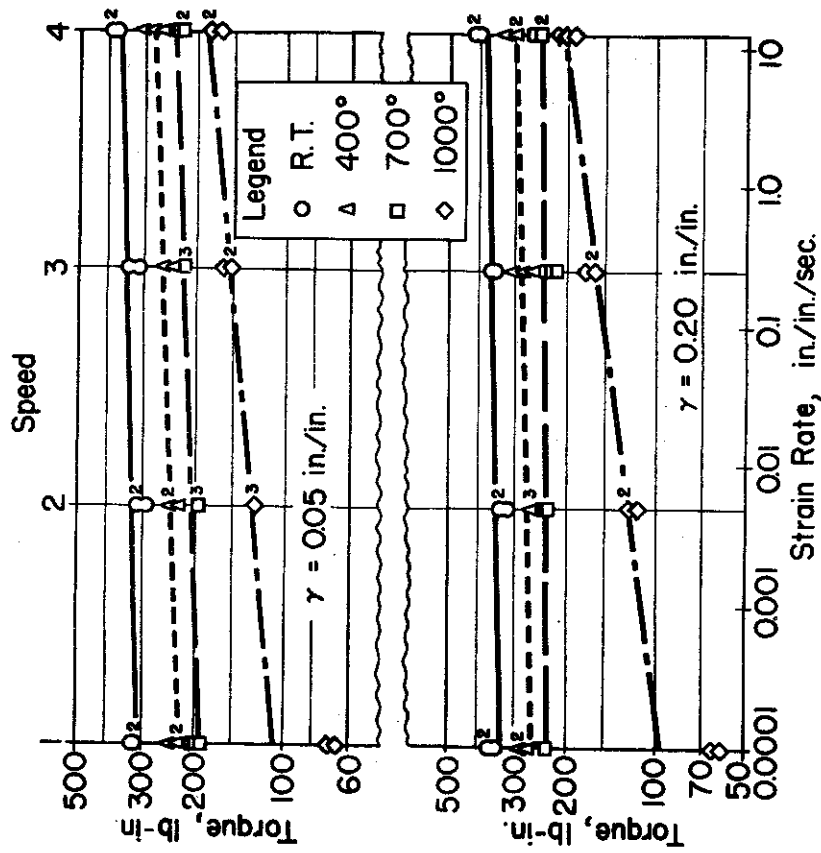


Fig.84 Effect of Rate of Strain on the Torque at Constant Shearing Strain in Torsion Tests of RC-130-B Titanium Alloy.

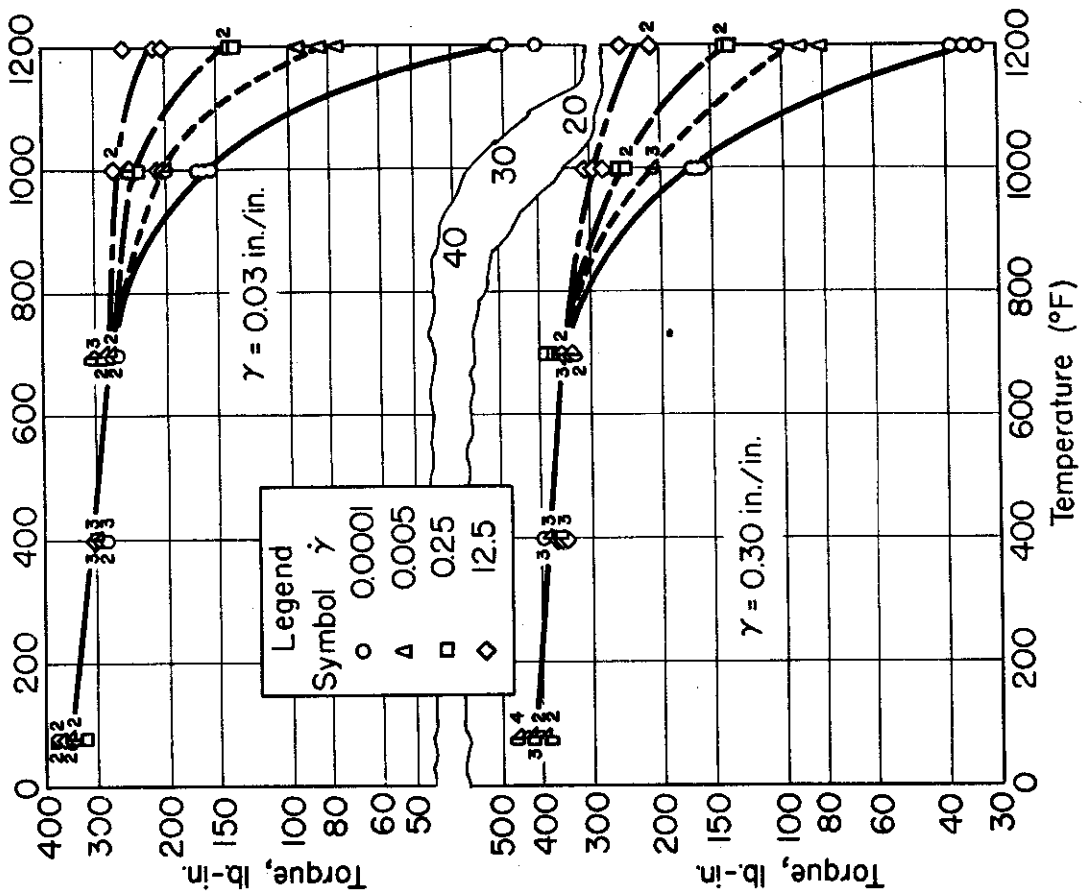


Fig.86 Effect of Temperature on the Torque at Constant Shearing Strain in Torsion Tests of SAE 4340 Steel.

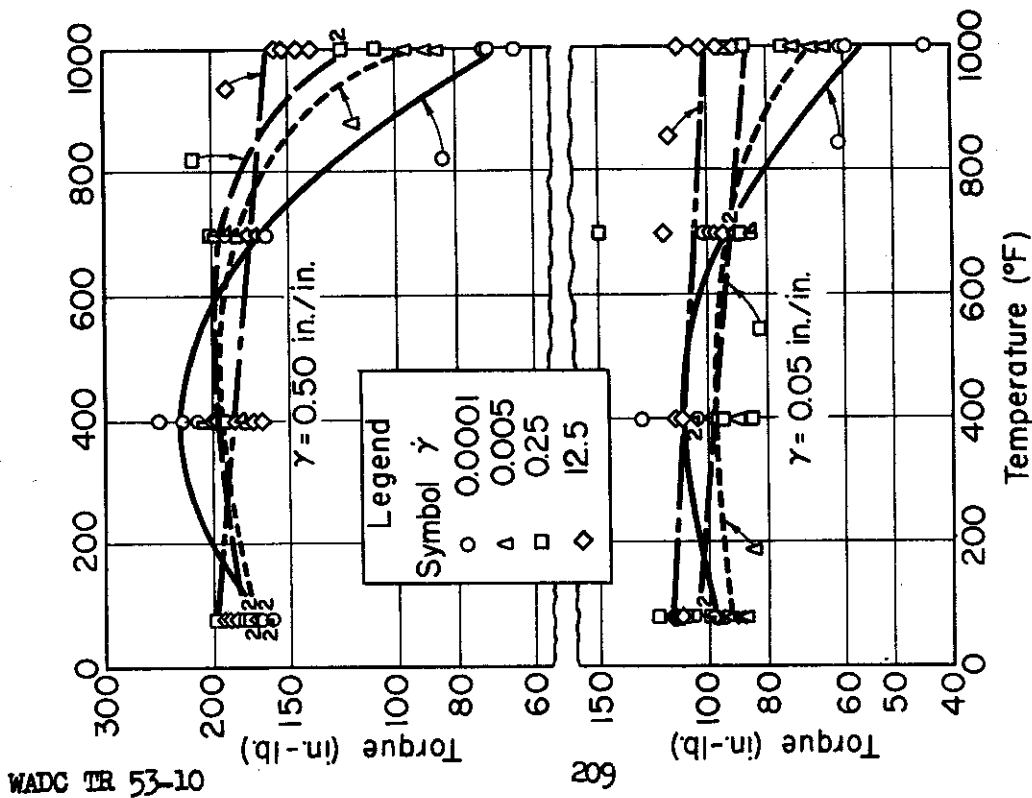


Fig.85 Effect of Temperature on the Torque at Constant Shearing Strain in Torsion Tests of SAE 1018 Steel.

WADC TR 53-10

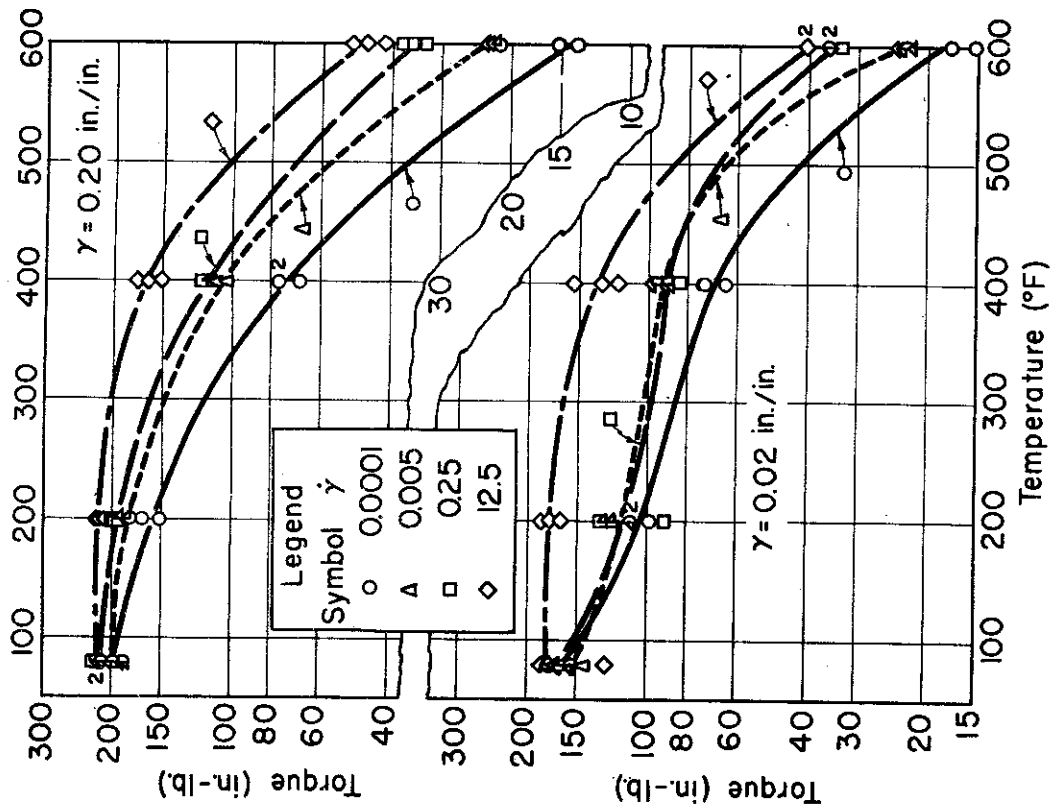


Fig.88 Effect of Temperature on the Torque at Constant Shearing Strain in Torsion Tests of 75S-T Aluminum Alloy.

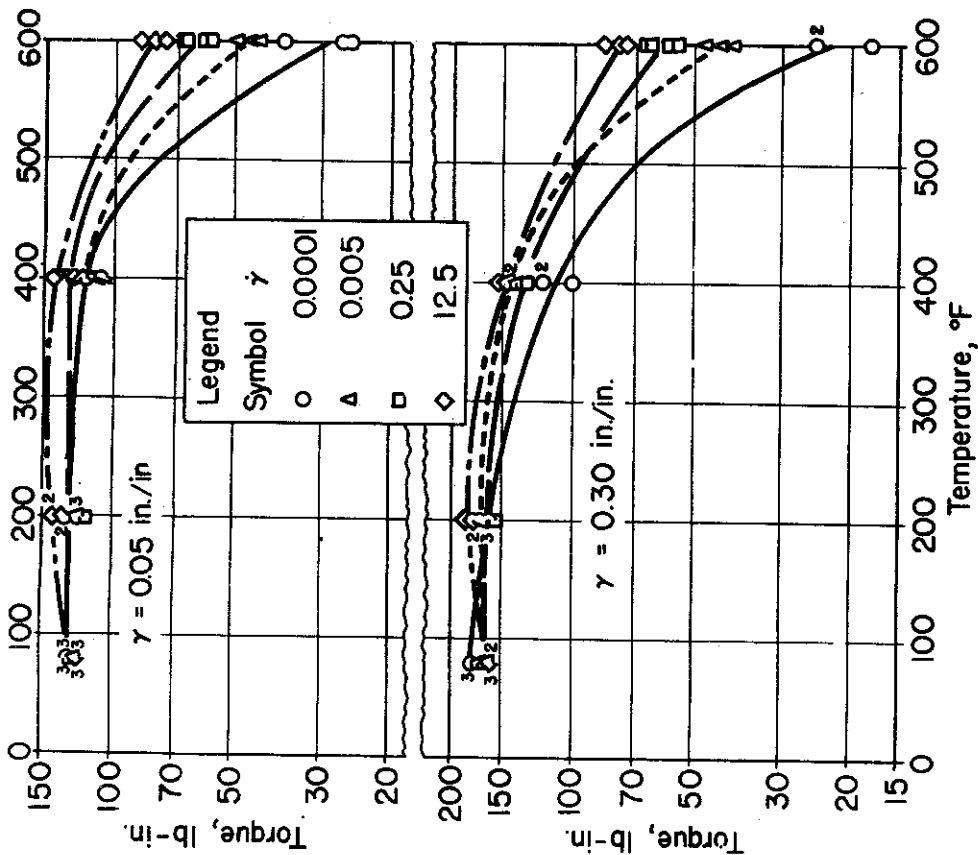


Fig.87 Effect of Temperature on the Torque at Constant Shearing Strain in Torsion Tests of 24 S-T Aluminum Alloy.

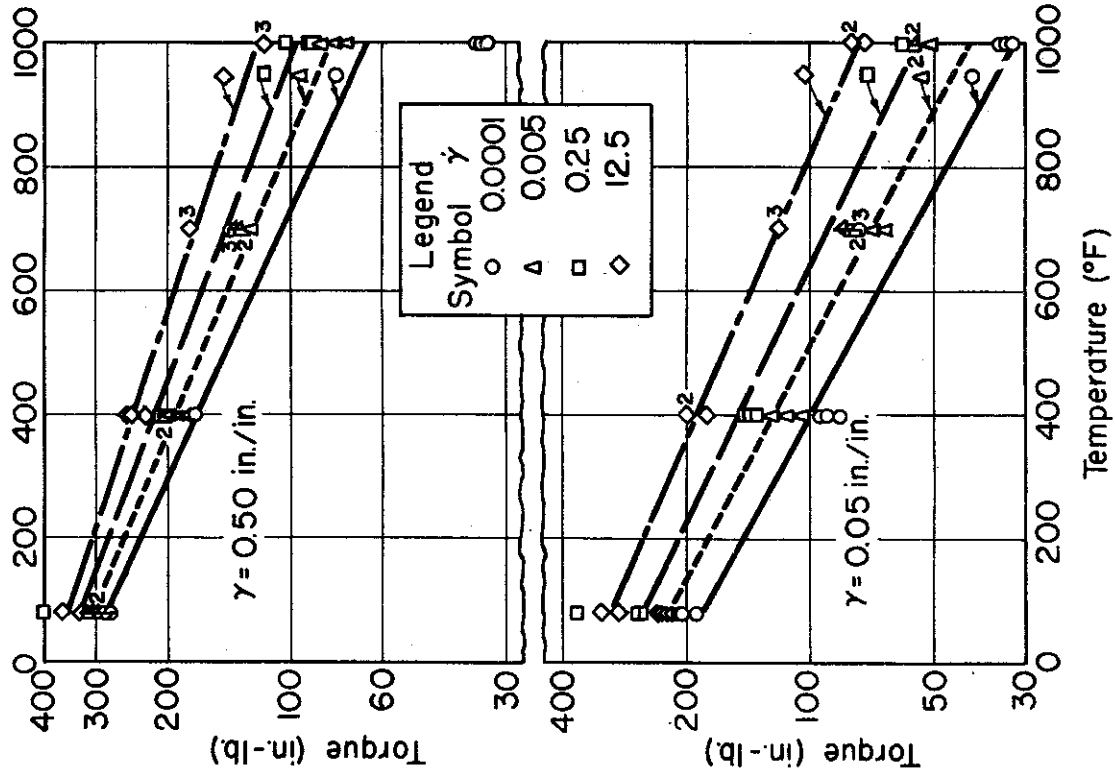


Fig.90 Effect of Temperature on the Torque at Constant Shearing Strain in Torsion Tests of RC-70 Titanium.

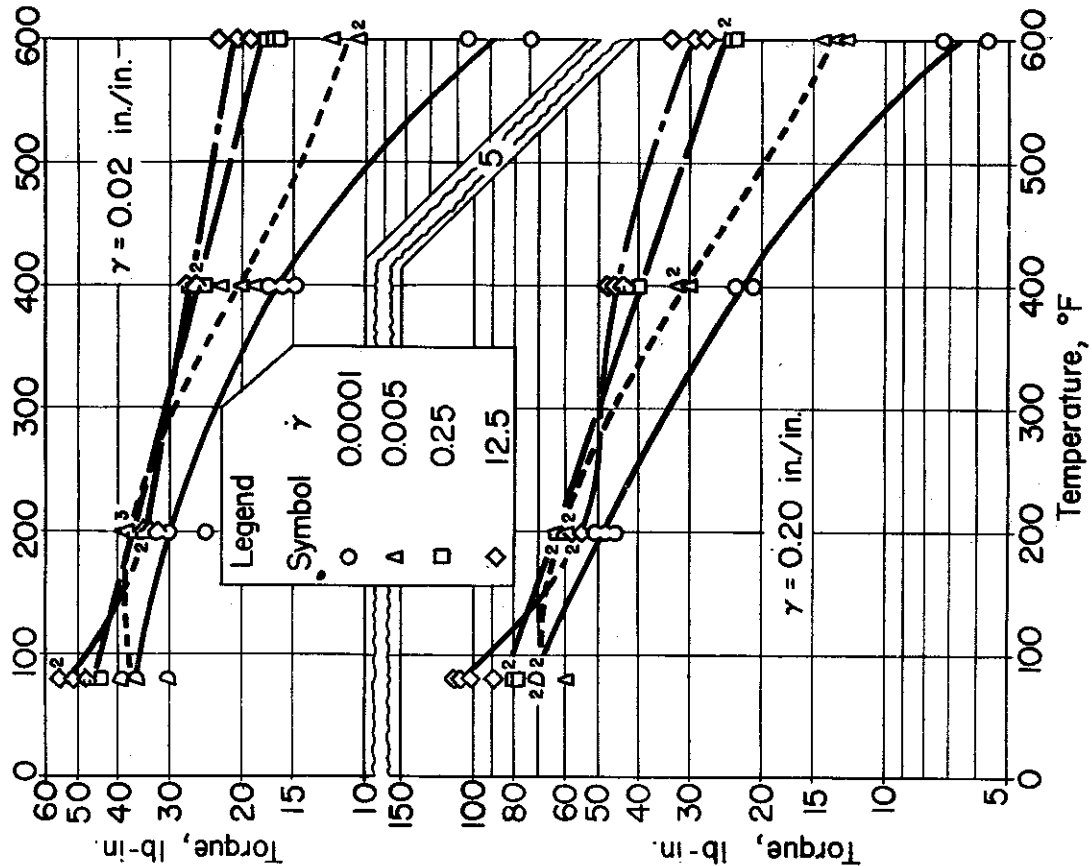


Fig.89 Effect of Temperature on the Torque at Constant Shearing Strain in Torsion Tests of FS-1 Magnesium Alloy

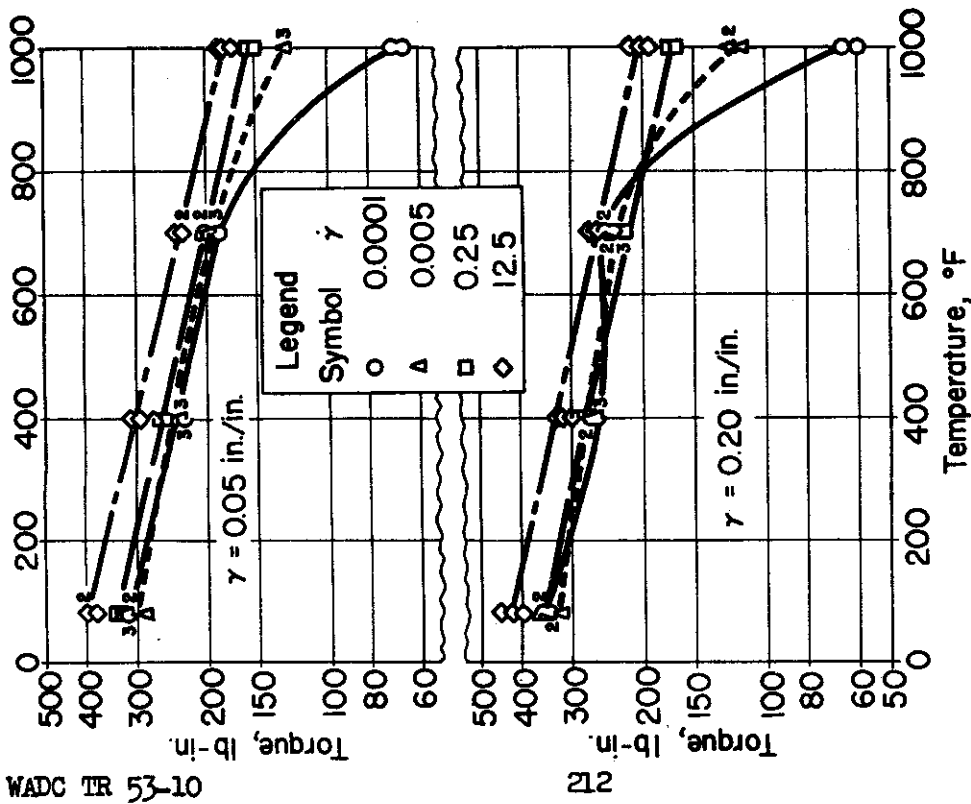


Fig.91 Effect of Temperature on the Torque at Constant Shearing Strain in Torsion Tests of RC-130-B Titanium Alloy.

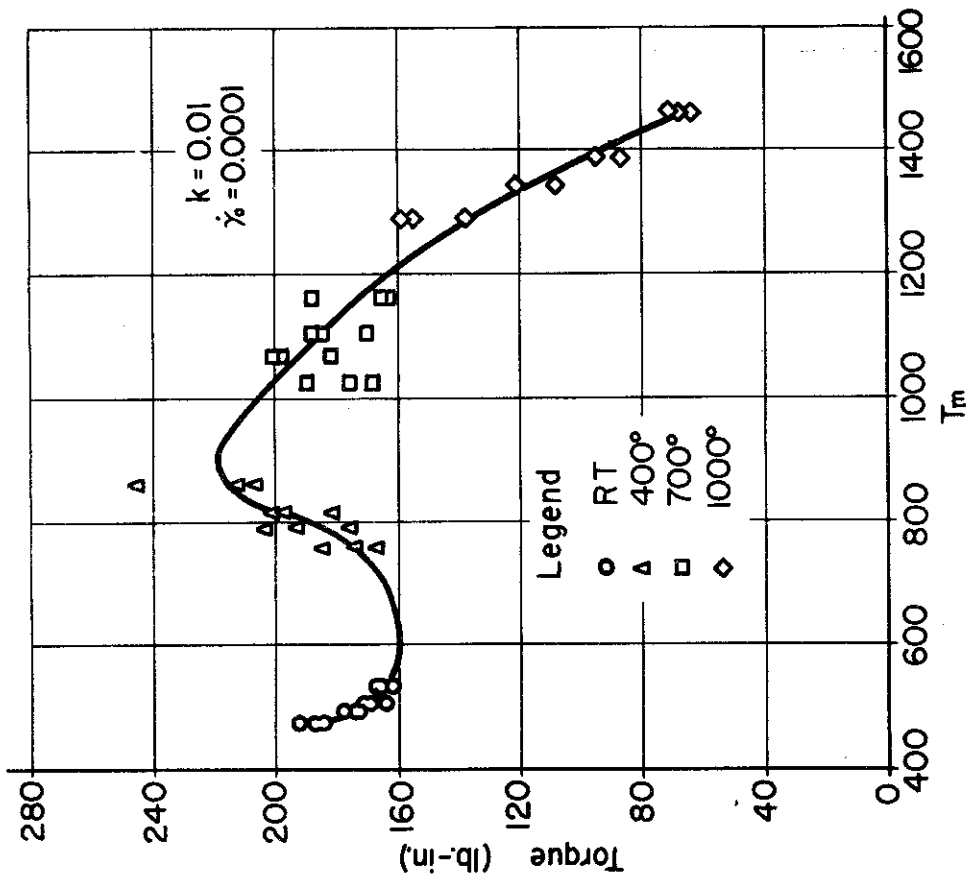


Fig.92 Variation of Torque at Shearing Strain, $\gamma=0.50$ in./in. with the Parameter T_m for SAE 1018 Steel in Torsion.

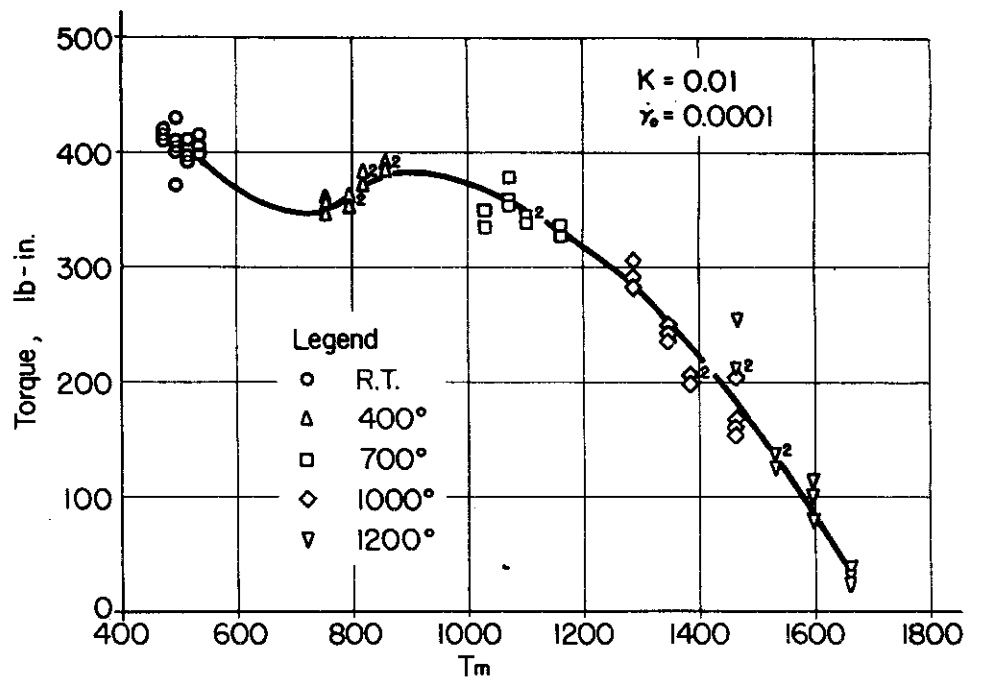


Fig.93 Variation of Torque at Shearing Strain, $\gamma = 0.30$ in./in. with the Parameter T_m for SAE 4340 Steel in Torsion.

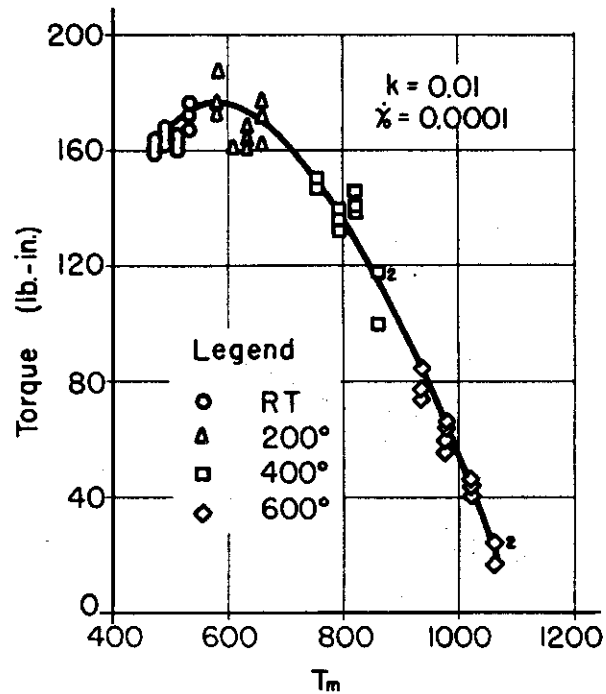


Fig.94 Variation of Torque at Shearing Strain, $\gamma = 0.30$ in./in. with the Parameter T_m for 24S-T Aluminum Alloy in Torsion.

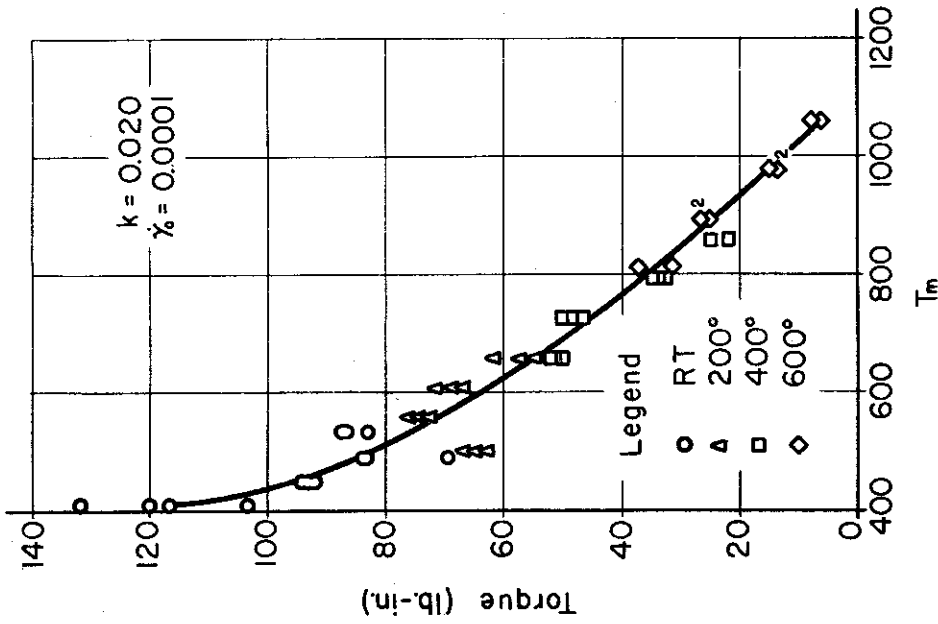


Fig.96 Variation of Torque at Shearing Strain, $\gamma = 0.30$ in./in. with the Parameter T_m for FS-1 Magnesium Alloy in Torsion.

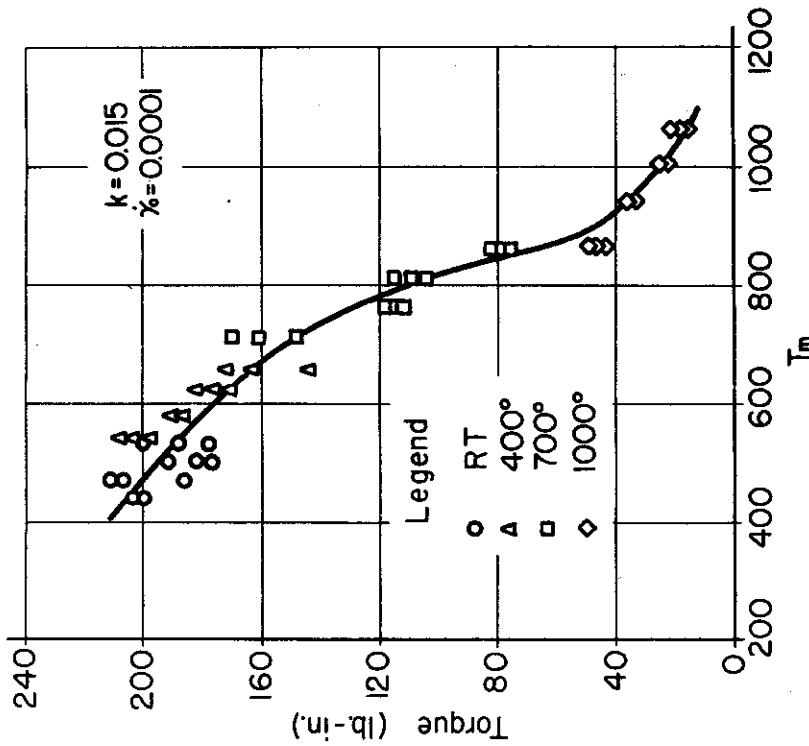


Fig.95 Variation of Torque at Shearing Strain, $\gamma = 0.10$ in./in. with the Parameter T_m for 75S-T Aluminum Alloy in Torsion.

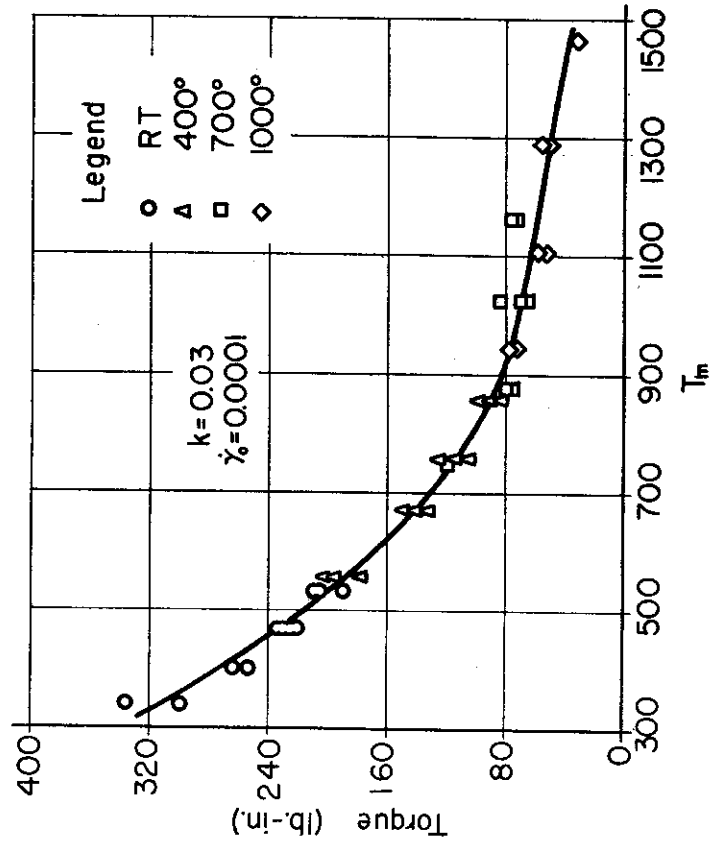


Fig.97 Variation of Torque at Shearing Strain, $\gamma=0.05$ in./in. with the Parameter T_m for RC-70 Titanium in Torsion.

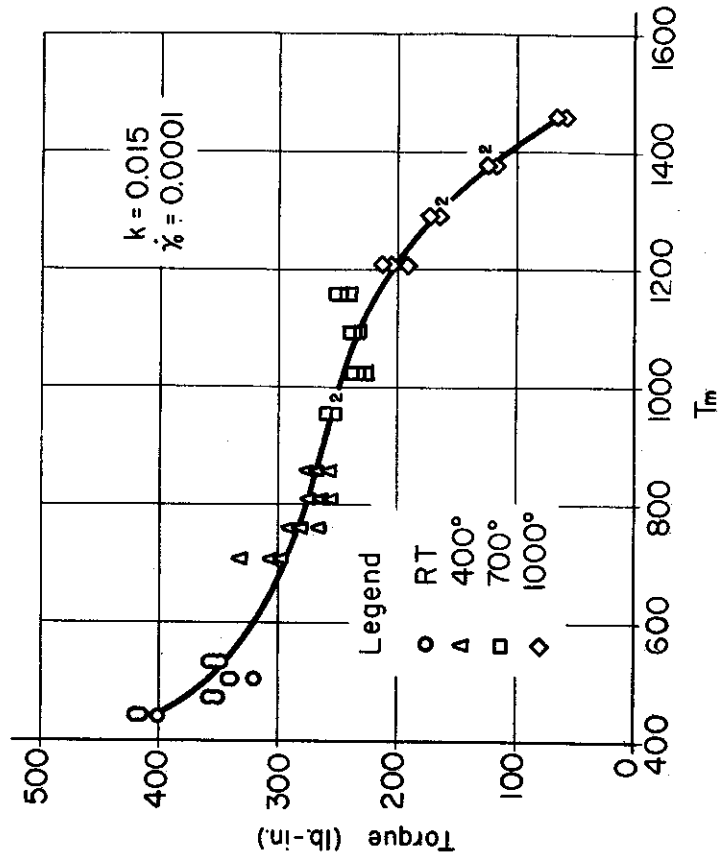


Fig.98 Variation of Torque at Shearing Strain, $\gamma=0.20$ in./in. with the Parameter T_m for RC-130-B Titanium Alloy in Torsion.

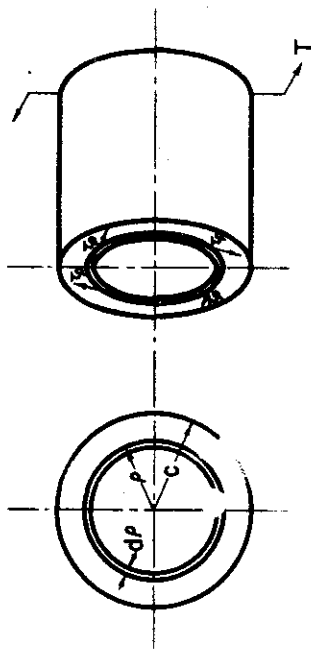


Fig.99 Snearing Stresses in Torsion of a Round Bar

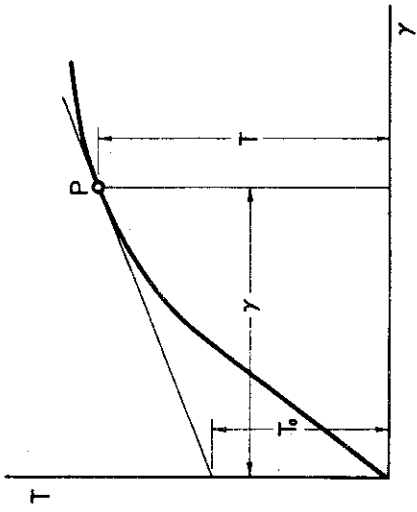


Fig.100 Torque-Twist Curve for Defining T_0

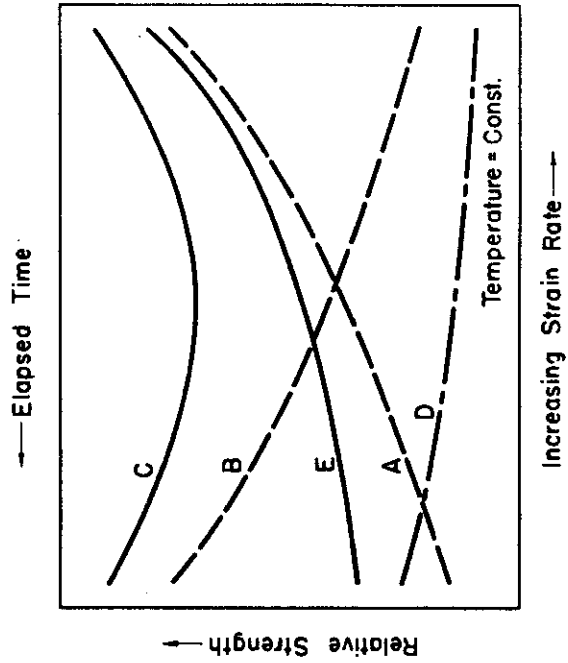


Fig. 101 Contributions to the Relative Strength Caused by Time-Dependent and Temperature-Dependent Changes During Testing.